UNIVERSITY OF CALIFORNIA, MERCED

FOREST MANAGEMENT, WILDFIRE, AND CLIMATE IMPACTS ON THE HYDROLOGY OF SIERRA NEVADA MIXED-CONIFER WATERSHEDS

A dissertation submitted in partial fulfillment of the requirements for the degree of Doctor of Philosophy

by

Philip Saksa

in

Environmental Systems

2015

Committee Members:

Professor Roger Bales, Advisor

Professor Martha Conklin, Chair

Associate Professor Qinghua Guo

Adjunct Professor & Research Scientist, Mohammad Safeeq

The dissertation of Philip Saksa is approved, and it is acceptable in quality and form for publication on microfilm and electronically:

Professor Roger Bales, Advisor	Date
Associate Professor Qinghua Guo	Date
Adjunct Professor & Research Scientist Mohammad Safeeq	Date
Professor Martha Conklin, Chair	Date

University of California, Merced

Table of Contents

List of Figures

List of Tables

Acknowledgements

First, I would like to acknowledge my committee members: Roger Bales for his scientific guidance and big-picture thinking, Martha Conklin for her research ideas and enthusiasm, Qinghua Guo for his encouragement and remote sensing expertise, and Mohammad Safeeq for his modeling expertise. Many thanks to Naomi Tague and the Ecohydrology Lab at UC Santa Barbara for guiding me through the intricacies of RHESSys modeling. Thanks to all my colleagues at the Sierra Nevada Research Institute, who taught me to ski in the backcountry, were fieldwork giants, and for keeping the fun in our science adventures. Thanks also go out to everyone who worked on the Sierra Nevada Adaptive Management Project, there are too many to name; your perseverance, dedication, stubbornness, productivity, scientific integrity, communication skills, humor, and patience are a model for everyone in collaborative science. A big thanks to my family, especially my parents George & Charlotte, for their constant support and the opportunities they provided, without which this would never have been possible. Lastly, thank you Vanessa, for letting me pick your brain about statistics and being persuaded to go on mountain snow adventures, despite your southern California preference for sunny coastlines, wetland habitat, and a balmy 22 degrees (Celsius, of course).

Curriculum Vita

Ph.D. Environmental Systems. University of California, Merced. 2015.
Advisor: Roger Bales, Professor of Engineering

M.S. Forestry. Louisiana State University. 2007.
Advisor: Jun Xu, Professor of Forest Hydrology

B.S. Environmental Science. Ohio State University. 2003.

Abstract

Forest Management, wildfire, and climate impacts on the hydrology of Sierra Nevada mixed-conifer watersheds by Philip Saksa. Ph.D. Environmental Systems. University of California, Merced. Committee Chair: Roger Bales. The research presented in this dissertation aims to 1) assess the water balance of headwater catchments in the Sierra Nevada and determine if fuel treatments implemented in 2012 impacted runoff, 2) use a hydro-ecologic model to simulate the effects of fuel treatments and modeled wildfire at a larger fireshed scale, and 3) to investigate the interaction of vegetation disturbance and projected temperature increases through 2100 to determine relative impacts on hydrologic fluxes. The high variability in annual precipitation, combined with low post-treatment precipitation, masked any detectable changes in headwater catchment runoff from fuel treatments. Model results, however, do show the potential of increased runoff with treatments at both the headwater and fireshed scales, particularly in the high precipitation region of the American River Basin, where vegetation is less water-limited. While the potential for increasing runoff with fuel treatments exists, and may be a co-benefit of reduced fire risk, high-precision equipment for measuring stream discharge may be necessary to verifiable detect these increases. Although increasing temperatures adversely affect snowpack storage, changes in runoff and evapotranspiration are limited to the highest potential temperature increases towards the end of the century, and have less of an impact than vegetation disturbances.

Summary Introduction

Forestland in the California Sierra Nevada is facing increasing pressure from a warming climate, elevated wildfire risk, and limited resources for effective management. Precipitation that originates in the Sierra is the source of more than half of the annual water supply in the state [*Kattelmann et al.*, 1983; *Department of Water Resources*, 2009], and is used for hydropower, agricultural irrigation, and municipal water supplies. The issues confronting forestland and forest management directly impact California's major water source, and there is an impetus to restore the resiliency of the forest to these pressures by applying localized integrated management [*Stephens et al.*, 2013]. The research presented in this dissertation aims to 1) assess the water balance of headwater catchments in the Sierra Nevada and determine if fuel treatments implemented in 2012 impacted annual runoff, 2) use a hydro-ecologic model to simulate the effects of fuel treatments and modeled wildfire at a larger fireshed scale, and 3) to investigate the interaction of vegetation change and temperature increases to determine relative impacts forcing on hydrologic fluxes.

In the first chapter, two sets of paired mixed-conifer headwater catchments are characterized using distributed snow and soil moisture measurements and combined with stream discharge over four water years, 2010-2013. Using the distributed observations, and a LiDAR-based vegetation dataset, the headwater catchment water balance is simulated using the Regional Hydro-Ecologic Simulation System (RHESSys). Observations and model simulations are used to assess the impact of fuel treatments on evapotranspiration and runoff.

The second chapter addresses water quantity measurement and modeling to determine the impacts of forest fuel treatments and wildfire on hydrologic fluxes at the fireshed scale. For this study, a spatially explicit hydro-ecologic model, calibrated in the first chapter on the observed headwater data, was used to scale from small to large catchments. The ability of the headwater calibrations to be transferred to fireshed scale-models is assessed, based on geologic and hydrologic similarities between catchments.

The water balance response to changes in forest structure is determined by differences in Leaf Area Index (LAI), overstory canopy cover, and understory shrub cover.

In the third chapter, I use the calibrated hydro-ecologic model (RHESSys) to analyze impacts to annual hydrologic fluxes with projected changes in the minimum and maximum daily temperatures for Representation Concentration Pathways (RCP) 4.5 and 8.5 at 2050 and 2100. These temperature perturbations are combined with forest thinning treatments and wildfire events to investigate interacting effects of external climate forcing and internal vegetation dynamics on snowpack, soil moisture, and runoff.

Chapter 1: Forest thinning impacts on the water balance of Sierra Nevada mixed-conifer headwater basins

Abstract

Paired headwater catchments in the mixed-conifer zone of the American and Merced River basins were selectively thinned in 2012. Distributed observations of snow storage, soil storage, and stream discharge from 2010 to 2013 were used to calculate the annual water balance and constrain a hydro-ecologic model (RHESSys). Forest thinning effects were simulated using changes in Leaf Area Index, canopy cover, and shrub cover. In the American basin, model results show runoff increased of 14% in response to reductions in Leaf Area Index (-8%), canopy cover (-3%), and shrub cover (-4%). In the Merced basin catchment, treatments had little impact on forest structure or runoff, as vegetation growth in areas not thinned offset reductions from treatments. Observed treatment effects on runoff could not be confirmed in either basin because of the high variability in precipitation in annual precipitation and the low 2013 post-treatment precipitation. When forest thinning is intensive enough to change forest structure, model results show the low-magnitude vegetation reductions can modify catchment-scale water balance in the high-precipitation region of the American River basin. Given the short study period and climate variability, modeling tools were necessary to determine vegetation treatment impacts on the water balance. Hydrologic modeling, constrained by multiple data points, provides a confident and useful tool for analyzing watershed response to forest thinning.

Introduction

The movement of water through mountainous catchments in the western United States depends on the interaction of climate, vegetation, and subsurface processes. Characterizing these components, and their influence on snowpack and water supply, is a priority for effective management of land and water resources. The major land manager in the Sierra Nevada, the U.S. Forest Service, undertakes vegetation treatments to reduce

the risk of large high-intensity wildfires. Vegetation density in these forests is high compared to a century ago [*Collins et al.*, 2011b], and thinning prescriptions range from low-intensity Strategically Placed Landscape Treatments [*Finney*, 2001] to more-intensive restoration treatments [*North et al.*, 2007; *Wayman and North*, 2007].

Forest management practices to encourage fire-resilient landscapes include prescribed burning and selective thinning to reduce surface and ladder fuels and lower crown density, while maintaining larger fire-resistant trees [*Agee and Skinner*, 2005]. Reviewing more than 90 catchment studies of vegetation-treatment effects on streamflow, Stednick [1996] and Bosch and Hewlett [1982] show there is a distribution of impacts on runoff relating to the magnitude of vegetation change, post-treatment precipitation levels, and the rate of vegetation re-growth. The magnitude and pattern of treatments affects snow interception [*Storck et al.*, 2002] and melt [*Essery et al.*, 2008a], water use by vegetation [*Whitehead et al.*, 1984; *Whitehead and Kelliher*, 1991; *Moore et al.*, 2004], and thus runoff [*Ffolliott et al.*, 1989; *Zou et al.*, 2010].

In the Sierra Nevada, canopy interception and evaporation loss has been estimated at 12% to 20% of the annual water budget [*Rowe and Hendrix*, 1951; *Kittredge*, 1953; *Armstrong and Stidd*, 1967]. Kittredge [1953] developed linear relationships between precipitation and interception rates in different forest canopy cover, finding an increase in the slope coefficient with increases in canopy cover, which indicates greater interception capacity in high-precipitation events. Forest cover also impacts surface energy input to the snowpack on the ground, reducing surface shortwave radiation and increasing longwave radiation [*Essery et al.*, 2008a]. Snowmelt rate and timing can have a significant role in the routing and volume of precipitation moving through a catchment. Lundquist *et al.* [2013] suggest that in regions with warm winters such as the mid-elevation Sierra, lower canopy cover decreases mid-winter and early spring melt because of the smaller influence of low angle-sun shortwave energy and greater influence of vegetative longwave energy associated with the warmer temperatures. Analyzing the specific relationship between forest gap size and net radiation, Lawler and Link [2011] compare the magnitude of incoming allwave radiation at an Idaho forest with gap sizes of

1 to 6 tree heights (25-150 m). They determine that net radiation is lowest in gaps of 1 to 2 tree heights (25-50 m), but start to exceed open area radiation in the northern portions of gaps 3 tree heights (75 m) and larger, where incoming shortwave and vegetation longwave energy rates are highest.

Watershed-scale transpiration response to forest thinning depends on regional precipitation amounts and rate of understory or overstory vegetation regrowth following treatments. Zhang *et al.* [2001] used empirical relationships developed from worldwide catchment water balance studies to estimate the increasing response of ET to changes in forest cover with increasing annual precipitation rates. Considering forested watersheds across the conterminous United States, Sun *et al.* [2015] use the Water Supply Stress Index model to calculate a potential range of water yield increases from 0% to 63% with a 50% reduction in LAI. Biederman *et al.* [2014] show that reduced transpiration in disturbed forests may not always lead to expected streamflow increases, however, offset by increased evaporation and sublimation rates.

In the Sierra Nevada, Marvin (1996) applied multiple regressions of runoff response to forest treatments, mean annual precipitation, mean annual runoff, and runoff fraction from 31 experimental catchments in the western United States to model treatment effects in the Sierra Nevada, showing that a 10% increase in mixed-conifer zone harvesting would have no statistical significance on annual runoff (-0.2 - 1.2 cm). Marvin (1996) notes that it is more difficult to determine effects of treatments on runoff in the arid west than the catchments used by Bosch and Hewlett (1982), although the model treatments are less than the 20% threshold that Stednick (1996) suggests is generally required to detect changes in runoff. Using existing literature, Kattelmann et al. (1983) qualitatively hypothesize that removing all vegetation in the Sierra could increase runoff 30-40%, while managing National Forest land specifically for water production could increase runoff by 2-6%. Constraints of management, access, and economics lower this estimate to about 0.5-2% (0.3-1.2 cm), and Kattelmann et al. (1983) instead emphasize the benefit of treatments in delaying snowpack ablation.

While a number of long-term research catchments have provided a wealth of information on forested mountain hydrology [*Hicks et al.*, 1991; *Swank et al.*, 2001; *Troendle et al.*, 2001; *Chauvin et al.*, 2011], there have been few ongoing initiatives in the Sierra Nevada for similar experimental watershed studies. The objectives of this study were to (1) measure the water balance in Sierra Nevada mixed-conifer headwater catchments across a range of latitudes and precipitation rates, (2) develop a well-constrained hydrologic modeling tool grounded with multiple observed datasets, and (3) evaluate watershed response to thinning treatments currently used by land managers with observations and modeling.

Methods

Two sets of paired mixed-conifer headwater catchments were monitored over four water-years, October 1, 2009 to September 30, 2013. Bear Trap Creek (treatment) and Frazier Creek (control) are in the American River basin, and Big Sandy Creek (treatment) and Speckerman Creek (control) are in the Merced River basin, with elevations from 1560 m to 2188 m (Figure 1.1). Forest thinning for fuels reductions were implemented in the treatment watersheds during autumn 2012. Pre- and post-treatment LiDAR data, combined with forest-plot measurements, were used to determine the area and extent of vegetation removed. Changes to water yield resulting from the forest thinning were assessed using observations of water storage in the snowpack and soil, and stream discharge to calibrate and evaluate model simulations.

Site characteristics

Soils in the American are well drained with Bear Trap Creek having the Crozier-Cohasset, Crozier-McCarthy-Cohasset, and Hurlbut-Deadwood complexes and Frazier Creek having the Crozier-Cohasset, Crozier-McCarthy-Cohasset, and Crozier-Mariposa-Cryumbrepts complexes [*Soil Survey Staff*, 2011]. Merced soils are also well drained with Speckerman Creek having Ledford family-Entic-Xerumbrepts and Chaix-Chawanakee families with Big Sandy Creek having Ledford family-Entic Xerumbrepts and Umpa family soil series [*Soil Survey Staff*, 2011]. Soil samples were collected at all 128 moisture-sensor locations and analyzed for texture. Nearly all of the soils contained

greater than 50% sand, and they all contained less than 50% silt and 30% clay. Soils in the American were classified as loam or sandy loam, and soils in the Merced were sand or sandy loam. Textures were more variable between individual sensor locations than between sensor depths.

Forest-plot vegetation surveys were completed at both sites, as described in Fry *et al.* [2015], and provided the following species composition. Mixed-conifer forest in the American River sites is dominated by white fir (*Abies concolor*) and Douglas-fir (*Pseudotsuga menziesii*), with an understory of manzanita (*Arctostaphylos spp.*). Mixed-conifer in the Merced River sites is dominated by white fir and incense cedar (*Calocedrus decurrens*), with understory shrub species including mountain whitethorn (*Ceanothus cordulatus*), deerbrush (*Ceanothus integerrimus*), and greenleaf manzanita (*Arcostaphylos patula*). Forest structure in the American River sites from plot data showed lower canopy cover, lower basal area (e.g. LAI), and higher shrub cover than the Merced River sites [*Fry et al.*, 2015].

Field measurements

The following instruments were installed at each site for the purposes of calculating a water balance and constraining hydrologic-model parameters. Meteorological stations in the upper and lower elevations of each pair of catchments recorded precipitation, temperature, wind speed/direction, and radiation. Tipping-bucket instruments were used at the stations to record precipitation, limiting their effectiveness to rain events. Precipitation data from external sites were also incorporated to maintain consistency of the measurement method between rain and snow events, with the precipitation phase at the upper and lower stations determined using snow-depth sensors. At the American River sites, additional precipitation data were taken from the Blue Canyon meteorological station (1610 m), operated by the US Bureau of Reclamation, 22-km to the northeast and similar in elevation to the lower meteorological station. In the Merced River site, precipitation data from the US Bureau of Reclamation Poison Ridge meteorological station (2100 m) were used, which is 8 km to the southeast and similar in elevation to the upper meteorological station.

Distributed snow-depth sensors (15 per pair of catchments) and soil-moisture sensors (64 per pair of catchments) provided continuous hourly measurements over a range of elevation, slope, aspect and forest cover, similar to Bales *et al.* [2011]. Stream stage was recorded at each watershed outlet by pressure-sensitive depth recorders. Stream discharge was then measured using the salt-dilution method to develop a stage-discharge rating curve. Discharges were measured over a range of flows during the four years, with a minimum of 16 data points available. A majority of discharge measurements were recorded at low to medium stream discharge, while higher discharges are generally under-represented.

One of the goals in deploying distributed environmental monitoring sensors is to ensure representative characterization of the mean and variability over the landscape. To determine the representativeness of the snow-depth sensor siting, a grid survey of 119 points in a 1-km^2 area around Duncan Peak was completed on March 23-26, 2009 and showed the 7 wired snow sensors represented 20% of the range of snow depths measured with the survey. A second survey on April 15 and 26, 2012 showed the wired sensors represented 24% of the surveyed snow depth range, but 9 new sensors for a distributed wireless network prototype had also been deployed by then [*Kerkez et al.*, 2012], and improved that number to 61%. Mean values for all methods were similar for both years; the 2009 mean depths were 212 cm and 208 cm for the survey and wired sensors respectively. The 2012 respective mean depths were 168 cm, 155 cm, and 160 cm for the survey, wired sensors, and new wireless sensors.

Forest Treatments

Strategically Placed Landscape Treatments (SPLATs) were implemented in the fall of 2012. Forest vegetation structure was determined using allometric equations from tree lists in the Forest Vegetation Simulator, populated using the forest-plot data, to calculate Leaf Area Index (LAI) and Canopy Cover (CC). Understory vegetation was also incorporated into the model using a linear equation developed from the forest-plot measurements [*Fry et al.*, 2015] (Equations 1, 2); we assumed these relationships in overstory and understory structure were constant in all model scenarios. Shrub cover was

calculated in each vegetation community type for the American River (Equation 1, R^2 = 0.16) and Merced River (Equation 2, R^2=0.25) sites as

$$SC = 63.079 - 0.244BA - 0.257CC \quad [1]$$

$$SC = 55.273 - 0.294BA - 0.256CC \quad [2]$$

where *SC* is shrub cover, *BA* is basal area (m^2 ha^{-1}) and *CC* is canopy cover. The low correlation coefficients were a result of the highly scattered relationships, but the equations are functionally relevant where higher-density vegetation and overstory cover produces lower predicted shrub cover. The Bear Trap watershed was completely covered by the mature mixed conifer classification and Frazier watershed was 95% mature mixed conifer, 3% young mixed conifer, and 2% cedar forest. Speckerman watershed contained 82% mature mixed conifer with 18% live oak-pine forest and Big Sandy was covered by all vegetation types at 56% mature mixed conifer, 33% live oak-pine, 6% open pine-oak woodland, and 5% closed canopy conifer forest.

Hydrologic Modeling

The RHESSys model [*Tague and Band*, 2004] combines a meteorological-forcing model (MTNCLM, [*Hungerford et al.*, 1989]), biogeochemical-cycling model (BIOME-BGC, [*Running and Hunt*, 1993]), and hydrologic model (TOPMODEL, [*Beven and Kirkby*, 1979] or DHSVM, [*Wigmosta et al.*, 1994]). The spatial environment in the model is created using a 20-m DEM, soil layer from the SSURGO database [*Soil Survey Staff*, 2011], and the vegetation layer described above. Daily precipitation from the nearby Blue Canyon and Poison Ridge was input, split into separate rain and snow series using the snow-depth sensors around each of the four meteorological stations. Daily minimum and maximum temperatures were input from the upper and lower met stations at each study site.

Precipitation input to the RHESSys model as individual rain and snow events was used because it replicated observed snow events more accurately than the model estimate

of precipitation phase based on a linear transition over a given temperature range. Using two climate zones in the model for the upper and lower climate stations, both catchments had a mean wintertime temperature (Nov-Apr) of 4.3^{o}C, but 40% of precipitation was snow in Bear Trap and 60% was snow in Big Sandy, due to the higher elevation range in Big Sandy. Summer (May-Oct) mean daily temperature was 18.3^{o}C in Bear Trap and 17.8^{o}C in Big Sandy. The respective mean elevations for Bear Trap and Big Sandy are 1723 m and 2140 m, but Bear Trap ranges from 1619 to 1826 meters while Big Sandy ranges from 1808 to 2473 m. The standardized lapse rate of 6.5^{o}C km^{-1} [*Barry and Chorley*, 1987] suggests that if these basins were co-located, Big Sandy would be 2.7^{o}C cooler than Bear Trap.

Snowmelt in RHESSys was calibrated to replicate mean basin snowpack using a radiation melt coefficient of 0.4, and temperature snowmelt coefficient of 0.0005 and 0.001 for the American and Merced treatment catchments, respectively. After manual calibration of snow processes, streamflow was calibrated using the Monte Carlo based method with 5000 normally distributed random parameter sets (Table 1.1). Parameters controlling soil physical properties of pore size index (*po*) and air entry pressure (*pa*), along with parameters controlling flow properties of hydraulic conductivity (*k*), decay of hydraulic conductivity with depth (*m*), vertical hydraulic conductivity (*svk*), and groundwater storage (*gw1*, *gw2*) were used in calibration. Acceptable parameter sets were determined by comparing observed and modeled daily stream discharge using a Nash-Sutcliffe Efficiency (NS_e; Nash and Sutcliffe, 1970) and of daily streamflow and log-transformed streamflow greater than 0.60, and discharge within 20% of annual and 25% of August flows. These restrictions support constrained simulations of annual discharge, peak storm flow events, and the seasonal trends typical of a Mediterranean climate.

Results

Field Measurements

Annual precipitation in the American River sites ranged from 160 cm in 2012 to 275 cm in 2011, and in the Merced River sites ranged from 83 cm in 2012 to 202 cm in 2011

(Figure 1.2). Precipitation in the Merced catchments was 50 to 80% of the levels in the American, with the largest differences in the two dry years of 2012 and 2013. Precipitation trends were consistent with regional values reported by the California Department of Water Resources (DWR), where the 8-station Northern California Precipitation Index was at 63% (2012) to 145% (2011) of the long-term mean (1922-1988) and the 5-station Southern California Precipitation Index was 61% (2012) to 160% (2011) of the mean (1956-2005). Observed snow depth was converted to snow water equivalent (SWE) using a linear relationship between the day of year and snowpack density from the nearest similar elevation snow pillow [*Liu et al.*, 2013]. At the higher elevation stations of Duncan Peak and Fresno Dome (elevation, ~2100 m), snowfall comprised 69% and 52% of the precipitation over the four years, while at the lower elevation stations of Bear Trap (1560 m) and Big Sandy (1790 m), snowfall rates were at 41% and 40%.

Runoff in the American headwaters (41-167 cm) was higher than in the Merced headwaters (23-112 cm), reflecting the higher precipitation of the more-northern sites. Within the American River, the Frazier Creek control catchment consistently had higher runoff (62-167 cm) than the Bear Trap treatment catchment (41-134 cm) in the pre-treatment years of 2010-2012 (Figure 1.2). Runoff in the post-treatment year of 2013 was much more similar, with Frazier and Bear Trap Creek at 44 and 43 cm, respectively. Within the Merced River, runoff in the Speckerman control catchment was lower in the wetter years of 2010 and 2011 (39-77 cm) than in the Big Sandy treatment catchments (52-112 cm). Runoff in the both of the drier years was within 1 - 2 cm between the catchments, including the pre-treatment 2012 and post-treatment 2013 years. To determine if the forest thinning had an effect on observed daily discharge, F-tests ($p<0.05$) were performed on the paired streams. The results showed significant differences in the control-treatment discharge relationship, not only in the pre- and post-treatments years, but also for all four individual years due to the high inter-annual precipitation variability (Figure 1.3).

Runoff ratio, defined as the fraction of annual precipitation leaving the catchment as runoff, was more consistent between the catchments in the wetter 2010 and 2011 years than during the drier 2012 and 2013 years (Figure 1.4). The Merced control watershed (Speckerman) runoff ratio was most consistent of all the basins, ranging from 0.26 to 0.38 over all the years, but the American control watershed (Frazier) was the most variable ratio, ranging from 0.26 to 0.61. The Merced treatment catchment (Big Sandy) runoff ratio ranged from 0.28 to 0.55 and the American treatment catchment (Bear Trap) ranged from 0.25 to 0.49. Comparing the American catchments, the runoff ratio of Bear Trap (treatment) was 0.12 to 0.13 lower than Frazier (control) in the pre-treatment years (2010-2012), but 0.01 higher in the post-treatment year of 2013. In the Merced headwaters, the Big Sandy (treatment) runoff ratio was 0.08 (2010) and 0.17 (2011) higher than Speckerman (control), but 0.1 (2011) and 0.2 (2012) lower in the pre- and post-treatment dry years, respectively.

Annual evapotranspiration and changes in subsurface storage are calculated as a loss term using precipitation minus runoff (Figure 1.2), and range from 119 to 141 cm in Bear Trap and from 98 to 125 cm in Frazier. The relatively constant values resulted in a low coefficient of variation (CV) of 0.07 in Bear Trap and 0.11 in Frazier. Runoff in the American sites depended on annual precipitation and varied substantially through the study period (CV: Bear Trap = 0.61, Frazier = 0.60), from 41 to 134 cm in Bear Trap and 44 to 167 cm in Frazier. In the Merced study region, the evapotranspiration and storage loss term was more dependent on annual precipitation, with similar rates for the first two years of higher precipitation, 100 and 90 cm in Big Sandy with 113 and 125 cm in Speckerman, and then similar for the last two years of lower precipitation, 60 and 56 cm in Big Sandy with 59 and 54 cm in Speckerman. The loss term CV was higher over the four years than in the American River catchments, at 0.29 for Big Sandy and 0.42 for Speckerman. Runoff variability was similar to the American watersheds (CV: Big Sandy = 0.75, Speckerman = 0.55), ranging from 53 to 112 cm in Big Sandy and 24 to 77 cm in Speckerman.

Soil-moisture values increased with fall rain events, as early as the first few days of the water year (early October). Moisture values typically showed sustained saturation through the winter season. Soils in the top 1 m stored 20 - 30 cm of water during the wet winter season in Merced catchments, while soils in the American catchments stored 25 to 35 cm, possibly reflecting the lower sand content. Soil storage recession started as early as day 200 in the dry years, but as late as day 270 in the wet year, and directly coincide with observed snowpack melt out dates. Despite the low precipitation in 2012 and 2013, a combination of drier ridge and hillslope soil moisture combined with summer storms that maintained higher soil moisture in the riparian zone, resulted in a greater soil storage standard deviation at both sites, and higher summer mean soil storage overall in the American River site (Figure 1.5).

Modeling

Calibration was completed for water years 2010-2012, as all three years exhibited substantially different precipitation levels. The snow calibrations were completed for the treatment and control watersheds, but the measured snowpack accumulation and ablation was not representative of the control basins, as none of the parameter sets met the minimum streamflow calibration criteria for Frazier Creek or Speckerman Creek. Treatment effects were modeled using the thinned watersheds, with the vegetation conditions before and after treatment simulated over all four years of observed measurements. From the 5000 parameter sets tested, 6 sets of Bear Trap, (American River) and 17 sets for Big Sandy (Merced River) sets met the criteria described above (Table 1.1, Figure 1.6). Water year 2013 was post-treatment and not used for calibrations, thus having an expected lower range of performance for Bear Trap (NS_e = 0.34-0.74, $\log NS_e$ = 0.68-0.79) and Big Sandy (NS_e = 0.27-0.75, $\log NS_e$ = 0.29-0.81).

Snowpack calibrations in the American River sites were most representative of observations during 2010 and 2013, and underestimated snowpack in much of 2012 and the accumulation phase of 2011. In the Merced River sites, snowpack calibration replicated 2010 snowpack well, but underestimated mid-season snowpack in 2011 and 2012, with faster than observed spring melt in 2013. Model root-zone soil storage and

streamflow recession timing depended on snowpack melt out date and summer storm events. Simulation of melt-out dates that were later than observed at both sites in 2010 and in Bear Trap in 2011 propagated to late simulation of soil storage and streamflow recession. Confidence intervals were greater in Big Sandy than in Bear Trap, even with the higher number of simulations. Modeled soil-water storage was most similar to observations in the dry 2012 and 2013 years, with wetting-up and drying-out periods that were often delayed compared to observations. The wettest year of 2011 in Big Sandy, where the model showed elevated moisture content relative to observations in the top meter of soil, and where soil infiltration exceeded drainage rates in the model, but not in observations. Simulated discharges often replicated the rapid response to specific storm or melt events, but did not recess as quickly as observed from peak flows. The shapes of summer recession curves were more consistent in the model than observed, possibly reflecting subsurface properties not captured in the model.

Forest thinning represented an 8.0% LAI reduction within the Bear Trap watershed and no LAI changes within the Big Sandy catchment. The small reductions in vegetation from fuel treatments in Big Sandy were offset by increases in vegetation in other parts of the watershed over the 5 years (2007-2013) between LiDAR flights. Bear Trap watershed LAI values were 9.9 prior to treatment and 9.1 following treatment. Leaf Area Index was 6.6 for both scenarios of Big Sandy, but the post-treatment vegetation was composed of marginally increased shrub vegetation and decreased overstory. Model results for Bear Trap show that with the treatments, runoff increased 14% on average (Figure 1.7). Changes in runoff and evapotranspiration were statistically significant within the 95% confidence interval from the 6 parameter sets and were consistent in dry to wet precipitation conditions, adding 12.2-13.6 cm of annual runoff and reducing evapotranspiration by 10.9-11.9 cm. Runoff and evapotranspiration did not change significantly in Big Sandy, associated with the light treatments, where overall LAI remained the same, canopy cover increased 1.1%, and shrub cover increased 7.2%.

Discussion

Observed Water Balance Treatment Effects

Differences in post-treatment observed runoff between the two American River watersheds (Figures 1.2, 1.5) can be attributed to forest-treatment effects, but may also reflect uncharacterized differences in subsurface storage properties. Between 2012 (pre-treatment) and 2013 (post-treatment), precipitation increased 5%, and the Bear Trap (treatment) runoff increased 5%, but the Frazier (control) runoff decreased 29%. The Bear Trap loss term (P − Q) increased 6%, but in Frazier it increased 28%. Subsurface bedrock in Bear Trap is dominated by the Shoo Fly Complex, metasedimentary sandstone and shale with low potential for storage and flow [*Saucedo and Wagner*, 1992]. Frazier Creek underlying bedrock is dominated by volcanic pyroclasts [*Saucedo and Wagner*, 1992], which can have high potential storage and flow, or respond similarly to Bear Trap geology depending on the amount of weathering [*Tague and Grant*, 2004].

The elevated response of Frazier compared to Bear Trap could have been an response to multiple impacts: higher transpiration demand from the untreated catchment, a second low-precipitation year routing more precipitation into subsurface storage that was already depleted from the first dry year, or a combination of both processes. Stream discharge calculations based on stage measurements and a rating curve, also introduce uncertainty, especially for high discharge events beyond the established rating curve. A small number of peak-flow events occurred every year, but the uncertainty associated with those events increases in the low precipitation years of 2012 and 2013, when high-flow events become a greater fraction of the annual runoff. The peak-flow uncertainty may have contributed to the observed changes in the dry pre- and post-treatment years between the American control and treatment catchments.

In the Merced River both the Big Sandy (treatment) and Speckerman (control) catchments responded similarly pre- and post-treatment, but also have similar bedrock compositions of grano-diorite batholith [*Bateman*, 1989]. A slight increase in precipitation of 2 cm (2%) from 2012 to 2013, combined with decreases in ET plus storage of 4 cm (7%) for Big Sandy and 5 cm (8%) for Speckerman, led to runoff increases of 6 cm (26%, Big Sandy) and 7 cm (29%, Speckerman).

High variability in annual precipitation and low post-treatment precipitation resulted in the inability to detect changes in stream discharge following fuel treatments. Bosch and Hewlitt [1982] note that streamflow response to forest treatments depends on mean annual precipitation and treatment year precipitation. Long-term post-disturbance monitoring would be needed to confirm some of the changes in runoff characteristics, as Troendle and King [1985] found increases in peak streamflow decades after a forested catchment was harvested that were not detectable shortly after treatments.

Modeled Water Balance Treatment Effects

Model results of mean annual increased runoff (+14%) and decreased evapotranspiration in Bear Trap (-14%) was unexpected, given the small LAI reduction of 8%. This result indicates that the vegetation in this region of high precipitation is not water limited, and so hydrologic fluxes respond directly to differences in vegetation densities. Although treatments within the Big Sandy watershed were light, lower precipitation rates in this lower-precipitation area may limit responses of runoff and ET to vegetation thinning. Running and Coughlan [1988] show that in Forest-BGC, changes in LAI will scale directly with vegetative water use in areas that are not resource limited (e.g. Bear Trap), but variation in the higher range of LAI may not show a response in more water-limited ecosystems (e.g. Big Sandy). This effect exists because increasing vegetation density in a water-limited region results in higher plant stress simulated with the lower water use, where increasing the vegetation density in a water-rich environment will result in higher use of the available water resource.

Hydro-ecologic model uncertainty originates from observations used for input and calibration, model structure and algorithms, and equifinality of model parameters. The distributed measurements of snow depth and soil moisture are designed to characterize the spatial variability, and thus reduce uncertainty in these observations. The snow-depth surveys completed around the American River upper meteorological station are some indication that we are capturing the local spatial mean of snow depth. Precipitation can be highly variable in mountain regions due to topography, orographic effects, and precipitation phase. Compared to studies in the Kings River basin [*Bales et al.*, 2011;

Goulden et al., 2012; *Hunsaker et al.*, 2012], the closely located Merced sites had similar annual runoff and evapotranspiration rates, but the American showed higher ET associated with the greater vegetation density and precipitation. Although the annual precipitation measured in the American River region was high during the study period, the Blue Canyon meteorological station (5280' elevation, 191 cm yr^{-1} mean precipitation) was within the range of measurements reported by nearby stations including Drum Power House (3400', 159 cm yr^{-1}), Hell Hole (4580', 121 cm yr^{-1}), and Huysink (6600', 216 cm yr^{-1}) [*California Department of Water Resources*, 2015].

Model calibration of snow accumulation and melt timing was challenging as the catchment elevations transition from rain-dominated to snow-dominated precipitation. Using the model to determine the precipitation phase with the temperature-based linear equation to transition from rain to snow resulted in very low snowpack estimates, particularly in the American. Comparing temperature records of the meteorological stations and snow-depth sensors showed that temperatures observed at the meteorological stations may not be representative of the regional elevation. Mean daily winter temperatures recorded at the lower-elevation met station for the American exceeded the maximum daily temperatures recorded in the adjacent valley at times in the winter, and valley maximum temperatures exceeded met-station maximums during the summer (Figure 1.8). Modeled snowfall events were then better simulated in this transitional region by inputting snow and rain precipitation separately, determined on a daily basis by an increase or decrease in the snow depth sensors at each meteorological station. Garcia *et al.* [2013] also showed that met-station location and temperature-interpolation methods can significantly affect the success of model calibration.

Given the potentially high temperature inputs, adjusting temperature-based melt was another possible method to better capture the snow pattern. In using standard met-station data, however, we wanted to maintain the meteorological-station inputs that most model users would have access to, and determine the model adjustments needed based on these standard inputs. Compared to the basin-scale snowpack calibrations completed for this research, Ray *et al.* [in preparation] calibrated annual snow water equivalent using one

station in the Providence Creek to the same spatial location in the model. The Providence Creek model successfully simulated stream discharge using RHESSys for the watershed as well as two adjacent catchments using the same model parameters. The difference in stream-discharge calibration success suggests that snowpack calibration at even one point within the watershed may be an improved method over distributed regional snowpack.

Surface temperatures vary considerably in mountain regions, as much as 10^{o}C on open ground ([*Parker*, 1952] as referenced in the MTN-CLIM manuscript [*Running et al.*, 1987]). Adjustments for LAI and aspect incorporated to the MTN-CLIM meteorological routines by Running *et al.* [1987] attempt to account for these variations, but even the evaluation sites for the meteorological model show a range of seasonal temperature estimates that differed 0.04-3.14^{o}C from observations, despite correlation coefficients consistently around 0.90. At the elevation range of Bear Trap and Big Sandy, where daily mean temperatures are often near the freezing point, even small model temperature offsets can result in the difference between more snow or rain and in temperatures directing the model to transfer incoming energy to the snowpack into snowmelt (lower energy, faster ablation) or sublimation (higher energy, slower ablation). Although we specifically considered spatial variability of snow and soil moisture in these basin, it would also be useful to explicitly capture spatial characteristics of surface temperatures in the future for better temperature-dependent snowmelt simulation in these rain-snow transition elevations. A precipitation gauge that can record both rain and snow events located within the modeled basin, combined with at least one transect of co-located temperature and snow depth sensors on each opposing hillslope would improve model estimates of temperature and snow pattern.

Spatial data uncertainty associated with LiDAR and forest-plot estimates of LAI and canopy cover may also be resulting in higher melt rates when used with RHESSys. Estimations of vegetation cover vary by remote sensing product, and Chen et al. [2004] noted that LiDAR estimates of completely open canopy in 10 m^2 plots were always detected as having some vegetation cover using IKONOS 4-m spectral estimates of forest cover, suggesting shading from trees or scattering from adjacent pixels were causing

detection at the open sites. Assuming LiDAR estimates of open areas are higher than spectral estimates, then snowpack radiation and melt is elevated compared to other remote-sensing estimates. As a result, to capture the snowpack persistence and melt timing observed, we found it necessary to decrease radiation melt to 40% in the model, associated with a mean canopy cover of 50% and 40% in Bear Trap and Big Sandy, respectively.

Further research into the differences of methods used for model input of forest structure are needed (e.g. *Varhola and Coops*, 2013) as remote sensing technology moves towards higher resolution products, with applications to the vegetation-hydrology interface. Estimates of vegetation structure and density not only affect the snowpack processes, but also the magnitude of changes to the water balance when disturbance or growth occurs. Jensen *et al.* [2011] found a 10% average difference between 1-km MODIS and 30-m LiDAR estimates of LAI, increasing to 50% difference in dense vegetation regions (LAI≥5) due to MODIS optical sensor saturation. A 10% LAI difference is greater than any treatment effect on vegetation in this study, and will affect the magnitude of water balance response with increases or decreases in vegetation. Su et al. [2016] have shown that using a combination of ground and remote sensing biomass data can produce a highly correlated ($R^2 = 0.75$) spatial vegetation estimation over a large area, but with a high Root Mean Square Error of 42 Mg ha^{-1} compared to the mean 120 Mg ha^{-1}, a range which would again affect the magnitude of water balance response to vegetation disturbances.

The Monte Carlo parameterization method was used to address issues of parameter equifinality and to create a distribution of model calibration and simulated response to treatments. Bear Trap watershed in the American River had a smaller range of simulation confidence intervals, reflecting the smaller number of parameter sets and smaller range of parameters in acceptable calibrations (Table 1.1, Figure 1.6). Big Sandy watershed in the Merced River had a much wider confidence band, associated with the greater number of acceptable calibrations and greater parameter ranges. The lack of transferable snowpack simulation to the nearby control basins, and unsuccessful adjustment of snowmelt

parameters for stream discharge simulation, shows the challenge of modeling this region on a daily timestep. The majority of discharge occurs in winter and spring, and is driven by intermittent snowmelt periods. Although we achieved acceptable snowpack simulation in the control basins compared to our measurements, the lack of success in streamflow simulations shows the challenge of constraining models to multiple datasets and the need for concentrating distributed measurements within headwater catchments. The precipitation data used, and observations recorded around the ridge meteorological stations near the study watersheds and at the stream outlets may not have accurately represented snow patterns within all headwaters, which was critically for successful daily discharge simulations.

Data-based modeling

Silberstein [2006] argued that improved modeling for water resources and land management cannot exist without improved data collection, "because we cannot manage what we do not measure". The limitations and uncertainties of using models to answer hydrologic questions are well known, yet continue to be used ubiquitously. The approach used in this study, integrating distributed observed datasets to constrain model parameters, produces a confident and verifiable tool for evaluating watershed-scale responses to changes in vegetation. Using multiple datasets for model constraint did not provide the highest model fit for snowpack, stream discharge, or even soil storage that could have been accomplished by calibrating only discharge, but Seibert and McDonnell [2002] comment that lower model fits may be necessary with these types of additional data to produce a better overall model of catchment behavior. The short study-period and high precipitation variability limited the ability of field observations alone to conclusively determine watershed response to fuels treatments. The data-informed modeling, however, provides the ability to evaluate the changes in vegetation over a greater time-period and range of precipitation than was available in the post-treatment year of observation. Thus, modeling can be a useful tool for extending observations, but only provides confident results when constrained by field data.

Conclusions

Model results show that an 8% reduction in vegetation from fuels treatments can result in a 14% runoff increase in high precipitation areas, such as the American River basin. Simulated evapotranspiration and runoff were sensitive to the relatively small changes in vegetation over the range of low to high precipitation rates experienced during the study. Combined with the high precipitation rates in the American River basin, this result suggests that the region is not water limited, or the remaining vegetation would have absorbed the additional water availability.

Modeling tools to evaluate watershed response to fuels treatments were necessary to address the challenges of a short study period and high precipitation variability. Using a spatially distributed dataset of snow and soil moisture observations, we were able to develop a well-constrained model for simulating watershed response to vegetation treatments. The high variability in annual precipitation, combined with low post-treatment precipitation, masked any detectable changes in headwater catchment runoff from fuel treatments. Using this approach of hydrologic modeling, informed by multiple observed datasets, provides a confident and useful tool for evaluating catchment response to changes in vegetation.

References

Agee, J. K., and C. N. Skinner (2005), Basic principles of forest fuel reduction treatments, For. Ecol. Manage., 211(1-2), 83–96, doi:10.1016/j.foreco.2005.01.034.

Armstrong, C. F., and C. K. Stidd (1967), A moisture-balance profile on the Sierra Nevada, J. Hydrol., 5, 258–268, doi:10.1016/S0022-1694(67)80105-7.

Bales, R. C., J. W. Hopmans, A. T. O'Geen, M. Meadows, P. C. Hartsough, P. Kirchner, C. T. Hunsaker, and D. Beaudette (2011), Soil Moisture Response to Snowmelt and Rainfall in a Sierra Nevada Mixed-Conifer Forest, Vadose Zo. J., 10(3), 786, doi:10.2136/vzj2011.0001.

Barry, R. G., and R. J. Chorley (1987), Atmosphere, weather and climate, 5th ed., Routledge, London, UK.

Bateman, P. C. (1989), Geologic map of the Bass Lake quadrangle, west-central Sierra Nevada, California, Geologic Quandrangle Map GQ-1656.

Beven, K. J., and M. J. Kirkby (1979), A physically based, variable contributing area model of basin hydrology, Hydrol. Sci. Bull., 24(1), 43–69.

Biederman, J., A. Harpold, D. Gochis, B. Ewers, D. Reed, S. Papuga, and P. Brooks (2014), Increased evaporation following widespread tree mortality limits streamflow response, Water Resour. Res., 50, 5395–5409, doi:10.1002/2013WR014994.

Bosch, J., and J. Hewlett (1982), A review of catchment experiments to determine the effect of vegetation changes on water yield and evapotranspiration, J. Hydrol., 55, 3–23, doi:10.1016/0022-1694(82)90117-2.

California Department of Water Resources (2015), Precipitation data for Drum Power House, Hellhole, and Huysink stations, Calif. Data Exch. Cent., 10/1/2009–9/302013. Available from: http://cdec.water.ca.gov/ (Accessed 21 October 2015)

Chauvin, G. M., G. N. Flerchinger, T. E. Link, D. Marks, a. H. Winstral, and M. S. Seyfried (2011), Long-term water balance and conceptual model of a semi-arid mountainous catchment, J. Hydrol., 400(1-2), 133–143, doi:10.1016/j.jhydrol.2011.01.031.

Chen, X., L. Vierling, E. Rowell, and T. DeFelice (2004), Using lidar and effective LAI data to evaluate IKONOS and Landsat 7 ETM+ vegetation cover estimates in a ponderosa pine forest, Remote Sens. Environ., 91(1), 14–26, doi:10.1016/j.rse.2003.11.003.

Collins, B. M., R. G. Everett, and S. L. Stephens (2011), Impacts of fire exclusion and recent managed fire on forest structure in old growth Sierra Nevada mixed-conifer forests, Ecosphere, 2(4), 14, doi:10.1890/ES11-00026.1.

Essery, R., J. Pomeroy, C. Ellis, and T. Link (2008), Modelling longwave radiation to snow beneath forest canopies using hemispherical photography or linear regression, Hydrol. Process., 22(15), 2788–2800.

Ffolliott, P. F., G. J. Gottfried, and M. B. Baker (1989), Water Yield From Forest Snowpack Management: Research Findings in Arizona and New Mexico, Water Resour. Res., 25(9), 1999–2007, doi:10.1029/WR025i009p01999.

Finney, M. (2001), Design of regular landscape fuel treatment patterns for modifying fire growth and behavior, For. Sci., 47(2), 219–228.

Fry, D., J. Battles, B. Collins, and S. Stephens (2015), Sierra Nevada Adaptive Management Project Final Report, Appendix A - Fire and Forest Ecosystem Health Report.

Garcia, E. S., C. L. Tague, and J. S. Choate (2013), Influence of spatial temperature estimation method in ecohydrologic modeling in the Western Oregon Cascades, Water Resour. Res., 49(3), 1611–1624, doi:10.1002/wrcr.20140.

Goulden, M. L., R. G. Anderson, R. C. Bales, a. E. Kelly, M. Meadows, and G. C. Winston (2012), Evapotranspiration along an elevation gradient in California's Sierra Nevada, J. Geophys. Res., 117(G3), G03028, doi:10.1029/2012JG002027.

Hicks, B. J., R. L. Beschta, and R. D. Harr (1991), Long-Term Changes in Streamflow Following Logging in Western Oregon and Associated Fisheries Implications, J. Am. Water Resour. Assoc., 27(2), 217–226, doi:10.1111/j.1752-1688.1991.tb03126.x.

Hungerford, R. D., R. R. Nemani, S. W. Running, and J. C. Coughlan (1989), MTCLIM : A Mountain Microclimate Simulation Model; INT-414, Ogden, UT.

Hunsaker, C. T., T. W. Whitaker, and R. C. Bales (2012), Snowmelt Runoff and Water Yield Along Elevation and Temperature Gradients in California's Southern Sierra Nevada1, J. Am. Water Resour. Assoc., 48(4), 667–678, doi:10.1111/j.1752-1688.2012.00641.x.

Jensen, J. L. R., K. S. Humes, A. T. Hudak, L. a. Vierling, and E. Delmelle (2011), Evaluation of the MODIS LAI product using independent lidar-derived LAI: A case study in mixed conifer forest, Remote Sens. Environ., 115(12), 3625–3639, doi:10.1016/j.rse.2011.08.023.

Kattelmann, R. C., N. H. Berg, and J. Rector (1983), the Potential for Increasing Streamflow From Sierra Nevada Watersheds, J. Am. Water Resour. Assoc., 19(3), 395–402, doi:10.1111/j.1752-1688.1983.tb04596.x.

Kerkez, B., S. D. Glaser, R. C. Bales, and M. W. Meadows (2012), Design and performance of a wireless sensor network for catchment-scale snow and soil

moisture measurements, Water Resour. Res., 48(9), 1–18, doi:10.1029/2011WR011214.

Kittredge, J. (1953), Influences of forests on snow in the ponderosa-sugar pine-fir zone of the Central Sierra Nevada, Hilgardia, 22(1), 1–96.

Lawler, R. R., and T. E. Link (2011), Quantification of incoming all-wave radiation in discontinuous forest canopies with application to snowmelt prediction, Hydrol. Process., doi:10.1002/hyp.8150.

Liu, F., C. Hunsaker, and R. C. Bales (2013), Controls of streamflow generation in small catchments across the snow-rain transition in the Southern Sierra Nevada, California, Hydrol. Process., 27(14), 1959–1972, doi:10.1002/hyp.9304.

Lundquist, J. D., S. E. Dickerson-Lange, J. a. Lutz, and N. C. Cristea (2013), Lower forest density enhances snow retention in regions with warmer winters: A global framework developed from plot-scale observations and modeling, Water Resour. Res., 49(4), n/a–n/a, doi:10.1002/wrcr.20504.

Marvin, S. (1996), Possible changes in water yield and peak flows in response to forest management, in Sierra Nevada Ecosystem Project: Final Report to Congress, vol. 101, pp. 154–199.

Moore, G. W., B. J. Bond, J. a Jones, N. Phillips, and F. C. Meinzer (2004), Structural and compositional controls on transpiration in 40- and 450-year-old riparian forests in western Oregon, USA., Tree Physiol., 24(5), 481–91.

Nash, J. E., and J. V Sutcliffe (1970), River flow forecasting through conceptual models part I --- A discussion of principles, J. Hydrol., 10(3), 282–290.

North, M., J. Innes, and H. Zald (2007), Comparison of thinning and prescribed fire restoration treatments to Sierran mixed-conifer historic conditions, Can. J. For. Res., 37(2), 331–342, doi:10.1139/X06-236.

Parker, J. (1952), Environment and Forest Distribution of the Palouse Range in Northern Idaho, Ecology, 33(4), 451–461.

Rowe, P., and T. Hendrix (1951), Interception of rain and snow by second-growth ponderosa pine, Trans. Aermican Geophys. Uion, 32(6), 903–908.

Running, S., and J. Coughlan (1988), A General Model of Forest Ecosystem Processes for regional applications I. Hydrologic balance, canopy gas exchange and primary production processes., Ecol. Modell., 42, 125–154.

Running, S. W., and E. R. Hunt (1993), Generalization of a forest ecosystem process model for other biomes, BIOME-BGC, and an application for global-scale models, in Scaling physiological processes: leaf to globe, edited by J. R. Ehleringer and C.

B. Field, pp. 141–158, Academic Press, San Diego.

Running, S. W., R. R. Nemani, and R. D. Hungerford (1987), Extrapolation of synoptic meteorological data in mountainous terrain and its use for simulating forest evapotranspiration and photosynthesis, Can. J. For. Res., 17(6), 472–483.

Saucedo, G. J., and D. L. Wagner (1992), Geologic Map of the Chico quadrangle, Regional Geologic Map 7A.

Seibert, J., and J. J. McDonnell (2002), On the dialog between experimentalist and modeler in catchment hydrology: Use of soft data for multicriteria model calibration, Water Resour. Res., 38(11), 23, 1–14, doi:10.1029/2001WR000978.

Silberstein, R. P. (2006), Hydrological models are so good, do we still need data?, Environ. Model. Softw., 21(9), 1340–1352, doi:10.1016/j.envsoft.2005.04.019.

Soil Survey Staff, . (2011), Soil Survey Geographic (SSURGO) Database.

Stednick, J. (1996), Monitoring the effects of timber harvest on annual water yield, J. Hydrol., 176(1-4), 79–95, doi:10.1016/0022-1694(95)02780-7.

Storck, P., D. P. Lettenmaier, and S. M. Bolton (2002), Measurement of snow interception and canopy effects on snow accumulation and melt in a mountainous maritime climate, Oregon, United States, Water Resour. Res., 38(11), 1123.

Su, Y., Q. Guo, B. Xue, T. Hu, O. Alvarez, S. Tao, and J. Fang (2016), Spatial distribution of forest aboveground biomass in China: Estimation through combination of spaceborne lidar, optical imagery, and forest inventory data, Remote Sens. Environ., 173, 187–199, doi:10.1016/j.rse.2015.12.002.

Sun, G., P. V. Caldwell, and S. G. McNulty (2015), Modeling the potential role of forest thinning in maintaining water supplies under a changing climate across the Conterminous United States, Hydrol. Process., n/a–n/a, doi:10.1002/hyp.10469.

Swank, W., J. Vose, and K. Elliott (2001), Long-term hydrologic and water quality responses following commercial clearcutting of mixed hardwoods on a southern Appalachian catchment, For. Ecol. Manage., 143, 163–178, doi:10.1016/S0378-1127(00)00515-6.

Tague, C., and G. E. Grant (2004), A geological framework for interpreting the low-flow regimes of Cascade streams, Willamette River Basin, Oregon, Water Resour. Res., 40(4), 1–9, doi:10.1029/2003WR002629.

Tague, C. L., and L. E. Band (2004), RHESSys: Regional Hydro-Ecologic Simulation System—An Object-Oriented Approach to Spatially Distributed Modeling of Carbon, Water, and Nutrient Cycling, Earth Interact., 8(19), doi:http://dx.doi.org/10.1175/1087-3562(2004)8<1:RRHSSO>2.0.CO;2.

Troendle, C. A., and R. M. King (1985), The effect of timber harvest on the Fool Creek watershed, 30 years later, Water Resour. Res, 21(12), 1915–1922.

Troendle, C. A., M. S. Wilcox, G. S. Bevenger, and L. S. Porth (2001), The Coon Creek Water Yield Augmentation Project: implementation of timber harvesting technology to increase streamflow, For. Ecol. Manage., 143, 179–187, doi:10.1016/S0378-1127(00)00516-8.

Varhola, A., and N. C. Coops (2013), Estimation of watershed-level distributed forest structure metrics relevant to hydrologic modeling using LiDAR and Landsat, J. Hydrol., 487, 70–86, doi:10.1016/j.jhydrol.2013.02.032.

Wayman, R. B., and M. North (2007), Initial response of a mixed-conifer understory plant community to burning and thinning restoration treatments, For. Ecol. Manage., 239(1-3), 32–44, doi:10.1016/j.foreco.2006.11.011.

Whitehead, D., and F. M. Kelliher (1991), A canopy water balance model for a {\em Pinus radiata} stand before and after thinning, Agric. For. Meteo., 55, 109–126, doi:10.1016/0168-1923(91)90025-L.

Whitehead, D., P. G. Jarvis, and R. H. Waring (1984), Stomatal conductance, transpiration, and resistance to water uptake in a Pinus sylvestris spacing experiment, Can. J. For. Res., (14), 692–700.

Wigmosta, M. S., L. W. Vail, and D. P. Lettenmaier (1994), A distributed hydrology-vegetation model for complex terrain, Water Resour. Res., 30(6), 1665, doi:10.1029/94WR00436.

Zhang, L., W. R. Dawes, and G. R. Walker (2001), Response of mean annual evapotranspiration to vegetation changes at catchment scale, Water Resour. Res., 37(3), 701–708.

Zou, C. B., P. F. Ffolliott, and M. Wine (2010), Streamflow responses to vegetation manipulations along a gradient of precipitation in the Colorado River Basin, For. Ecol. Manage., 259(7), 1268–1276, doi:10.1016/j.foreco.2009.08.005.

Table 1.1. Calibrated parameter ranges for Bear Trap and Big Sandy catchments. Streamflow statistics of Nash-Sutcliffe Efficiency (NS_e>0.6) and log-transformed NS_e ($logNS_e$>0.6) were used to determine acceptable parameter sets.

Parameter	Description	Range	Bear Trap	Big Sandy
m	decay of hydraulic conductivity, dimensionless	0 - 20	5.6 – 12.3	0.6 – 19.9
k	hydraulic conductivity, m day^{-1}	0 - 300	2.0 – 6.6	5 - 294
svk	vertical hydraulic conductivity, m day^{-1}	0 - 300	7 – 250	2 – 294
po	soil pore size index, dimensionless	0 - 3	1.4 – 3.0	0.1 – 3.0
pa	soil air entry pressure, m	0 - 3	0.6 – 2.6	0.2 – 2.9
gw1	groundwater bypass flow, dimensionless	0 - 0.4	0.0 – 0.15	0.2 – 0.4
gw2	groundwater to stream, dimensionless	0 - 0.4	0.0 – 0.01	0.1 – 0.4
NS_e	Nash-Sutcliffe Efficiency (NS_e)	-∞ - 1	0.60 – 0.64	0.67 – 0.78
$logNS_e$	log-transformed Nash-Sutcliffe Efficiency ($logNS_e$)	-∞ - 1	0.75 – 0.84	0.62 – 0.70

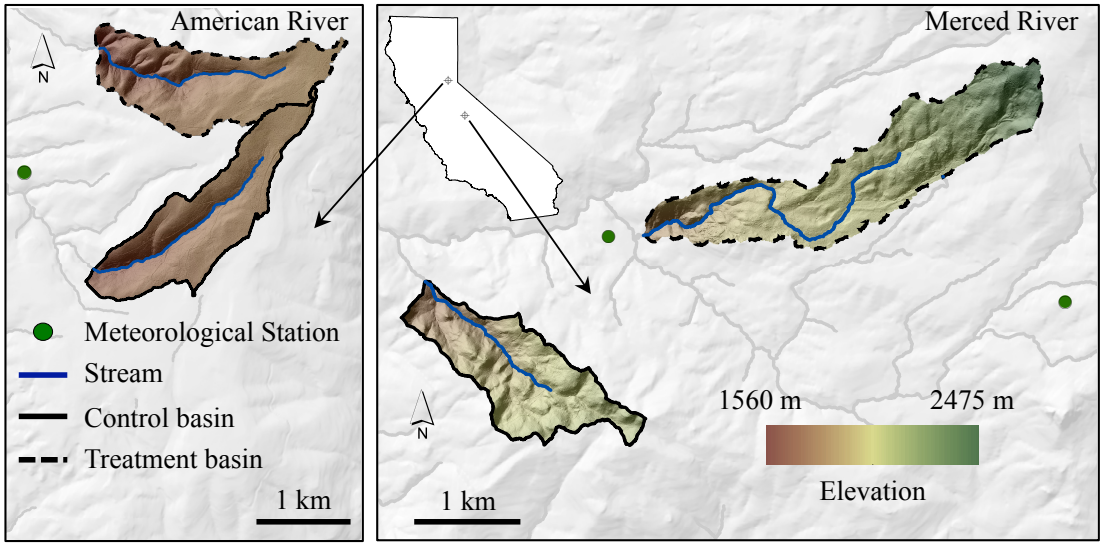

Figure 1.1. Locations of the headwater research catchments in the American and Merced River basins. The upper elevation meteorological station in the American is located off the map to the north of the basins, and the color elevation band applies to all catchments.

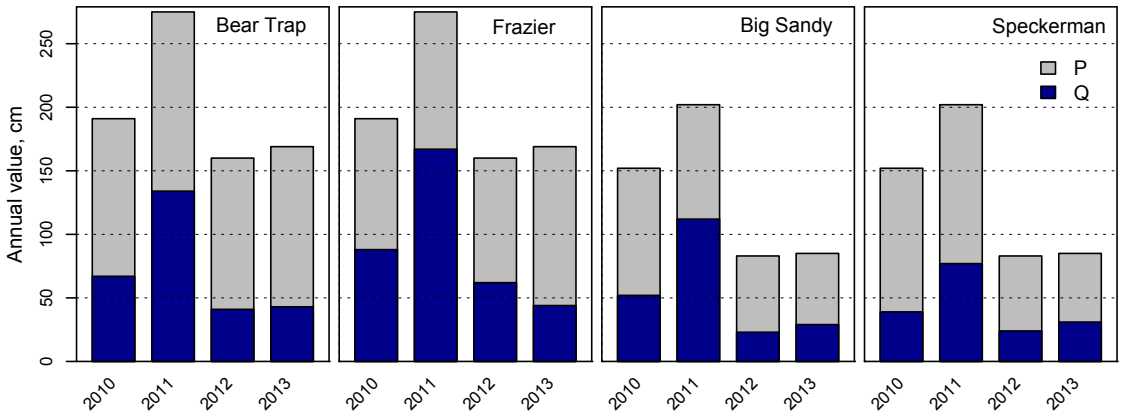

Figure 1.2. Interannual variability of precipitation (P) and runoff (Q) observed during the four-year study. Precipitation rates are the same for Bear Trap and Frazier in the American River and for Big Sandy and Speckerman in the Merced River. Years 2010 to 2012 are pre-treatment and 2013 is the post-treatment year.

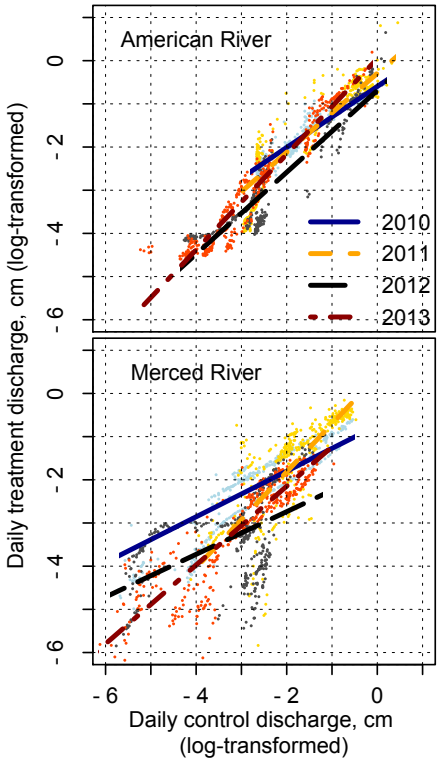

Figure 1.3. Log-transformed daily stream runoff in the American and Merced River headwater catchments by water year. Treatment and control discharge was significantly different in all years (F-test, $p<0.05$), including before (2010-2012) and after (2013) treatment.

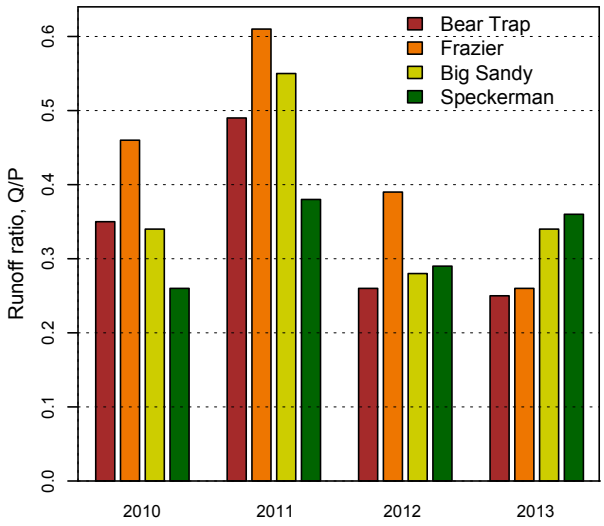

Figure 1.4. Runoff ratios for each year and headwater catchment, defined as the fraction of precipitation that leaves the catchment by runoff. Precipitation rates are the same for Bear Trap and Frazier in the American River and the same for Big Sandy and Speckerman in the Merced River. Years 2010 to 2012 are pre-treatment and 2013 is the post-treatment year.

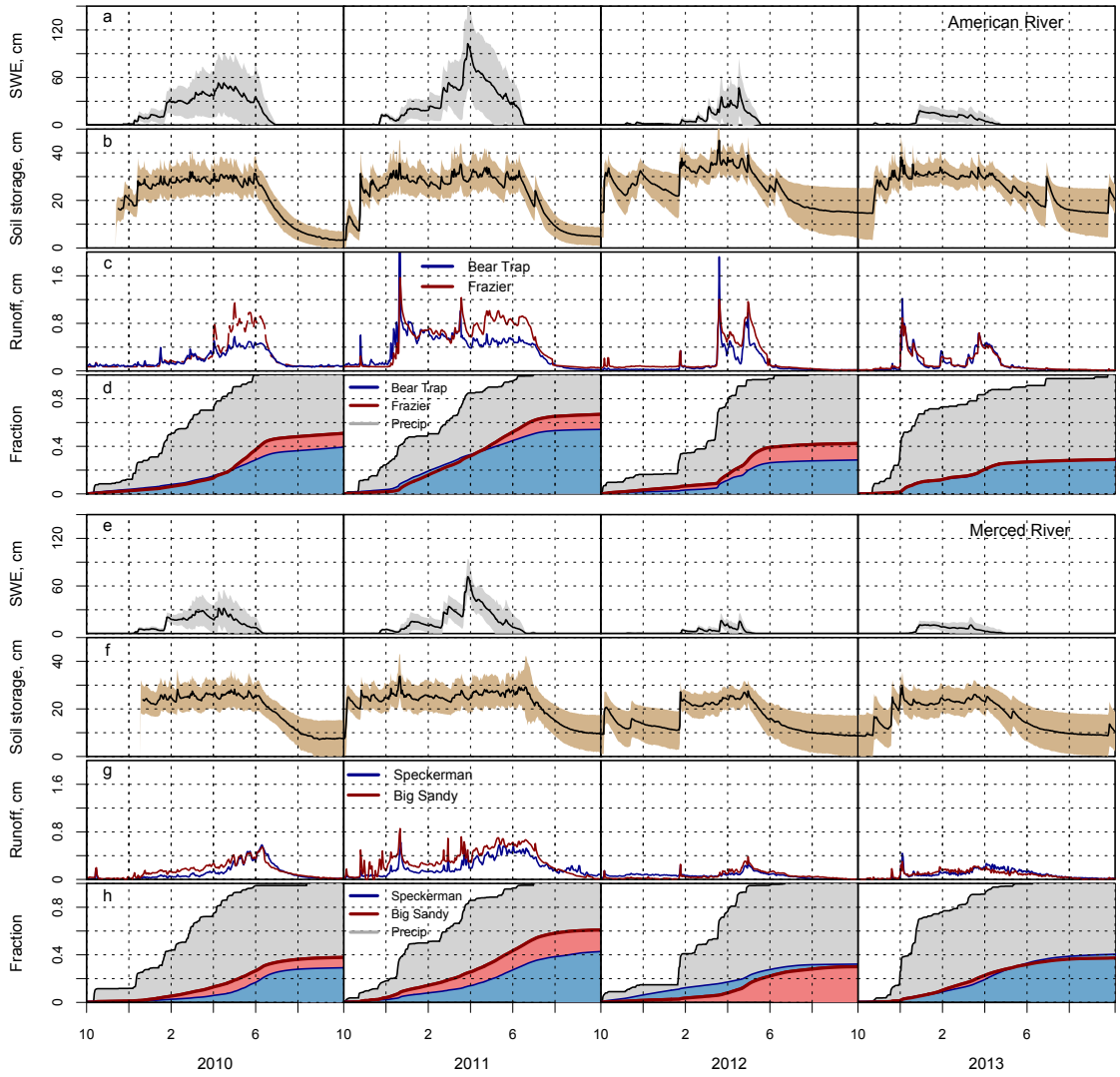

Figure 1.5. Daily snow water equivalent (SWE) (a,e), soil storage (b,f), and runoff (c,g) observations for the American and Merced River sites during water years 2010-2013. Black lines show mean of distributed observations; shaded area shows one standard deviation. Cumulative precipitation and runoff are also shown as a fraction of precipitation for each year (e,h).

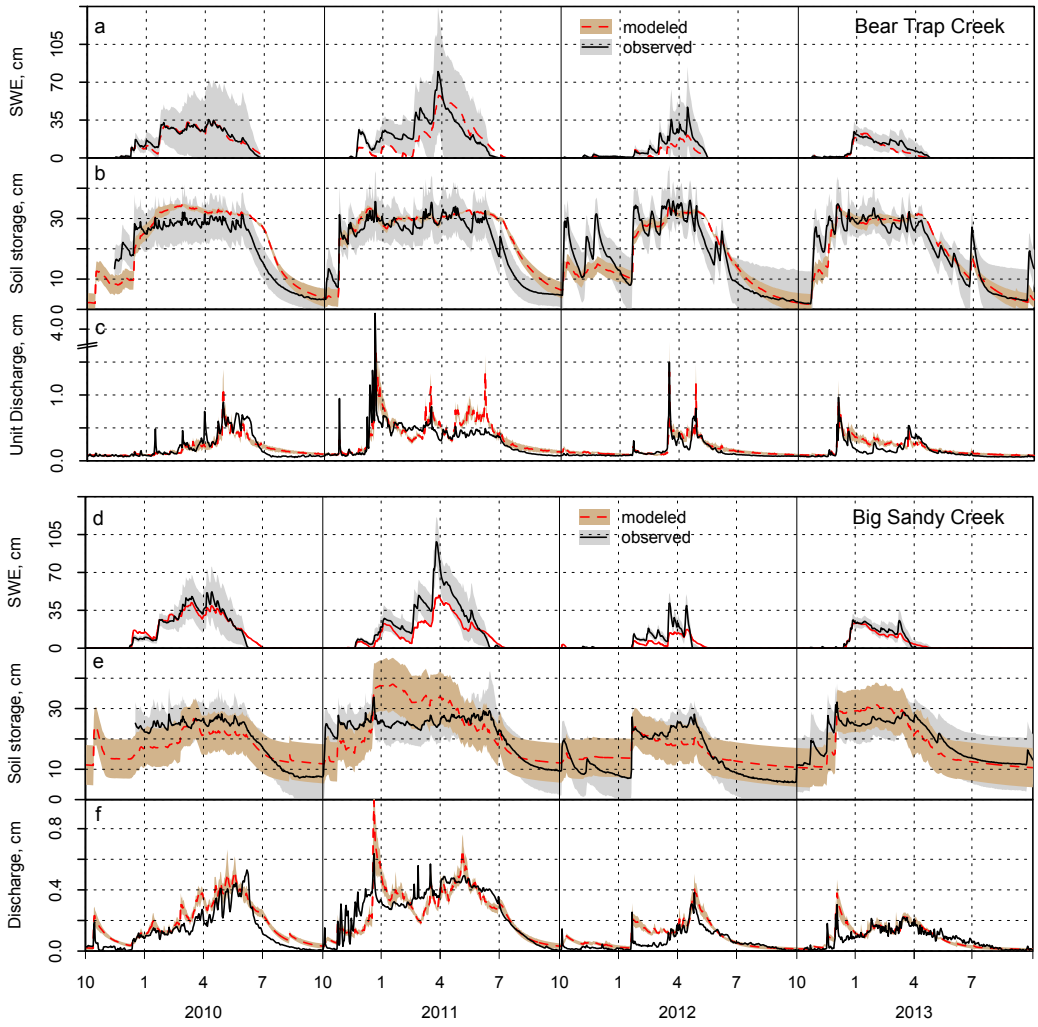

Figure 1.6. Model daily output of snow water equivalent (SWE) (a,d), root zone soil storage in the top 1-m (b,e), and stream discharge (c,f) compared to mean observation values in Bear Trap (top panel) and Big Sandy (bottom panel) catchments. Shaded areas represent one standard deviation from the mean, with model mean and standard deviations from the sets of calibrated parameters.

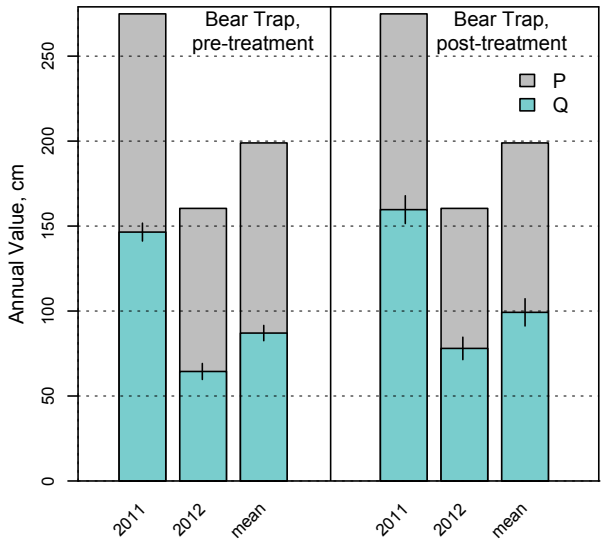

Figure 1.7. Modeled treatment effects on the water balance in Bear Trap over the range of observed annual precipitation (P) rates, including the mean from all four years of observations (2010-2013). Vertical bars indicate 95% confidence intervals of simulated annual runoff (Q).

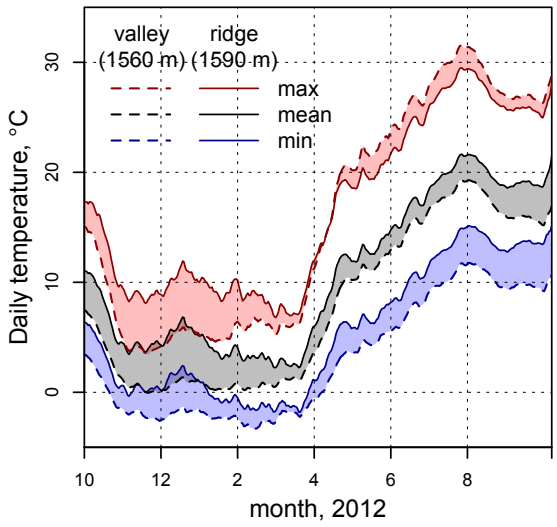

Figure 1.8. Distributed sensors show ridge temperatures recorded at the met station used for hydrological model input may not capture the temperature characteristics recorded by the snow depth sensor in the valley. Temperature inputs drive the model snow accumulation and melt processes, which can be challenging to simulate at the rain/snow transitional elevations. The ridge meteorological station sensor is at 1590 m and the valley snow depth sensor is at 1560 m. Shaded areas highlight the temperature differences and daily values are smoothed using a running 30-day mean.

Chapter 2: Forest fuels treatment and wildfire effects on Sierra Nevada mixed-conifer runoff

Abstract

We used an eco-hydrologic model (RHESSys) calibrated with spatially distributed field measurements to assess the impacts of forest fuels treatments and wildfire on hydrologic fluxes in Sierra Nevada firesheds. Fuels treatments were implemented during 2011-2012 in the American River and Lewis Fork watersheds. This study uses the measured vegetation change from treatments and the results from wildfire modeling of vegetation change to determine impacts on catchment water balance. A well-constrained headwater model is used to determine how annual hydrologic fluxes respond to vegetation changes from treatments and fires in these larger firesheds, based on geologic and hydrologic similarities. Treatments in the American River resulted in a vegetation decrease of 8%, leading to a 13% runoff increase. Wildfire with and without treatments reduced vegetation by 38% and 50%, increasing runoff by 55% and 67%, respectively. Treatments in Lewis Fork also reduced vegetation by 8%, but the runoff response was limited to an increase of less than 3% compared to no treatment. Wildfire with and without treatments reduced vegetation by 40% and 43%, increasing runoff by 13% and 15% respectively. The results suggest that forest vegetation in Lewis Fork is more water-limited than in the American, where treatments had a greater impact on the water balance. Changes to catchment-scale water balance simulation were more sensitive to canopy cover than Leaf Area Index, indicating the pattern and location of vegetation treatments is more important than the total amount of biomass removed.

Introduction

The risk of high-intensity wildfire in the Sierra Nevada is increasing [*Miller et al.*, 2009] because of changes in climate [*Westerling et al.*, 2006] and high vegetation densities compared to the previous century [*Collins et al.*, 2011b]. There is a need to restore the resiliency of the forest to pressures of climate and wildfire by applying localized integrated management [*Stephens et al.*, 2013]. The collective impacts of forested-watershed management, wildfire, and climate will modify the responses of evapotranspiration and runoff in these mountain catchments. As the major source of California's annual water supply [*CA Department of Water Resources*, 2013], predicting the changes in Sierra Nevada runoff in response to forest vegetation management, disturbance, and growth is a priority.

Fuels treatments can be used in Sierra Nevada mixed-conifer forest to reduce wildfire hazard [*Stephens*, 1998; *Stephens and Moghaddas*, 2005], but Collins *et al.* [2011a] showed the effectiveness of fuels treatments on burn probabilities was reduced after 20 years of regrowth. Runoff response to fuels treatments depends on the pattern and magnitude of prescribed fire [*Robichaud and Waldrop*, 1994; *Robichaud*, 2000; *Fernandez et al.*, 2008], shrub removal [*Fernandez et al.*, 2008], and thinning [*Robles et al.*, 2014]. The runoff response to wildfire depends on similar characteristics, such as location in the catchment, fire intensity, and fire severity [*Ice et al.*, 2004]. The rate of vegetation regrowth will affect long-term runoff effects [*Potts et al.*, 2010; *Hawthorne et al.*, 2013]. Shakesby and Doerr [2006] note that post-fire runoff research at the watershed scale tends to focus on changes to peak flows and erosion potential more than on water yield.

The application of hydrologic modeling to ungauged basins has been the subject of much recent study [*Sivapalan*, 2003; *Wagener and Montanari*, 2011; *Hrachowitz et al.*, 2013], given the increasing use of modeling tools and decreasing emphasis on measurements in hydrology [*Silberstein*, 2006]. One approach for modeling basins lacking observations has been to transfer model parameters from another instrumented basin [*van der Linden and Woo*, 2003; *Heuvelmans et al.*, 2004; *Bárdossy*, 2006]. There

are a number of attributes that can be considered when regionalizing model parameters from gauged basins, including spatial proximity, physical similarity, and regression of model parameters and physical characteristics [*Merz and Blöschl*, 2004; *Bao et al.*, 2012]. Studies comparing the methods have noted that parameters of some gauged (donor) basins can be completely transferred to ungauged (receiver) watersheds based on spatial proximity and hydrologic similarity [*Kokkonen et al.*, 2003; *Parajka et al.*, 2005], which eliminates the necessary assumption of linearity associated with the regression method [*Parajka et al.*, 2005].

The U.S. Forest Service, the largest public land manager in the Sierra Nevada, has undertaken efforts to incorporate adaptive management into the institution's land management practices [*e.g. Bormann et al.*, 1994, 2007]. One of these land-management approaches, Strategically Placed Landscape Treatments (SPLATs; Bahro and Barber, 2004), are fuels treatments designed to disrupt fire paths and reduce overall fire severity. The Sierra Nevada Adaptive Management Project [SNAMP, UC Science Team 2015] was initiated to study the effect of SPLATs on forest health, wildfire, wildlife, and hydrology with the goal of producing scientific research results that would enable the Forest Service to assess and improve management practices.

Development of forest-management strategies should incorporate water yield into the management framework [*Adams*, 2013]. Explicit quantification and verification of water-balance response to vegetation management and disturbance is required, however, in order for management of forests and water to succeed. Development of regional prediction and verification tools are also needed to transfer observed hydrologic conditions to unmonitored firesheds and projected forest-vegetation conditions. The objectives of this study were to: 1) estimate the effects of implemented SPLATs and modeled wildfires on the fireshed water-balance, 2) determine the factors controlling fireshed-scale hydrologic response to changes in vegetation, and 3) assess the transferability of a well-calibrated headwater catchment hydrologic model (1-3 km^2) to scales of fire-management projects (firesheds, 10-25 km^2).

Methods

This study was completed in the larger framework of the Sierra Nevada Adaptive Management Project [SNAMP; Hopkinson and Battles, 2015], a multi-faceted research and assessment component of a prototype adaptive-management program carried out by Region 5 of the U.S. Forest Service. The study design for the hydrologic component of SNAMP was to intensively monitor headwater-scale catchments to develop a watershed model grounded in distributed observations. We then transfer the calibrated headwater model to assess watershed response to vegetation growth and disturbance at the fireshed scale. A fireshed generally spans thousands of acres, and is determined by landscape fire characteristics such as regime, history, risk, and potential behavior [*Bahro and Barber*, 2004].

Study site and treatments

Paired headwater catchments in the American River (central Sierra) and Merced River (southern Sierra) SNAMP study sites (Figure 2.1) were instrumented with snow-depth, soil-moisture, meteorological and stream-discharge sensors for water-balance estimation, using the Regional Hydro-Ecologic Simulation System (RHESSys) to integrate data [*Chapter 1, this document*]. The stream outlets draining the firesheds were not gaged due to the remote and steep terrain. The only monitored stream-discharge site directly downstream from the firesheds drains the entire North Fork of the Middle Fork of the American River.

The American catchments are underlain by upper-elevation Miocene-Pliocene volcanic and lower-elevation sedimentary bedrock of the Shoo Fly complex [*Saucedo and Wagner*, 1992]. The bedrock underlying the Merced & Lewis Fork catchments consists of plutonic Early Cretaceous Bass Lake Tonalite [*Bateman*, 1989]. Fireshed elevations range from 490 m to 2190 m, transitioning from rain- to snow-dominated precipitation. Vegetation communities are mainly comprised of mixed-conifer forests.

SPLATs were implemented in the fall of 2012 by the local forest districts in accordance with the record of decision for the Sierra Nevada Forest Plan Amendment

[*USDA*, 2004]. Vegetation removal was concentrated in 25% and 32% of the American and Lewis study firesheds, respectively. Fuels treatments consisted of forest thinning by removing a fraction of the trees below 76.2 cm diameter at breast height, mastication and prescribed ground burning. Changes in forest vegetation were determined by differences in Leaf Area Index (LAI), canopy cover, and shrub cover calculated from LiDAR and vegetation-plot data collected before and after treatments. Overstory LAI was calculated using the data in Jones *et al.* [2015] based on specific leaf area, species, and vegetation community type (Appendix Tables A2.1, A2.2).

Vegetation-management scenarios

For each scenario, we used the four years of observed meteorological inputs (water years 2010-2013) to produce a mean annual value of surface runoff, evapotranspiration, and subsurface outflow. Model runs were conditioned for two water years (2008-2009) using the individual scenario vegetation maps before simulating hydrologic responses, removing the effects of gradually transitioning between vegetation states. Four vegetation scenarios were considered: an untreated forest, a forest with SPLATs implemented, an untreated forest followed by wildfire, and a forest with SPLATs implemented followed by wildfire. Fire simulations and projected vegetation growth for 30 years were completed by Fry *et al.* [2015], using the Forest Vegetation Simulator [FVS, *Dixon*, 2002] and FlamMap [*Finney*, 2006]. A point-in-time snapshot of the vegetation conditions was captured at 0, 10, 20, and 30 years.

The four years of meteorological observations were simulated for each vegetation condition to capture the range of dry to wet precipitation conditions that occurred during this study. Post-fire vegetation scenarios start at 10 years, allowing for a decade of growth following the simulated wildfire events, and avoid issues such as soil hydrophobicity, reduced soil infiltration capacity, and diminished litter cover that can occur immediately after fire. We differed from the exact FVS scenarios by adding in the shrub cover using the linear relationship equations [Chapter 1] because understory vegetation can be an important additional source of transpiration loss following disturbance.

RHESSys Model

The Regional Hydro-Ecologic Simulation System is a watershed model with the ability to incorporate implicit [TOPMODEL; *Beven and Kirkby*, 1979] and explicit [DHSVM; *Wigmosta et al.*, 1994] flow routing. Tague and Band [2001] discuss the advantage of explicit routing in portraying seasonal shifts of soil moisture and drainage patterns at the expense of the computation efficiency associated with implicit routing. We use an explicit routing approach for the vegetation scenario simulations, given the strong seasonality of the Mediterranean climate and abundance of available spatial data for the study area. Model calibration in the American headwater was completed in a sub-catchment of the fireshed, and in Lewis Fork was completed in a nearby headwater of the adjacent Merced River basin. Radiation melt fraction was reduced to 0.40 in the headwater models match the observed snowpack, but was increased to 1.0 in these fireshed catchments to match the melt-out date of the headwater catchments.

Modeling the impact of vegetation on catchment water balance is focused on the following equations, reproduced from Tague and Band [2004]. LAI is split into sunlit and shaded fractions, based on the photosynthesis model of Chen *et al.* [1999].

$$LAI_{proj_{sunlit}} = 2.0 \times \cos(\theta_{noon}) \times \left[1.0 - exp^{(-0.5)(1-GF)(LAI_{proj})/\cos(\theta_{noon})}\right] \quad [1]$$

$$LAI_{proj_{shade}} = LAI_{proj} - LAI_{proj_{sunlit}} \quad [2]$$

where $LAI_{proj_{sunlit}}$ is the projected sunlit LAI, θ_{noon} is the solar angle at noon, *GF* is the canopy gap fraction, *LAIproj* is the projected total LAI, and $LAI_{proj_{shade}}$ is the projected shaded LAI.

LAI and vegetation cover modify snowmelt rates by changing the amount of net surface radiation impacting the snowpack (Equations 4-6), and on a smaller magnitude change interception and evaporation rates. Transpiration rates were modified as limitations on maximum stomatal conductance, with LAI used to scale transpiration up to the landscape patch (Equation 3; Jarvis, 1976). The limitations of stomatal conductance for sunlit and shaded canopy were calculated as linear scalars

$$gs = f(ppfd)f(CO_2)f(LWP)f(vpd)(LAI)(gs_{max}) \quad [3]$$

where *gs* is stomatal conductance (m s^{-1}), *ppfd* is photosynthetic flux density, CO_2 is carbon dioxide concentration, *LWP* is leaf water potential, *vpd* is vapor pressure deficit, and gs_{max} is maximum conductance. The surface energy balance for snowmelt is affected by a Beer's law approximation of the amount of incoming shortwave radiation (Equations 4,5), combined with longwave radiation (Equation 6). Incoming direct and diffuse shortwave radiation are calculated as

$$K_{direct} = (1 - \propto_{direct})K_{direct'}(1 - corr\ exp^{-ext_{coef}}) \quad [4]$$

$$K_{diffuse} = (1 - \alpha_{direct})K_{diffuse'}\{1 - exp^{-[(1-GF)PAI]^{0.7}} + S_c\} \quad [5]$$

where α_{direct} is the vegetation-specific albedo, K_{direct}' and $K_{diffuse}$' are the direct and diffuse solar radiation at the top of each vegetation layer, *corr* is an option correction factor for low sunlight angles with sparse canopy, ext_{coef} is the Beer's Law extinction coefficient, *GF* is the canopy gap fraction, *PAI* is the plant area index, and S_c is the scattering coefficient. Longwave radiation was calculated as

$$L = 41.868[ess_{atm}\sigma(T_{air} + 272)^4 - 663] \quad [6]$$

where ess_{atm} is the emissivity of the atmosphere , σ is the Stefan-Boltzmann constant, and T_{air} is the air temperature (*K*).

Results

Vegetation scenarios

Modeled scenarios in the American range from 3.5 to 11.1 LAI, over which mean canopy cover increased from 43% to 78%. The vegetation scenarios modeled in Lewis Fork are between 5.2 and 10.5 LAI, where the mean canopy cover is maintained between 70% and 80%. Implementation of SPLATs in the American resulted in a LAI decrease of 8.0% over the treated fireshed area; SPLATs in Lewis Fork resulted in a LAI decrease of 7.5% in the fireshed.

Model simulations for the American show the SPLATs increased runoff 12.3%, a statistically significant increase using a 95% confidence interval calculated from the multiple parameters sets, with smaller decreases in both evapotranspiration and subsurface outflow (Figure 2.2). The reduced ET increases soil saturation and associated hydraulic conductivity, routing more of the excess soil infiltration to runoff and leaving less precipitation available to percolate through to subsurface bypass flow. Although decreases in evapotranspiration were relatively small, corresponding increases in runoff were larger because it is a smaller fraction of precipitation. After 10 years of vegetation regrowth following SPLATs, runoff returned to initial pre-treatment levels. Vegetation growth following both no treatment and SPLATs resulted in trends of increasing subsurface flow over the entire growth period, but were only significant at the 95% confidence interval at 20 and 30 years of growth in the pre-treatment scenario, and at the 30-year interval for the treatment. Runoff increases from treatment were maintained at the significance level up to 20 years, but were not significantly higher by year 30. Model simulations of evapotranspiration in the American showed no significant differences between the treatment scenarios for any of the regrowth intervals. Model simulations for Lewis Fork show the SPLATs resulted in no significant differences to the initial mean annual water balance (Figure 2.2e-g). Evapotranspiration was constant for the entire period of vegetation growth, with a no significant differences in the decreasing trend of runoff and increasing trend of subsurface outflow.

Fire modeled on the American in the treatment and no treatment vegetation densities, followed by 10 years of vegetation growth, resulted in a 38.1% and 49.8% reduction in LAI respectively (Figure 2.2e). Fire modeled on Lewis Fork in the treatment and no

treatment vegetation densities, followed by 10 years of vegetation growth, resulted in a 39.5% and 42.5% reduction in LAI respectively (Figure 2.2h). This reflects the success of the SPLATs in reducing fire intensity for the American catchments, leading to reduced vegetation mortality. Compared to no treatment, both fire scenarios resulted in lower ET, higher runoff, and lower groundwater infiltration at all of the regrowth intervals: 10, 20, and 30 years. No differences in groundwater existed between the fire scenarios, but ET was lower in years 10 and 20 for the fire without treatment, and runoff was higher in all years simulated. The response of runoff and groundwater in both fire scenarios were the same, with all time intervals resulting in higher runoff and lower groundwater compared to pre-treatment vegetation conditions. Evapotranspiration showed no response to any of the variability in vegetation densities between fire or treatment model scenarios or regrowth intervals.

Model sensitivity

The sensitivity of the RHESSys water-balance response to changes in LAI and canopy cover was assessed to determine controlling factors of model vegetation structure on water balance components. Pre-treatment LAI and canopy cover were each increased and reduced by 50%, similar to the highest magnitude of vegetation change, to measure water balance response to the individual changes in vegetation structure (Figure 2.3). Changes in LAI had lower magnitude effects on the water balance in comparison to changes in canopy cover. Both LAI and canopy cover had smaller impacts on snowpack and soil storage, but canopy cover changes impacted evapotranspiration and runoff extensively. The runoff response in the American was much more sensitive to changes in canopy cover than Lewis Fork, because of the higher precipitation and evapotranspiration.

Water-balance partitioning of precipitation into evapotranspiration, runoff, and subsurface outflow were assessed for conditions over the observed period (water years 2010-2013), and reported here as a mean fraction of precipitation with a 95% confidence interval. Initial assessment of water balance response to changes in vegetation are made without regard to specific management scenarios to determine overarching responses to

catchment-scale changes in vegetation (Figure 2.4). Changes in catchment-scale vegetation are also simulated by uniform incremental increases and decreases in LAI or canopy cover, from 50% to 150%. Canopy cover becomes saturated at 100%, resulting in more-limited LAI changes as more of the catchment reaches complete canopy cover.

In the American catchments, vegetation changes in the modeled scenarios mimics the pattern of canopy cover changes, where in the Lewis Fork catchments the vegetation change follows the pattern of LAI. The difference in the responses can be attributed to the individual vegetation structures in each catchment, and the range of modeled LAI values. Comparing the co-located LAI and canopy cover values from the vegetation layer, the American catchments have a forest structure where canopy cover increases continuously over the range of mapped LAI values (0-15), but in the Lewis Fork catchment canopy increases sharply between 0.0 and 4.0 LAI and becomes saturated above an LAI of 6.0 (Figure 2.5).

Model transferability

Within the framework of RHESSys, stream discharge at the outlet of the modeled watershed is normally used to determine the best-fit parameter sets for subsurface bypass flow. Tague et al. [2013] assessed the ability of RHESSys to function in ungauged basins. The authors demonstrated that the calibration parameters are specifically focused on modeling a simplistic groundwater system, and that the values of these parameters depend on the bedrock geology. Bedrock geology is similar within the Merced headwater and Lewis Fork study sites. Both basins are dominated by the same grano-diorite batholith, with less than 1% of each basin represented by crystalline metamorphic rock [*Bateman*, 1989]. These geologic units have been assumed to have similar hydrogeologic behavior, with insignificant amounts of water entering deep storage and flowing into streams [*Clow et al.*, 2003].

The American basin headwater catchment contains 69% of the Shoo Fly Complex and 31% of the volcanic pyroclasts, with the fireshed having 74% and 26% of the respective geologies. Due to metamorphosis, the Shoo Fly Complex can be assumed to be

highly crystalline and thus have minimal groundwater flow [*Clow et al.*, 2003]. Tague and Grant [2004] have shown that volcanic deposits can either have a significant groundwater component or act similarly to crystalline bedrock, depending on the amount of weathering the deposits have experienced. Although there are two possible hydrologic characteristics of volcanics, the headwater catchment is nested within the fireshed, and overlie the same continuous bedrock compositions. Therefore, based on the work of Tague et al. [2013], we suggest that the calibration parameter sets from the headwater models can be used directly in the fireshed models.

Discharge from the headwater basins was compared to discharge data from the closest available sites downstream of the firesheds. In the American, data from the North Fork of the Middle Fork of the American River (unpublished data, courtesy of the Placer County Water Agency) was used for comparison. In the Lewis Fork, discharge data were available directly downstream (unpublished data, courtesy of the California Department of Water Resources), however data from the gauging site were only available for 2012 and 2013. Fuels treatments were also implemented in 2011 and 2012, so there may be some influence of treatments in the comparisons. Runoff timing controls annual values, so the area-normalized discharge was compared using cumulative fractions of precipitation to compare timing and in absolute values to determine annual rates (Figure 2.6).

The cumulative discharge of headwater and downstream sites for both the American and Lewis Fork catchments exhibit high correlation coefficients (>0.90), indicating similar runoff timing between headwater and fireshed-scale catchments. The firesheds generally have faster mid-winter runoff and reduced summer baseflow runoff, associated with the more rain-dominated lower elevations of the firesheds. In the American, annual runoff from fireshed catchments was within 25% of the headwater catchments, but ranges from lower in 2013 (42 cm, 78%) to higher in 2011 (150 cm, 119%). Runoff in the Lewis Fork fireshed catchment was lower in both 2012 (16 cm, 69%) and 2013 (14 cm, 47%), compared to the Merced headwater catchment.

Simulations of the fireshed catchments in both American and Lewis Fork sites reflected the faster winter runoff observed in the downstream discharge data, but consistently reported lower annual runoff than the headwater catchments. In the American, runoff in water year 2010 was substantially underestimated in the model results, and did not reflect the higher runoff observed in the North Fork of the Middle Fork compared to the headwater catchment in 2011. The Lewis Fork model captures the relative magnitude of annual rates compared to the Merced headwater in the more limited 2012 and 2013 observation period.

Discussion

Vegetation Scenarios

Model results of SPLAT implementation, both with and without wildfire, had a greater effect on runoff in the American than in Lewis Fork (Figure 2.2). The difference in the two study area responses can largely be attributed to the differences in precipitation rates and canopy cover. Changes in vegetation in Lewis Fork had minimal effect on annual ET rates, suggesting the forest maintains more-consistent canopy cover and is water limited compared to the American, where changes in ET were more closely linked to canopy cover and forest density. This difference in responses can be illustrated using the range of vegetation changes, where a 7.5-42.5% reduction in Lewis Fork vegetation led to a 0.5-2.9% decrease in ET and a 2.7-15.2% increase in runoff (Figure 2.4). Alternatively, the 8.0-49.8% reduction in Last Chance vegetation resulted in a 4.1-22.8% decrease in evapotranspiration and a 12.0-66.7% increase in runoff (Figure 2.4).

Robles *et al.* [2014] calculated a 9-10% increase in runoff following thinning in ponderosa pine forests of central Arizona, with a 50% basal area decrease and 40.6 cm of winter precipitation. Their result follows the trend of higher runoff increases with higher precipitation in this study, given the 15.2% and 22.8% runoff increase with the 42.5% and 49.8% LAI decrease in the Lewis Fork (130 cm yr^{-1}) and the American (199 cm yr^{-1}), respectively. Zou *et al.* [2010] use this precipitation trend to suggest vegetation manipulations in the forested upper basin of the Colorado River have higher potential to

increase runoff than lower basin landscapes, using previous forest thinning studies to propose a 6.3-25.0% potential runoff increase given a mean precipitation of 40 cm. Robles *et al.* [2014] also estimated that runoff increases would be eliminated 6-7 years after thinning, similar to both sites in this study, where runoff increases from thinning were also absent within 10 years of vegetation regrowth.

High-intensity wildfire impacts on runoff can be greater than thinning, not only from the higher biomass removed, but also from the variability in burn severity, from light understory burns to stand-replacing crown fires. In a central Arizona ponderosa pine and mixed conifer forest, no increases in seasonal or mean annual streamflow were observed after a prescribed burn over 45% of the watershed [*Gottfried and DeBano*, 1990]. Following a stand-replacing fire in central Washington, Helvey [1980] showed flow rates approximately doubled over the entire flow-duration curve. In addition to vegetation impacts, wildfire can also reduce forest soil infiltration and hydraulic conductivity rates due to the formation of a hydrophobic surface layer [*Robichaud*, 2000].

The few studies that address the persistence in soil water repellence have recorded the effect undetectable within a year [*Huffman et al.*, 2001; *Macdonald and Huffman*, 2004] to six years after fire [*Dyrness*, 1976; *Henderson and Golding*, 1983]. Soil recovery rates can depend on vegetation, as Cerdà and Doerr [2005] found soil stabilization under herb and shrub regrowth in as little as two years, but increasing hydrophobicity and runoff under Mediterranean pines over the decade of measurements. Wildfire effects were modeled starting 10 years after the fire event, at which time we assumed the post-fire impacts were no longer a factor, with stabilization of the soil and vegetation. The maximum runoff increase of 23% in response to the simulated post-fire vegetation reduction of nearly 50% in the American was likely mitigated by the increased understory vegetation cover, calculated in response to the reduced overstory (Figure 2.5).

Controlling factors of water balance response to vegetation change

Canopy cover exerted greater influence on the modeled water balance than LAI, as evidenced by the higher magnitude of response in ET and runoff to changes in the canopy

(Figures 2.3, 2.4). This reflects the photosynthetic model of Chen *et al.* [1999], where LAI is partitioned into sunlit and shaded portions. The sunlit portion of LAI intercepts most of the photosynthetically active photon flux density (PPFD), and has the highest potential rate of photosynthesis and transpiration. When canopy cover is reduced, the amount of sunlit LAI also decreases linearly. When LAI values are modified instead, the proportion of sunlit LAI changes at a lower rate, or may not change at all if the total LAI exceeds the calculation for sunlit LAI (Equations 1,2). Thus, the forest structure and method of vegetation change is as important as how much vegetation is actually on the landscape. Model projections often focus specifically on LAI when considering vegetation changes (*i.e.* [*Running and Nemani*, 1991; *Tague et al.*, 2008]), but changes in vegetation cover may be more significant than changes in LAI.

Model transferability

The direct transfer of calibrated model parameters has been shown to be a preferred method of simulating nearby ungauged basins with similar physiographic characteristics [*Kokkonen et al.*, 2003; *Parajka et al.*, 2005]. The headwater and fireshed catchments in this study have similar geologic and vegetation characteristics, but differ in elevation range and basin size. The lower elevation range in the larger catchments result in more rain and faster winter runoff, which was reflected in the observations and model results (Figure 2.2). Goulden and Bales [2014] note that lower-elevation basins in the Sierra Nevada also have a higher potential evapotranspiration because of the warmer winter temperatures.

This study also found higher ET in the model simulations of lower elevation range, reflected in the consistently lower annual runoff. Observations in the American catchments, however, show the North Fork of the Middle Fork has similar or higher rates of runoff than the Bear Trap headwater catchment for three out of the four years. The differences in the observations and model results may be due to lower vegetation densities outside the measurement area of this study. Additionally, the increased winter runoff from greater amounts of precipitation falling as rain may reduce water availability later in the year, when forest water demand is higher [*Tague and Peng*, 2013].

Conclusions

Model simulations show that the Strategically Placed Landscape Treatments would increase runoff in the high precipitation region of the American River basin. In Lewis Fork, however, fuels treatments over a larger portion of the fireshed or in a more intensive application may be necessary to measurably change the vegetation structure and catchment-scale water balance. Precipitation and canopy cover controlled the magnitude of runoff increases, from 2% in Lewis Fork to 13% in the American, following the 8% reduction in vegetation from fuels treatments. The high-intensity fires modeled in this study also result in even greater vegetation reductions and can lead to large runoff increases. These results, however, did not address potentially adverse issues related to wildfires such as soil erosion into the stream channel, hydrophobic soils, and elevated snowmelt rates.

The spatial pattern and magnitude of vegetation change impacted the response of evapotranspiration and runoff at the catchment scale. Simulating reductions in vegetation by perturbing LAI only resulted in limited impacts on the water balance. Simulating the same reduction by manipulating canopy cover resulted in a water balance response of much greater magnitude, specifically in the high-precipitation American catchments. The representation of forest vegetation structure in hydrologic modeling is important to capture, and will affect model results of projected changes in vegetation.

Calibrated watershed models, constrained with observed data, were transferred to ungauged catchments of similar geology and hydrology to assess watershed response to changes in forest vegetation from growth, treatments, and wildfire. There are a number of uncertainties associated with modeling ungauged catchments, but these uncertainties can be limited by having a well-constrained model in a nearby catchment of similar geologic characterization.

References

Adams, M. A. (2013), Mega-fires, tipping points and ecosystem services: Managing forests and woodlands in an uncertain future, For. Ecol. Manage., 294(2013), 250–261, doi:10.1016/j.foreco.2012.11.039.

Bahro, B., and K. Barber (2004), Fireshed Assessment: An Integrated Approach to Landscape Planning. USDA Forest Service Pacific Southwest Region, R5-TP-017.

Bao, Z., J. Zhang, J. Liu, G. Fu, G. Wang, R. He, X. Yan, J. Jin, and H. Liu (2012), Comparison of regionalization approaches based on regression and similarity for predictions in ungauged catchments under multiple hydro-climatic conditions, J. Hydrol., 466-467, 37–46, doi:10.1016/j.jhydrol.2012.07.048.

Bárdossy, A. (2006), Calibration of hydrological model parameters for ungauged catchments, Hydrol. Earth Syst. Sci., 11(2), 703–710, doi:10.5194/hessd-3-1105-2006.

Bateman, P. C. (1989), Geologic map of the Bass Lake quadrangle, west-central Sierra Nevada, California, Geologic Quandrangle Map GQ-1656.

Beven, K. J., and M. J. Kirkby (1979), A physically based, variable contributing area model of basin hydrology, Hydrol. Sci. Bull., 24(1), 43–69.

Bormann, B., P. Cunningham, M. H. Brooks, V. W. Manning, and M. W. Callopy (1994), Adaptive ecosystem management in the Pacific Northwest. USDA Forest Service Pacific Northwest Forest and Range Experiment Station, Portland, OR PNW-GTR-34.

Bormann, B. T., R. W. Haynes, and J. R. Martin (2007), Adaptive Management of Forest Ecosystems: Did Some Rubber Hit the Road?, Bioscience, 57(2), 186, doi:10.1641/B570213.

California Department of Water Resources (2013), California Water Plan, Update 2013, Sacramento, CA.

Cerdà, A., and S. H. Doerr (2005), The influence of vegetation recovery on soil hydrology and erodibility following fire: an eleven-year investigation, Int. J. Wildl. Fire, 14(4), 423–437.

Chen, J. ., J. Liu, J. Cihlar, and M. . Goulden (1999), Daily canopy photosynthesis model through temporal and spatial scaling for remote sensing applications, Ecol. Modell., 124(2-3), 99–119, doi:10.1016/S0304-3800(99)00156-8.

Clow, D. W., L. Schrott, R. Webb, D. H. Campbell, A. Torizzo, and M. Dornblaser (2003), Ground water occurrence and contributions to streamflow in an alpine catchment, Colorado Front Range, Groundwater, 41(7), 937–950,

doi:10.1111/j.1745-6584.2003.tb02436.x.

Collins, B., S. Stephens, G. Roller, and J. Battles (2011a), Simulating fire and forest dynamics for a landscape fuel treatment project in the Sierra Nevada, For. Sci., 57(2), 77–88.

Collins, B. M., R. G. Everett, and S. L. Stephens (2011b), Impacts of fire exclusion and recent managed fire on forest structure in old growth Sierra Nevada mixed-conifer forests, Ecosphere, 2(4), 14, doi:10.1890/ES11-00026.1.

Dixon, G. E. (2002), Essential FVS: A user's guide to the Forest Vegetation Simulator. Internal Report, Fort Collins, CO: USDA Forest Service, Forest Management Serivce Center. 226p. (Revised: February 25,2015

Dyrness, C. T. (1976), Effect of Wildfire on Soil Wettability in the High Cascades of Oregon. USDA Pacific Northwest Forest and Reange Experiment Station, PNW-202: Portland, OR.

Fernandez, C., J. Vega, T. Fonturbel, E. Jimenez, and J. Perez (2008), Immediate effects of prescirbed burning, chopping and clearing on runoff, infiltration and erosion in a shrubland area in Galicia (NW Spain), L. Degrad. Dev., 19, 502–515.

Finney, M. (2006), An overview of FlamMap fire modeling capabilities, in Fuels Management - How to Measure Success, edited by P. Andrews and B. Butler, pp. 213–220, U.S. Department of Agriculture, Forest Service, Rocky Mountain Research Station: Fort Collins, CO, Portland, OR.

Fry, D., J. Battles, B. Collins, and S. Stephens (2015), Sierra Nevada Adaptive Management Project, Appendix A - Fire and Forest Ecosystem Health Report.

Gottfried, G. J., and L. F. DeBano (1990), Streamflow and water quality responses to preharvest prescribed burning in an undisturbed ponderosa pine watershed. USDA Forest Service, Rocky Mountain Forest and Range Experiment Station, RM-GTR-191: Flagstaff and Tempe, AZ.

Goulden, M. L., and R. C. Bales (2014), Mountain runoff vulnerability to increased evapotranspiration with vegetation expansion, Proc. Natl. Acad. Sci., 1–5, doi:10.1073/pnas.1319316111.

Hawthorne, S. N. D., P. N. J. Lane, L. J. Bren, and N. C. Sims (2013), The long term effects of thinning treatments on vegetation structure and water yield, For. Ecol. Manage., 310, 983–993, doi:DOI 10.1016/j.foreco.2013.09.046.

Helvey, J. (1980), Effects of a north central Washington wildfire on runoff and sediment production, J. Am. Water Resour. Assoc., 16(4), 627–634.

Henderson, G. S., and D. L. Golding (1983), The effect of slash burning on the water

repellency of forest soils at Vancouver, British Columbia, Can. J. For. Res., 13, 353–355.

Heuvelmans, G., B. Muys, and J. Feyen (2004), Evaluation of hydrological model parameter transferability for simulating the impact of land use on catchment hydrology, Phys. Chem. Earth, Parts A/B/C, 29(11-12), 739–747, doi:10.1016/j.pce.2004.05.002.

Hopkinson, P., and J. J. Battles, editors (2015), Learning adaptive management of Sierra Nevada forests : An integrated assessment. Final report of the Sierra Nevada Adaptive Management Project, Berkeley, CA: Center for Forestry, UC Berkeley.

Hrachowitz, M., H.H.G. Savenije, G. Bloschl, J.J. McDonnell, M. Sivapalan, J.W. Pomeroy, B. Arheimer, T. Blume, M.P. Clark, U. Ehret, F. Fenicia, J.E. Freer, A. Gelfan, H.V. Gupta, D.A. Hughes, R.W. Hut, A. Montanari, S. Pande, D. Tetzlaff, P.A. Troch, S. Uhlenbrook, T. Wagener, H.C. Winsemius, R.A. Woods, E. Zehe, and C. Cudennec (2013), A decade of Predictions in Ungauged Basins (PUB)—a review, Hydrol. Sci. J., 58(6), 1198–1255, doi:10.1080/02626667.2013.803183.

Huffman, E. L., L. H. MacDonald, and J. D. Stednick (2001), Strength and persistence of fire-induced soil hydrophobicity under ponderosa and lodgepole pine, Colorado Front Range, Hydrol. Process., 15(15), 2877–2892, doi:10.1002/hyp.379.

Ice, G., D. Neary, and P. Adams (2004), Effects of Wildfire on Soils and Watershed Processes, J. For., 102(6), 16–20.

Jarvis, P. (1976), The interpretation of the variations in leaf water potential and stomatal conductance found in canopies in the field, Philos. Trans. R. Soc. London, 273(927), 593–640.

Jones, D., K. O'Hara, J. Battles, and R. Gersonde (2015), Leaf Area Prediction Using Three Alternative Sampling Methods for Seven Sierra Nevada Conifer Species, Forests, 6(8), 2631–2654, doi:10.3390/f6082631.

Kokkonen, T. S., A. J. Jakeman, P. C. Young, and H. J. Koivusalo (2003), Predicting daily flows in ungauged catchments: Model regionalization from catchment descriptors at the Coweeta Hydrologic Laboratory, North Carolina, Hydrol. Process., 17(11), 2219–2238, doi:10.1002/hyp.1329.

van der Linden, S., and M. Woo (2003), Transferability of hydrological model parameters between basins in data-sparse areas, subarctic Canada, J. Hydrol., 270(3 - 4), 182–194, doi:10.1016/S0022-1694(02)00295-0.

Macdonald, L. H., and E. L. Huffman (2004), Post-fire Soil Water Repellency : Persistence and Soil Moisture Thresholds, Soil Sci. Soc. Am. J., 68, 1729–1734.

Merz, R., and G. Blöschl (2004), Regionalisation of catchment model parameters, J.

Hydrol., 287(1-4), 95–123, doi:10.1016/j.jhydrol.2003.09.028.

Miller, J. D., H. D. Safford, M. Crimmins, and a. E. Thode (2009), Quantitative evidence for increasing forest fire severity in the Sierra Nevada and southern Cascade Mountains, California and Nevada, USA, Ecosystems, 12, 16–32, doi:10.1007/s10021-008-9201-9.

Parajka, J., R. Merz, and G. Blöschl (2005), A comparison of regionalisation methods for catchment model parameters, Hydrol. Earth Syst. Sci., 9, 157–171, doi:10.5194/hessd-2-509-2005.

Potts, J. B., E. Marino, and S. L. Stephens (2010), Chaparral shrub recovery after fuel reduction: a comparison of prescribed fire and mastication techniques, Plant Ecol., 210(2), 303–315, doi:10.1007/s11258-010-9758-1.

Robichaud, P. R. (2000), Fire effects on infiltration rates after prescribed fire in Northern Rocky Mountain forests, USA, J. Hydrol., 231-232, 220–229, doi:10.1016/S0022-1694(00)00196-7.

Robichaud, P. R., and T. A. Waldrop (1994), A Comparison of Surface Runoff and Sediment Yields From Low- and High-Severity Site Preparation Burns, J. Am. Water Resour. Assoc., 30(1), 27–34.

Robles, M. D., R. M. Marshall, F. O'Donnell, E. B. Smith, J. A. Haney, and D. F. Gori (2014), Effects of climate variability and accelerated forest thinning on watershed-scale runoff in southwestern USA ponderosa pine forests., PLoS One, 9(10), e111092, doi:10.1371/journal.pone.0111092.

Running, S. W., and R. R. Nemani (1991), Regional hydrologic and carbon balance responses of forests resulting from potential climate change, Clim. Change, 19(4), 349–368, doi:10.1007/BF00151173.

Saucedo, G. J., and D. L. Wagner (1992), Geologic Map of the Chico quadrangle, Regional Geologic Map 7A.

Shakesby, R., and S. Doerr (2006), Wildfire as a hydrological and geomorphological agent, Earth-Science Rev., 74(3-4), 269–307, doi:10.1016/j.earscirev.2005.10.006.

Silberstein, R. P. (2006), Hydrological models are so good, do we still need data?, Environ. Model. Softw., 21(9), 1340–1352, doi:10.1016/j.envsoft.2005.04.019.

Sivapalan, M. (2003), Prediction in ungauged basins: a grand challenge for theoretical hydrology, Hydrol. Process., 17(15), 3163–3170, doi:10.1002/hyp.5155.

Stephens, S., J. Agee, P. Fule, M. P. North, W. Romme, T. Swetnam, and M. Turner (2013), Managing Forest and Fire in Changing Climates, Science (80-.)., 342, 41–42.

Stephens, S. L. (1998), Evaluation of the effects of silvicultural and fuels treatments on potential fire behaviour in Sierra Nevada mixed-conifer forests, For. Ecol. Manage., 105(1-3), 21–35, doi:10.1016/S0378-1127(97)00293-4.

Stephens, S. L., and J. J. Moghaddas (2005), Experimental fuel treatment impacts on forest structure, potential fire behavior, and predicted tree mortality in a California mixed conifer forest, For. Ecol. Manage., 215(1-3), 21–36, doi:10.1016/j.foreco.2005.03.070.

Tague, C., and G. E. Grant (2004), A geological framework for interpreting the low-flow regimes of Cascade streams, Willamette River Basin, Oregon, Water Resour. Res., 40(4), 1–9, doi:10.1029/2003WR002629.

Tague, C., and H. Peng (2013), The sensitivity of forest water use to the timing of precipitation and snowmelt recharge in the California Sierra: Implications for a warming climate, J. Geophys. Res. Biogeosciences, 118(2), 875–887, doi:10.1002/jgrg.20073.

Tague, C., L. Seaby, and a. Hope (2008), Modeling the eco-hydrologic response of a Mediterranean type ecosystem to the combined impacts of projected climate change and altered fire frequencies, Clim. Change, 93(1-2), 137–155, doi:10.1007/s10584-008-9497-7.

Tague, C. L., and L. E. Band (2001), Evaluating explicit and implicit routing for watershed hydro-ecological models of forest hydrology at the small catchment scale, Hydrol. Process., 15(8), 1415–1439, doi:10.1002/hyp.171.

Tague, C. L., and L. E. Band (2004), RHESSys: Regional Hydro-Ecologic Simulation System—An Object-Oriented Approach to Spatially Distributed Modeling of Carbon, Water, and Nutrient Cycling, Earth Interact., 8(19), doi:http://dx.doi.org/10.1175/1087-3562(2004)8<1:RRHSSO>2.0.CO;2.

Tague, C. L., J. S. Choate, and G. Grant (2013), Parameterizing sub-surface drainage with geology to improve modeling streamflow responses to climate in data limited environments, Hydrol. Earth Syst. Sci., 17(1), 341–354, doi:10.5194/hess-17-341-2013.

USDA, (2004), Sierra Nevada Forest Plan Amendment, Record of Decision. USDA Forest Service Pacific Southwest Region: Vallejo, CA.

Wagener, T., and A. Montanari (2011), Convergence of approaches toward reducing uncertainty in predictions in ungauged basins, Water Resour. Res., 47(6), 1–8, doi:10.1029/2010WR009469.

Westerling, A. L., H. G. Hidalgo, D. R. Cayan, and T. W. Swetnam (2006), Warming and earlier spring increase western U.S. forest wildfire activity., Science, 313(5789),

940–3, doi:10.1126/science.1128834.

Wigmosta, M. S., L. W. Vail, and D. P. Lettenmaier (1994), A distributed hydrology-vegetation model for complex terrain, Water Resour. Res., 30(6), 1665, doi:10.1029/94WR00436.

Zou, C. B., P. F. Ffolliott, and M. Wine (2010), Streamflow responses to vegetation manipulations along a gradient of precipitation in the Colorado River Basin, For. Ecol. Manage., 259(7), 1268–1276, doi:10.1016/j.foreco.2009.08.005.

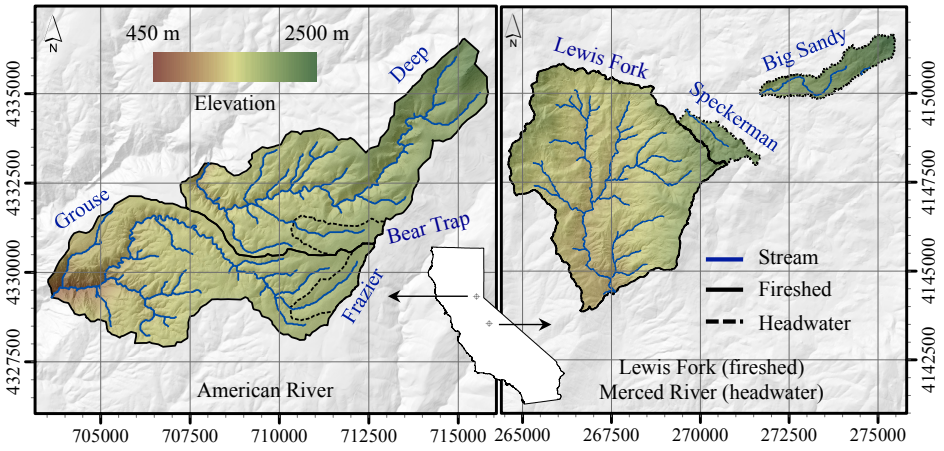

Figure 2.1. Location of the research catchments, within the American River basin in Tahoe National Forest (left panel) and Lewis Fork in Sierra National Forest (right panel). Gridlines indicate 2500 meter spacing of Universal Transverse Mercator projection; the same elevation band applies to both maps.

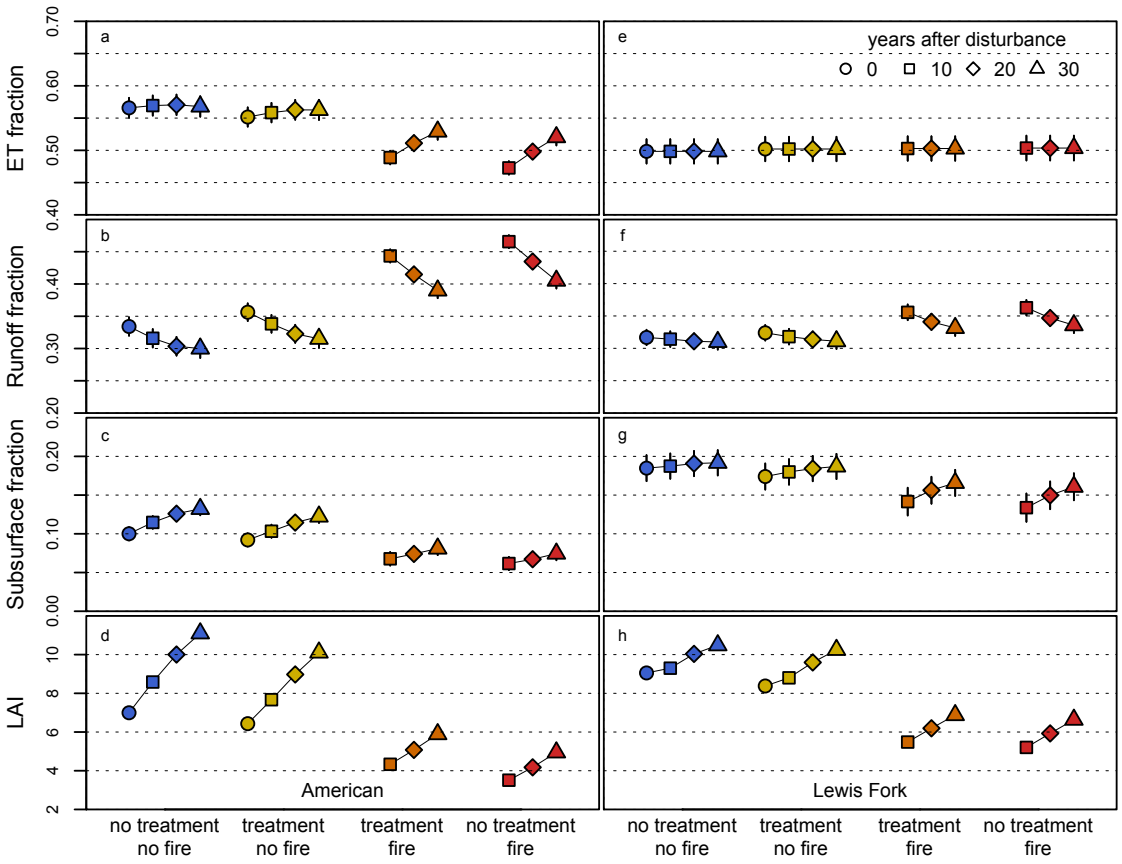

Figure 2.2. Changes in the partitioning of precipitation into evapotranspiration (a,e), runoff (b,f), and subsurface flow (c,g) in response to mean LAI (d,h) of simulated management scenarios over 30 years. Each water balance component is shown here as a fraction of precipitation, and was modeled over the four years of observed data (water years 2010-2013). Bars indicate 95% confidence interval.

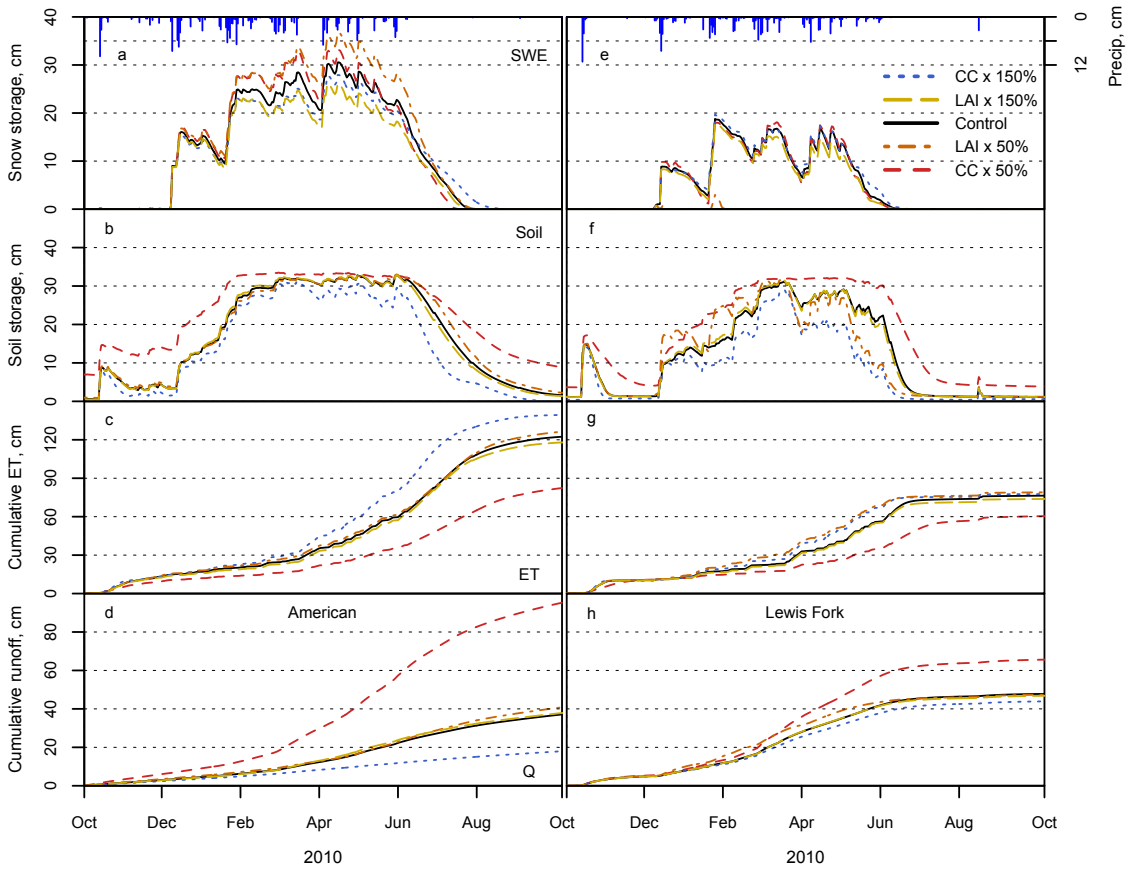

Figure 2.3. Sensitivity of the water balance for water year 2010 for the American (left panel) and Lewis Fork (right panel) to ±50% leaf area index and canopy cover on snow storage (a,e), soil storage (b,f), evapotranspiration (c,g), and runoff (d,h) in response to 50% and 150% vegetation change by modifying leaf area index or canopy cover.

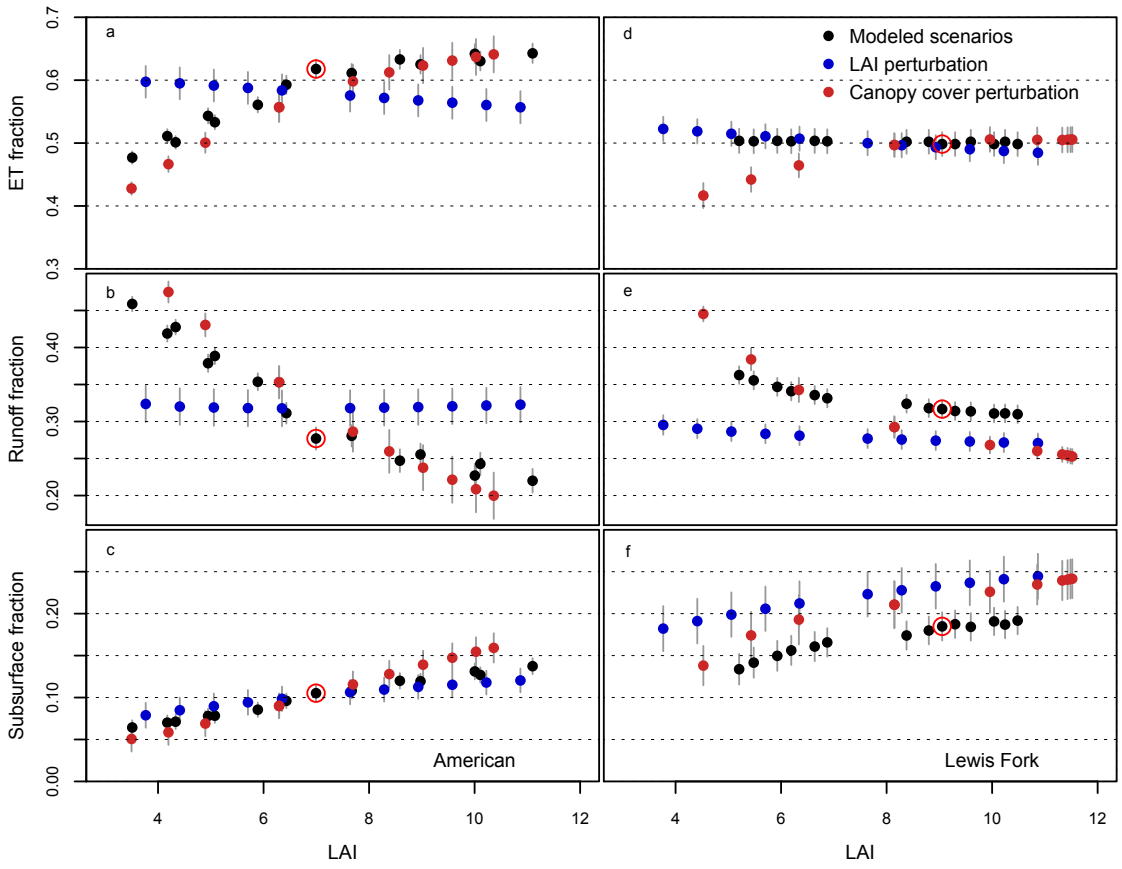

Figure 2.4. Fireshed water balance response to simulated vegetation change from the no treatment scenario (red circles), as fraction of precipitation, averaged over water years 2010-2013. Bars indicate 95% confidence interval.

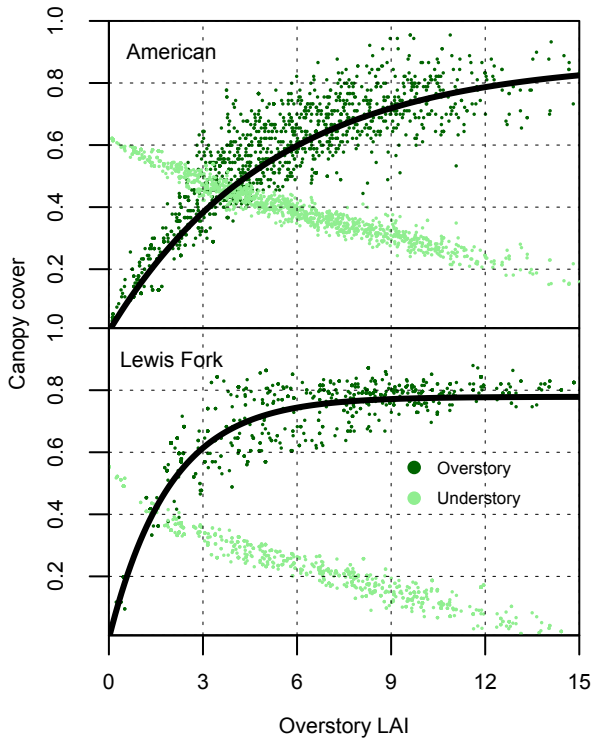

Figure 2.5. Overstory and understory canopy cover within the range of mapped vegetation overstory Leaf Area Index in the pre-treatment vegetation maps for the American and Lewis Fork study areas. The vegetation maps input for each scenario modified overstory vegetation using both canopy cover and LAI; only canopy cover was modified for understory because we had no LAI data for the lower vegetation layer.

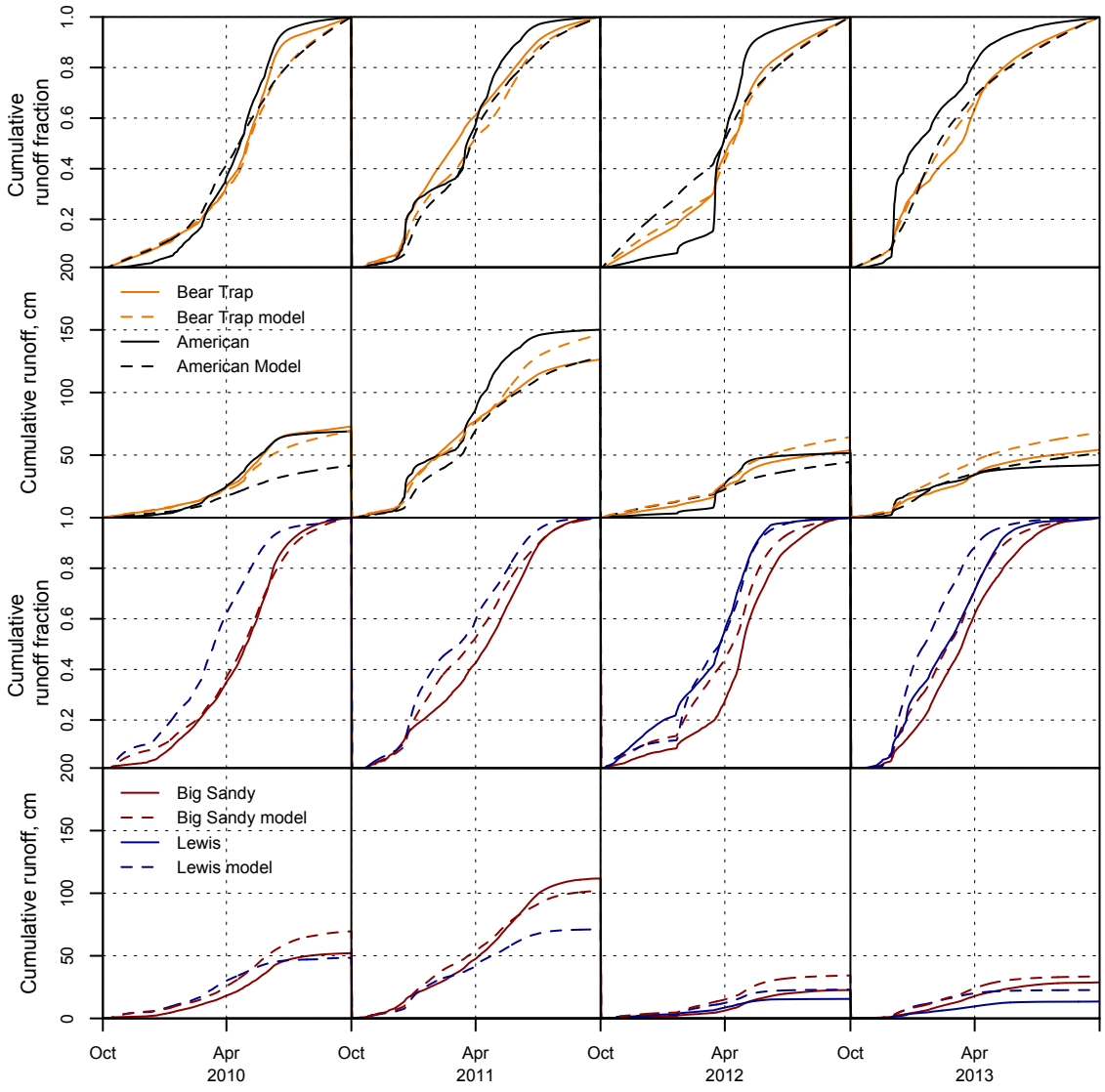

Figure 2.6. Cumulative discharge of observations and model simulation for the headwater (Bear Trap, Big Sandy) and downstream (American, Lewis Fork) catchments from 2010 to 2013. Cumulative fractions are used to compare timing of runoff and cumulative runoff normalized over the watershed area is used to compare annual runoff totals. The observation data for Lewis Fork was only available during 2012-2013.

Chapter 3. Vegetation and climate effects on Sierra Nevada mixed-conifer headwater hydrology.

Abstract

Forested watersheds in the Sierra Nevada are sensitive to the influence of a warming climate, where increased temperatures elevate the amount of precipitation falling as rain and reduce the natural water storage that exists in the winter snowpack. We used a hydro-ecologic model (RHESSys) constrained by runoff, distributed snow, and distributed soil moisture measurements, to simulate the impacts of projected temperature increases and forest disturbance on two headwater catchments in the central and southern Sierra. Increasing temperatures were projected for Representation Concentration Pathways (RCP) 4.5 and 8.5 at 2050 and 2100, and combined with forest thinning treatments and wildfire events to investigate interacting effects of external climate forcing and internal vegetation dynamics on snowpack, evapotranspiration, and runoff. The results presented here show that although future climate forcings will reduce the fraction of precipitation falling as snow, and the winter seasonal snowpack storage, the variability of interannual precipitation and vegetation perturbations from fuel treatments and wildfire will likely exert a greater influence on annual evapotranspiration and runoff.

Introduction

It has long been known that watersheds on the western slopes of the Sierra Nevada, and the critical water supplies originating in these areas, are sensitive to climate warming [*Pupacko*, 1993; *Jeton et al.*, 1996]. Many of the winter storms that provide the deep seasonal snowpack in the western Sierra occur at temperatures above -3^{o}C [*Bales et al.*, 2006], making precipitation vulnerable to a transition towards a higher rainfall fraction and reduced snowpack storage in a warmer climate [*Knowles*, 2002; *Miller et al.*, 2003]. The frequency of wildfires is also increasing in the western U.S. because of the warmer temperatures, and in the Sierra mixed-conifer zone, a buildup of fuels in forests with a century-long history of suppressing the frequent low-intensity burns that previously kept vegetation densities low [*Westerling et al.*, 2006]. Combined with demand increases, climate warming may place the provision of sustainable water supplies at risk.

Climate projections for California show a 1.7-5.8^{o}C increase in temperatures by the year 2100, with precipitation modified by 5-20% [*Cayan et al.*, 2008]. In a low emissions projection, southern Sierra precipitation is not projected to change from the historical record, but the central- and northern-Sierra may experience precipitation increases up to 20% before 2050 [*Garfin et al.*, 2013]. Projected trends change towards the end of the century, however, with all of the Sierra Nevada expected to see reduced precipitation, up to 20% in the southernmost Sierra with a high emissions scenario [*Garfin et al.*, 2013]. Garfin et al. [2013] note that the confidence in these predictions is low to medium, given the high variability of climate model projections and low precipitation changes relative to the extreme variability of short-term precipitation in the southwest United States.

A number of studies focusing on watershed response to changes in climate have been completed for the western slope of the Sierra Nevada, which has been identified as more sensitive to changes in temperature than the eastern slope due to the larger area of lower elevation [*Pupacko*, 1993]. Investigating the sensitivity of mean annual streamflow to climate, Duell [1994] reported that average annual streamflow from the North Fork of the American River could range from a 9% increase (+2^{o}C, +25% Precip), to a 68% decrease (+4^{o}C, -25% P). For projected temperature increases of 2-5^{o}C in the American and

Merced river basins, and no change in precipitation amount or timing, Dettinger *et al.* [2004] reported that average annual runoff generally remained constant, with the major changes resulting from the fraction of precipitation falling as rain and earlier snowmelt. These trends that have already been observed in the last half of the 20th century [*Stewart et al.*, 2004]. An analysis of historical streamflow in the Sacramento River basin streamflow found that the interannual variability in precipitation explained 95.4% of differences in annual streamflow volumes while only 2.7% was explained by temperature [*Risbey and Entekhabi*, 1996]; findings consistent with the minimum 80% of streamflow explained by precipitation reported by Duell [1994].

The latest IPCC North American regional assessment lists wildfire as one of the key risks to ecosystems from climate change [*Romero-Lankao et al.*, 2014]. Westerling *et al.* [2006] discuss the competing influences of climate and forest management on increasing wildfire occurrence across the western U.S., suggesting that although recent climate change was the primary driver in Northern California, fire exclusion is also an important contributing factor in this region. In response to these changing conditions, Millar *et al.* [2007] encourage a proactive planning approach for forest management. Fuels treatments are an effective forest-management tool for mitigating wildfire risk in Sierra Nevada forests [*Stephens*, 1998; *Collins et al.*, 2011a], and include selective thinning and prescribed burning for promoting fire-resilient landscapes [*Agee and Skinner*, 2005].

Forest vegetation density and structure impact interception of precipitation [*Storck et al.*, 2002; *Moeser et al.*, 2015], evapotranspiration rates [*Dore et al.*, 2010, 2012; *Hawthorne et al.*, 2013], and the surface energy balance for snowmelt [*Essery et al.*, 2008b; *Ellis et al.*, 2011; *Mahat and Tarboton*, 2012; *Lundquist et al.*, 2013]. Molotch and Meromy [2014] found elevation, temperature, and precipitation were more influential than vegetation, using regression tree analysis to rank relative physiographic and climatic influence on snow cover for all the major Sierra Nevada watersheds. Both forest cover and temperature increases showed significant, non-linear effects on snowpack and streamflow in the upper Tuolumne [*Cristea et al.*, 2014], however, using the Distributed Hydrology Soil Vegetation Model (DHSVM; [*Wigmosta et al.*, 1994]). The relative

effects of temperature and vegetation may then depend on the specific montane elevation range, vegetation type, and annual precipitation received in a watershed, requiring more localized analyses to determine the dominant influences on evapotranspiration and runoff. The specific aim of this study is to project the interacting effects of climate warming with forest disturbances on the water balance of mountain headwater catchments that have a Mediterranean climate and span the elevation range that transitions from rain- to snow-dominated precipitation.

Methods

This study uses a hydro-ecologic model (RHESSys), constrained with distributed snow, distributed soil moisture, and stream discharge measurements, to project water balance response of two Sierra Nevada mixed-conifer headwater catchments to temperature and vegetation perturbations. Two types of vegetation disturbances are simulated, a forest thinning treatment implemented in 2012, and impacts of wildfires modeled with and without the thinning. Temperature increases from two climate scenarios are also simulated, Representative Concentration Pathways (RCP) 4.5 and 8.5, at 2050 and 2100. The climate and vegetation scenarios are then simulated together to determine the dominant factors controlling evapotranspiration and runoff, assessed over the range of dry to wet precipitation conditions observed during the four-year study period.

Study Sites

Two headwater catchments at different latitudes along the western slope of the Sierra Nevada were monitored for climate, stream discharge, and distributed snow depth and soil moisture during water years 2010-2013. The watersheds are dominated by mixed-conifer forests, a forest type covering 13-14% (~ 52,500-56,50 km^2) of California [*Barbour and Minnich*, 2000], and have well drained soils, classified as loamy-sand in Bear Trap and sandy or sandy-loam in the Big Sandy watershed. Bear Trap Creek is located in the headwaters of the American River Basin, located in the central-Sierra, and Big Sandy Creek is located in the Merced River Basin, located in the southern-Sierra. The headwaters receive well-mixed rain and snow at the watershed outlet, but are snow

dominated at the upper elevations, suggesting these basins would be sensitive to lower snowfall and higher rainfall from increases in temperature.

Model scenarios

Four vegetation scenarios were combined with the climate projections to determine dominant influences in forest hydrology: pre-treatment, post-treatment, pre-treatment after fire, and post-treatment after fire (Figure 3.1, Table 3.2). Strategically Placed Landscape Treatments (SPLATs, [*Finney*, 2001]), a forest fuels reduction strategy to reduce fire risk by treating part of the landscape, were implemented at the fireshed scale during the summer of 2012. As part of the larger SPLAT implementation, selective thinning was done in Bear Trap and a commercial thinning was completed in Big Sandy. LiDAR flights in 2007 and late 2012 captured changes in vegetation, which were combined with aerial images to create spatial layers of vegetation type, Leaf Area Index (LAI), and canopy cover [*Su et al.*, 2015].

Understory vegetation was also estimated using a linear equation developed from forest plot data relating basal area and canopy cover with shrub cover fraction [Chapter 1]. The differences in vegetation density were used to run the Forest Vegetation Simulator (FVS, [*Dixon*, 2002]) with the Fire and Fuels Extension (FFE, [*Reinhardt and Crookston*, 2003]) and the Fire Area Simulator (FARSITE, [*Finney*, 2004]) to assess treatment impact on wildfire severity [*Fry et al.*, 2015]. Post-fire vegetation densities were assessed starting 10 years following the simulated wildfire events, setting aside the need to consider effects such as soil hydrophobicity, reduced soil infiltration capacity, and diminished litter cover that can occur immediately after fire.

The climate scenarios are based on changes projected in the minimum and maximum daily temperatures for the Representation Concentration Pathways (RCP) 4.5 and 8.5 at 2050 and 2100. RCP 4.5 is defined as a 4.5 W m^{-2} increase in radiative forcing relative to pre-industrialization with stabilization by 2100; RCP 8.5 represents an 8.5 W m^{-2} radiative increase by 2100 that continues to rise [*van Vuuren et al.*, 2011]. Mean annual minimum and maximum temperature anomalies were calculated using the 4-year annual

mean of 2010-2013 as a baseline. A four-year trailing ensemble mean was calculated using the Coupled Model Intercomparison Project Phase 5 (CMIP5) output for the Community Climate System Model version 4 (CCSM4) and the Model for Interdisciplinary Research on Climate version 5 (MIROC5) (Figure 3.2). Using the temperature anomalies to produce a uniform offset in minimum and maximum temperatures on our observed temperature datasets precluded the need for downscaling climate projections.

Model simulations

The Regional Hydro-Ecologic Simulation System (RHESSys, [*Tague and Band*, 2004]) was used to simulate the hydrologic response to vegetation and climate scenarios. Model calibration was completed for water years 2010-2012, during which annual precipitation varied from drier than normal to wetter than normal conditions. Monte-Carlo style calibrations were completed by running 5000 sets of random parameters and using the parameter sets that conformed to a Nash-Sutcliffe and log-transformed Nash-Sutcliffe statistic higher than 0.60, as well as annual and August streamflow rates within 25% of observed values. Six parameter sets met the criteria for the Bear Trap watershed and 17 sets were acceptable for the Big Sandy watershed, providing a range of modeled responses to temperature and vegetation perturbations. The study sites, instrumentation, treatments, and model construction were described in detail previously [Chapter 1, this document].

Increasing temperatures at the elevation range of these watersheds are expected to have a significant impact on the amount of precipitation received as snow versus rain, and the persistence of snowpack during the winter and into spring. RHESSys calibration was completed using a separate rain and snow precipitation input, and changes to initial snowfall rates were implemented using the linear transition of snowfall temperatures in the model, from -1 to 3^{o}C. Three inputs contribute to snowmelt rates: temperature, precipitation falling as rain, and radiation. All three components are affected by air temperature, and the relevant top level equations are listed below from Tague and Band

[2004]. Melt attributed to temperature is based on an empirical relationship to sensible and latent heat, and is calculated

$$M_T = \beta_{MT} T_{air}(1 - 0.8F) \quad [1]$$

where β_{MT} is the temperature melt coefficient, calibrated to 0.0005 for Bear Trap and 0.001 for Big Sandy, T_{air} is the temperature in Celsius and F is the fraction of forest cover. Snowmelt from advection due to rainfall is calculated

$$M_v = (\rho_{water} T_{air}, TF cp_{water})/\lambda_f \quad [2]$$

where ρ_{water} is the density of water, TF is net throughfall onto the snowpack, cp_{water} is the heat capacity of water, and λ_f is the latent heat of fusion. Lastly, melt due to radiation is calculated as

$$M_{rad} = (K_{direct} + K_{diffuse} + L)/\lambda_f \rho_{water} \quad [3]$$

where K_{direct} and $K_{diffuse}$ are direct and diffuse shortwave radiation, and L is longwave radiation. Melt only occurs when the snowpack is ripe, but snow loss also can occur by sublimation from radiation energy input, calculated by adding the latent heat of vaporization to the latent heat of fusion in Equation 3.

Results

Model scenarios

Mean annual water balance components of evapotranspiration, and runoff were assessed in response to vegetation and climate scenarios over the complete observation period (water years 2010-2013). Mean annual precipitation was 199 cm in Bear Trap and 130 cm in Big Sandy. Selective thinning implemented in Bear Trap reduced mean LAI from 9.9 to 9.1, with modeled wildfire reducing LAI to 8.8 with SPLATs and 7.7 without SPLATs. Mean LAI in Big Sandy was 5.0, with the commercial thinning reducing mean LAI over the watershed less than 0.1. A small section of Big Sandy was thinned, with LAI being reduced by as much as 4.0, but the minor amount of area thinned combined

with incremental increases in growth elsewhere, led to the small changes in basin-scale LAI. Wildfire in Big Sandy reduced LAI to 3.8, with thinning effects on wildfire again reducing mean LAI over the watershed less than 0.1. Because the vegetation structure did not change substantially after treatments, results reported for the Big Sandy catchment are limited to pre-treatment and post-fire vegetation change.

Mean daily winter temperatures during the months of heaviest precipitation (Nov-Apr), were 4.3^{o}C in both Bear Trap and Big Sandy catchments. Temperatures projected with RCP 4.5 increased 1.2^{o}C by 2050 and 1.6^{o}C by 2100 in Bear Trap, with slightly smaller increases at Big Sandy, 1.0^{o}C by 2050 and 1.4^{o}C by 2100. In the RCP 8.5 projections, temperature increases by 2050 and 2100 are 1.8^{o}C and 4.7^{o}C in Bear Trap and 1.6^{o}C and 4.4^{o}C in Big Sandy, respectively.

Model simulations

Simulations showed that vegetation changes had greater effects on runoff and evapotranspiration than the changes in temperature (Figure 3.3). 95% confidence intervals were calculated for the 6 parameterized Bear Trap models and 17 parameterized Big Sandy models, with runoff and evapotranspiration responses are reported as fractions of precipitation. Confidence intervals were small for both pre-treatment and post-fire scenarios in Big Sandy. Confidence intervals in Bear Trap increased with decreasing vegetation, resulting in higher uncertainties of water balance response with greater vegetation disturbance. In the Bear Trap watershed, the scenario of greatest vegetation change (no treatment, fire) increased the mean runoff fraction by 0.20 (from 0.44 to 0.64) and decreased the mean fraction of evapotranspiration by 0.20 (from 0.47 to 0.27), in response to the 22% LAI decrease (from 9.9 to 7.7). In comparison, the climate scenario of greatest temperature increases (RCP 8.5, 2100) resulted in a smaller reduction in runoff, from 0.44 to 0.41, and smaller evapotranspiration increase, from 0.47 to 0.48. Responses of mean runoff and evapotranspiration fractions in 2050 and 2100 to RCP 4.5 temperature increases were limited to less than 0.03, as was the response to RCP 8.5 in 2050.

In the Big Sandy watershed, the simulated response of evapotranspiration and runoff to the 26% LAI decrease (from 5.0 to 3.7) from modeled wildfire was more limited than in Bear Trap, increasing the runoff fraction by 0.06 (from 0.35 to 0.41) and decreasing the evapotranspiration fraction by 0.06 (from 0.54 to 0.48). A similar response in the reduction of evapotranspiration of 0.05 (from 0.54 to 0.49) was simulated due to the RCP 8.5 temperature increase by 2100, but the response of runoff was not significant, only increasing from 0.35 to 0.36. Precipitation not accounted for in runoff or evapotranspiration is routed to deeper groundwater storage and is attributed to the difference in responses to the temperature increase in Big Sandy. This component is assumed to constitute net subsurface outflow from the catchment. Response to all other climate scenarios also resulted in changes of less than 0.03 in evapotranspiration and runoff fractions, similar to Bear Trap.

Precipitation variability

Runoff in Bear Trap responded to both vegetation and precipitation rates, but the response to the range of precipitation exceeded 75 cm while the response to even the highest vegetation disturbance was limited to less than 50 cm of increased runoff (Figure 3.4). Trends of runoff and evapotranspiration response with increasing temperatures were the same in all climate scenarios except for RCP 8.5 in 2100, where evapotranspiration increases are greater in the wet years (<5 cm). In Big Sandy, precipitation variability between wet and dry years had a greater effect on evapotranspiration and runoff than the reductions in vegetation from wildfire (Figure 3.4). The range of annual precipitation resulted in evapotranspiration differences near 40 cm without treatment or fire, and runoff differences close to 70 cm with post-fire vegetation. Water balance response to reductions in LAI from wildfire were smaller, with evapotranspiration decreases and runoff increases of under 20 cm. Temperature increases affected runoff less than evapotranspiration, with runoff increases of less than 10 cm during the highest projected temperature increases for RCP 8.5 in 2100. Elevated temperatures in 2050 and 2100 moderated the ET response to fire during mean to high precipitation years. Evapotranspiration in the untreated Big Sandy catchment resulted in lower ET with

increasing temperatures, but in the post-fire scenario resulted in higher ET until the highest temperature increases of RCP 8.5 in 2100.

Hydrologic timing and storage

Precipitation falling as rain or snow, along with the accumulation and melt of the seasonal snowpack, determines the timing of soil infiltration, runoff, and availability of water in the soil for use by vegetation. Projected temperature increases affect both precipitation phase and melt rate, with vegetation density affecting snowmelt by modifying the surface energy balance. Simulations of temperature and vegetation impacts on hydrologic storage and timing were thus assessed for a mean precipitation year (2010, Figure 3.5).

In Bear Trap, post-fire vegetation reduces snowpack persistence by about 3 weeks, with temperature increases by 2100 in RCP 4.5 advancing the melt-out date by about 4 weeks (Figure 3.5a, 3.5b). Increases in temperature by 2100 in RCP 8.5 show no persistent snowpack, with the amount of precipitation falling as snow reduced from 40% to 10% overall (Table 3.1). Soil storage from the reduced post-fire vegetation is increased during the dry season from minimal storage to within 15 cm of saturated winter conditions (~35 cm). Soil storage with increased temperatures begins the recession to dry summer conditions earlier, associated with the reduced snowpack. Evapotranspiration with increased temperatures becomes more limited in the early summer because of the earlier soil drying. The reduced post-fire vegetation resulted in ET reductions during all seasons, and is not limited by soil storage. Runoff timing is accelerated with both scenarios of increased temperatures and reduced vegetation, with peak runoff about 8 weeks earlier. Post-fire vegetation results in much higher runoff, with increased peaks and frequency of high-flow events, where increased temperature scenarios result in lower peak flows spread more evenly across the winter months.

In Big Sandy, post-fire vegetation resulted in the loss of a persistent winter snowpack, similar to temperature increases by 2100 with RCP 8.5 (Figure 3.5g, 3.5h). Increases in temperature by 2100 with RCP 4.5 and 8.5 are projected to reduced snowfall from 60%

to 53% and 29% of precipitation, respectively. Reductions in vegetation and increases in temperature show much more similar responses in Big Sandy than they did in Bear Trap. Soil storage from infiltration increases earlier in the winter and becomes more saturated (30 cm) than in the control (23 cm), but the dry season recession curve also starts about three weeks earlier than in the control scenario. Evapotranspiration response to the vegetation reductions is muted, but ET is reduced in all vegetation and temperature simulations from the earlier drawdown in soil storage. Peak runoff timing is shifted about 12 weeks, from early-June to early-March, in the post-fire and RCP 8.5 scenarios, with slightly higher peaks in the post-fire vegetation simulation than with projected increases in temperature. The earlier peak runoff in the RCP 4.5 scenario is only shifted about 8 weeks, to mid-April.

Discussion

Model simulations

Ficklin and Barnhardt [2014] suggest using multiple parameter sets and General Circulation Model outputs, as significant differences in hydrologic projections will occur from uncertainty in model parameterization and climate scenario. In this study, we used the ensemble means from two climate models and two emissions scenarios, with 6 (Bear Trap) and 17 (Big Sandy) parameter sets to incorporate some accounting of uncertainty. Additional uncertainties can originate from climate downscaling, which was not done in this study, and model structure [*Wilby and Harris*, 2006]. The simulations completed in this study apply a uniform increase in the minimum and maximum daily temperatures, using projected temperature anomalies for 2050 and 2100. Studies often use a single mean temperature adjustment to project effects of climate warming on Sierra Nevada watersheds [e.g. *Young et al.*, 2009; *Meyers et al.*, 2010], but minimum and maximum temperatures may have periods of non-linear increases, which can modify the diurnal temperature range [*Easterling*, 1997; *Vose et al.*, 2005]. In the RCP 4.5 projections, minimum and maximum temperatures increased an average of 0.017 and 0.020 ^{o}C yr^{-1} in the American and 0.016 and 0.019 ^{o}C yr^{-1} in the Merced between 2013 and 2100, respectively. RCP 8.5 projections of minimum and maximum temperatures resulted in

mean increases of 0.044 and 0.055 ^{o}C yr^{-1} in the American and 0.045 and 0.053 ^{o}C yr^{-1} in the Merced between 2013 and 2100, respectively. The rate differences of minimum and maximum temperature increases will also affect the Jarvis-based calculations of stomatal conductance [*Jarvis*, 1976] used to estimate transpiration in RHESSys, which incorporates functions of mean and minimum daily temperatures to limit maximum conductance.

The simulation results of temperature perturbations generally agree with the findings of Dettinger *et al.* [2004], that without statistically significant changes in precipitation, annual volumes of streamflow will generally remain steady in the American and Merced River basin areas with increasing temperatures. Dettinger *et al.* [2004] did find a general trend of +8% precipitation yr^{-1} with climate warming, but the effect was small compared to the interannual variation, which was also found to have a large effect on runoff in this study (Figure 3.4). Previous work in the Merced River [*Christensen et al.*, 2008] also showed the sensitivity of transpiration to precipitation at an elevation range similar to Big Sandy, with their model extending into higher elevations where transpiration became increasing sensitive to changes in temperature. Although the results of this study are based on CMIP5 data, with much of the previous research based on CMIP3 data, Ficklin *et al.* [2015] found that the hydrologic projections from both climate datasets are comparable for the Sierra Nevada. The headwater models used in this study are on much smaller scale than much of the previous watershed-scale research on hydrologic impacts of climate warming, but both headwaters and large-scale basins span the transition from rain- to snow-dominated precipitation, explaining the similarity in responses.

Precipitation variability

The strong response of evapotranspiration to vegetation density in Bear Trap, and to annual precipitation in Big Sandy suggests that within a Budyko [1974] framework of competing water and energy limitations of photosynthesis (and transpiration), the Bear Trap region tends to be energy limited while the Big Sandy region tends to be more water limited (Figure 3.6). The difference in energy and water limitations will affect the magnitude of the water balance response to changes in vegetation and temperature, as

Zhang *et al.* [2001] showed the potential for increased response of evapotranspiration with reduced forest cover in regions with higher precipitation. In both sites, yearly runoff was influenced by interannual precipitation variability more than temperatures, similar to results from previous work in the western Sierra [*Duell*, 1994; *Risbey and Entekhabi*, 1996].

Individual years of 2011 and 2012 were selected from the four years of simulation (2010-2013) to provide a spectrum of response to climate and vegetation perturbations during a wet and dry year, respectively. Antecedent moisture conditions can modify watershed response to disturbance, so the progression of dry to wet years may be important. Precipitation in 2010 was close to the long-term mean for both regions, followed by the wet year of 2011, and dry years of 2012 and 2013. Subsurface storage capacity and groundwater flow dynamics will impact the magnitude of low summer streamflow response to low precipitation years and temperature increases in seasonal snow regions [*Jefferson et al.*, 2008; *Tague and Grant*, 2009; *Huntington and Niswonger*, 2012]. Improved characterization of subsurface properties in Sierra watersheds are needed to enhance our understanding and predictive capability of runoff response to climate [*Shaw et al.*, 2014].

Hydrologic timing and storage

Both reduced vegetation and increased temperatures result in more energy being absorbed by the snowpack, with persistent snow cover eliminated by 2100 in RCP 8.5 (Figure 3.5b, 3.5h). The increased winter (Nov-Apr) snowmelt is split between absorption into soil storage and increasing streamflow, but ET generally remains limited in the winter to the same rates. The faster melt also reduces soil storage, evapotranspiration and streamflow in May through July in both Bear Trap and Big Sandy (Figure 3.5). Dividing the daily estimate of potential ET into soil storage availability shows the progression of the soil storage recession curve impacts ET rates, with greater impacts on Big Sandy than Bear Trap (Figure 3.5e, 3.5k). These results agree with Tague and Peng [2013], showing that ET response to temperature increases will depend on timing of snowmelt.

The response of snowmelt to the vegetation loss from wildfire in Big Sandy was much greater than in Bear Trap. LAI drives radiation attenuation [*Varhola and Coops*, 2013], and in RHESSys, radiation transferred through the canopy to the snowpack follows a Beer's Law type of exponential curve. In Bear Trap, LAI was reduced from 9.9 to 7.7 in the post-fire scenario, is within the saturated range of radiation absorption by the canopy, and is similar to previous reported LAI values for ponderosa pine forests in the area [*Goldstein and Hultman*, 2000; *Gersonde et al.*, 2004; *Campbell et al.*, 2009]. In Big Sandy, the LAI was reduced from 5.0 to 3.7, which is similar to previous LiDAR LAI estimates for the Sierra National Forest [*Zhao et al.*, 2012; *Tang et al.*, 2014]. The lower LAI in Big Sandy is within the exponential increase of radiation with changes in vegetation, resulting in snowpack patterns more similar to RCP 8.5 in 2100. The combination of reduced vegetation and elevated snowmelt led to the highest peak runoff in the post-fire scenario, compared to the control or climate projections.

Conclusions

Simulating the water balance response to temperature and vegetation perturbations showed the variability of precipitation, and vegetation changes from fuel treatments and wildfire, exerted a greater influence on annual evapotranspiration and runoff than temperature increases. Climate warming will eliminate the persistent seasonal snowpack at these elevations by 2100 in the RCP 8.5 projections, becoming rain-dominated as the amount of precipitation falling as snow is reduced from the current 40-60% down to 10-29%. The early snowmelt has cascading effects of the rate and timing of soil storage, evapotranspiration, and runoff. Increases in temperatures resulted in earlier peak runoff, but post-fire vegetation also increased peak runoff rates, especially in the American River headwaters. The highest temperature projections (+4.6^{o}C) begin to show increasing water loss through evapotranspiration in the American River headwaters, a region of high precipitation. In the more water-limited Merced River headwaters, evapotranspiration reductions in summer from the early snowmelt are greater than the elevated ET from

temperatures increases in the winter months, resulting in reduced annual ET by 2100 under both RCP 4.5 and 8.5 scenarios.

Acknowledgements

This is a SNAMP publication. The Sierra Nevada Adaptive Management Project (SNAMP) is funded by USDA Forest Service Region 5, USDA Forest Service Pacific Southwest Research Station, US Fish and Wildlife Service, California Department of Water Resources, California Department of Fish and Game, California Department of Forestry and Fire Protection, and the Sierra Nevada Conservancy. The authors would like to thank California Department of Water Resources, US Forest Service, Sierra Nevada Research Institute, and Sierra Nevada Adaptive Management Project personnel for their support and assistance. We acknowledge the World Climate Research Programme's Working Group on Coupled Modelling, which is responsible for CMIP, and we thank the climate modeling groups for producing and making available their model output. For CMIP the U.S. Department of Energy's Program for Climate Model Diagnosis and Intercomparison provides coordinating support and led development of software infrastructure in partnership with the Global Organization for Earth System Science Portals.

References

Agee, J. K., and C. N. Skinner (2005), Basic principles of forest fuel reduction treatments, For. Ecol. Manage., 211(1-2), 83–96, doi:10.1016/j.foreco.2005.01.034.

Bales, R. C., N. P. Molotch, T. H. Painter, M. D. Dettinger, R. Rice, and J. Dozier (2006), Mountain hydrology of the western United States, Water Resour. Res., 42(8), 1–13, doi:10.1029/2005WR004387.

Barbour, M., and R. Minnich (2000), California upland forests and woodlands, in North American Terrestrial Vegetation, edited by M. Barbour and W. Billings, pp. 159–200, Cambridge University Press.

Budyko, M. (1974), Climate and Life, Academic Press, San Diego, CA.

Campbell, J., G. Alberti, J. Martin, and B. E. Law (2009), Carbon dynamics of a ponderosa pine plantation following a thinning treatment in the northern Sierra Nevada, For. Ecol. Manage., 257(2), 453–463, doi:10.1016/j.foreco.2008.09.021.

Cayan, D. R., E. P. Maurer, M. D. Dettinger, M. Tyree, and K. Hayhoe (2008), Climate change scenarios for the California region, Clim. Change, 87(S1), 21–42, doi:10.1007/s10584-007-9377-6.

Christensen, L., C. L. Tague, and J. S. Baron (2008), Spatial patterns of simulated transpiration response to climate variability in a snow dominated mountain ecosystem, Hydrol. Process., 22(January), 3576– 3588, doi:10.1002/hyp.

Collins, B., S. Stephens, G. Roller, and J. Battles (2011), Simulating fire and forest dynamics for a landscape fuel treatment project in the Sierra Nevada, For. Sci., 57(2), 77–88.

Cristea, N. C., J. D. Lundquist, S. P. Loheide, C. S. Lowry, and C. E. Moore (2014), Modelling how vegetation cover affects climate change impacts on streamflow timing and magnitude in the snowmelt-dominated upper Tuolumne Basin, Sierra Nevada, Hydrol. Process., 28(12), 3896–3918, doi:10.1002/hyp.9909.

Dettinger, M. D., D. R. Cayan, M. K. Meyer, and A. E. Jeton (2004), Simulated Hydrologic Responses to Climate Variations and Change in the Merced, Carson, and American River Basins, Sierra Nevada, California, 1900–2099, Clim. Change, 62(1-3), 283–317, doi:10.1023/B:CLIM.0000013683.13346.4f.

Dixon, G. E. (2002), Essential FVS: A user's guide to the Forest Vegetation Simulator.

Internal Report, Fort Collins, CO: USDA Forest Service, Forest Management Service Center. 226p. (Revised: February 25, 2015).

Dore, S. et al. (2010), Carbon and water fluxes from ponderosa pine forests disturbed by wildfire and thinning, Ecol. Appl., 20(3), 663–683.

Dore, S., M. Montes-Helu, S. C. Hart, B. a. Hungate, G. W. Koch, J. B. Moon, A. J. Finkral, and T. E. Kolb (2012), Recovery of ponderosa pine ecosystem carbon and water fluxes from thinning and stand-replacing fire, Glob. Chang. Biol., 18(10), 3171–3185, doi:10.1111/j.1365-2486.2012.02775.x.

Duell, L. F. W. (1994), The sensitivity of northern Sierra Nevada streamflow to climate change, J. Am. Water Resour. Assoc., 30(5), 841–859.

Easterling, D. R. (1997), Maximum and Minimum Temperature Trends for the Globe, Science (80-.)., 277(5324), 364–367, doi:10.1126/science.277.5324.364.

Ellis, C. R., J. W. Pomeroy, R. L. H. Essery, and T. E. Link (2011), Effects of needleleaf forest cover on radiation and snowmelt dynamics in the Canadian Rocky Mountains, Can. J. For. Res., 41(3), 608–620, doi:10.1139/X10-227.

Essery, R., J. Pomeroy, C. Ellis, and T. Link (2008), Modelling longwave radiation to snow beneath forest canopies using hemispherical photography or linear regression, Hydrol. Process., 2800(June), 2788–2800, doi:10.1002/hyp.

Ficklin, D., S. Letsinger, I. Stewart, and E. Maurer (2015), Assessing differences in snowmelt-dependent hydrologic projections using CMIP3 and CMIP5 climate forcing data for the western United States, Hydrol. Res., doi:10.2166/nh.2015.101.

Ficklin, D. L., and B. L. Barnhart (2014), SWAT hydrologic model parameter uncertainty and its implications for hydroclimatic projections in snowmelt-dependent watersheds, J. Hydrol., 519(PB), 2081–2090, doi:10.1016/j.jhydrol.2014.09.082.

Finney, M. (2001), Design of regular landscape fuel treatment patterns for modifying fire growth and behavior, For. Sci., 47(2), 219–228.

Finney, M. (2004), FARSITE: fire area simulator-model development and evaluation, Washington DC.

Fry, D., J. Battles, B. Collins, and S. Stephens (2015), Sierra Nevada Adaptive Management Project Final Report, Appendix A - Fire and Forest Ecosystem Health Report.

Garfin, G., A. Jardine, R. Merideth, M. Black, S. LeRoy, and Eds. (2013), Assessment of Climate Change in the Southwest United States: A Report Prepared for the national Climate Assessment, Washington, DC: Island Press.

Gersonde, R., J. J. Battles, and K. L. O'Hara (2004), Characterizing the light environment in Sierra Nevada mixed-conifer forests using a spatially explicit light model, Can. J. For. Res., 34, 1332–1342, doi:10.1139/X04-013.

Goldstein, A., and N. Hultman (2000), Effects of climate variability on the carbon dioxide, water, and sensible heat fluxes above a ponderosa pine plantation in the Sierra Nevada (CA), Agric. For. …, 101, 113–129.

Hawthorne, S. N. D., P. N. J. Lane, L. J. Bren, and N. C. Sims (2013), The long term effects of thinning treatments on vegetation structure and water yield, For. Ecol. Manage., 310, 983–993, doi:DOI 10.1016/j.foreco.2013.09.046.

Huntington, J. L., and R. G. Niswonger (2012), Role of surface-water and groundwater interactions on projected summertime streamflow in snow dominated regions: An integrated modeling approach, Water Resour. Res., 48(11), W11524, doi:10.1029/2012WR012319.

Jarvis, P. (1976), The interpretation of the variations in leaf water potential and stomatal conductance found in canopies in the field, Philos. Trans. R. Soc. London, 273(927), 593–640.

Jefferson, A., A. Nolin, S. Lewis, and C. Tague (2008), Hydrogeologic controls on streamflow sensitivity to climate variation, Hydrol. Process., 4385(June), 4371–4385, doi:10.1002/hyp.

Jeton, A. E., M. D. Dettinger, and J. L. Smith (1996), Potential Effects of Climate Change on Streamflow , Eastern and Western Slopes of the Sierra Nevada , California and Nevada, Sacramento, CA.

Knowles, N. (2002), Potential effects of global warming on the Sacramento/San Joaquin watershed and the San Francisco estuary, Geophys. Res. Lett., 29(18), 2–5, doi:10.1029/2001GL014339.

Lundquist, J. D., S. E. Dickerson-Lange, J. a. Lutz, and N. C. Cristea (2013), Lower forest density enhances snow retention in regions with warmer winters: A global framework developed from plot-scale observations and modeling, Water Resour. Res., 49(4), n/a–n/a, doi:10.1002/wrcr.20504.

Mahat, V., and D. G. Tarboton (2012), Canopy radiation transmission for an energy balance snowmelt model, Water Resour. Res., 48(1), W01534, doi:10.1029/2011WR010438.

Meyers, E. M., B. Dobrowski, and C. L. Tague (2010), Climate Change Impacts on Flood Frequency , Intensity , and Timing May Affect Trout Species in Sagehen Creek , California, Trans. Am. Fish. Soc., 1657–1664, doi:10.1577/T09-192.1.

Millar, C. I., N. L. Stephenson, and S. L. Stephens (2007), Climate change and forests of the future : Managing in the face of uncertainty, Ecol. Appl., 17(8), 2145–2151, doi:10.1890/06-1715.1.

Miller, N. L., K. E. Bashford, and E. Strem (2003), Potential impacts of climate change of California hydrology, J. Am. Water Resour. Assoc., 39(4), 771–784, doi:10.1111/j.1752-1688.2003.tb04404.x.

Moeser, D., M. Stahli, and T. Jonas (2015), Improved snow interception modeling using cnaopy parameters derived from airborn LiDAR data, Water Resour. Res., 51, 5041–5059, doi:10.1002/2014WR016724.

Molotch, N. P., and L. Meromy (2014), Physiographic and climatic controls on snow cover persistence in the Sierra Nevada Mountains, Hydrol. Process., 28(16), 4573–4586, doi:10.1002/hyp.10254.

Pupacko, A. (1993), Variations in Northern Sierra Nevada Streamflow: Implications of Climate Change, J. Am. Water Resour. Assoc., 29(2), 283–290, doi:10.1111/j.1752-1688.1993.tb03208.x.

Reinhardt, E., and N. Crookston (2003), The fire and fuels extension to the forest vegetation simulator. RMRS-GTR-116, Ogden, UT.

Risbey, J. S., and D. Entekhabi (1996), Observed Sacramento Basin streamflow response to precipitation and temperature changes and its relevance to climate impact studies, J. Hydrol., 184, 209–223.

Romero-Lankao, P., J. B. Smith, D. J. Davidson, N. S. Diffenbaugh, P. L. Kinney, P. Kirshen, P. Kovacs, and L. V. Ruiz (2014), North America, in Climate Change 2014: Impacts, Adaptation, and Vulnerability. Part B: Regional Aspects. Contribution of Working Group II to the Fifth Assessment Report of the Intergovernmental Panel on Climate Change, edited by V. R. Barros et al., pp. 1439–1498, Cambridge University Press, Cambridge, UK and New York, NY.

Shaw, G. D., M. H. Conklin, G. J. Nimz, and F. Liu (2014), Groundwater and surface water flow to the Merced River, Yosemite Valley, California: ^{36}Cl and Cl^- evidence, Water Resour. Res., 50, 1943–1959, doi:10.1002/2013WR014222.Received.

Stephens, S. L. (1998), Evaluation of the effects of silvicultural and fuels treatments on potential fire behaviour in Sierra Nevada mixed-conifer forests, For. Ecol. Manage., 105(1-3), 21–35, doi:10.1016/S0378-1127(97)00293-4.

Stewart, I. T., D. R. Cayan, and M. D. Dettinger (2004), Changes in snowmelt runoff timing in western North America under a "business as usual" climate change scenario, Clim. Change, 62, 217–232.

Storck, P., D. P. Lettenmaier, and S. M. Bolton (2002), Measurement of snow interception and canopy effects on snow accumulation and melt in a mountainous maritime climate, Oregon, United States, Water Resour. Res., 38(11), 1123.

Su, Y., Q. Guo, D. L. Fry, B. M. Collins, M. Kelly, J. P. Flanagan, and J. J. Battles (2015), A new vegetation mapping strategy for conifer forests by combining airborne lidar data and aerial imagery, For. Ecol. Manage., in review.

Tague, C., and G. E. Grant (2009), Groundwater dynamics mediate low-flow response to global warming in snow-dominated alpine regions, Water Resour. Res., 45(7), 1–12, doi:10.1029/2008WR007179.

Tague, C., and H. Peng (2013), The sensitivity of forest water use to the timing of precipitation and snowmelt recharge in the California Sierra: Implications for a warming climate, J. Geophys. Res. Biogeosciences, 118(2), 875–887, doi:10.1002/jgrg.20073.

Tague, C. L., and L. E. Band (2004), RHESSys: Regional Hydro-Ecologic Simulation System—An Object-Oriented Approach to Spatially Distributed Modeling of Carbon, Water, and Nutrient Cycling, Earth Interact., 8(19), doi:http://dx.doi.org/10.1175/1087-3562(2004)8<1:RRHSSO>2.0.CO;2.

Tang, H., M. Brolly, F. Zhao, A. H. Strahler, C. L. Schaaf, S. Ganguly, G. Zhang, and R. Dubayah (2014), Deriving and validating Leaf Area Index (LAI) at multiple spatial scales through lidar remote sensing: A case study in Sierra National Forest, CA, Remote Sens. Environ., 143, 131–141, doi:10.1016/j.rse.2013.12.007.

Varhola, A., and N. C. Coops (2013), Estimation of watershed-level distributed forest structure metrics relevant to hydrologic modeling using LiDAR and Landsat, J. Hydrol., 487, 70–86, doi:10.1016/j.jhydrol.2013.02.032.

Vose, R. S., D. R. Easterling, and B. Gleason (2005), Maximum and minimum temperature trends for the globe: An update through 2004, Geophys. Res. Lett., 32(23), 1–5, doi:10.1029/2005GL024379.

van Vuuren, D. P. et al. (2011), The representative concentration pathways: An overview, Clim. Change, 109(1), 5–31, doi:10.1007/s10584-011-0148-z.

Westerling, A. L., H. G. Hidalgo, D. R. Cayan, and T. W. Swetnam (2006), Warming and earlier spring increase western U.S. forest wildfire activity., Science, 313(5789), 940–3, doi:10.1126/science.1128834.

Wigmosta, M. S., L. W. Vail, and D. P. Lettenmaier (1994), A distributed hydrology-vegetation model for complex terrain, Water Resour. Res., 30(6), 1665, doi:10.1029/94WR00436.

Wilby, R. L., and I. Harris (2006), A framework for assessing uncertainties in climate change impacts: Low-flow scenarios for the River Thames, UK, Water Resour. Res., 42(2), 1–10, doi:10.1029/2005WR004065.

Young, C., M. Escobar_Arias, M. Fernandes, B. Joyce, M. Kiparsky, J. Mount, V. Mehta, D. Purkey, J. Viers, and D. Yates (2009), Modeling the hydrology of climate change in California's Sierra Nevada for subwatershed scale adaptation1, J. Am. Water Resour. Assoc., 45(6), 1409–1423.

Zhang, L., W. R. Dawes, and G. R. Walker (2001), Response of mean annual evapotranspiration to vegetation changes at catchment scale, Water Resour. Res., 37(3), 701–708.

Zhao, F. et al. (2012), Measuring gap fraction, element clumping index and LAI in Sierra Forest stands using a full-waveform ground-based lidar, Remote Sens. Environ., 125, 73–79, doi:10.1016/j.rse.2012.07.007.

Table 3.1. Mean daily temperatures for the months of highest precipitation (Nov-Apr) and the fraction of precipitation falling as snow under each climate scenario.

		2013	RCP 4.5 2050	RCP 4.5 2100	RCP 8.5 2050	RCP 8.5 2100
Bear Trap	November – April mean temperature	4.3°C	5.5°C	5.9°C	6.1°C	8.8°C
	Mean annual snow fraction	0.40	0.33	0.27	0.29	0.10
Big Sandy	November - April mean temperature	4.3°C	5.3°C	5.7°C	5.9°C	8.7°C
	Mean annual snow fraction	0.60	0.57	0.53	0.54	0.29

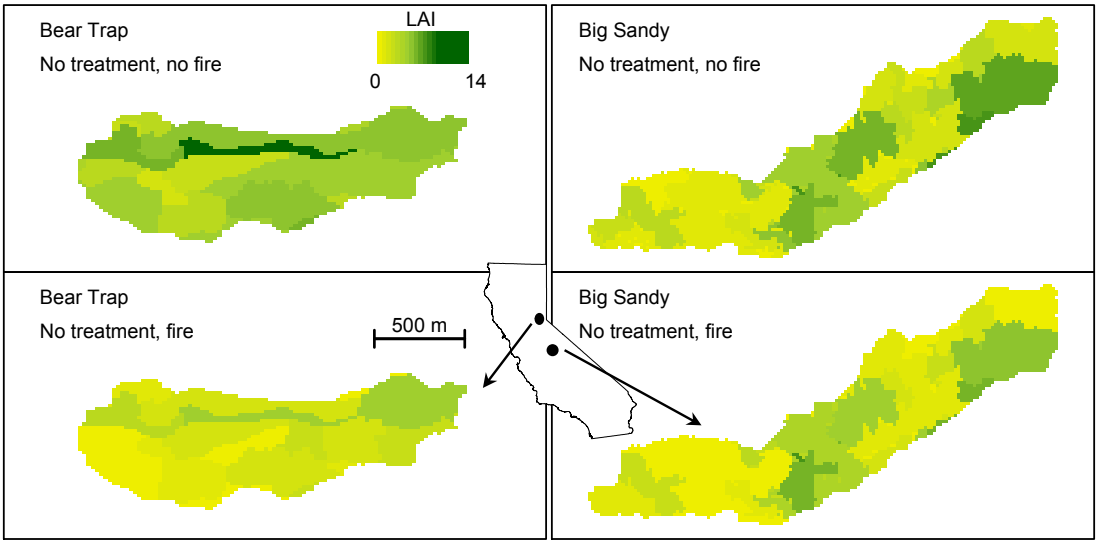

Figure 3.1. Leaf Area Index (LAI) values in the Bear Trap and Big Sandy catchments in the highest (no treatment, no fire) and lowest (no treatment, fire) vegetation density scenarios.

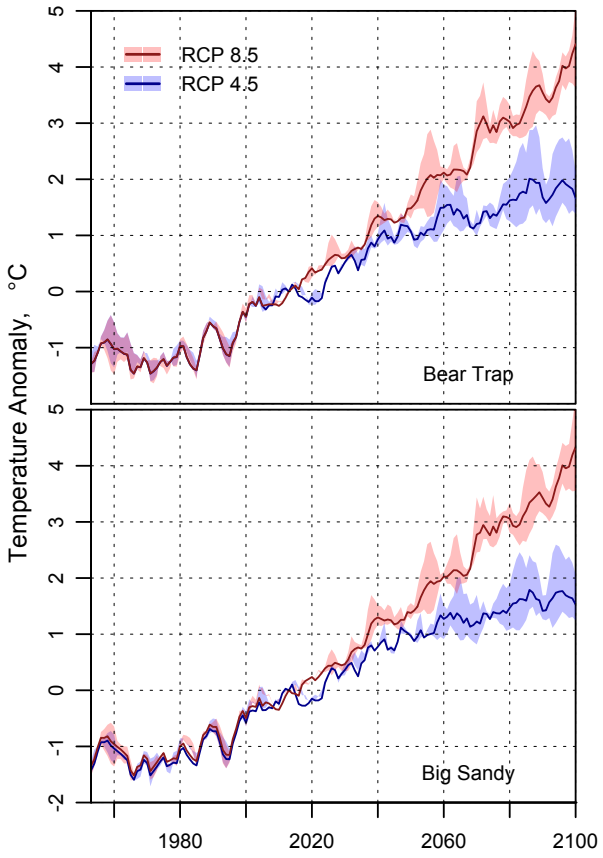

Figure 3.2. Climate scenario temperature anomalies based on the 2010 to 2013 four-year mean. Each line connects data points for annual mean temperature anomalies calculated as a four-year trailing mean from 1950 to 2100. Shaded areas note the range of daily minimum and maximum temperature anomalies from the two climate scenarios used to calculate the mean.

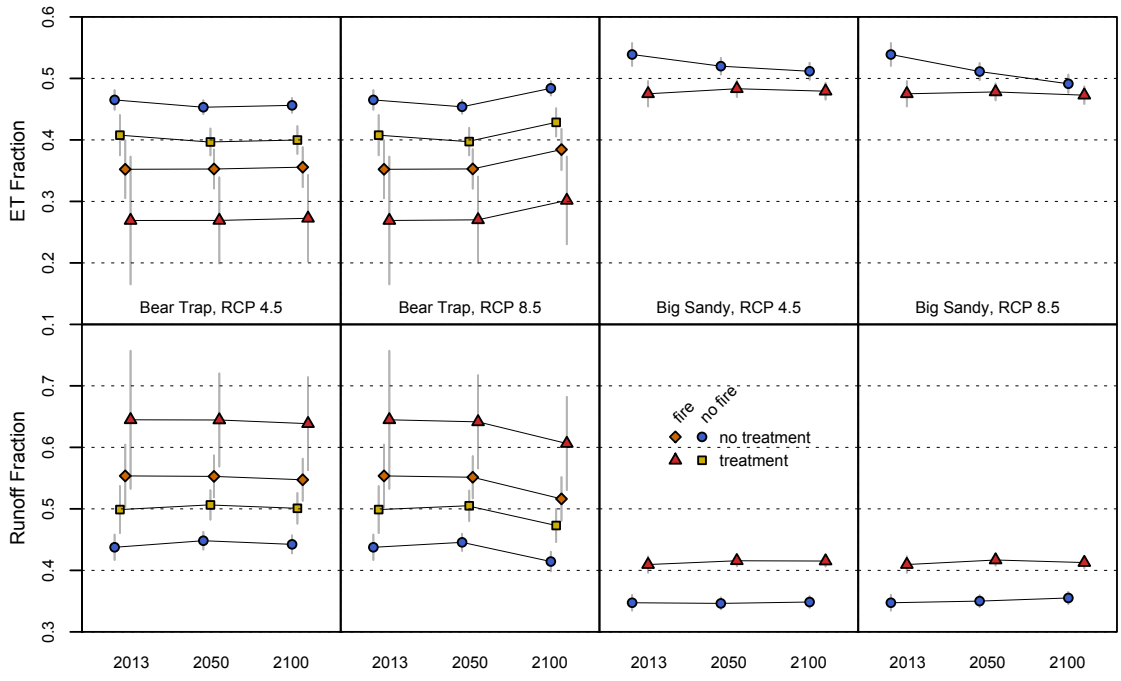

Figure 3.3. Simulation results of the runoff and evapotranspiration fractions for vegetation scenarios and projected temperature increase in 2050 and 2100. Vegetation structures in Big Sandy treatment, with and without fire, were not different than the no treatment scenarios and are not shown. Simulations were completed for water year 2010-13 conditions, during which mean precipitation was 199 cm in Bear Trap and 130 cm in Big Sandy. Vertical bars indicate the 95% confidence interval based on the multiple parameter sets for each catchment.

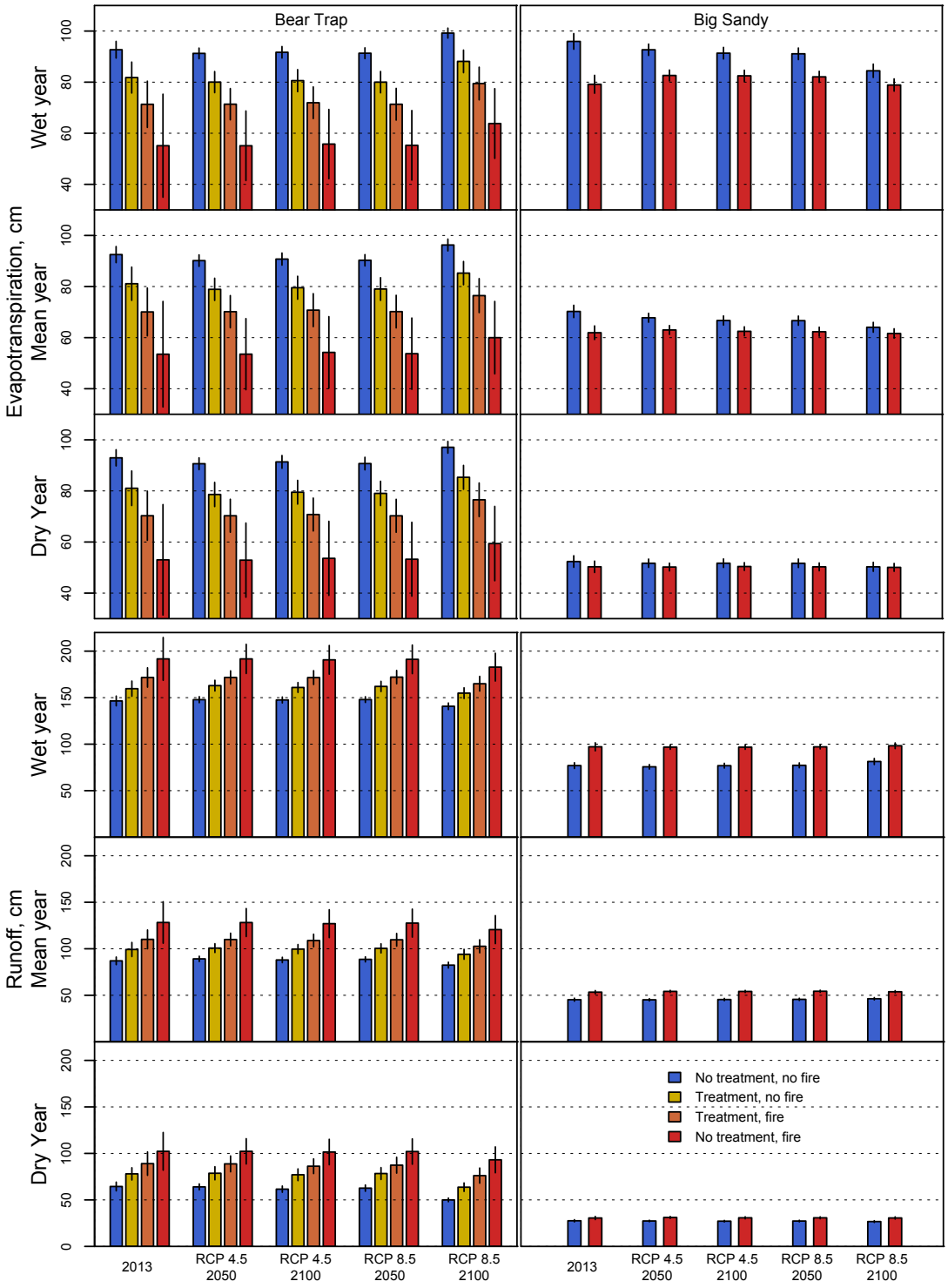

Figure 3.4. Evapotranspiration and runoff rates of forest disturbance scenarios during dry (2012), mean (all years), and wet (2011) precipitation conditions for current and projected temperatures. Big Sandy vegetation treatments were not different than having no treatment and are not shown.

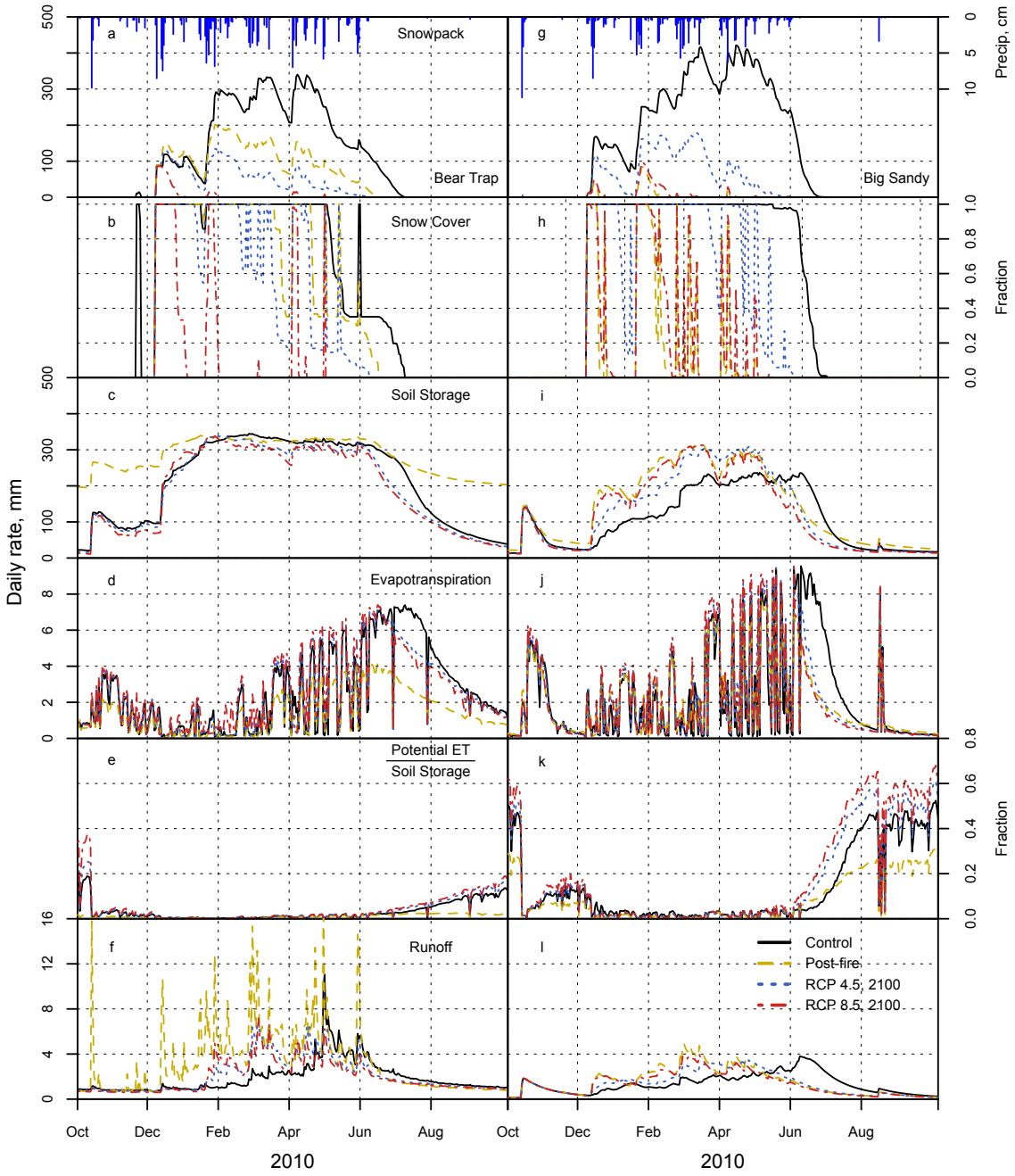

Figure 3.5. Daily rates of snow storage (a,g), basin snow cover fraction (b,h), soil storage (c,i), evapotranspiration (d,j), potential evapotranspiration divided by soil storage (e,k), and stream discharge (f,l) in the Bear Trap and Big Sandy catchments with vegetation and temperature perturbations. Vegetation densities are from control and post-fire conditions, and temperature increases are from year 2100 projections with RCP 4.5 and 8.5 climate scenarios.

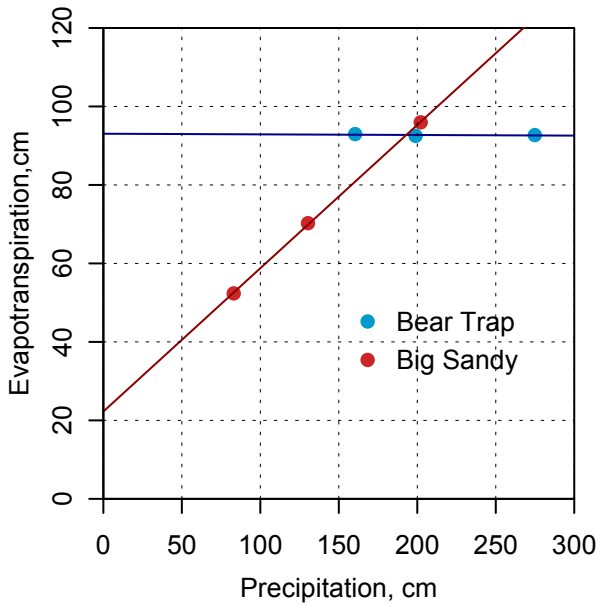

Figure 3.6. Annual evapotranspiration as a function of dry to wet precipitation conditions in Bear Trap and Big Sandy. Forest vegetation was constant (pre-treatment), with fitted lines highlighting the different trends between the two catchments.

Summary Conclusion

Study Results

Paired headwater catchments in the mixed-conifer zone of the American and Merced River basins were selectively thinned in 2012. Distributed observations of snow storage, soil storage, and stream discharge from 2010 to 2013 were used to calculate the annual water balance and constrain a hydro-ecologic model (RHESSys). Forest thinning effects were simulated using changes in Leaf Area Index, canopy cover, and shrub cover. In the American basin, model results show runoff increased of 14% in response to reductions in Leaf Area Index (-8%), canopy cover (-3%), and shrub cover (-4%). In the Merced basin catchment, treatments had little impact on forest structure or runoff, as vegetation growth in areas not thinned offset reductions from treatments. Observed treatment effects on runoff could not be confirmed in either basin because of the high variability in precipitation in annual precipitation and the low 2013 post-treatment precipitation. When forest thinning is intensive enough to change forest structure, model results show the low-magnitude vegetation reductions can modify catchment-scale water balance in the high-precipitation region of the American River basin. Given the short study period and climate variability, modeling tools were necessary to determine vegetation treatment impacts on the water balance. Hydrologic modeling, constrained by multiple data points, provides a confident and useful tool for analyzing watershed response to forest thinning.

We used the eco-hydrologic model (RHESSys) calibrated with spatially distributed field measurements to assess the impacts of forest fuels treatments and wildfire on hydrologic fluxes in Sierra Nevada firesheds. Fuels treatments were implemented during 2011-2012 in the American River and Lewis Fork watersheds. This study uses the measured vegetation change from treatments and the results from wildfire modeling of vegetation change to determine impacts on catchment water balance. A well-constrained headwater model is used to determine how annual hydrologic fluxes respond to vegetation changes from treatments and fires in these larger firesheds, based on geologic and hydrologic similarities. Treatments in the American River resulted in a vegetation decrease of 8%, leading to a 13% runoff increase. Wildfire with and without treatments

reduced vegetation by 38% and 50%, increasing runoff by 55% and 67%, respectively. Treatments in Lewis Fork also reduced vegetation by 8%, but the runoff response was limited to an increase of less than 3% compared to no treatment. Wildfire with and without treatments reduced vegetation by 40% and 43%, increasing runoff by 13% and 15% respectively. The results suggest that forest vegetation in Lewis Fork is more water-limited than in the American, where treatments had a greater impact on the water balance. Changes to catchment-scale water balance simulation were more sensitive to canopy cover than Leaf Area Index, indicating the pattern and location of vegetation treatments is more important than the total amount of biomass removed.

Forested watersheds in the Sierra Nevada are sensitive to the influence of a warming climate, where increased temperatures elevate the amount of precipitation falling as rain and reduce the natural water storage that exists in the winter snowpack. We used the hydro-ecologic model (RHESSys) constrained by runoff, distributed snow, and distributed soil moisture measurements, to simulate the impacts of projected temperature increases and forest disturbance on two headwater catchments in the central and southern Sierra. Increasing temperatures were projected for Representation Concentration Pathways (RCP) 4.5 and 8.5 at 2050 and 2100, and combined with forest thinning treatments and wildfire events to investigate interacting effects of external climate forcing and internal vegetation dynamics on snowpack, evapotranspiration, and runoff. The results presented here show that although future climate forcings will reduce the fraction of precipitation falling as snow, and the winter seasonal snowpack storage, the variability of interannual precipitation and vegetation perturbations from fuel treatments and wildfire will likely exert a greater influence on annual evapotranspiration and runoff.

Major Findings

This study showed that the location and intensity of fuels treatments will affect the magnitude of water balance response. Intensive treatments, including changes in canopy cover, will affect catchment-scale evapotranspiration and runoff, even when treatments are implemented over a small fraction of the watershed. Treatments were more intensive in the American compared to Lewis Fork, where the 8% LAI reduction in both basins

was a result of treating only 24% and 30% of the area. Vegetation change was higher in the treated areas of the American, including greater reductions in canopy cover. The higher localized vegetation change, combined with the higher precipitation, resulted in the significant runoff increase of 12% in the American.

Temperature increases for the highest magnitude of temperature warming, Representative Concentration Pathway 8.5, resulted in opposite responses in the American and Merced headwaters. Annual evapotranspiration increased in the American, associated with higher winter temperatures leading to increased evapotranspiration. In the Merced, however, decreases in late-spring evapotranspiration were greater than winter increases, leading to the decrease in annual evapotranspiration. As the Sierra Nevada transitions to warm temperatures in the coming century, the persistence of snowpack will determine the timing of the soil storage recession curve and water availability for vegetation during the spring period of highest potential evapotranspiration. The relative increases in winter seasonal evapotranspiration from warmer temperatures and decreases in spring from earlier soil storage recession will determine the runoff response in Sierra Nevada mid-elevation watersheds.

Uncertainties

Sources of uncertainty for simulating watershed hydrologic response to vegetation and climate disturbances are described in the first chapter, and can originate from environmental measurements used to run and evaluate the eco-hydrologic model, spatially explicit soil and vegetation data, RHESSys model structure, and external model results of forest growth and climate projections to simulate watershed hydrologic response.

The distributed measurement of snow depth and soil moisture were intended to capture the spatial variability of water storage in the snow and soil, and provide some estimate of variation on the modeled landscape. The multiple parameter sets used for each watershed model were also intended to provide a range of potential responses to

each scenario of vegetation and climate disturbance. Land managers can use the range of projected outcomes to make more informed decisions about the effects of management activities by having the ability to assess different approaches if the minimum or maximum projected response were to occur. The two climate models used for projecting the range of expected climate warming were designed to capture a range of temperature increases. The additional uncertainty in simulations of projected RCP 4.5 and RCP 8.5 temperature projections are shown in the expanded range of expected outcomes within the 95% confidence intervals in chapter 3.

Singh and Woolhiser [2002] note that error propagation through model processes is not well explored, suggesting further error analysis be developed to give even greater confidence in results, and will be necessary for models to become a practical tool. I have used a range of measurements and model predictions to account for environmental variability and model projection uncertainty, but the next progression of this research should include explicitly investigating error propagation, as the overall goal of these modeling efforts is to develop a tool that land managers can incorporate into their landscape management planning. Guo et al. [2008] suggest a probability distribution function approach to account for error propagation in spatial data applications, to be used in situations where data is not normally distributed or where standard errors cannot be calculated for all error sources.

Management Implications

The structure and density of forested watersheds in the Sierra Nevada impacts snowpack persistence, evapotranspiration loss, and runoff from precipitation. The contribution and fractioning of precipitation into these separate processes depends on annual precipitation and individual catchment physiography. Distributed measurements of snowpack and soil moisture in the rain-snow transition zone, combined with discharge measurements, were successful in developing a modeling tool that can be used in

estimating water balance response to projections of forest management and vegetation disturbance in the southern- and central-Sierra Nevada. The hydrologic model in this study was able contend with the short study period, high precipitation variability, and low post-treatment precipitation, to estimate evapotranspiration and runoff response over a range of vegetation densities.

Modeling tools cannot be developed, however, without the measurements required for constraining model estimates, and verification of projected responses. The highly variable range of snow depth and soil moisture values measured around the meteorological stations and stream discharge sites suggests distributed measurements are needed for representative observations. The snow depth survey around Duncan Peak found that the distributed measurements were successful at capturing a representative mean value, but also that only capturing a few measurements could lead to reporting non-representative high or low snow depth estimates. The inability to produce a calibrated model for two of the four-headwater basins suggests exactly that result. Although we were able to replicate the snow accumulation and ablation patterns we measured in our model simulations, the modeled stream discharge estimates did not match the observed values, suggesting a different snowmelt pattern or groundwater – surface water interactions within the basins than at the four locations we measured.

Model simulations suggest that treatments as implemented would increase runoff in the high precipitation region of Last Chance, but either treating a broader area or greater vegetation reductions over the same area may be necessary to measurably increase runoff in Sugar Pine. Given the single dry year of post-treatment precipitation, we were unable to verify the projected increases in runoff that the modeling estimated. Verification of responses would require long-term monitoring, to capture the range of precipitation conditions expected in this region of Mediterranean climate, with periodic sequences of multiple wet or dry years. The stage-discharge relationship method we use is a common low-cost method used in hydrology research, but measurements that are more precise may be necessary to better capture effects of vegetation change for the wide range of interannual precipitation and stream discharge conditions present in the

Mediterranean climate of the Sierra Nevada. Model sensitivity results also showed that forest disturbances would affect runoff the greatest during high-flow periods, which would likely exceed the established stage-discharge rating curves. The high-intensity fires modeled in this study can result in greater vegetation reductions and lead to increased runoff, however these results did not address potentially adverse issues related to these wildfires such as soil erosion into the stream channel, hydrophobic soils, and elevated snowmelt rates.

References

Guo, Q., Y. Liu, and J. Wieczorek (2008), Georeferencing locality descriptions and computing associated uncertainty using a probabilistic approach, Int. J. Geogr. Inf. Sci., 22(10), 1067–1090, doi:10.1080/13658810701851420.

Singh, V., and D. Woolhiser (2002), Mathematical modeling of watershed hydrology, J. Hydrol. Eng., 7(4), 270–292.

Appendix 1. Headwater and fireshed comparative analysis of geologic composition and hydrologic characteristics.

This analysis, and the upscaling methodology used in chapter 2, was completed by Ben Tobin, formerly a postdoctoral researcher at UC Merced and currently hydrologist for the Grand Canyon National Park.

The stream outlets draining the study firesheds were not gaged due to the remote and steep terrain. The only monitored stream discharge site directly downstream from the firesheds drains the entire North Fork of the Middle Fork of the American River, an area of 230.2 km^2 of which 43.2% are the study firesheds. Initial comparison of flow duration curves for the two headwater streams and the North Fork of the Middle Fork of the American River (NFMF) showed that headwaters and downstream sites have differing distributions of flow probabilities (Figure A1.1). This suggests that during these conditions flow at different scales and between basins is controlled by different flow paths or paths with different flow lengths. However, as flow drops below the 20^{th} percentile, the slope of the line representing the relationship between discharge and probability becomes more similar between headwaters and the NFMF. This suggests that the behavior of these headwater basins becomes more similar to the hydrologic behavior of the NFMF, until flow probabilities increases to above 90%, where discharge values for Frazier drop rapidly. This drop is due to the stream become ephemeral during extreme drought conditions in 2013. As flow decreases, the relative contribution of the two headwaters to discharge from the entire basin increases from approximately one percent to over four percent, showing the importance of these headwaters during low flow conditions (Figures A1.2, A1.3).

A direct comparison of area-normalized discharge between each headwater stream and the NFMF did not show a strong correlation between the headwaters and downstream sites (Figure A1.4). However, using the predictive format of linear regression models with the full discharge record for the headwater streams, the headwaters acted as predictors for downstream stream discharge and were highly significant for all three models tested (Table A1.1). Bear Trap discharge explained more of the variability in the

North Fork of the Middle Fork of the American River than Frazier, however, the combination of the two basins was shown to be the best fit model using AIC (Table A1.1). This model explained 63.7% of the variability in the downstream discharge for the entire available data record.

When looking specifically at low flow conditions, a stronger relationship is seen between the basins. During low flow conditions, Frazier explains more of the variability in the downstream discharge than Bear Trap, however model selection again shows that the linear regression model using both headwater streams provided the best fit (Table A1.2). The combined regression model explains 93.2% of the variability seen in the NFMF area normalized discharge data. This suggests that during low flow and baseflow conditions, the headwaters and full basin have statistically similar behavior.

Flow Durations curves for the Sugar Pine sites show a similar relationship to those seen in the Last Chance sites (Figure A1.5). During high flow conditions, both headwater streams and the Lewis Fork of the Fresno show very different flow probabilities. However, as flow probability decreases below 20%, the slopes of the curves become more similar. The data for the Lewis Fork has a lower resolution and is likely affected by water withdrawals during the upper portions of the flow duration curve [*California Environmental Protection Agency*, 2014], which combined to reduce the similarity of the Lewis Fork to the headwater streams, although a relationship is still present. Additionally, a comparison of the hydrographs of the headwaters and the Lewis Fork show that peak discharge and subsequent recessions occurred at approximately the same time at both scales (Figure A1.6).

A direct comparison of area-normalized discharge between each headwater stream and the Lewis Fork did not show a strong correlation between the headwaters and downstream sites (Figure A1.7). However, these hydrograph comparisons between the headwater sites and the Lewis Fork of the Fresno River were complicated by a number of factors including (1) numerous active water withdrawals upstream of the gaged site on the Lewis Fork, (2) low resolution of the Lewis Fork data during low flow conditions (data was recorded in cubic feet per second with no decimal places), and (3) the

headwater streams flow into the Merced River and are not hydrologically associated with the firesheds or the Lewis Fork of the Fresno River. These complications have likely resulted in lower correlations between headwater streams and the downstream discharge site. However, the regression analysis between discharge of the headwater streams (predictor variables) and discharge of the Lewis Fork (response) still show a similar pattern to those seen in the Last Chance sites. During the period of available data, the combined discharges of Big Sandy and Speckerman were seen to be the best fit model for discharge in the Lewis Fork (Table A1.3) and explained 43.5% of the variability in Lewis Fork Discharge.

During low flow conditions, the combined model is again the best fit and the ability of the headwater discharge values to predict Lewis Fork discharge increases and is able to explain 61% of the variability of the Lewis Fork of the Fresno River (Table A1.4). This model is not as good a fit as that seen for the Last Chance sites due to a combination of the low resolution of the data and the large number of water withdrawals upstream of the site. Using these methods, it was determined that Bear Trap Creek and Big Sandy Creek, both treated headwaters, would be the preferred catchments for transferring model parameters to the ungaged firesheds for flow storage and routing in the RHESSys model.

Table A1.1. Results of AIC analysis of regression model between listed variables and discharge of the North Fork of the Middle Fork of the American River.

Variables	*K*	*AIC*	*Akaike Weight*	r^2
BTP	3	6973.33	4.4×10^{-16}	0.618
FRZ	3	7393.36	2.7×10^{-107}	0.491
BTP + FRZ	4	6902.602	0.999	0.637

Table A1.2. Results of the AIC analysis of the regression model between listed variables and discharge of the North Fork of the Middle Fork of the American River during low flow conditions.

Variables	*K*	*AIC*	*Akaike Weight*	r^2
BTP	3	-914.15	9.1×10^{-100}	0.835
FRZ	3	-1307.62	2.5×10^{-14}	0.919
BTP+FRZ	4	-1370.25	1	0.932

Table A1.3. Results of AIC analysis of regression model between listed variables and discharge of the Lewis Fork of the Fresno River.

Variables	*K*	*AIC*	*Akaike Weight*	r^2
BSN	3	404.76	0.002	0.425
SPK	3	496.01	3.3×10^{-23}	0.352
BSN+SPK	4	392.49	0.997	0.435

Table A1.4. Results of AIC analysis of regression model between listed variables and discharge of the North Fork of the Middle Fork of the American River during low flow conditions.

Variables	*K*	*AIC*	*Akaike Weight*	r^2
BSN	3	-955.50	6.3×10^{-15}	0.593
SPK	3	-1005.93	5.6×10^{-4}	0.528
BSN+SPK	4	-1020.91	0.999	0.610

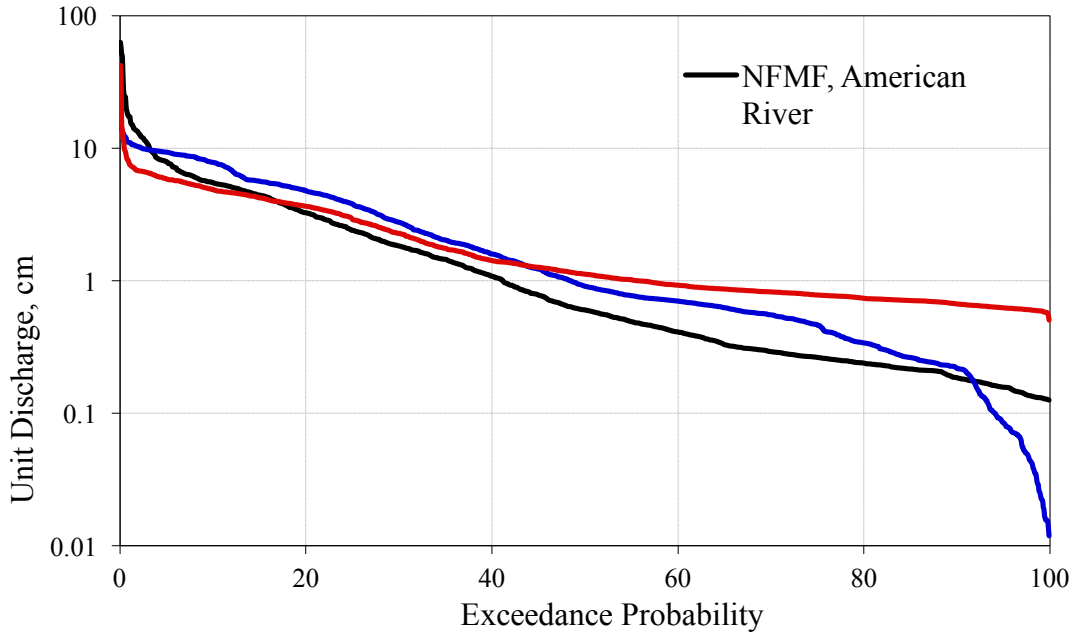

Figure A1.1. Last Chance flow duration curves for the North Fork of the Middle Fork (NFMF) of the American River, Frazier Creek, and Bear Trap Creek. Discharge is normalized over the watershed area.

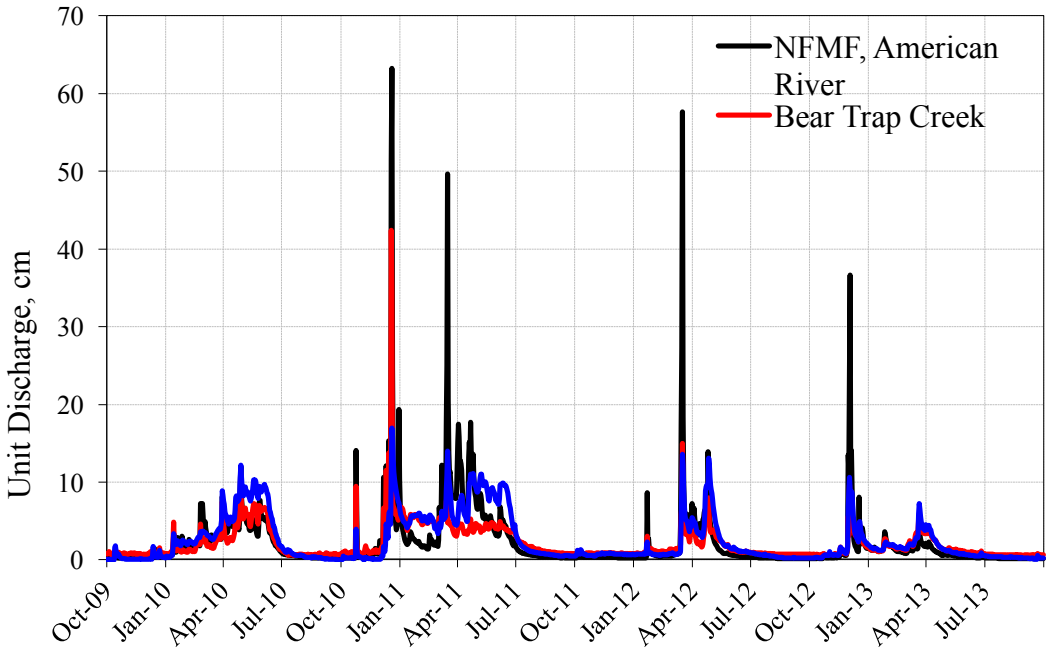

Figure A1.2. Last Chance discharge for the North Fork of the Middle Fork (NFMF) of the American River, Frazier Creek, and Bear Trap Creek. Discharge is normalized over the watershed area.

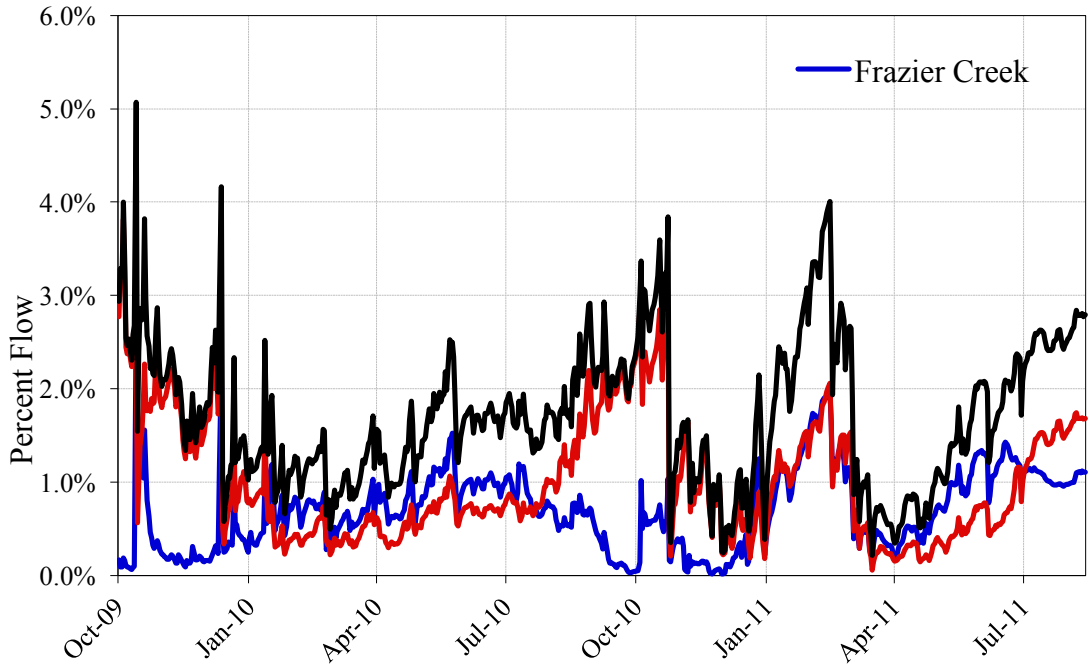

Figure A1.3. Percent contribution of headwater catchments to flow in the North Fork of the Middle Fork of the American River.

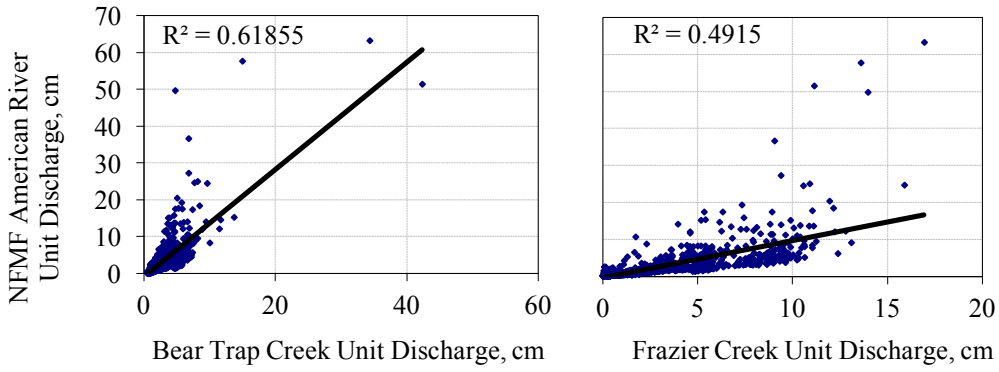

Figure A1.4. Linear relationships of area-normalized discharge for Bear Trap and Frazier Creek headwater catchments to the North Fork of the Middle Fork (NFMF) of the American River.

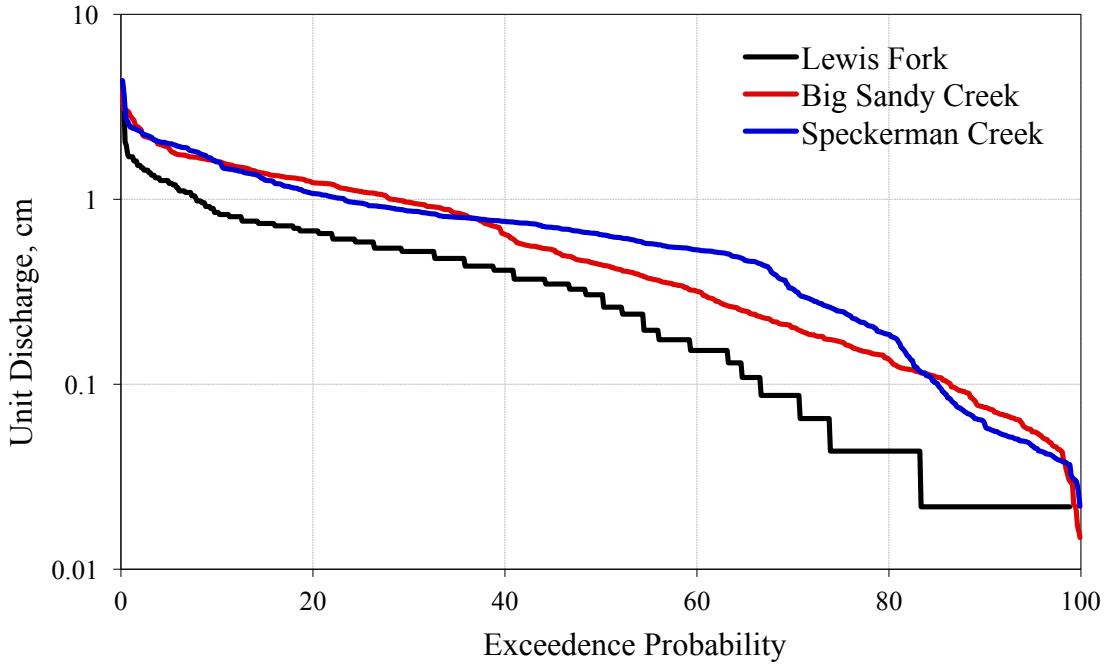

Figure A1.5. Flow Duration Curves of the Lewis Fork of the Fresno River, Big Sandy Creek, and Speckerman Creek. Discharge is normalized over the watershed area.

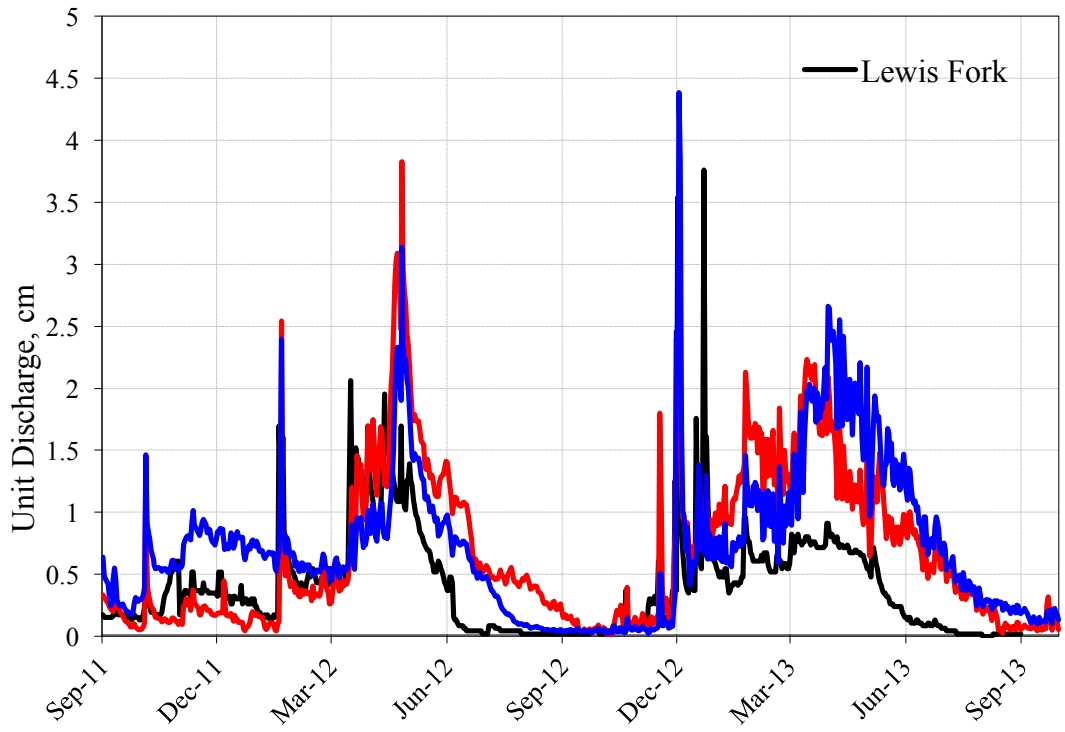

Figure A1.6. A comparison of area-normalized discharge for the headwater sites and the Lewis Fork of the Fresno River. Note: headwater sites do not flow into the Lewis Fork and thus a relative contribution plot was not created.

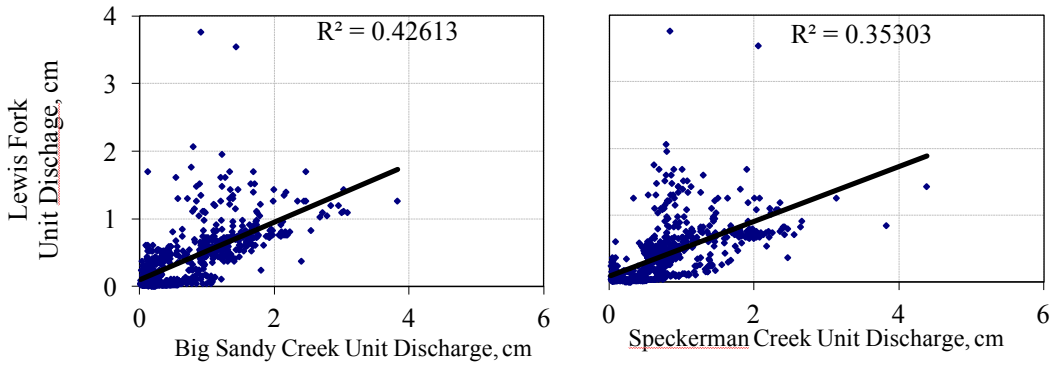

Figure A1.7. Linear relationships area-normalized discharge (cm) of Big Sandy and Speckerman Creek to Lewis Fork Creek.

Appendix 2. Supplemental tables of fireshed vegetation composition.

Table A2.1. Tree species composition of the vegetation community types in the American. Specific Leaf Area (SLA) of each species is also given and used with the percent basal area of each species to calculate SLA for each community type, similar to Jones *et al.* [2015].

Species	SLA, $m^2\ kg^{-1}\ C^{-1}$	Species contribution to forest type, percent				
		true fir forest, open	pine-fir forest, sparse cover	cedar-white fir mixed conifer forest, medium cover	mixed conifer forest, medium cover	mixed conifer forest, high cover
Abies concolor	8.0	37	25	39	25	34
Abies magnifica	6.7	19	15	1	1	5
Calocedrus decurrens	8.9	0	0	12	9	8
Cornus nuttallii	32.0	0	0	0.0	0	0
Quercus agrifolia	32.0	0	0	0.0	0	0
Pinus lambertiana	11.1	0	16	17	20	20
Pinus monticola	11.1	6	2	0	0	0
Pseudotsuga menziesii	12.2	17	16	15	20	19
Pinus ponderosa	8.1	21	26	14	23	11
Quercus kelloggii	32.0	0.0	0	1	2	3
Dequoiadendron giganteum	8.9	0.0	0	1	0	0
		Aggregate quantities				
SLA weighted mean, ($m^2\ kg^{-1}\ C^{-1}$)		8.7	9.0	9.5	10.1	10.1
Mean canopy cover fraction		0.390	0.384	0.480	0.458	0.562
Basal area, $m^2\ ha^{-1}$		2.2	10.4	17.1	24.3	45.1
Percent of area		1.7	2.7	5.4	5.9	84.3

Table A2.2. Tree species composition of the vegetation community types in Lewis Fork. Specific Leaf Area (SLA) of each species is also given and used with the percent basal area of each species to calculate SLA for each community type, similar to Jones *et al.* [2015]

		Species contribution to forest type, percent			
Species	SLA, $m^2\ kg^{-1}\ C^{-1}$	Open pine-oak woodland	Live oak-pine forest	Mature mixed conifer forest	Closed-canopy mixed conifer forest
Abies concolor	8	0	0	26	28
Calocedrus decurrens	8.9	0	4	33	39
Pinus lambertiana	11.1	0	0	9	16
Pinus ponderosa	8.1	51	30	18	13
Quercus Kelloggii	32	49	10	9	3
Quercus wislizeni	32	0	43	0	0
		Aggregate quantities			
SLA weighted mean, $m^2\ kg^{-1}\ C^{-1}$		19.8	19.7	10.4	9.5
Mean canopy cover fraction		0.173	0.436	0.677	0.8
Basal area $m^2\ ha^{-1}$		11.6	12.9	48	80.2
Percent of area		0.0	5.9	88.2	5.9

Appendix 3. Sierra Nevada Adaptive Management Project (SNAMP) water team data report to the California Department of Water Resources.

The following document was submitted to the California Department of Water Resources, documenting hydrologic characteristics and data collection for the study watersheds used in this dissertation and the Sierra Nevada Adaptive Management Project.

Sierra Nevada Adaptive Management Project

Water-Team Update

Task Order #UC 10-6

Deliverable #4.3.2

Contract #4600008548

Martha Conklin, Ph.D., Co-Principal Investigator

Roger Bales, Ph.D., Co-Principal Investigator

Phil Saksa, Ph.D. Candidate

Sarah Martin, Ph.D. Candidate

Ram Ray, Ph.D., Postdoctoral Researcher

Benjamin Tobin, Ph.D., Postdoctoral Researcher

Patrick Womble, Field Hydrologist

Sierra Nevada Research Institute

University of California, Merced

8 January 2015

Table of Contents

List of Figures

List of Tables

Executive Summary

This report is an update of results from the original documentation of the water component of the Sierra Nevada Adaptive Management Project (SNAMP), dated July 2012, which covered water years 2008-2011. The results presented here cover water years 2012 and 2013, the remaining 2 measurement years of the 7-year SNAMP study, with this current. This current and final year are focused on data analysis, hydrologic-modeling results (for both the catchment scale and upscaled to the fireshed), and integrating the hydrology results with the other components of SNAMP (including a 30-year hydrologic simulation). The background and methods from the original report are still current and are in Appendix C.

SNAMP is an integrated effort designed to study forest management from an ecosystem perspective - more specifically, to assess the effects of Strategically Placed Landscaped Treatments (SPLATs) in the mixed-conifer zone of the Sierra Nevada. In addition to water, investigations of forest health, forest fire, wildlife, and spatial processes is being conducted simultaneously in the same region. The hydrology (water) component focuses on detecting and predicting changes in the movement and timing of water flowing through these mountain catchments as a result of vegetation management, and on detecting changes to water quality. We hypothesize that the tree thinning and prescribed burning implemented with SPLATs will alter the timing of streamflow, increase water yields, and increase sediment movement within the stream channel due to the increased water yield.

The two SNAMP study areas are Last Chance, in the Tahoe National Forest, and Sugar Pine, in the Sierra National Forest. Within each study area, two headwater catchments were chosen for intensive monitoring, providing a treated and untreated watershed in both areas

The implementation of the Strategically Placed Landscape Treatments (SPLATs) were initiated in autumn 2011, and were completed in autumn 2012, a year later than scheduled. As a result, there is only one post-treatment water year (2013) instead of the two that were in the original study design. This delay in completion of SPLATs has led to a number of adjustments to the study timeline, with the delay in LiDAR analyses affecting interpretation of the hydrologic results. We require spatial information regarding the quantity of vegetation removed in the study sites, expected in fall 2014, in order to move forward with the final analysis and hydrologic modeling of the treatment effects on the water balance. In August 2013, the American River Fire burned through our treatment catchment, Bear Trap Creek. This complicates post-treatment analysis, but it also provides an opportunity to look at the effect of a low to medium-severity wildfire event.

Water years 2012 and 2013 were both dry years, with precipitation below average during both winters. Last Chance (Tahoe NF) recorded 146 and 154 cm while Sugar Pine (Sierra NF) recorded 97 and 128 cm of precipitation for 2012 and 2013, respectively. Annual stream discharge for both years was about 50 cm for the Last Chance headwater catchments and about 27 cm for the Sugar Pine headwater catchments. This resulted in a specific yield (discharge divided by precipitation) of approximately 0.37 in Last Chance and 0.24 in Sugar Pine for both years, which were lower yields than in the average and high precipitation years of 2010 (0.55 Last Chance, 0.41 Sugar Pine) and 2011 (0.58 Last Chance, 0.49 Sugar Pine). The dry conditions post-treatment also muted any hydrologic response to the treatments.

The Regional Hydro-Ecological Simulation System (RHESSys) has been set up to model the effects of the completed treatments, as well as the effects of further forest management and wildfire. The snow, soil-moisture, and streamflow data in this report are used to constrain the modeling, and preliminary calibrations are presented here. Finalization of the model, parameter calibration, and treatment results will be produced after the LiDAR vegetation layers are available.

Introduction

The Sierra Nevada Adaptive Management Project (SNAMP) is a joint effort by the University of California, state and federal agencies, and the public to study management of forest lands in the Sierra Nevada. The SNAMP team is assessing how forest vegetation treatments to prevent wildfire affect fire risk, wildlife, forest health and water. The USDA Forest Service's 2004 Sierra Nevada Forest Plan Amendment calls for managing the forest using the best information available to protect forests and homes. Vegetation management treatments are planned or being conducted in several places in the Sierra Nevada where fire risk is high. Millions of acres of Sierra Nevada forest are endangered by wildfire.

This report is summarizes the water quantity and quality monitoring for the Sierra Adaptive Management Project (SNAMP) for the water years 2012 and 2013. These results are an update to the July 2012 report on the period 2008-2011. The text of that report is appended. Figures 1-23 are incorporated into this report to provide a complete data record for the SNAMP. Data for water years 2012 and 2013 start at Figure 24. Additionally, analysis of water chemistry samples was incomplete at the time of the original report, but has since been completed and is included in this update.

This year the water team is focused on data analysis, hydrologic-modeling results (for both the catchment scale and upscaled to the fireshed), and integrating the hydrology results with the other components of SNAMP. In order to produce effective recommendations for land managers regarding the implemented forest treatments, it was decided to model the effects of these treatments on forest health, wildfire, water, and spotted owl habitat over 30 years. It has been estimated by previous studies that fire risk returns to pre-treatment levels within two to three decades. However, an integrated product over the extended timeline also required a new vegetation map that could be used for multiple analyses: forest growth and fire modeling, hydrology modeling, and spotted owl habitat assessment. This new spatial vegetation information was derived from a combination of lidar and forest plot data to produce more detailed information on forest community types, canopy cover, and vegetation density.

Methods

Methods described in the original 2012 data report are still current and are not repeated in this updated report. Presented here are some updates and additional information on data-collection and

additional methods for analysis. In August 2013, the American River fire burned our treated catchment, Bear Trap, and some instrumentation was lost and some data records were interrupted.

Snow Depth

Additional snow-depth measurements (2012-2013) were distributed around the meteorological stations and the stream instrument clusters at the northern site to measure variability across the landscape. These installations were part of the wireless sensor network testbed for the American River Project but relevant data collected at the SNAMP instrument locations are presented here. Snow depth was gap filled from adjacent measurements prior to spatial averaging.

Stream Water Quality

The water-quality attributes of water temperature, conductivity, dissolved oxygen, turbidity, and stage continued to be collected in all study catchments using multi-parameter continuously running sondes. Water-quality attributes and stream stage are reported here in 15-minute time intervals. The meteorological attributes of air temperature, precipitation, and snow depth, plotted on the following graphs for reference to the water-quality data, are reported in daily time intervals. Air temperature was recorded at the study-site met stations. In the original data report, we reported precipitation measurements from our study sites. Because the study-site rain gages were unheated and unshielded, there was concern over their accuracy. In the data report update, precipitation reported are from the nearby stations Blue Canyon (for Last Chance) and Westfall (for Sugar Pine). As the precipitation data are provided for explaining trends, we opted for the more accurate data set. The plotted snow-depth values represent means of all snow-depth measurements at a given site.

Starting in WY 2012 a second multiparameter sonde co-located with the original sondes was installed in all catchments except Frazier Creek. These sondes measured water temperature, conductivity, and turbidity for data redundancy. Data from all the multiparameter sondes were manually checked to remove any erroneous spikes due to maintenance of sensors, sampling in the stream, or (for turbidity and dissolved oxygen) periods when the sonde was buried in sediment. To reduce sensor background noise, the turbidity data were filtered to remove any values less than 5 NTU. The remaining values were considered actual turbidity events and were used in analysis. Gaps after the WY 2012 installation were filled using the secondary sonde. When data from the secondary sonde were unavailable, only water temperature and stage could be gap filled using data from the stand alone stage recorders.

Turbidity events were classified according to seasons, with fall defined as first fall rain event to before the beginning of snow accumulation, early/mid-winter as beginning of snow accumulation to peak accumulation, snowmelt as peak accumulation to complete melt out, and base flow as full melt out to first fall rains. Intensity values of storm events were analyzed by subtracting peak discharge values from background discharge values defined by a 15-day running average.

Adjacent to the multiparameter sondes, automated water samplers were installed to collect suspended sediment samples. These samplers were tied to the sonde turbidity measurements and programmed to increase sampling frequency during turbidity events. Manual grab samples for suspended sediment, major ions, and stable isotopes were also collected on a monthly to bi-monthly basis. Manual and automated suspended-sediment samples were filtered using 0.45-micron filters, dried, and weighed to determine suspended-sediment concentrations. Major-ion samples were filtered, then split in half for ion-chromatography analysis of major cation and anions as well as titration analysis for acid neutralization capacity (ANC). Isotope samples were processed using integrated-cavity laser spectroscopy to determine the delta D and delta ^{18}O of samples.

Load-cell pressure sensors were placed near the water-quality instrumentation to measure bedload movement and channel-bed-elevation changes. Bank pins were installed (6-9 locations per stream) at the southern site to measure streambank erosion according to the methods outlined in Martin (2009). Attempts were made to install them at the northern site, but due to the high cobble and boulder content of the stream banks, the rebar pins could not be set. Cross-sections at the scour-pan locations and bank surveys at the bank-pin locations were completed several times throughout the study, typically during late-summer/early-fall low flows. Additional data on particle-size distribution, and localized gradient were also collected.

Stream Water Quantity

Stage values measured by the two pressure-recording instruments within each stream showed good agreement, so the record with greater confidence (i.e. fewer relocations, fewer malfunctions, more stable cross-section, etc) was chosen as the primary record for calculating discharge. Where gap filling was necessary, it was performed using the record from the secondary stage instrument.

Results

Meteorological Data

Hourly meteorological data continued to be recorded at the four stations, capturing the range of environmental conditions present within the four study basins. Figures 24 and 25 show the daily observations of solar radiation, precipitation, temperature, relative humidity, and wind speed, as well as net radiation for observing energy exchanges between the ecosystem and atmosphere. The upper and lower elevations at Last Chance showed greater differences in the meteorological observations than the Sugar Pine stations.

Precipitation measured in Last Chance was 146 cm in 2012 versus 154 cm in 2013; while Sugar Pine had 97 and 128 cm in the same years (Figures 24-25). Spatial differences in precipitation showed the northern study area of Last Chance, located within the American River basin, had about 40-cm higher levels annually than the southern study area of Sugar Pine, located within the Merced River basin. Precipitation at the higher-elevation stations of Duncan Peak and Fresno Dome (elevation >2100 m) is dominated by snowfall, while the lower elevation stations of Bear Trap and Big Sandy (1500-1800 m elevation) recorded similar levels of rain and snow.

Temperatures at Bear Trap averaged 10.4^{o}C (ranging -12.3 to 34.0) and Duncan Peak averaged 8.3^{o}C (-13.7 to 33.2) at Last Chance, while Big Sandy averaged 7.1^{o}C (-17.0 to 30.8) and Fresno Dome averaged 8.5^{o}C (-13.6 to 29.3) at Sugar Pine for WY 2012 and 2013 (Figures 24-25). This reflects a temperature difference of only 1.2 ^{o}C per 300 m elevation for Last Chance, and 1.0 ^{o}C for Sugar Pine. Daily maximum temperatures between the two sites differ by about 1.8 ^{o}C, versus 1.0 ^{o}C for daily minimum temperatures.

Higher relative-humidity values were recorded at the lower-elevation sites, with mean-daily wind speeds around 2 m s^{-1}, and the major wind direction being S-SE for all sites for WY 2012 and 2013 (Figure 24-25). Wind speed and direction were not able to be gap filled, due to the individual nature of wind conditions at each site.

Upper-elevation stations received slightly higher total daily solar radiation inputs during the summer than lower elevations due to the lower horizon, and the southern study site received more than the northern study site (Figure 24-25). Approximate maximum radiation values for WY 2012 and 2013 were 32 MJ m^{-2} day^{-1} at Fresno Dome, 30 MJ m^{-2} day^{-1} at Big Sandy, 30 MJ m^{-2} day^{-1} at Duncan Peak, and 25 MJ m^{-2} day^{-1} at Bear Trap. Absolute radiation values cannot be obtained due to the limitations of the LI-COR pyranometer used.

Maximum summer net radiation followed a similar stratification with values of 23, 23, 18, and 15 MJ m^{-2} day^{-1} at Fresno Dome, Big Sandy, Duncan Peak, and Bear Trap respectively. Net solar radiation was small, and in many cases close to zero for water year days 60 to 150 for all sites. The Duncan Peak station (higher elevation) also showed greater variability in net radiation than did Bear Trap (lower elevation).

Snow Depth

Site-averaged snow depth peaked at 53 cm for WY 2012 and 18 cm for WY 2013 at Last Chance (Figure 26-27). Site averaged snow depth peaks were 48 cm and 58 cm for WY 2012 and 2013 respectively at Sugar Pine. The data show snow cover durations of 5 and 7 months for Last Chance and Sugar Pine respectively in 2012, with both sites having about 4 months in 2013. Snow in 2012 came during the later months of January-March, while in WY 2013 most of the snow fell in the earlier months of December and January. Many instrument locations had low or intermittent snow cover in both years, but some maintained some snow cover all winter. Open snow-depth measurements tended to maintain more snow cover, while under canopy were more likely to be intermittent; canopy edges generally showed intermediate values between open and under canopy sites.

Upper-elevation meteorological stations recorded the highest snow depths and latest snowmelt dates. Last Chance snow depth showed greater variability than did Sugar Pine, with Duncan Peak having the highest snow accumulations and Bear Trap showing intermittent snow cover throughout the two winter periods. Snow depths measured above the banks of the streams varied from intermittent patterns to high accumulation and late melt out. Mean snow depths in WY 2012 and WY 2013 in Last Chance were around 75 cm and 30 cm. In Sugar Pine, snow depth values were around 15 cm and 20 cm in WY 2012 and WY 2013 respectively. Last Chance showed greater variability among measurement locations while Sugar Pine showed more daily variability over the winter seasons.

Soil Moisture

Soil-moisture values were more variable in WY 2012-2013 than in WY 2010-2011. The dry water years led to more variability in precipitation and snow cover, resulting in the higher soil moisture variability. The sites surrounding the meteorological stations continued to exhibit more variability than the sites adjacent to the streams in these dry periods (Figures 28-29). Monitoring soil moisture at Duncan Peak continued to be challenging, as the sensors exhibited behavior that could not be reconciled with measurements recorded at the other sites, limiting observations at the upper elevations. The failure rate of soil-moisture sensors (Decagon EC-TM) overall was relatively high, about 20% over the 4-

year record. The Duncan Peak north-facing site had all soil-moisture sensors fail by 2013, and the sensors at the south-facing site were damaged following the American Fire in August 2013 (Figure 28).

Temperature

Average water temperature for WY 2012 and WY 2013 ranged from 0 to 15.0 ^{o}C in Frazier, 0 to 13.6 ^{o}C in Bear Trap, 0 to 18.0 ^{o}C in Big Sandy, and 0 to 13.0 ^{o}C in Speckerman (Figures 30-33). Of the two years, WY 2013 showed slightly warmer water temperatures in all catchments except Big Sandy where WY 2012 had roughly 1 ^{o}C higher maximum water temperature. Yearly means were 5.8 and 6.6 ^{o}C for Frazier, 5.8 and 6.8 ^{o}C for Bear Trap, 5.6 and 6.3 ^{o}C for Speckerman, 5.8 and 6.3 ^{o}C for Big Sandy, for WY 2012 and WY 2013 respectively. Water temperature patterns were similar in both water years and trended with air temperature, reaching lowest values in early winter and gradually rising through the season.

Conductivity

At both Sugar Pine catchments, manual and continuous measurements of conductivity show low, relatively stable values with little seasonal variation (Figures 30-33). Mean specific conductivity values for WY 2012 and WY 2013 are 18 µS and 17 µS at Speckerman, and 45 µS and 44 µS at Big Sandy respectively. Mean conductivity values for the Last Chance catchments were 46 µS and 44 µS for Frazier for WY 2012 and WY 2013. For Bear Trap the mean value for WY 2012 was 48 µS. Bear Trap's WY 2013 mean was found to be 43 µS. These values are higher than those in WY 2010 and WY 2011, as would be expected due to WY 2012 and WY 2013 being low water years with proportionally less low-conductivity rain/snow entering the stream.

The highest conductivity values in this period are seen during baseflow conditions and the lowest during peak spring snowmelt. Big Sandy, Frazier, and Bear Trap show a much more-pronounced seasonal trend in conductivity than did Speckerman. The higher mean conductivities and high seasonal variation imply that the groundwater input at Big Sandy and the Last Chance catchments may be older or that the soil/rock the water is in contact with is more easily reacted. Both explanations are plausible for the Last Chance sites given that Sugar Pine has predominantly granitic bedrock that is slow to weather, whereas the Last Chance catchments have a mixture of granitic and metamorphic rock types.

Dissolved Oxygen

Dissolved oxygen data in both Last Chance catchments showed percent saturation values that remained in the 75% and 95% saturation range for all four water years (Figures 30-33). The WY 2012

A depletion of sediment was seen at the seasonal and at the event scale (for multi-rise events). Figure 34 shows a series of discharge and turbidity events during the fall 2011 season at Speckerman Creek. The largest turbidity signal was seen early in the season, with a gradual decrease in turbidity signal values even though the peak discharges for events increased. This suggests that there may have been stores of sediment that had accumulated during the previous low-flow season and that were gradually depleted as the season progressed. Mechanisms for low-flow sediment accumulation may be physical weathering of channel banks as they dry and crumble, or bioturbation. Multi-rise events also showed a shift in hysteresis patterns indicative of depletion of sediments. Figure 35 shows a multi-rise discharge event in Big Sandy Creek that progresses from strongly clock-wise to a weakly clock-wise pattern and finally, to a linear pattern. This indicates a progressive lag in sediment transport that likely results from a depletion in localized stores and a shift from nearby, easy-to-transport sediments to more distant sediment sources or to more consolidated sources (consolidated banks or armored beds) that require greater flow energy to entrain. Snow cover did not appear to factor into fall having higher turbidity values than winter and spring due to the sediment sources being localized, and no differences in turbidity patterns between the seasons (Martin *et al.*, 2014).

Major Ions

Analysis of major cation and anions from streamwater samples and comparison of those ion concentrations with stream conductivity showed the general trends of Speckerman having the lowest concentrations and conductivities of the four watersheds (Figure 36). Big Sandy had intermediary concentrations and conductivities while Frazier and Bear Trap showed the highest concentrations and/or conductivity depending on the ion in question. Also the Last Chance samples showed a much larger spread of sample points than did the Sugar Pine sites.

For the cations Na^{+} and K^{+}, Speckerman, Big Sandy, and Frazier had increases in concentration that were proportional to increases in conductivity, while Bear Trap did not exhibit an increase in concentration with increasing conductivity. For Mg^{+2}, Speckerman did not show a concentration increase with increased conductivity and Bear Trap had only a slight increase (less steep slope) in concentration with increased conductivity. Big Sandy and Frazier had proportional increases similar to that for Na^{+} and K^{+}. For Ca^{+2} all streams except Speckerman showed higher concentrations associated with increased conductivities.

The F^{-} anion showed considerable spread in the data along with relatively low concentrations. For Cl^{-} and SO_4^{-2}, Bear Trap showed increasing ion concentrations with increasing conductivity, but the

other three streams had relatively stable ion concentrations even with increased conductivity. All four streams had proportional increases between ion concentration and conductivity for HCO_3^-.

These trends indicates that for Speckerman Na^+, K^+, and HCO_3^- are important constituents affecting stream conductivity, while Mg^{+2}, Ca^{+2}, and SO_4^{-2} play little role in that streams conductivity. The same constituent make-up seems to be the case for Big Sandy, however there is more scatter in the data. The similarities are likely due to very similar rock types and source waters between the two paired watersheds.

The Last Chance sites have very different constituent make-ups between the two watersheds. Ca^{+2}, Cl^-, and SO_4^{-2}, and HCO_3^- seem to be the most important constituents for stream conductivity (Mg^{+2} to a lesser degree) for Bear Trap, while Na^+ and K^+ seem to be unimportant. Frazier has a nearly opposite trend, with Na^+, K^+, Mg^{+2}, and HCO_3^- being the more important constituents (Ca^{+2} to a lesser degree) and Cl^- and SO_4^{-2} not contributing significantly to conductivity. These differences are likely due to variations in the bedrock chemistry between these two streams.

Stable Isotopes

Stable isotopes from stream samples showed slightly more negative δD and δO18 values for the Big Sandy and Speckerman samples as would be expected due to the southern catchments higher altitudes (Figure 37). Paired catchments showed similar values with the northern catchments showing a smaller range than the southern catchments. The isotopic signatures of the samples form a local meteoric water line (LMWL) that sits slightly to the left of the global meteoric water line (GMWL) in Figure 37 and fits well with samples from other Sierra Nevada sites.

Discharge

In Speckerman and Big Sandy Creeks, WY 2012 had a large rain event in early fall that was roughly equal to peak snowmelt discharge and a late fall event that exceeded peak snowmelt for the year (Figure 38). WY 2013 also had a late fall event that exceeded peak snowmelt for the year, representing the year's peak discharge. Big Sandy showed another significant event that exceeded peak snowmelt discharge prior to the late-fall annual peak event, but the same storm event led to less significant discharges in Speckerman. In Frazier and Bear Trap the WY 2012 fall rain events were much less significant and did not approach the peak discharge levels for the year. The highest discharge event for WY 2012 in Bear Trap was a mid-winter peak that corresponded to the highest daily precipitation for the year, while the second highest peak corresponded to a medium size precipitation peak during spring snowmelt. Frazier's largest peak discharge corresponded to the same medium-sized snowmelt-season

precipitation peak as in Bear Trap. The second largest discharge peak was during late winter and corresponded to a medium-sized precipitation event that occurred after the storm event with the largest daily precipitation. In WY 2013, the largest discharge peaks for both Last Chance catchments occurred in late fall, concurrent with the largest daily total precipitation. This late-fall event was 2-3 times the peak snowmelt discharge for that year.

The yearly peak discharges in Bear Trap are proportionally higher than snowmelt and baseflow compared to the other watersheds (Figure 38). This is likely due to limited site access during times of peak flow, resulting in the rating curve being less well constrained for the higher discharges. We believe that the peak-flow values may be slightly over estimated for this catchment, but the mid-range and lower flows are accurately represented. Additionally, due to the short duration of the peak flows, they do not significantly affect annual discharge estimations used in modeling.

For WY's 2012 and 2013 there were considerable differences in the shape of the hydrographs between the Sugar Pine and the Last Chance sites (Figure 38). Interestingly, where WY 2013 had significantly less snow than in WY 2012 at the Last Chance sites, the annual discharge peaks and the snowmelt discharges were of similar magnitude. At the Sugar Pine sites the two years were more similar in amount of snow (though not in timing as previously discussed), and while Speckerman had very similar snowmelt discharges for the two years, Big Sandy had somewhat lower snowmelt discharges in WY 2013 possibly due to the earlier peak snow accumulation and slightly earlier melt out for the year.

Basin Discharge Comparison

For both water years, Big Sandy had a discharge that was more similar to Speckerman (Figures 38, 41), than during the first two years of record. The dry years clearly had an effect on flow levels, and may complicate interpretation of treatment effects (Big Sandy, treatment; Speckerman, control). Discharge at Frazier and Bear Trap are also more similar than 2010 and 2011 years, but have kept the trend of Frazier generally having higher discharges than Bear Trap during winter flow and spring snowmelt (with the exception of a few short-duration early winter events where Bear Trap has slightly higher peak event flows) (Figures 38, 41). That inverse relationship continued in the dry years where Bear Trap consistently showed higher discharges than Frazier during baseflow conditions. This may be due to the overestimations in the rating curve at higher discharges as discussed above or due to the bedrock channel at Bear Trap limiting channel bed infiltration or subsurface streamflow. Bear Trap may also have more flow from springs this time of year.

Cumulative discharge comparisons highlight the similarities between the two dry water years and between streams. Total annual flows for WY 2012 and WY 2013 were calculated for each stream (Figure 39). Total flow for Speckerman was 0.46 $x10^6$ m^3 (16.3$x10^6$ ft^3) for WY 2012 and 0.59 $x10^6$ m^3 (21.0$x10^6$ ft^3) for WY 2013. Annual totals at Big Sandy were 0.53 $x10^6$ m^3 (18.7$x10^6$ ft^3) and 0.67 $x10^6$ m3 (23.8x106 ft^3) in WY 2012 and 2013 respectively. Frazier had totals of 0.99 $x10^6$ m^3 (34.9$x10^6$ ft^3) and 0.88 $x10^6$ m^3 (31.1$x10^6$ ft^3) for WY 2012 and 2013. Bear Trap totaled 0.95 $x10^6$ m^3 (33.6$x10^6$ ft^3) and 0.96 $x10^6$ m^3 (33.9$x10^6$ ft^3) for WY 2012 and 2013.

When discharge values are normalized over the watershed areas, the similarities between streams become even more apparent (Figure 40). The normalized total cumulative discharge at Speckerman was 24 cm in WY 2012 and 31 cm in WY 2013. At Big Sandy, cumulative discharge was 23 cm in WY 2012 and 28 cm in WY 2013. Frazier's cumulative totals for WY 2010 were 53 cm for WY 2012 and 59 cm for WY 2013. Bear Trap cumulative flows were the same, 54 cm for both years. Annual stream discharge was the lowest during WY 2012 out of all four of the observation years.

Runoff coefficients, expressed as the fraction of precipitation leaving the basin as stream discharge, were associated more with precipitation levels than basin size (Table 3, Figure 40). As a result, Last Chance showed higher runoff coefficients than Sugar Pine, and values from both study sites were similar between 2012 and 2013. Speckerman Creek and Big Sandy Creek had respective coefficients of 0.24 and 0.23 in 2012 and 0.24 and 0.22 in 2013, respectively. Bear Trap Creek and Frazier Creek had respective coefficients of 0.41 and 0.37 in 2012 and 0.34 and 0.35 in 2013.

Table 3. Interannual variability of precipitation and water yield observed in the study watersheds.

Site	Year	Stream	Precipitation, cm	Water Yield, cm	Runoff Coefficient*
Last Chance	2012	Bear Trap	146	54	0.41
		Frazier	146	53	0.37
	2013	Bear Trap	154	54	0.34
		Frazier	154	59	0.35
Sugar Pine	2012	Speckerman	97	24	0.24
		Big Sandy	97	23	0.23
	2013	Speckerman	128	31	0.24
		Big Sandy	128	28	0.22

* Runoff coefficient is calculated as Water Yield divided by Precipitation

Regional Hydro-Ecological Simulation System (RHESSys)

RHESSys calibration and parameterization continues for the SNAMP basins, with final products dependent upon the LiDAR-derived vegetation layers that should be completed within the next few months. Preliminary parameterization results using modeled vegetation growth show reasonable agreement with snow, soil moisture, and streamflow observations (Figure 42).

In the original report, model results were obtained using observed temperatures and precipitation separated into rain and snow. Results are now being obtained using the model to split the precipitation into the different phases of rain and snow. The met station temperatures used initially were not representative of the regional temperature range recorded by the distributed snow depth sensors. Lowering the met stations temperatures by 1-2 degrees so that modeled snow matched observed snow levels allowed a better snow/rain representation than splitting the phases manually.

Upscaling RHESSys to the larger firesheds (10-25 km^2) is ongoing. The headwaters and firesheds have similar geology, with the streamflow from the closest available stream gauge also showing similar streamflow patterns. Similar studies using RHESSys have shown that parameters developed in headwater regions can be transferred to larger watersheds based on these physical characteristics, and we are using the same approach. The model output is also shown for water year 2010 from Bear Trap Creek (Figures 22-23).

Conclusions

The four years of continuous snow, soil moisture, and stream discharge observations have been achieved over a range of conditions (Figure 41). Water year 2010 showed average winter precipitation, 2011 was wetter than average, while 2012 and 2013 were both low precipitation years. Forest treatments were started in the fall of 2011 and were finished in the fall of 2012. Water-year 2013 is the only post-treatment measurement year, and will be the basis for evaluating any observed effects of thinning on the water balance in these watersheds. However, the dry conditions in the final two water years may mask any treatment effects in the single 2013 post-treatment year. The American Fire also burned through the Last Chance treatment catchment (Bear Trap Creek) in August 2013, complicating the evaluation of future effects of the forest treatments, but also providing an opportunity to look at further vegetation reduction from a low to medium-severity wildfire event.

Stream water quality showed similar seasonal trends to those seen in water years 2010 and 2011 with water quality parameters measuring within the acceptable range for water quality standards. For water years 2010-2012, turbidity was found to be episodic with distinct seasonal patterns. In-channel sources were shown to dominate sediment supply and those supplies underwent seasonal cycles of accumulation and depletion. Four years of stream water chemistry data showed that Speckerman generally had lower ion concentrations than Big Sandy, which fit with the comparatively low conductivity observed in Speckerman. Major ion constituents also differed greatly between Frazier and Bear Trap possibly due to differences in geology between the two basins. Stable isotope data showed elevational trends as expected and trends fit well with those of other Sierra Nevada sites. Due to changes in water quality being closely tied to changes in discharge the dry conditions post treatment are likely to also mask any potential treatment effects on water quality.

The water-quantity and energy-balance data assembled and presented in the preceding data report and this update provide better than usual observations to constrain and evaluate the modeling capability for the SNAMP catchments. A majority of models reported in the literature are calibrated on streamflow alone, while this model will be compared to snow and soil moisture levels as well. The initial two water years of meteorological measurements (2008-2009) will be use to stabilize the model environment. The range of precipitation conditions, while potentially masking treatment effects, will be very useful in calibrating the model over a range of possible winter climates.

Bibliography

Martin, S.E., Conklin, M.H, Bales, R.C. 2014. Seasonal Accumulation and Depletion of Local Sediment Stores of Four Headwater Catchments. Water 6:2144-2163.

Williams, G.P. 1989. Sediment Concentration Versus Water Discharge during Single Hydrologic Events in Rivers. Journal of Hydrology 111(1-4):89-106.

Wood, P.A. 1977. Controls of Variation in Suspended Sediment Concentration in the River Rother, West Sussex, England. Sedimentology 24(3):437-445

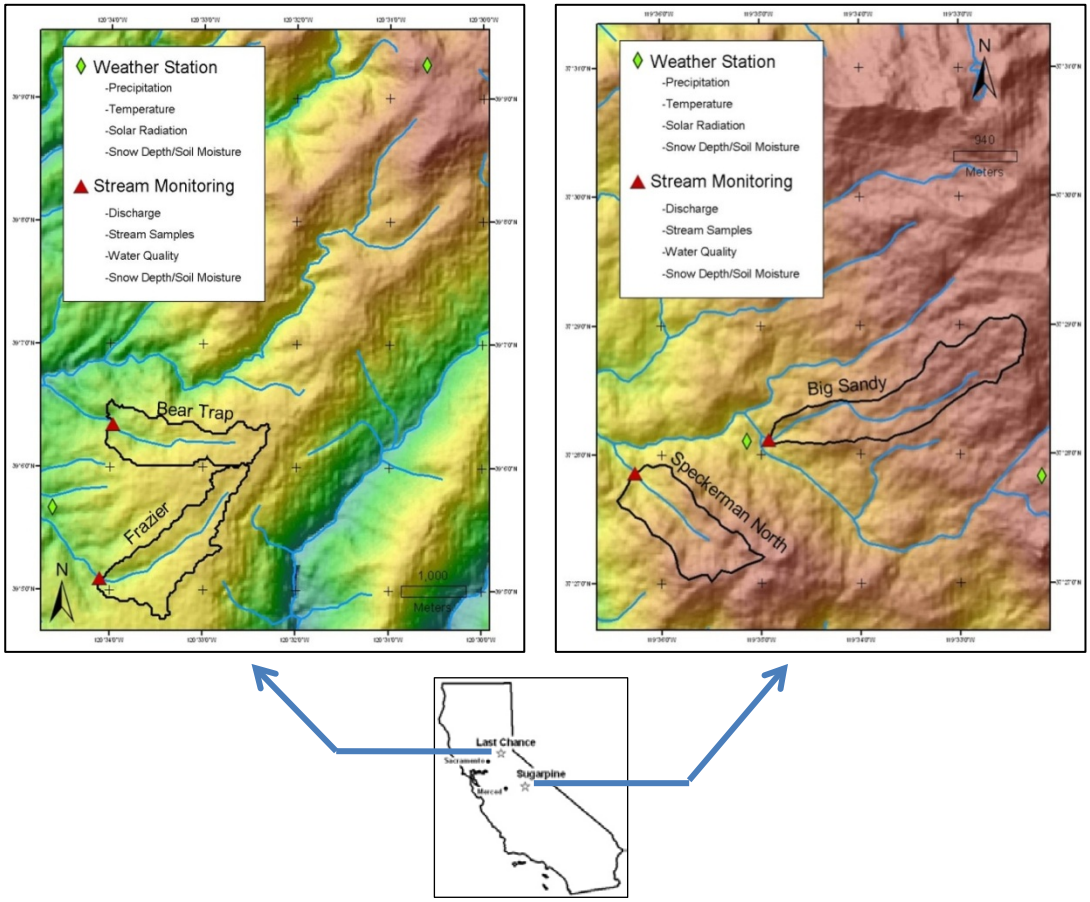

Figure 1. Layout of Last Chance (left panel) and Sugar Pine (right panel) study areas.

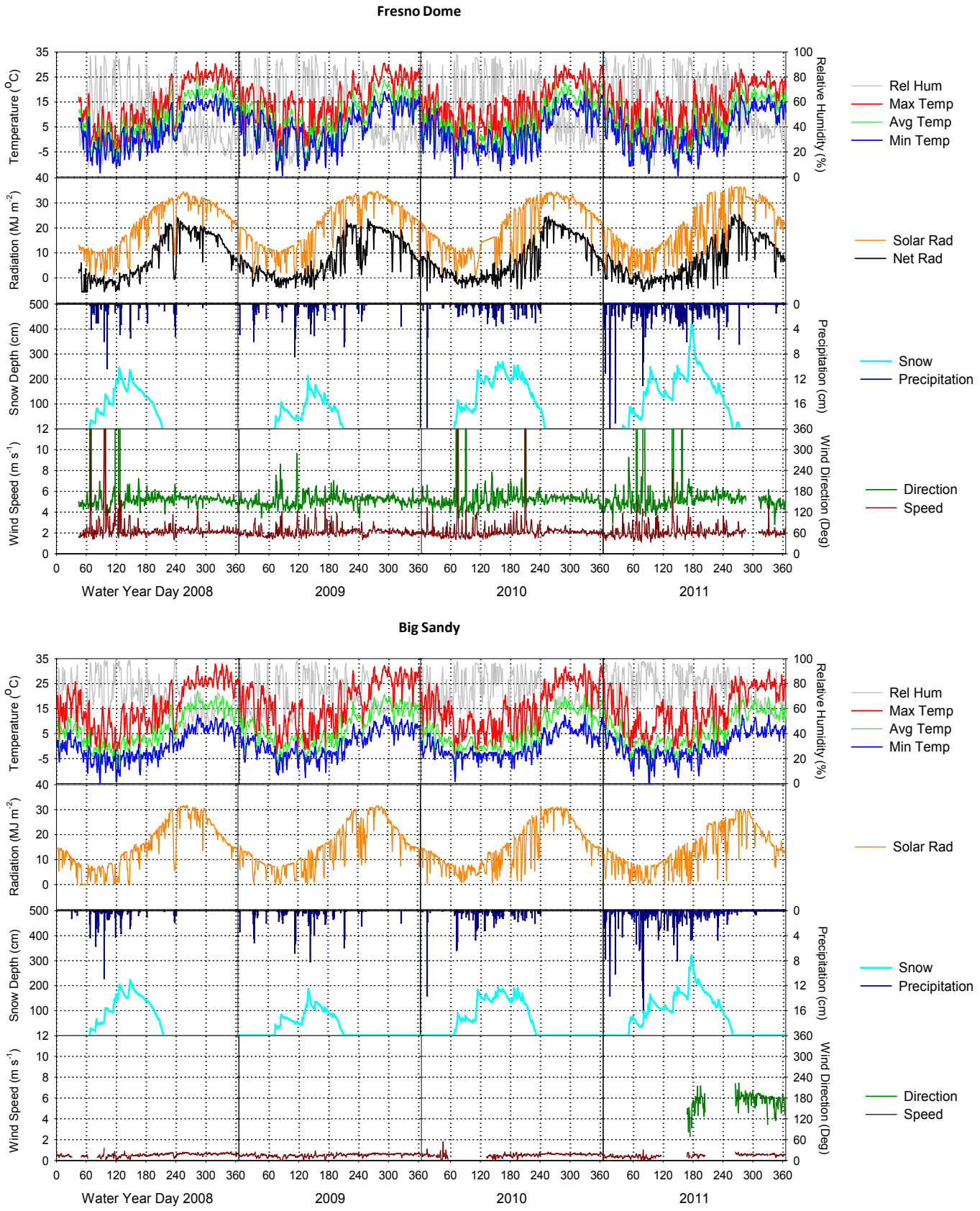

Figure 2. Daily values of data collected from the upper (Fresno Dome) and lower (Big Sandy) elevation meteorological stations in the Sugar Pine study area for water years 2008-2011.

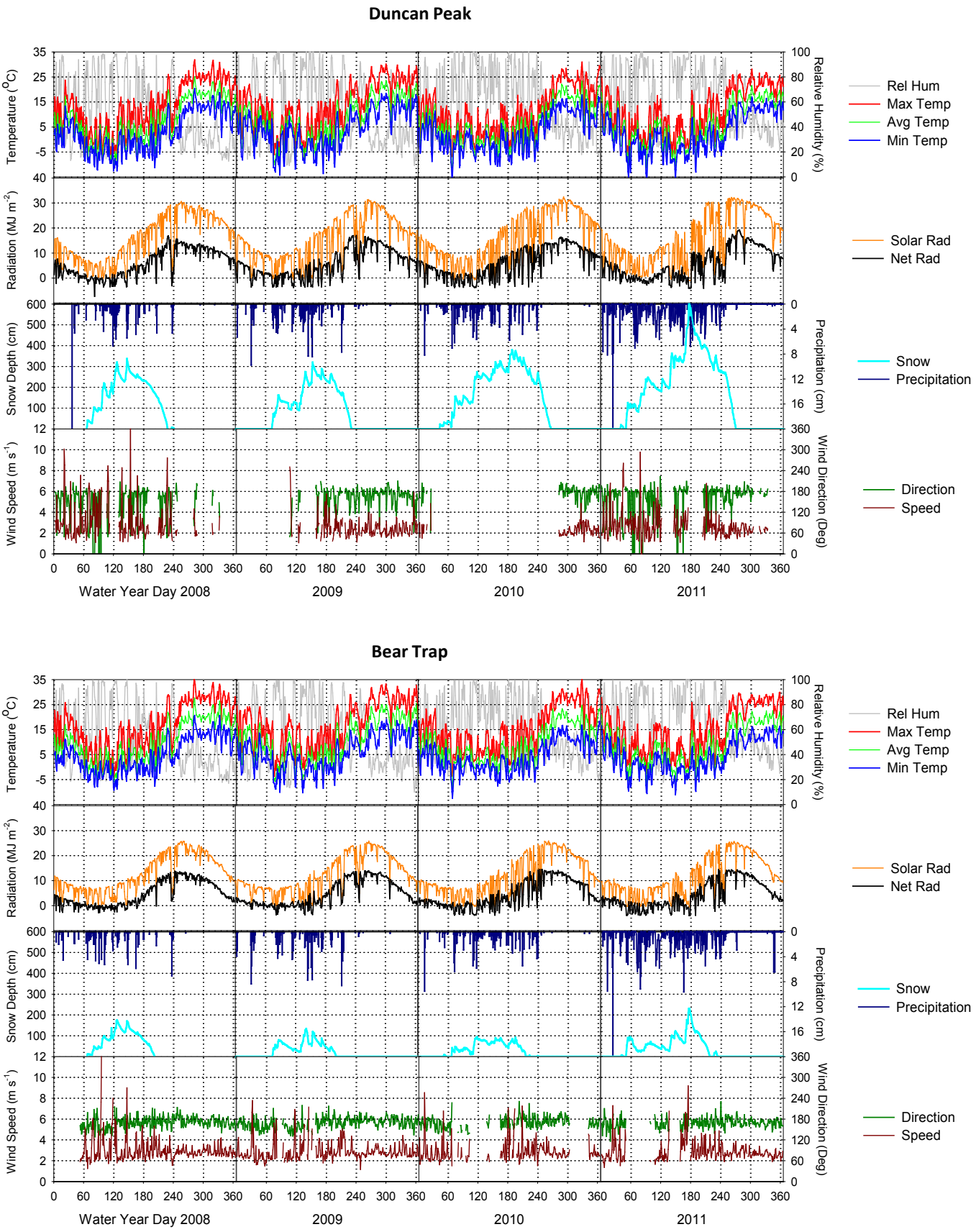

Figure 3. Daily values of data collected from the upper (Duncan Peak) and lower (Bear Trap) elevation meteorological stations in the Last Chance study area for water years 2008-2011.

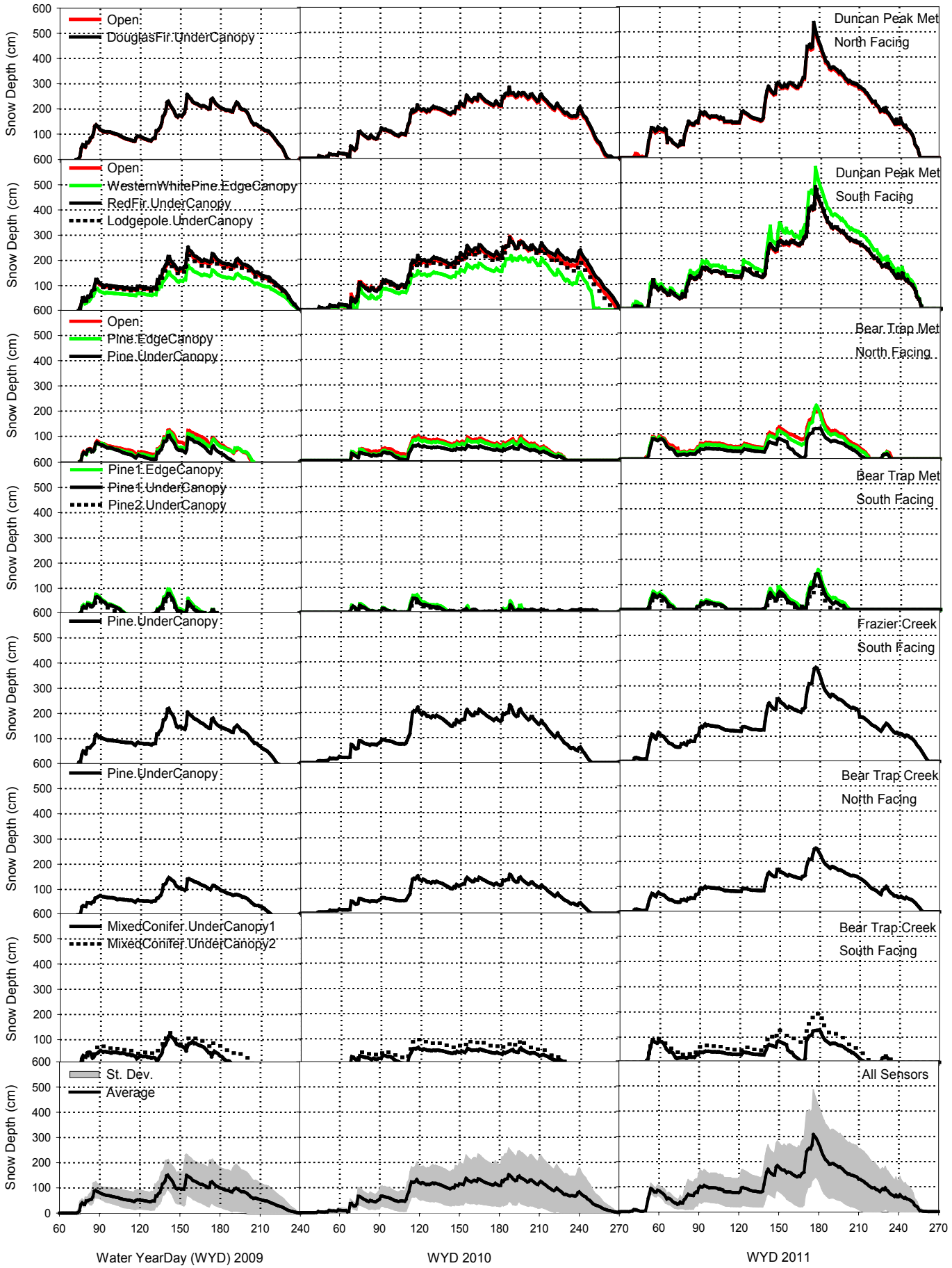

Figure 4. Daily mean snow depths recorded with a total of 16 sensors in 4 different locations incorporating the variable physiographic characteristics of aspect, canopy cover, and elevation that are present in the study area.

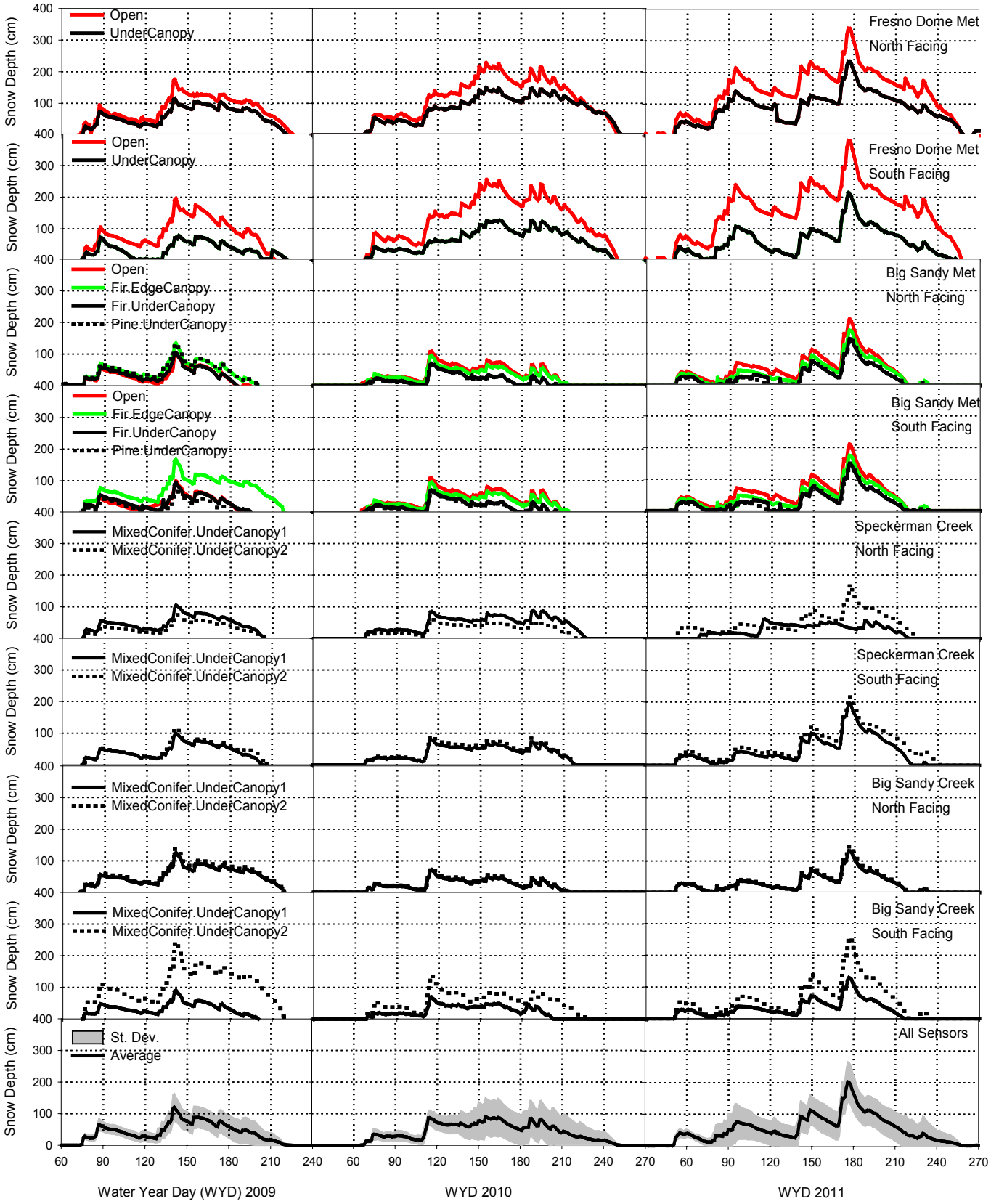

Figure 5. Daily mean snow depth for 2009-2011 from 18 sensors in 4 different locations, covering physiographic characteristics of aspect, slope, elevation, and canopy cover present in the Sugar Pine study area.

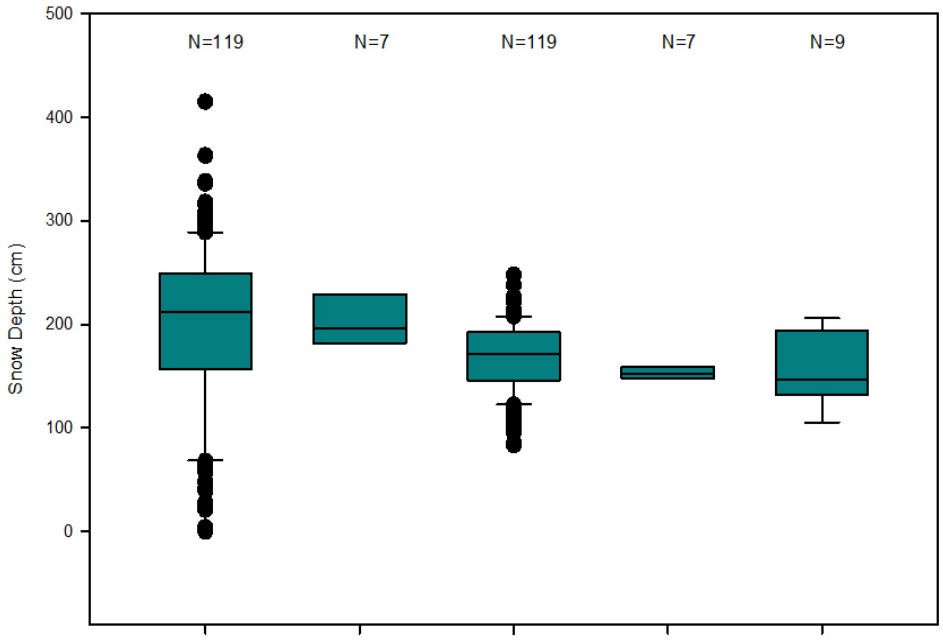

	2009 Survey	2009 Sensors	2012 Survey	2012 Sensors	2012 Sensors
Max	405	257	248	180	206
Mean	212	208	168	155	160
Median	226	196	172	152	146
Min	0	176	83	141	105

Figure 6. Snow depths recorded during surveys around Duncan Peak in 2009 and 2012, the wired depth sensors on the same day, and the new wireless sensors in 2012. The wireless sensors show an improved ability to capture snow variability over the north- and south-facing wired nodes. The boxes bound the 25th and 75th percentiles with a line for the median value in the middle. Error bars represent the 10th and 90th percentiles, with outliers shown as points. Descriptive values of the measurements are also shown in the table.

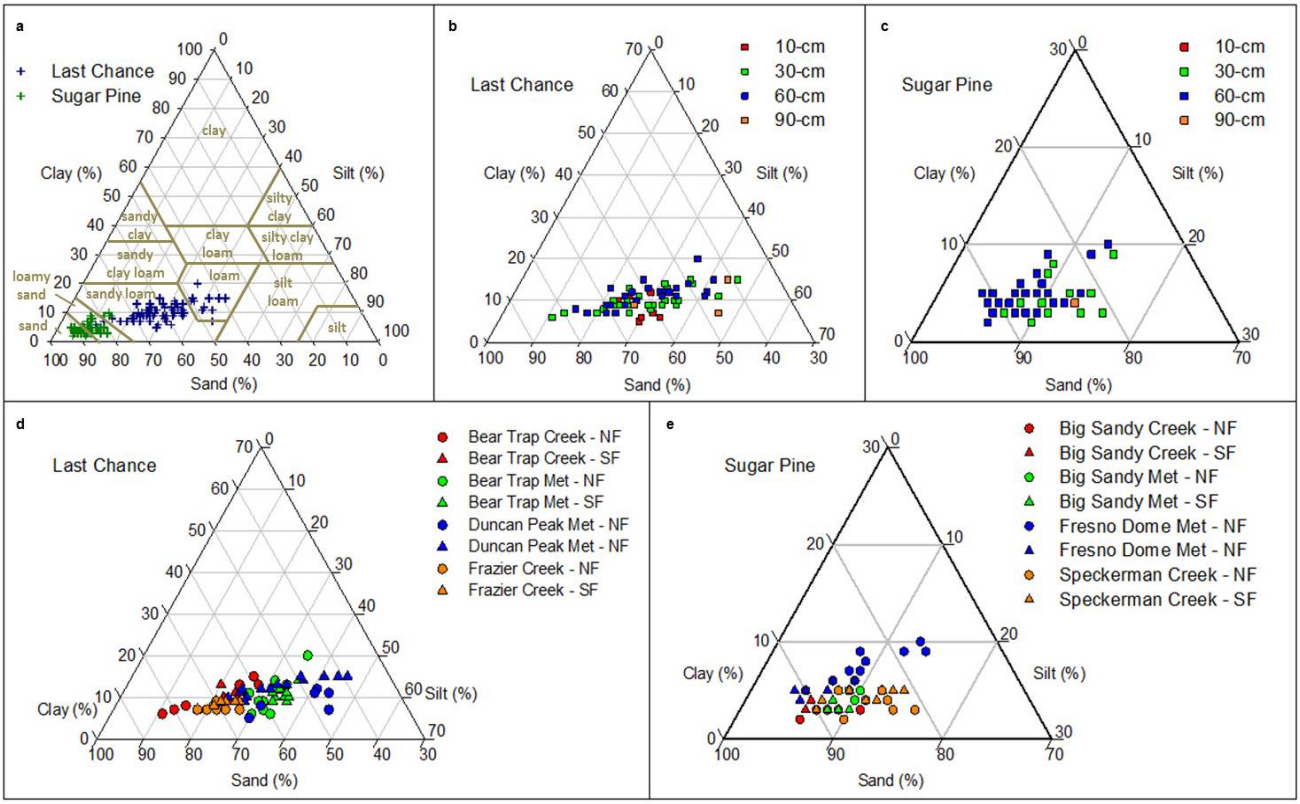

Figure 7. Soil texture analysis from samples collected where every moisture sensor was installed. Panels show the USDA soil texture classifications for all samples (a), and are also stratified by depth below surface (b,c) and sample site (d,e). All soils were in one of four classifications (loam, sandy loam, loamy sand, sand), with soils generally having greater than 50% sand, less than 50% silt and less than 30% clay. Soils in the Sugar Pine region were sandier than in Last Chance, and textures were more similar by sample site than by depth. Sample sites denoting NF and SF are on a north-facing aspect and south-facing aspect, respectively.

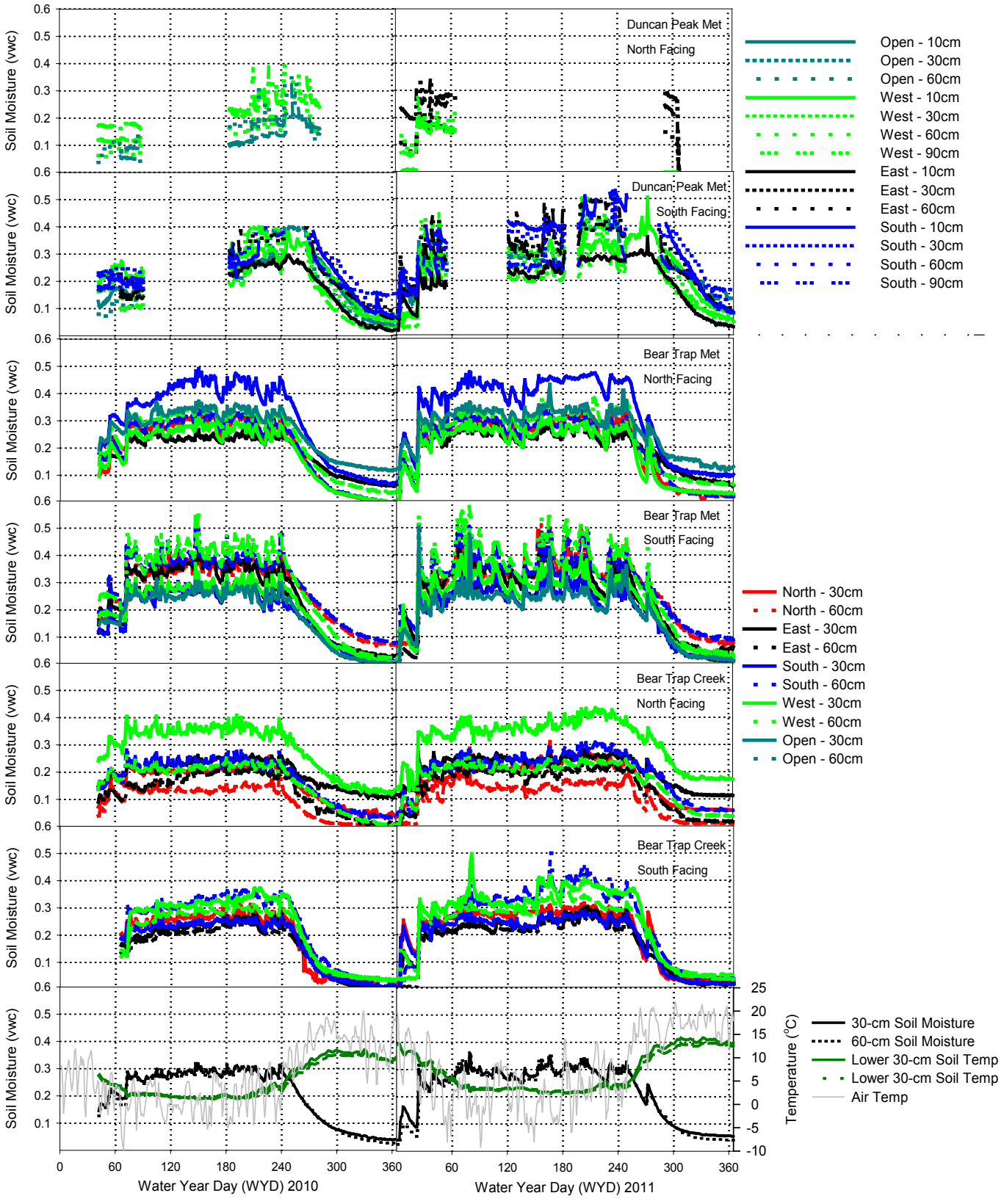

Figure 8. Soil moisture recorded with 43 sensors in the 4 general study locations. Most sensors were placed at 30- and 60-cm below the surface in a cardinal direction 1 m from the trunk of a tree where snow depth was also measured. A few sensors were placed at different depths for additional observations. The sensors at Duncan Peak exhibited erratic behavior not observed at the other sites, with these time periods removed a limited number of observations were recorded.

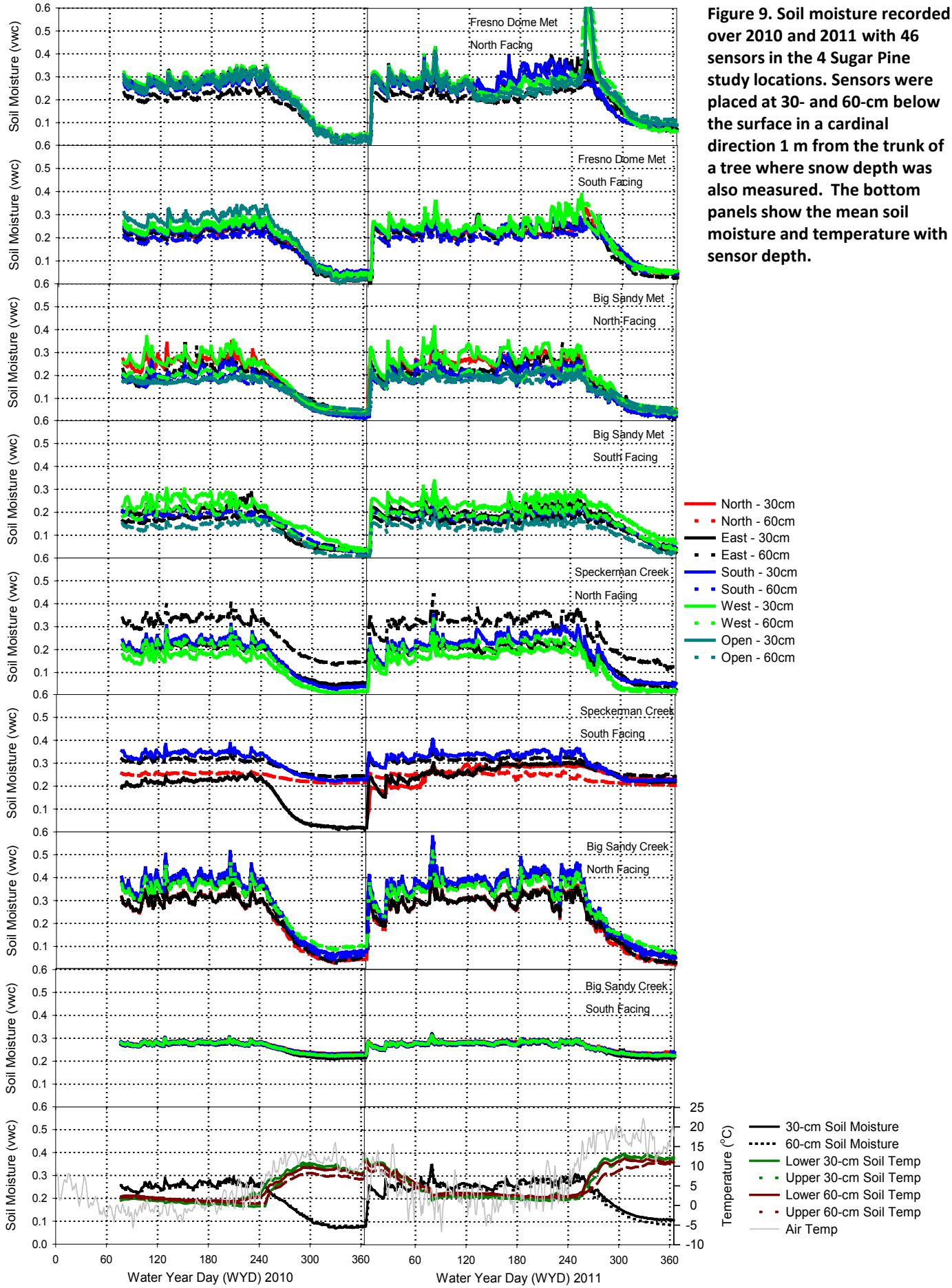

Figure 9. Soil moisture recorded over 2010 and 2011 with 46 sensors in the 4 Sugar Pine study locations. Sensors were placed at 30- and 60-cm below the surface in a cardinal direction 1 m from the trunk of a tree where snow depth was also measured. The bottom panels show the mean soil moisture and temperature with sensor depth.

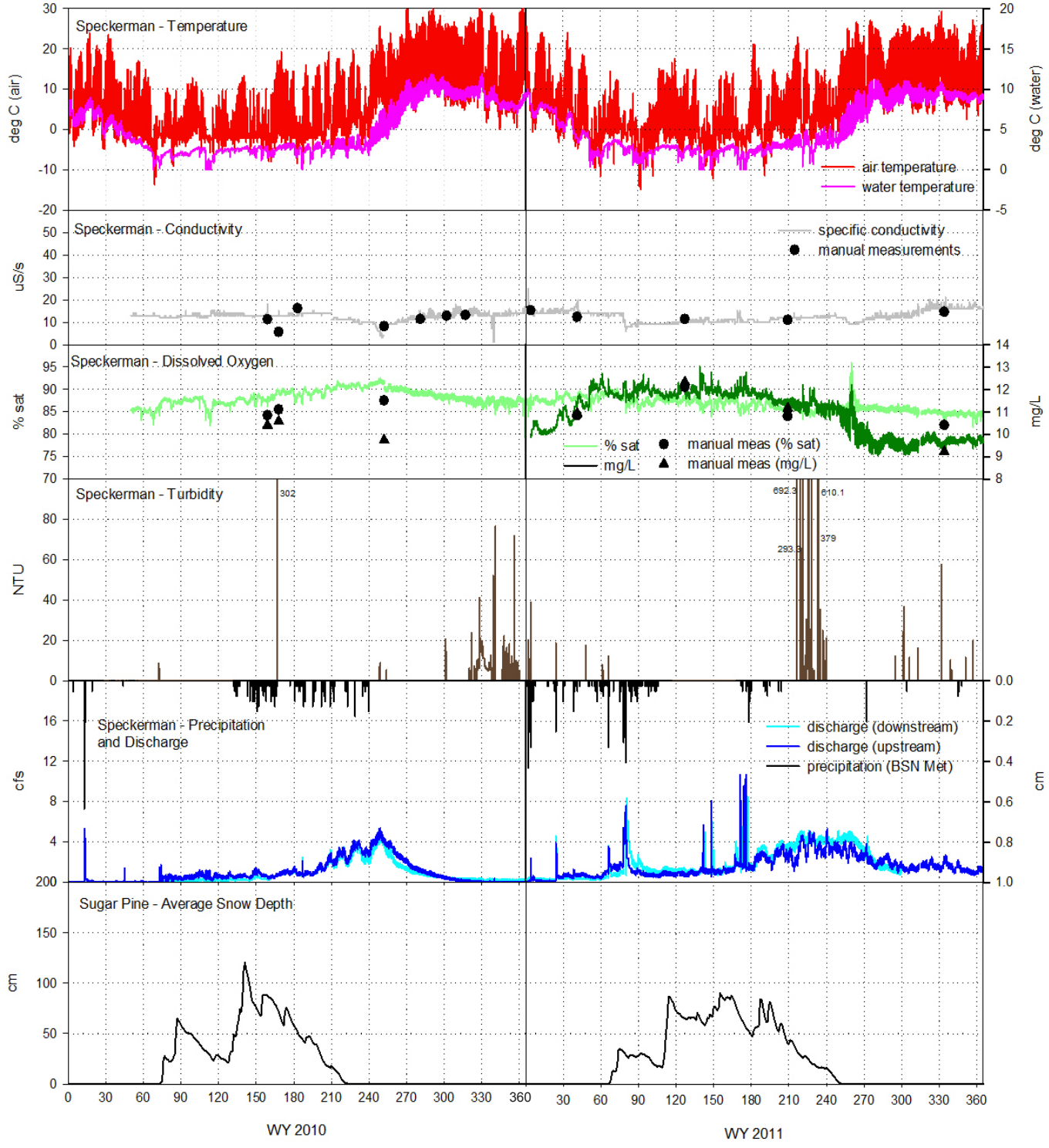

Figure 10. Speckerman Creek water-quality data. Water temperature, conductivity, dissolved oxygen, turbidity, and discharge are plotted as 15-minute time-interval data from Speckerman Creek. Air temperature and precipitation were collected at Big Sandy Met and plotted on an hourly time interval. Snow depth data are plotted using daily averages and spatial averages of all sensors across the Sugar Pine site.

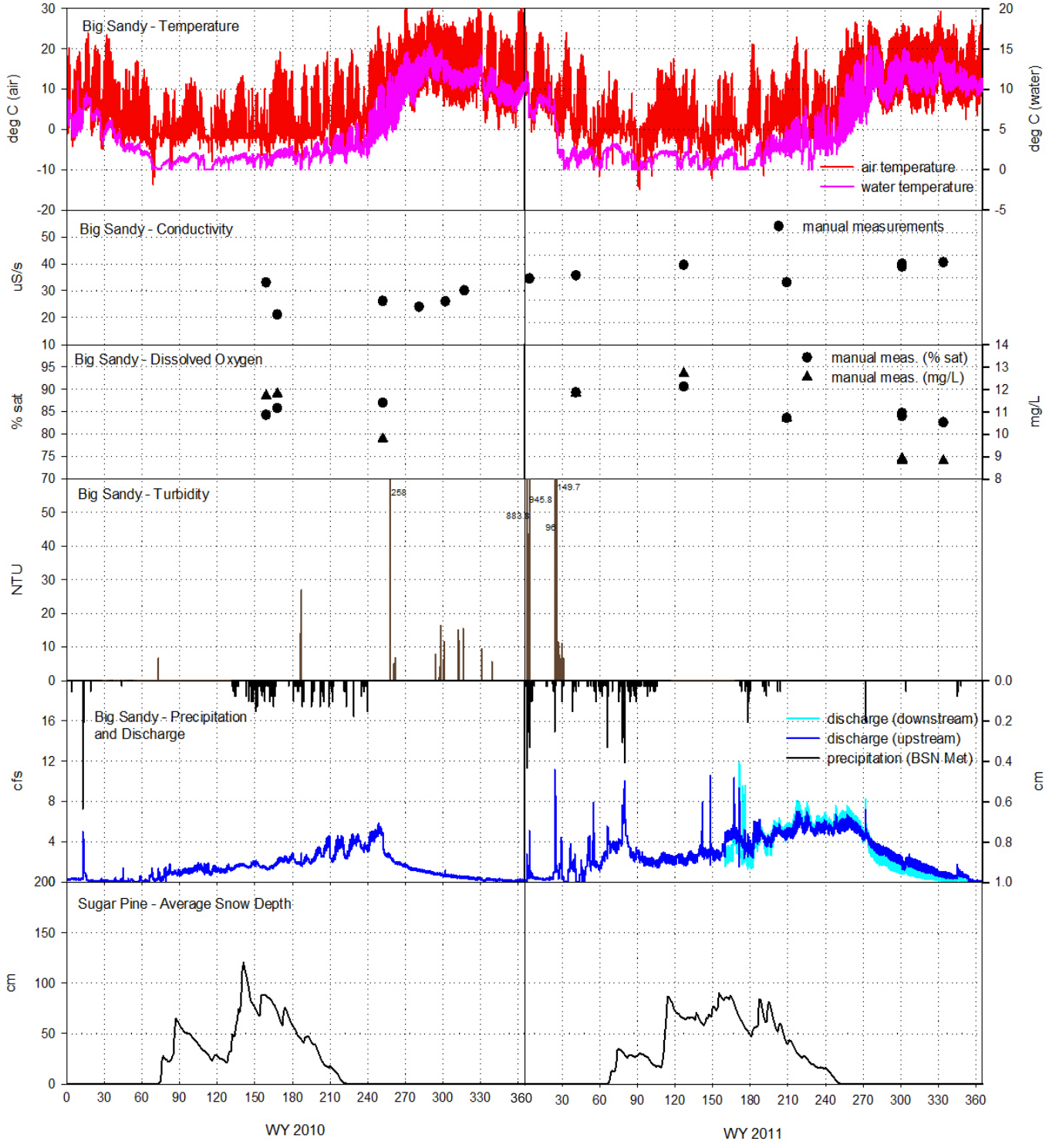

Figure 11. Big Sandy Creek water-quality data. Water temperature, conductivity, dissolved oxygen, turbidity, and discharge are plotted as 15-minute time-interval data from Big Sandy Creek. Air temperature and precipitation were collected at Big Sandy Met and plotted on an hourly time interval. Snow depth data are plotted using daily averages and spatial averages of all sensors across the Sugar Pine site.

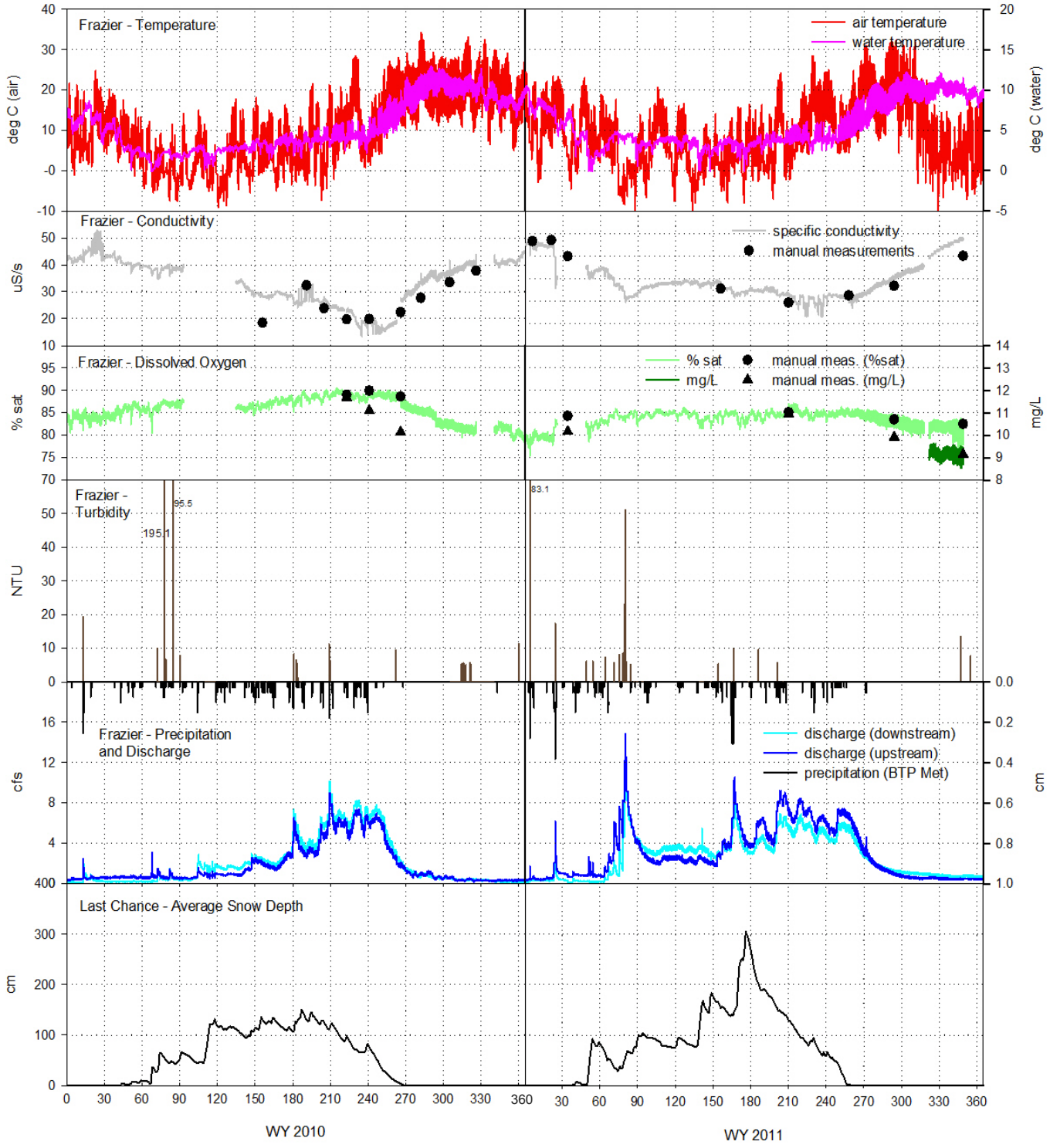

Figure 12. Frazier Creek water-quality data. Water temperature, conductivity, dissolved oxygen, turbidity, and discharge are plotted as 15-minute time-interval data from Frazier Creek. Air temperature and precipitation were collected at Bear Trap Met and plotted on an hourly time interval. Snow depth data are plotted using daily averages and spatial averages of all sensors across the Last Chance site.

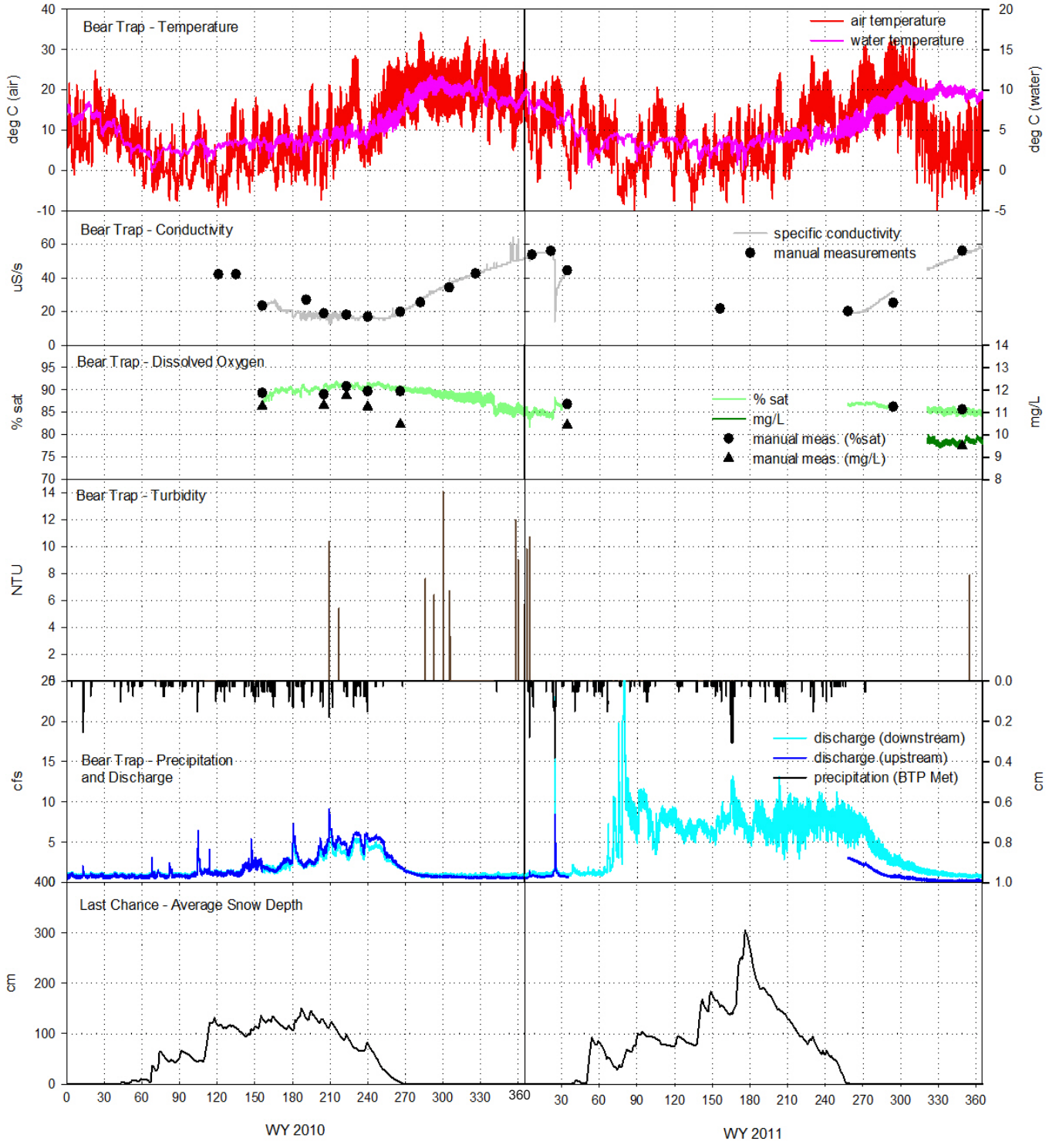

Figure 13. Bear Trap Creek water-quality data. Water temperature, conductivity, dissolved oxygen, turbidity, and discharge are plotted as 15-minute time-interval data from Bear Trap Creek. Air temperature and precipitation were collected at Bear Trap Met and plotted on an hourly time interval. Snow depth data are plotted using daily averages and spatial averages of all sensors across the Last Chance site.

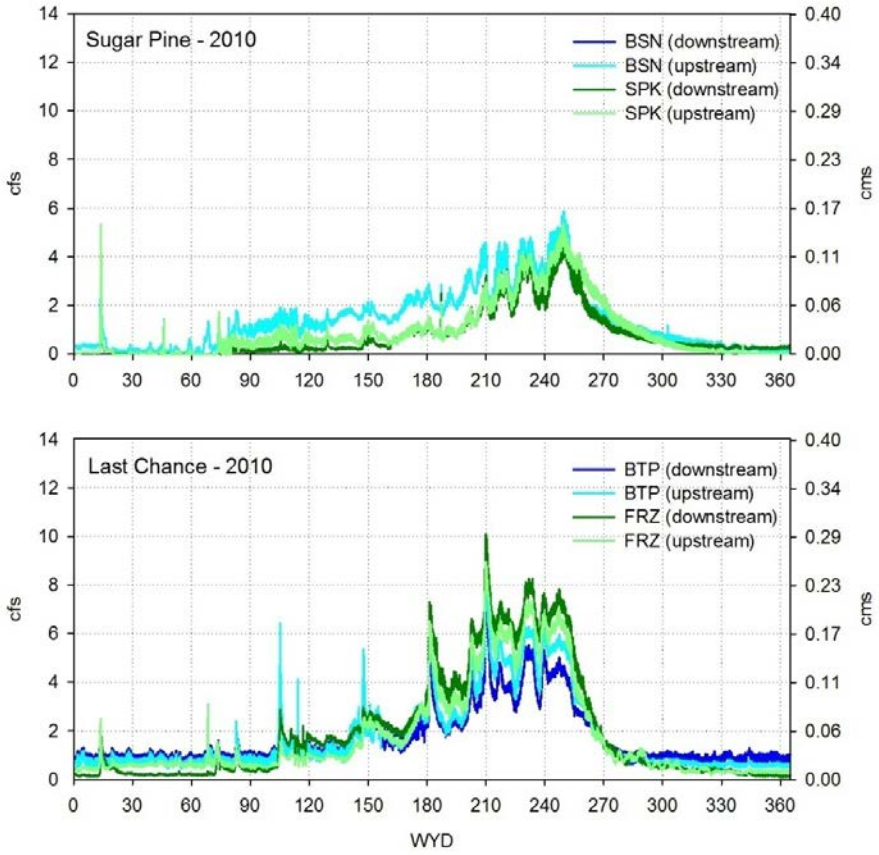

Figure 14. Water year 2010 15-minute discharge data for the Sugar Pine and Last Chance sites.

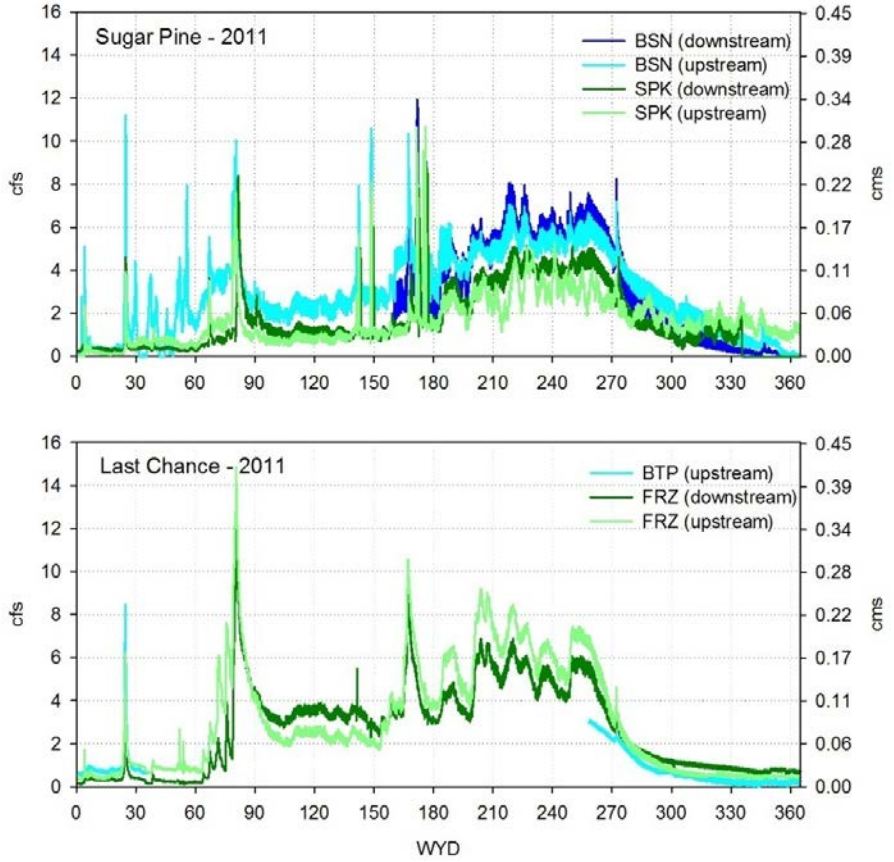

Figure 15. Water year 2011 15-minute discharge data for the Sugar Pine and Last Chance sites.

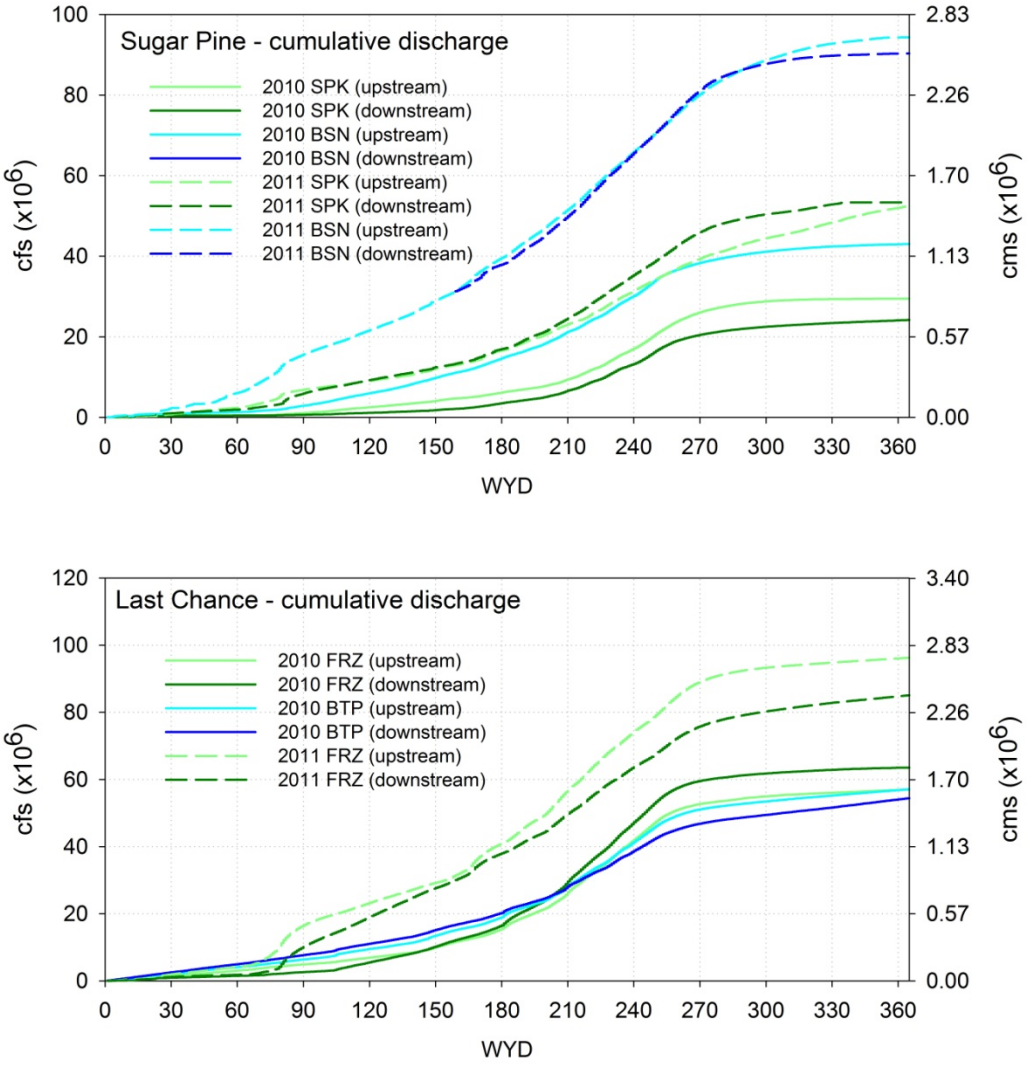

Figure 16. Cumulative discharge plots based on 15-minute discharge data for Sugar Pine and Last Chance sites.

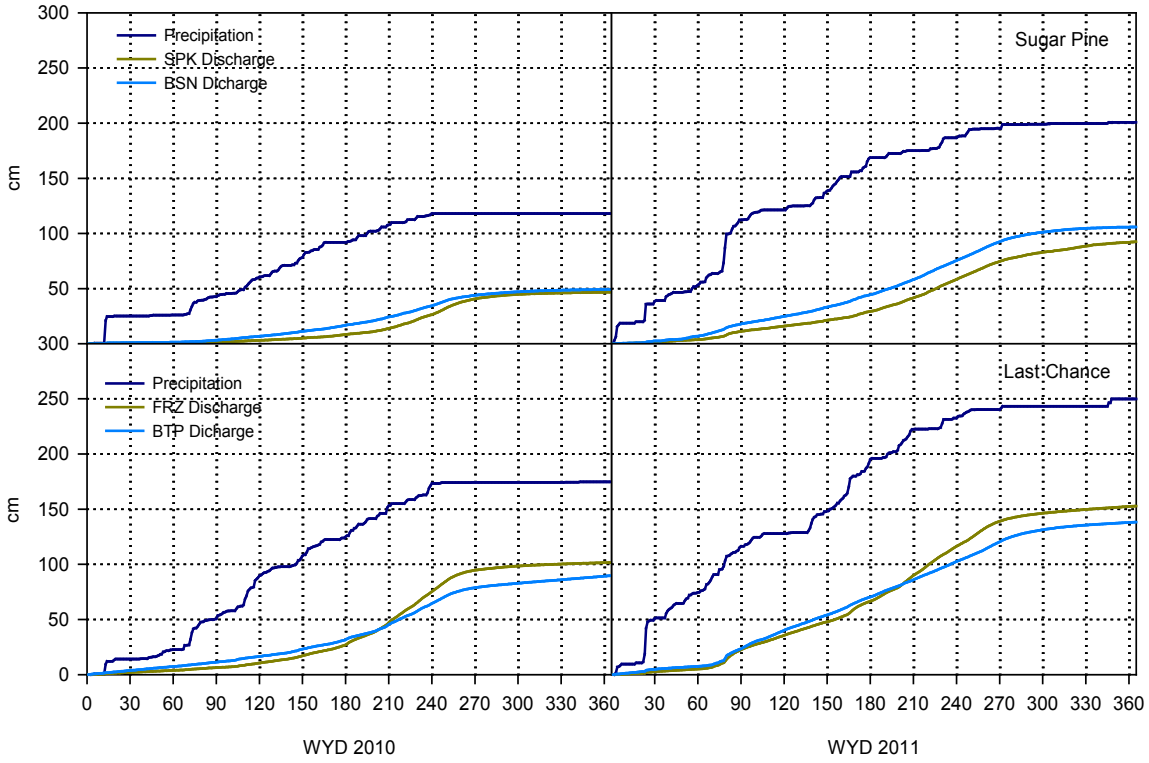

Figure 17. Cumulative daily precipitation and discharge for the Sugar Pine and Last Chance sites.

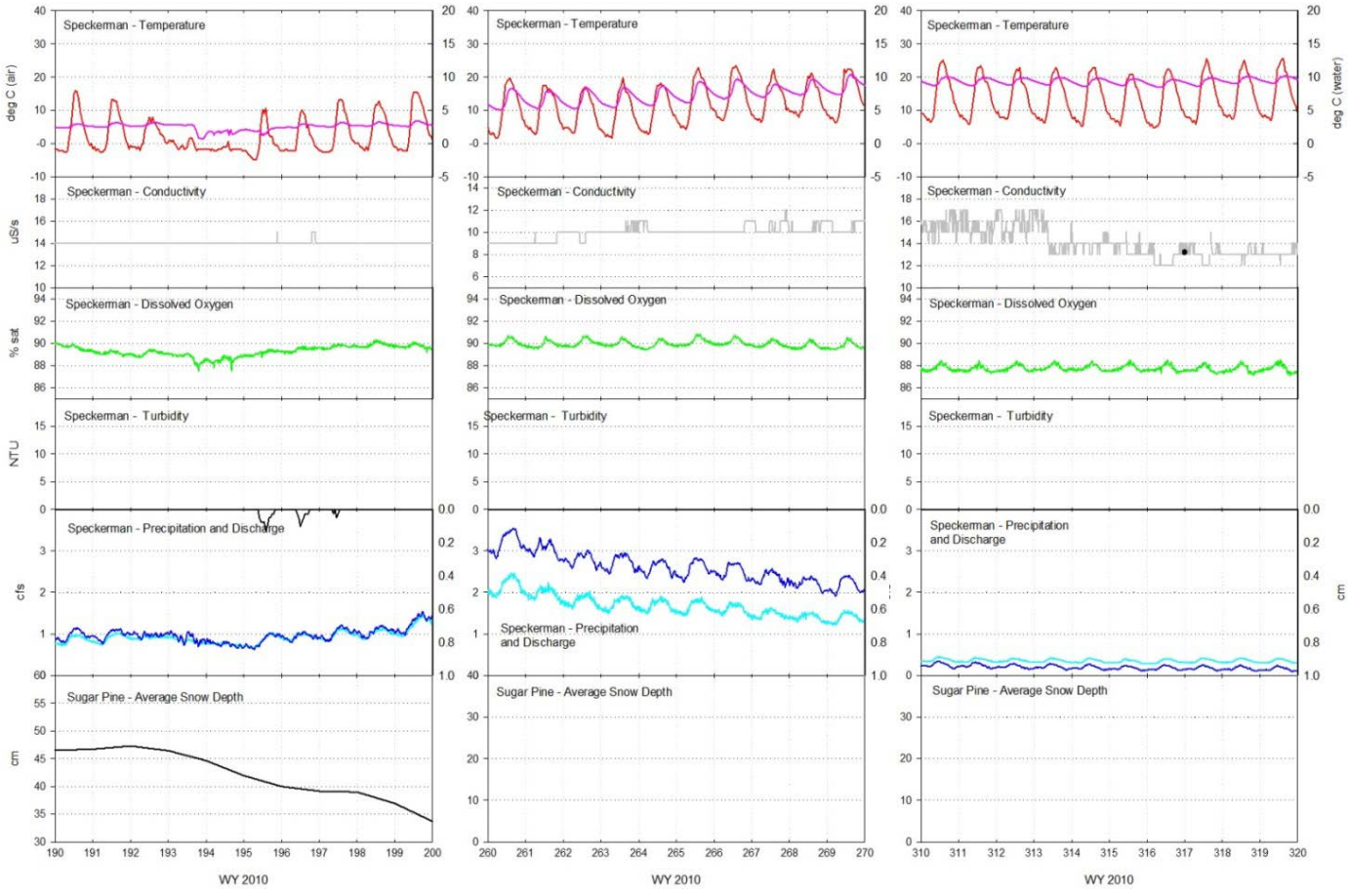

Figure 18. Speckerman Creek ten-day periods during snow melt (left), spring recession, and baseflow (right)

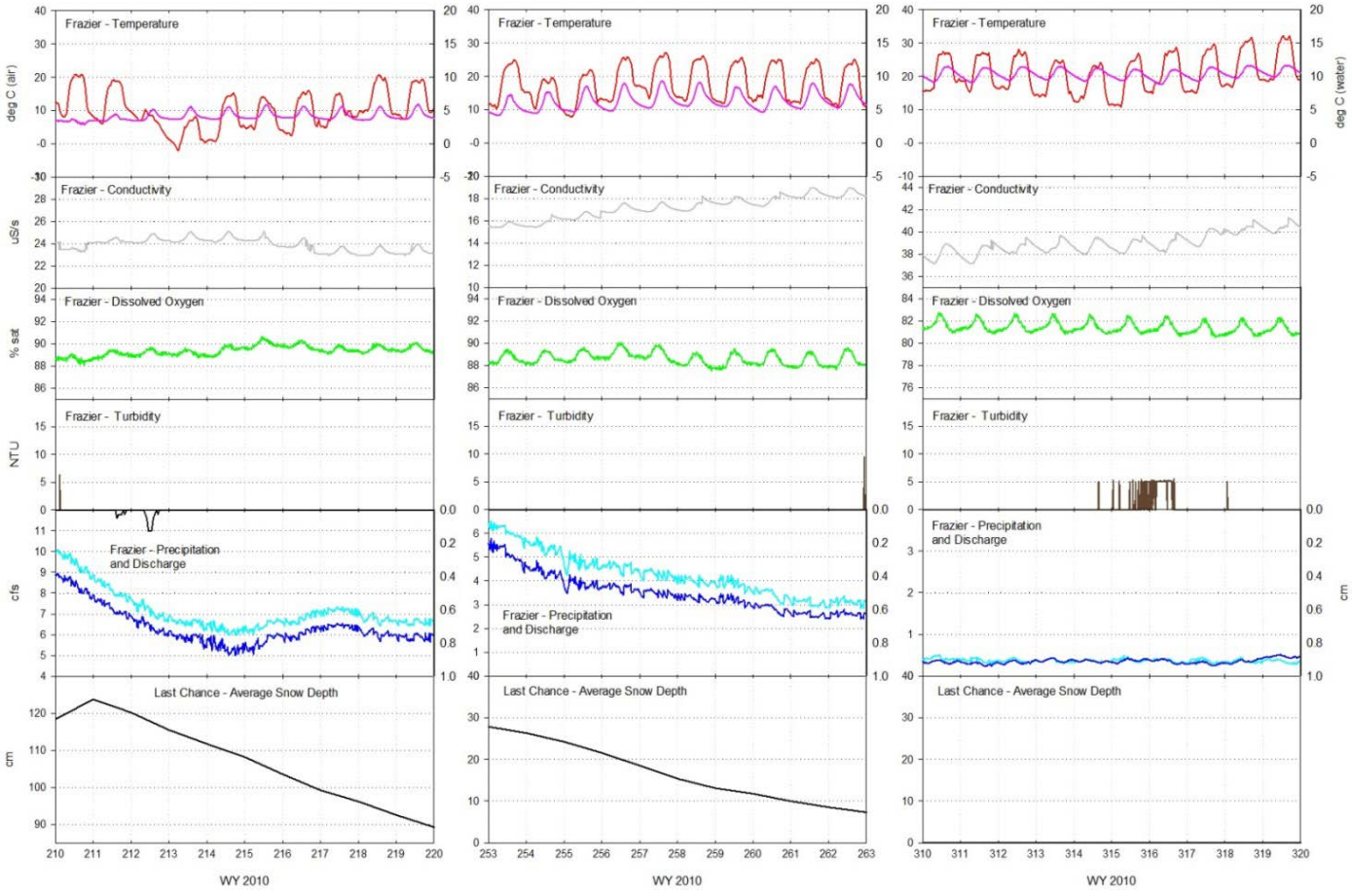

Figure 19. Frazier Creek ten-day periods during snow melt (left), spring recession, and baseflow (right)

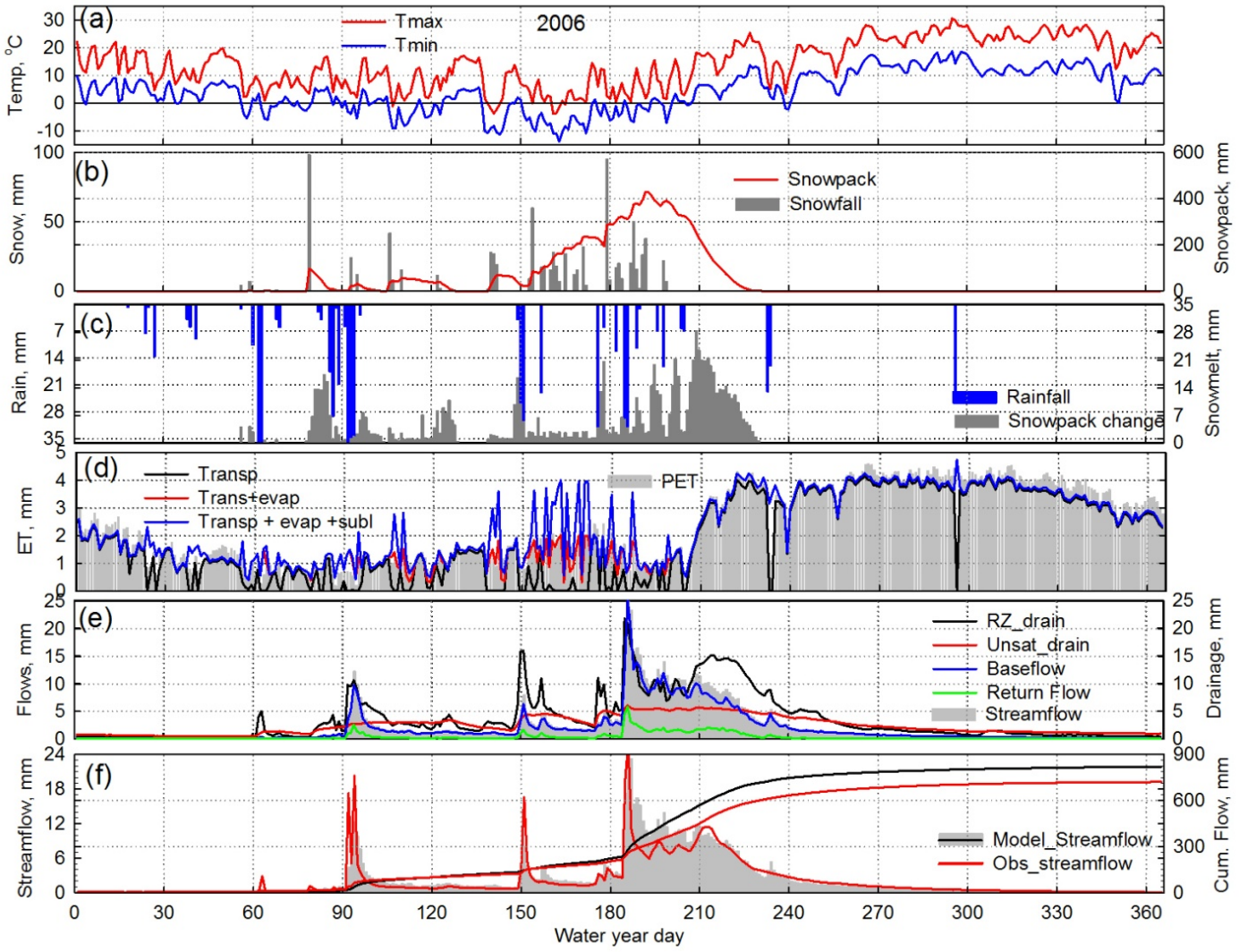

Figure 20: RHESSys output using daily observed temperatures, snowfall and rainfall as inputs. Output variables are snowmelt, evaporation, transpiration, sublimation, Potential ET (PET), Root-Zone (RZ) and unsaturated zone drainage, baseflow, return flow. Also included is the comparison of daily and cumulative observed (obs) and simulated streamflow for catchment P303, Kings River Experimental Watershed in water year 2006.

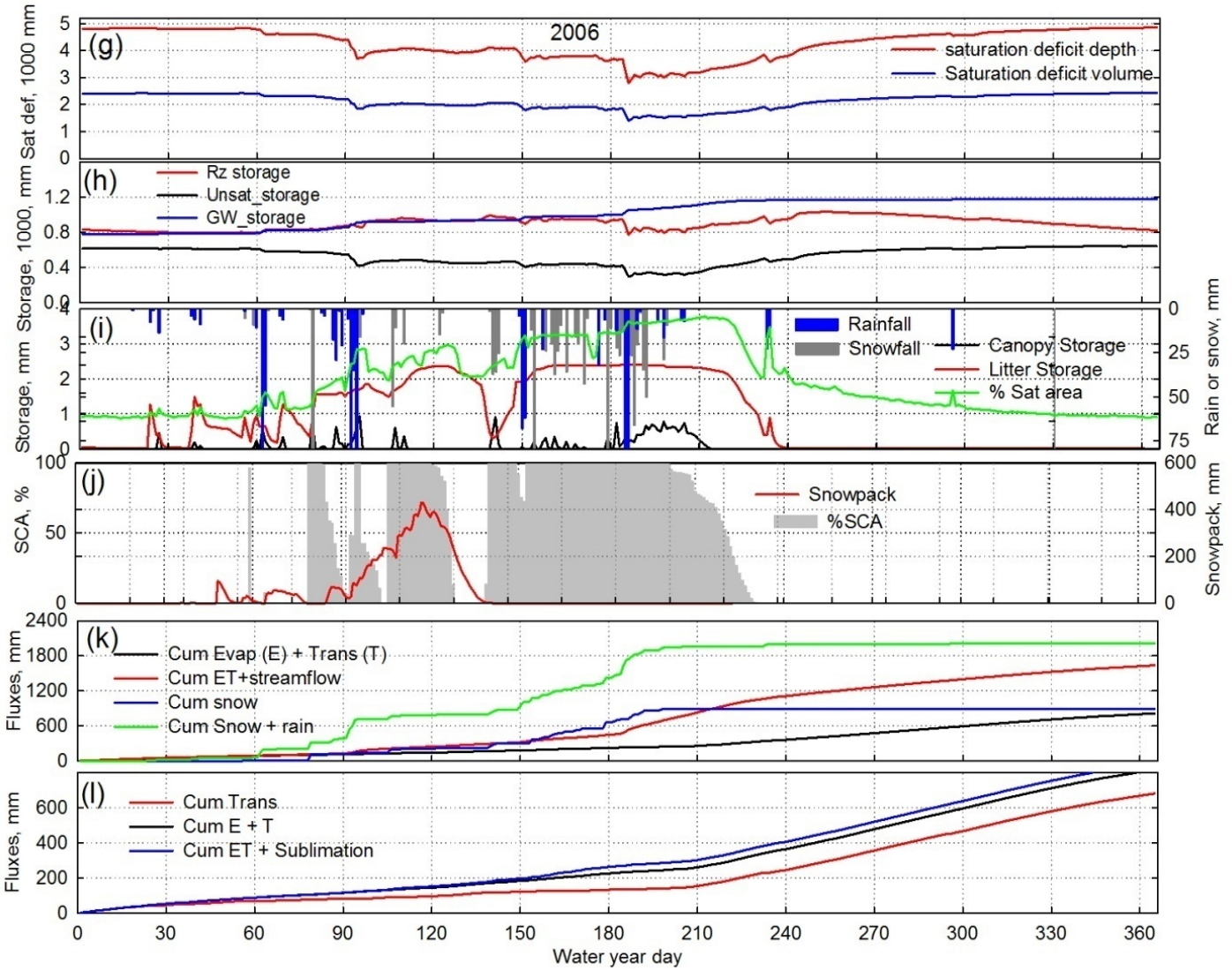

Figure 21: Additional daily model output used for diagnosis and constraining parameters: saturation deficit, snowpack, snow cover area (SCA), evaporation, transpiration, sublimation, root-zone (RZ), unsaturated zone groundwater (GW), canopy and litter storage. (P303, Kings River Watershed)

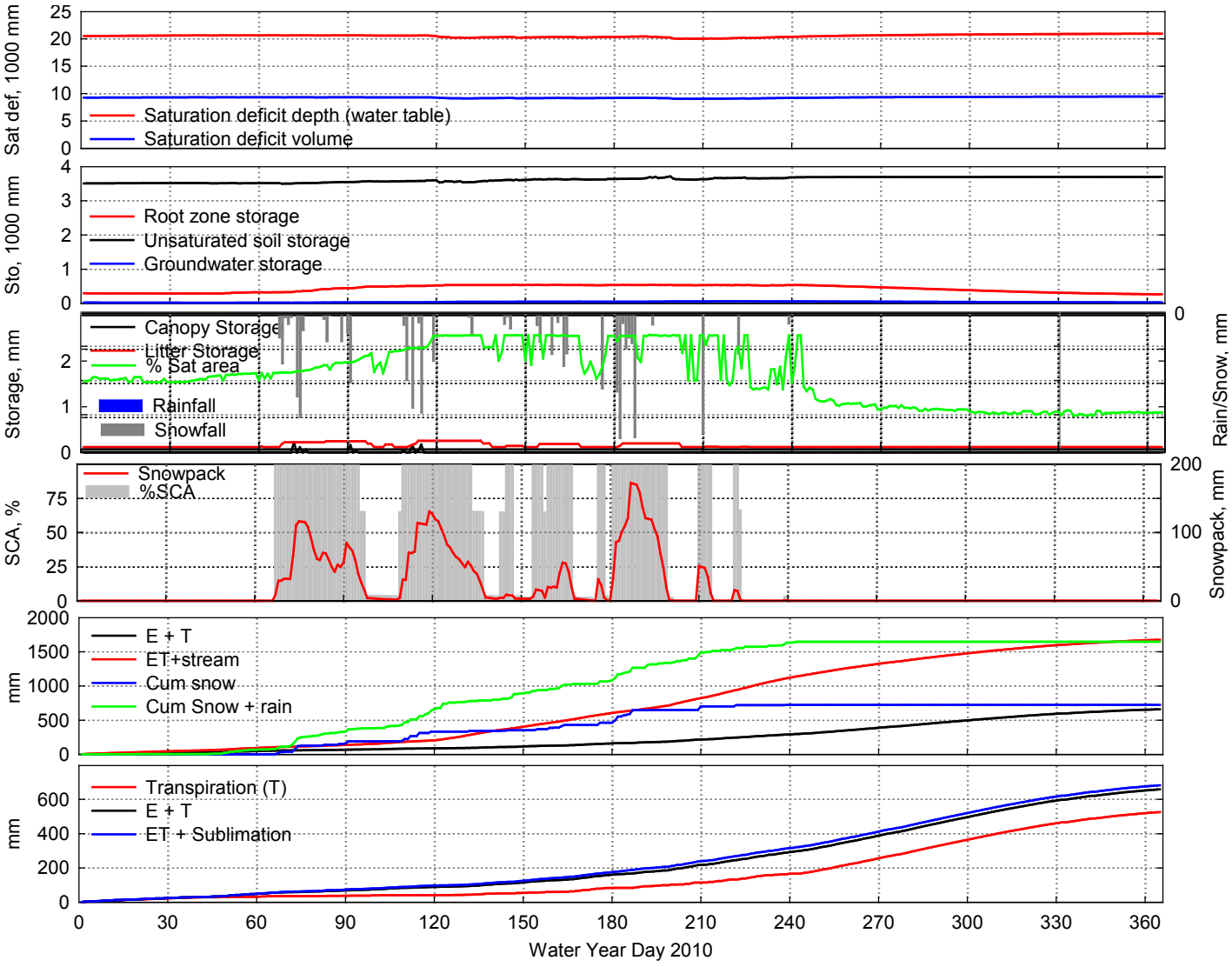

Figure 22: RHESSys output using daily observed temperatures, snowfall and rainfall as inputs. Output variables are snowmelt, evaporation, transpiration, sublimation, Potential ET (PET), Root-Zone (RZ) and unsaturated zone drainage, baseflow, return flow. Also included is the comparison of daily and cumulative observed (obs) and simulated streamflow for Bear Trap Creek in water year 2010.

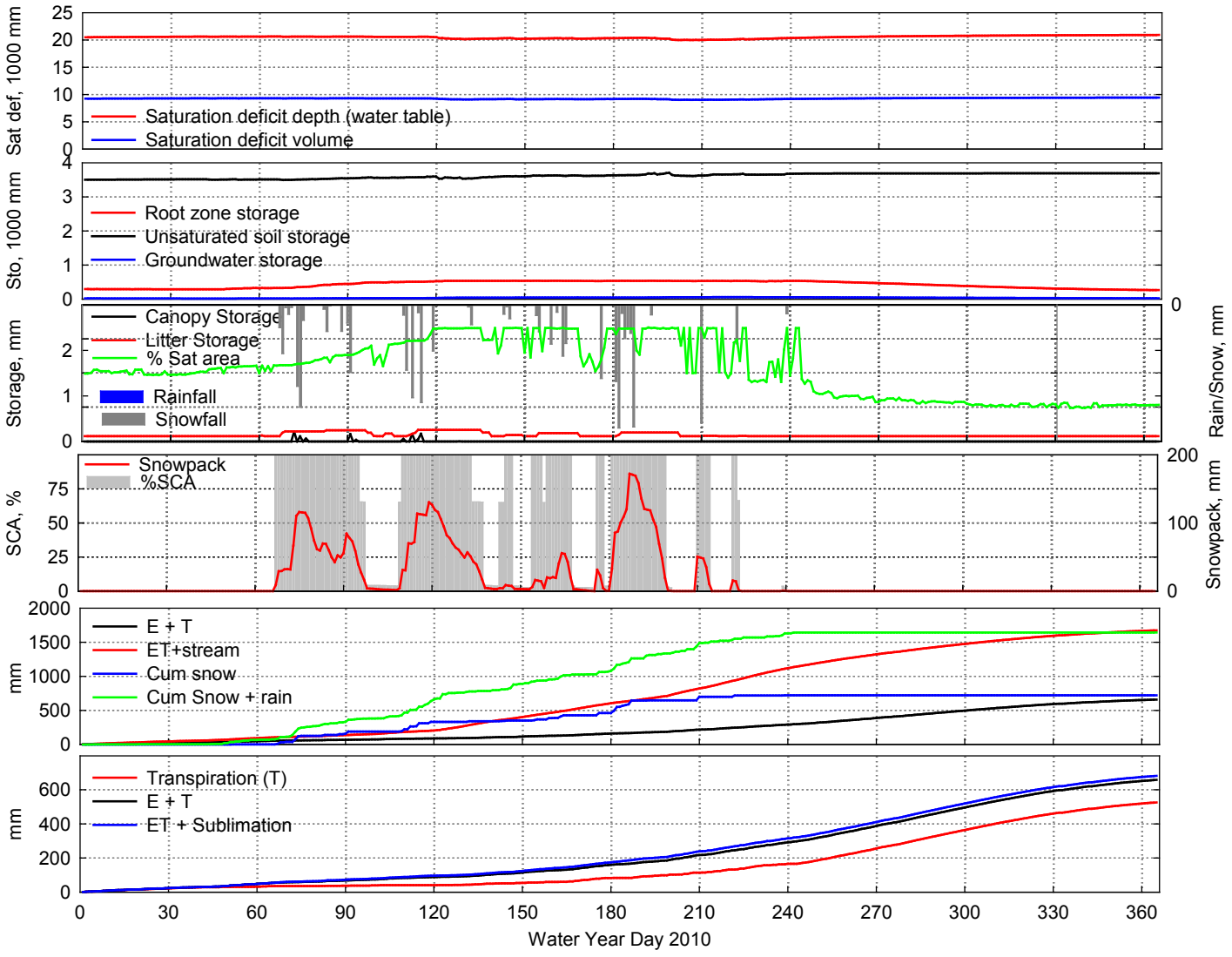

Figure 23: Additional model output used for diagnosis and constraining parameters: saturation deficit, snowpack, snow cover area (SCA), evaporation, transpiration, sublimation, root-zone (RZ), unsaturated zone groundwater (GW), canopy and litter storage. (Bear Trap Creek)

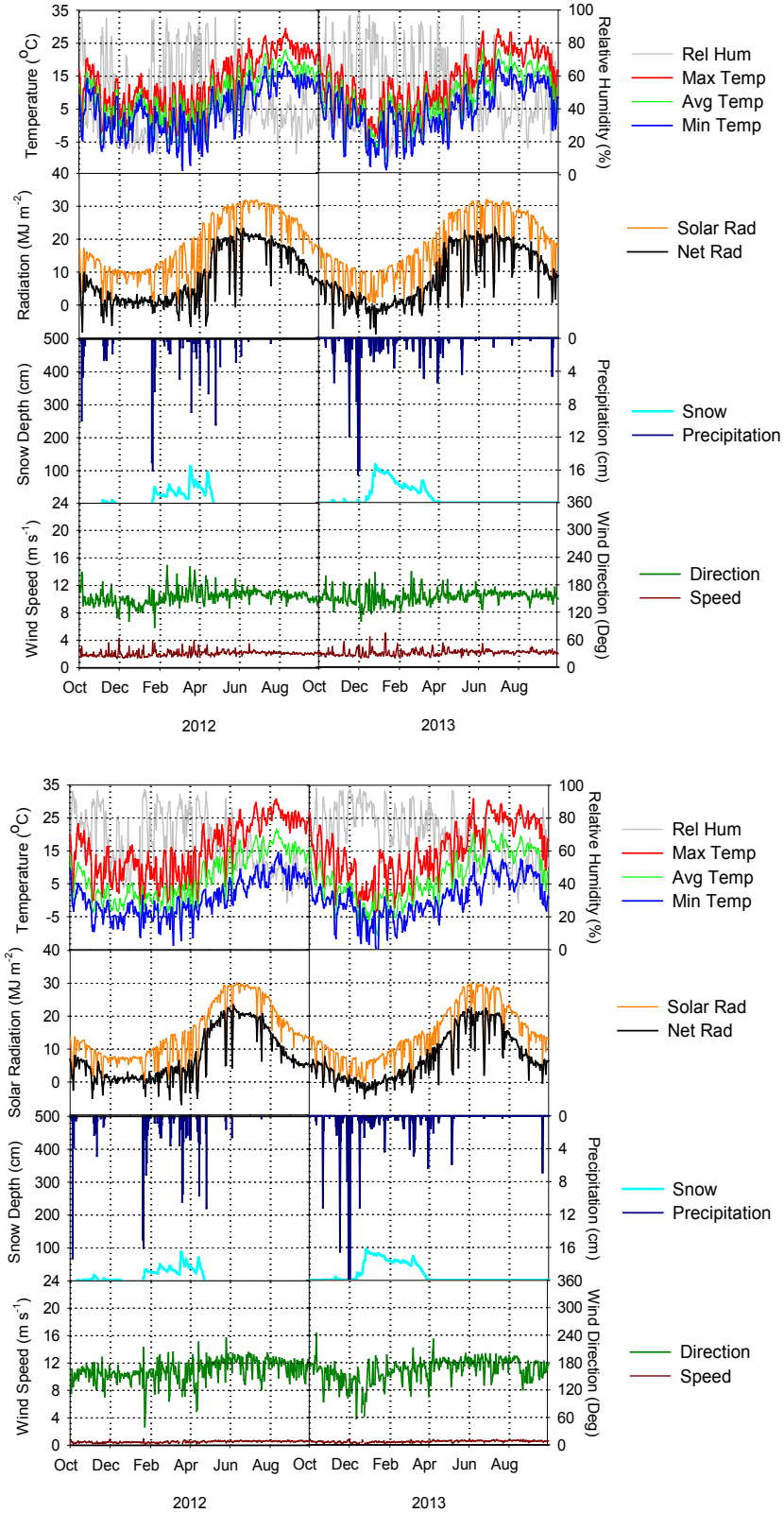

Figure 24. Daily data collected from the upper (Fresno Dome) and lower (Big Sandy) elevation meteorological stations in the Sugar Pine study area for water years 2012-2013.

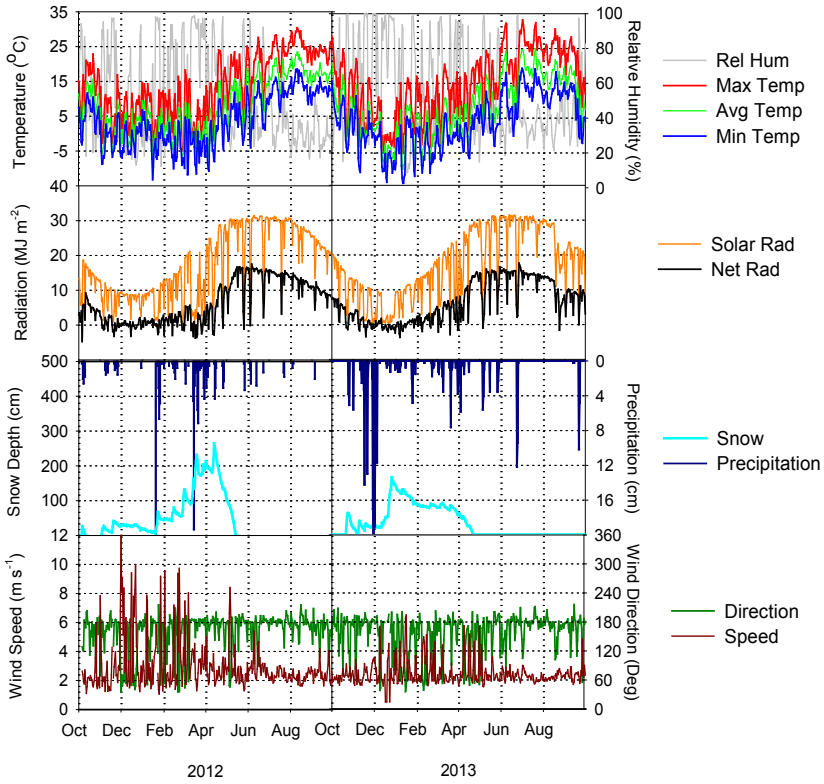

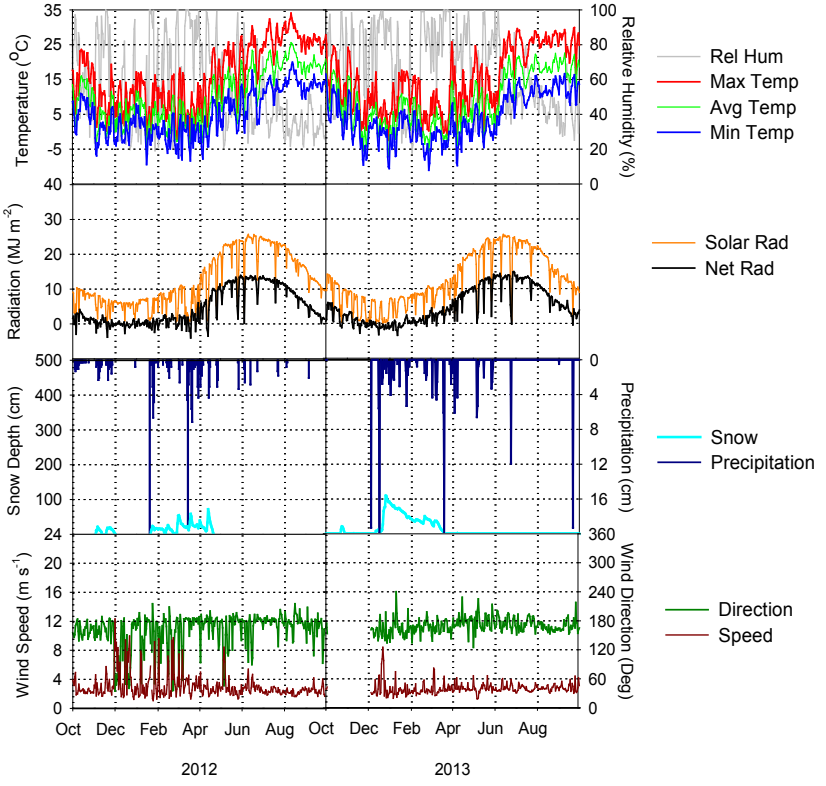

Figure 25. Daily data collected from the upper (Duncan Peak) and lower (Bear Trap) elevation meteorological stations in the Sugar Pine study area for water years 2012-2013.

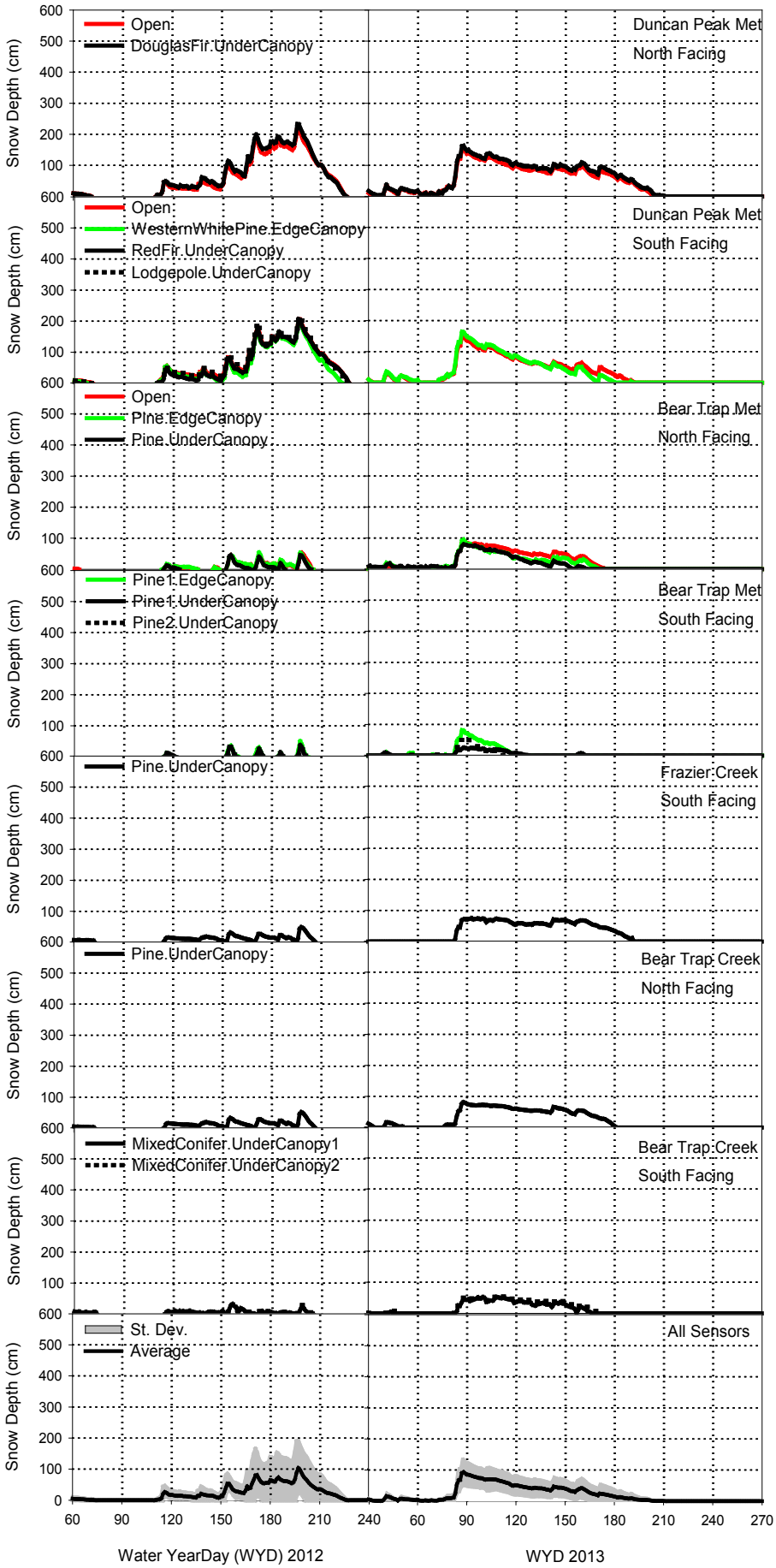

Figure 26. Daily mean snow depth recorded with a total of 16 sensors in 4 different locations incorporating the variable physiographic characteristics of aspect, canopy cover, and elevation that are present in the study area.

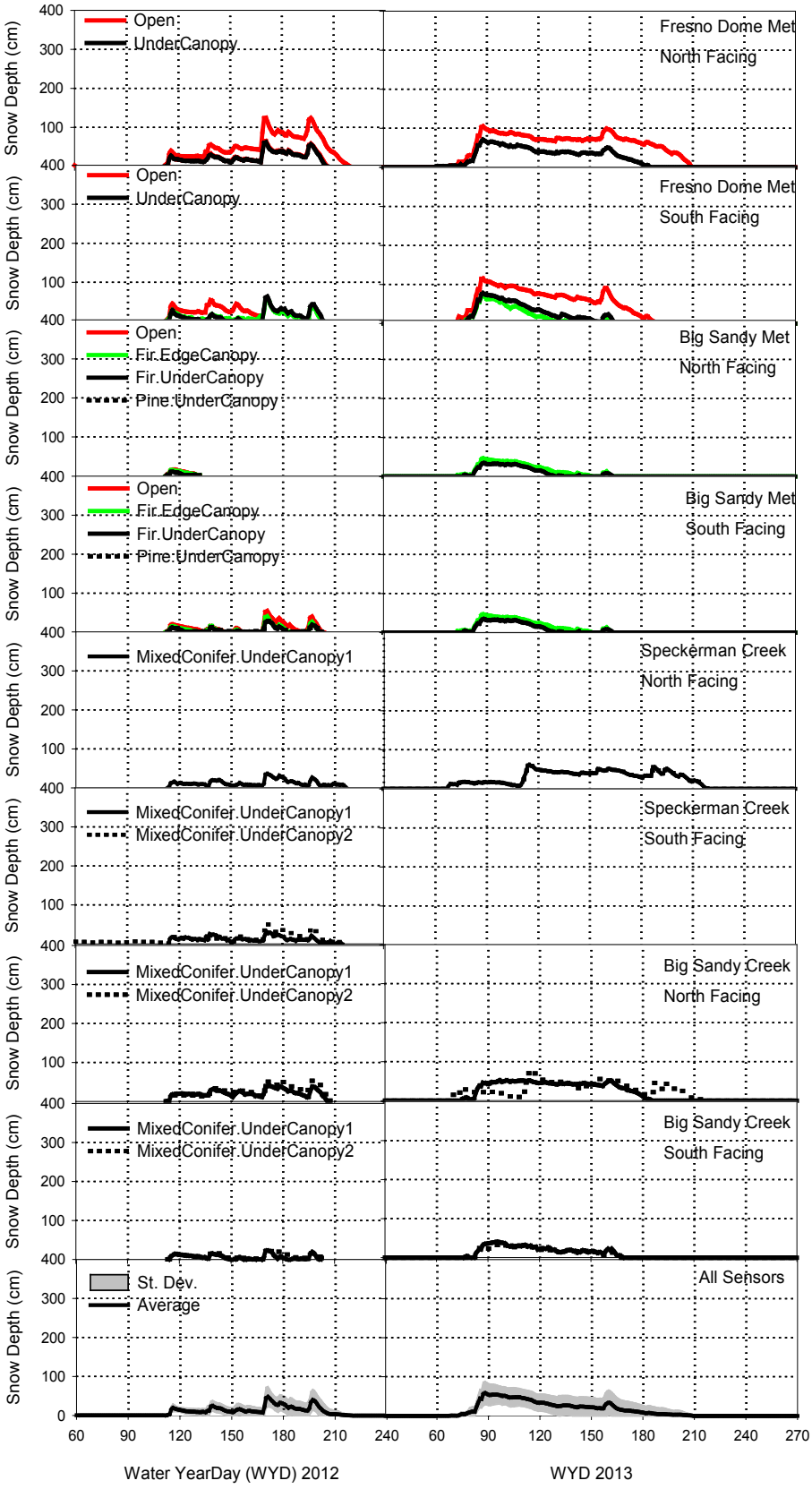

Figure 27. Daily mean snow depth for 2011-2012 from 18 sensors in 4 different locations, covering physiographic characteristics of aspect, slope, elevation, and canopy cover present in the Sugar Pine study area.

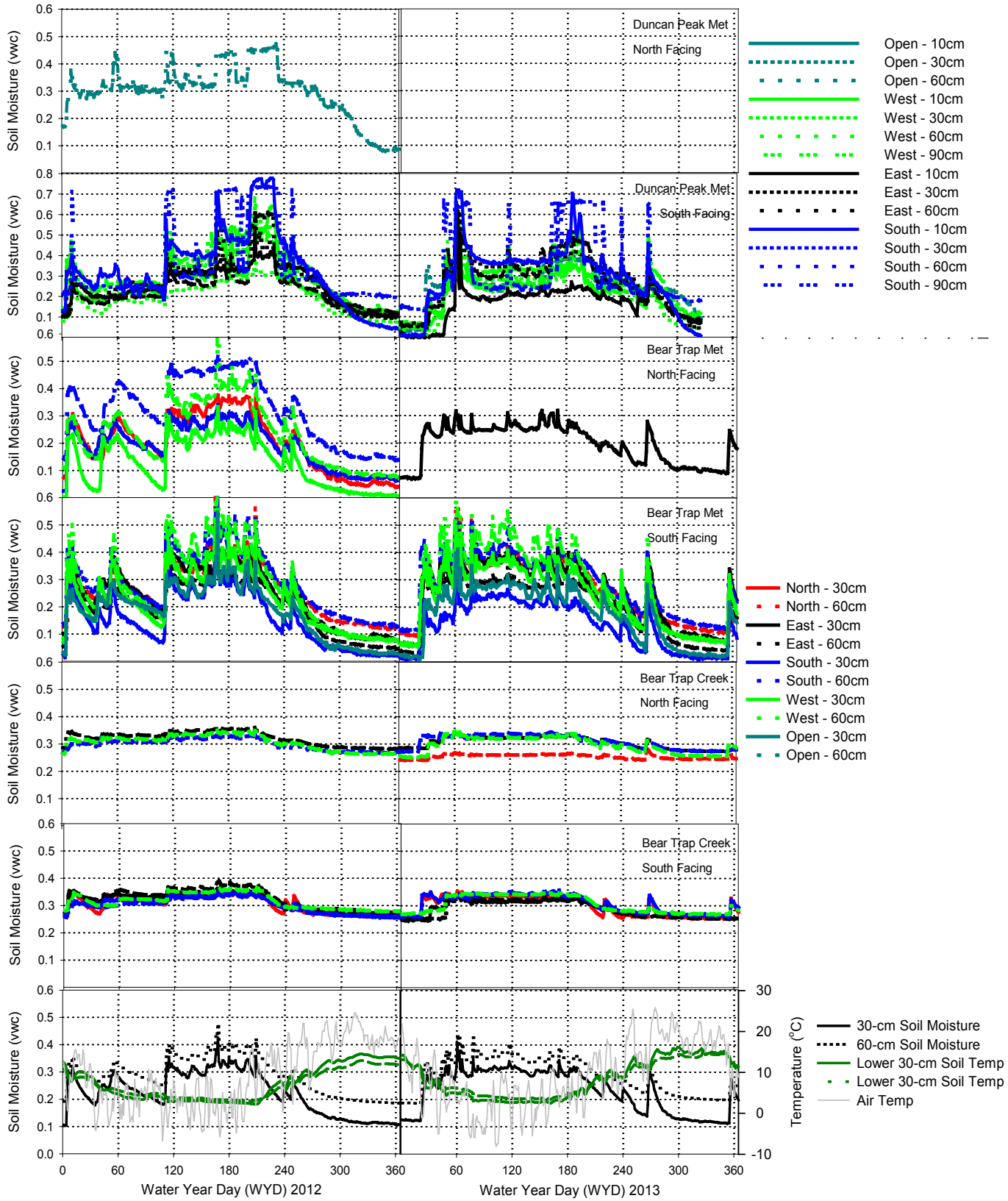

Figure 28. Soil moisture recorded with 43 sensors in the 4 general study locations. Most sensors were placed at 30- and 60-cm below the surface in a cardinal direction 1 m from the trunk of a tree where snow depth was also measured. A few sensors were placed at different depths for additional observations. The sensors at Duncan Peak exhibited erratic behavior not observed at the other sites, with these time periods removed a limited number of observations were recorded.

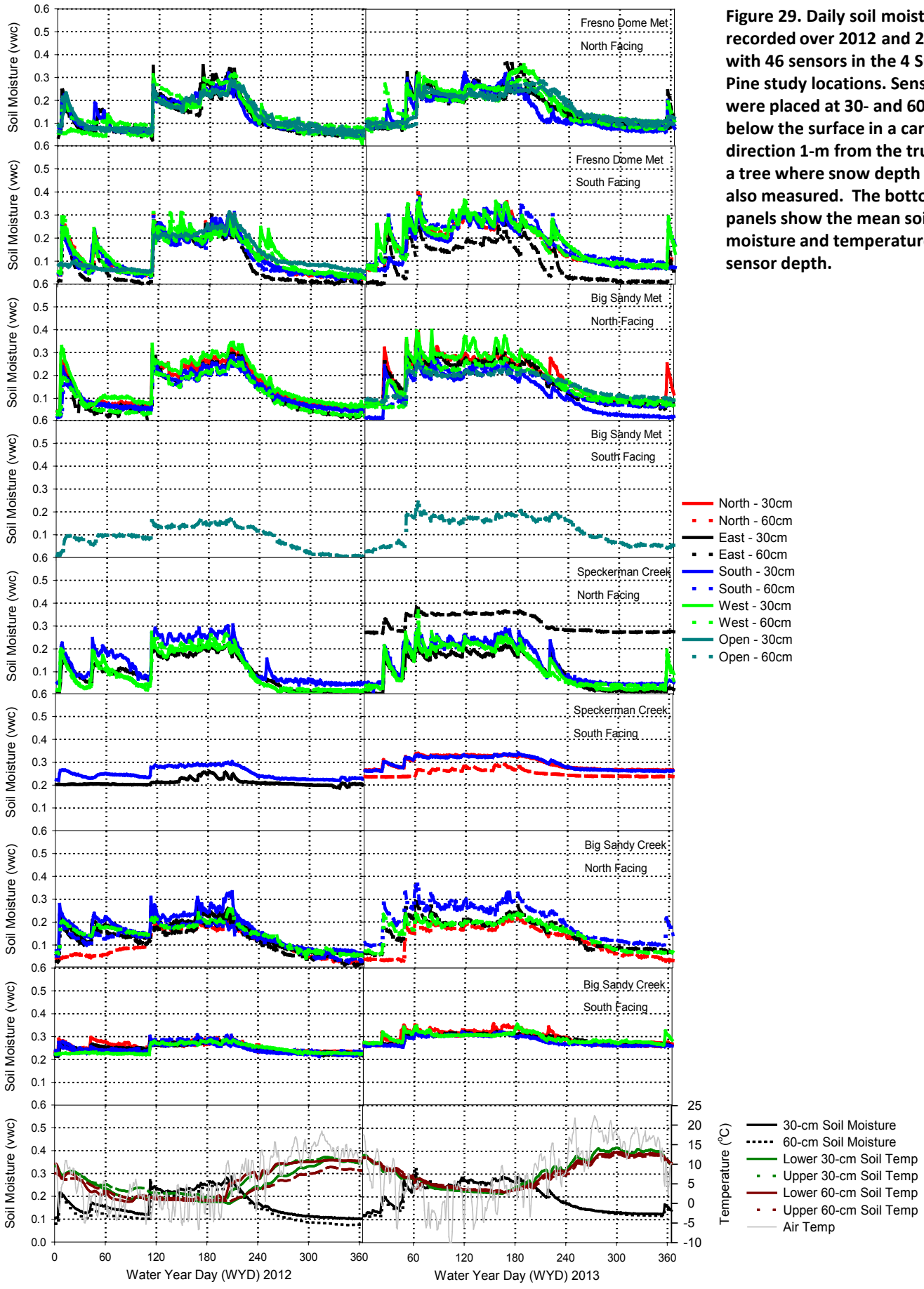

Figure 29. Daily soil moisture recorded over 2012 and 2013 with 46 sensors in the 4 Sugar Pine study locations. Sensors were placed at 30- and 60-cm below the surface in a cardinal direction 1-m from the trunk of a tree where snow depth was also measured. The bottom panels show the mean soil moisture and temperature by sensor depth.

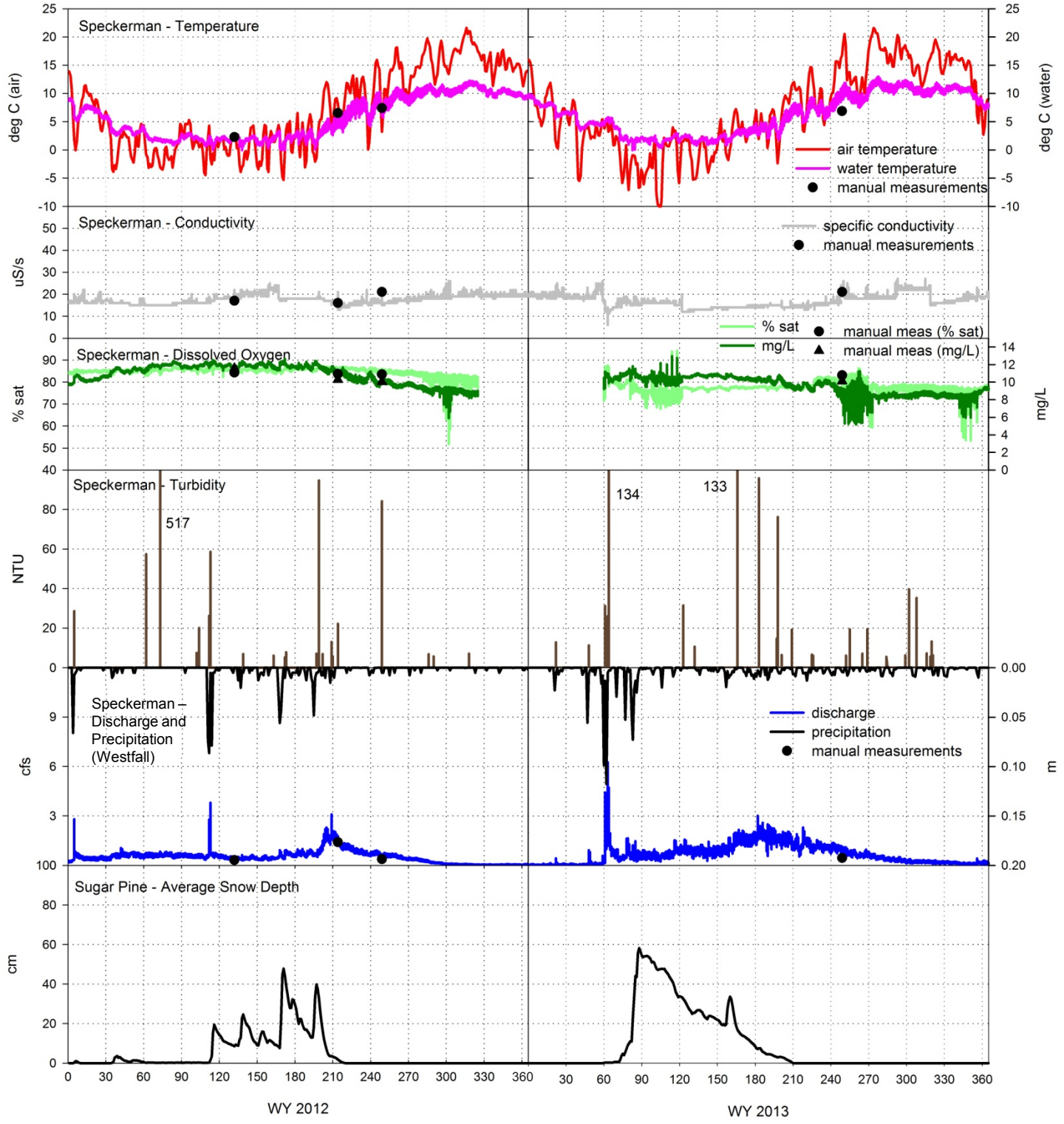

Figure 30. Speckerman Creek water-quality data for WY 2012 and WY 2013. Water temperature, conductivity, dissolved oxygen, turbidity, and discharge are plotted as 15-minute time-interval data from Speckerman Creek. Air temperature was collected at Big Sandy Met and plotted on a daily time interval. Precipitation data are from the Westfall meteorological station operated by the US Army Corps of Engineers. Snow depth data are plotted using daily averages and spatial averages of all sensors across the Sugar Pine site.

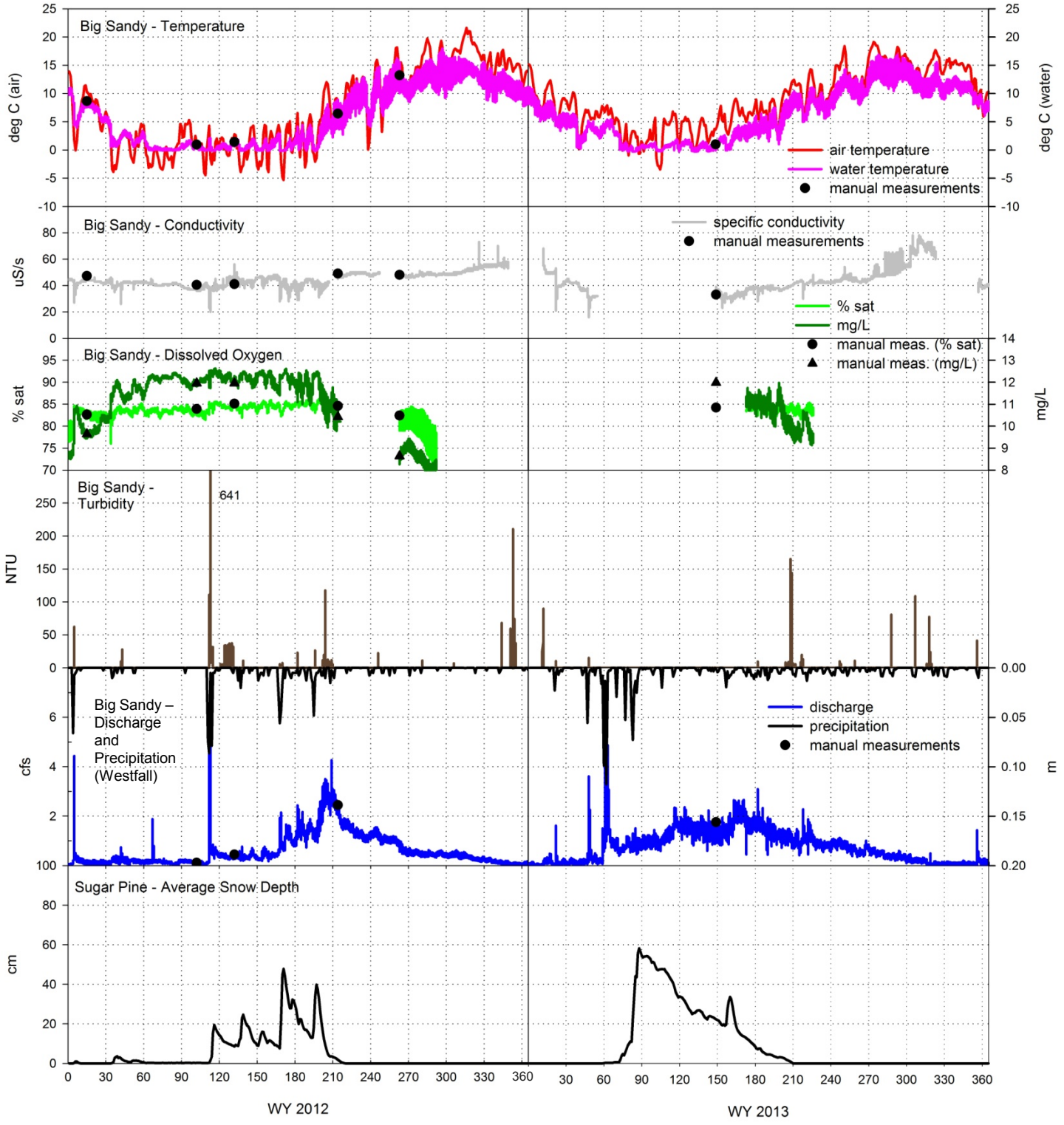

Figure 31. Big Sandy Creek water-quality data for WY 2012 and WY 2013. Water temperature, conductivity, dissolved oxygen, turbidity, and discharge are plotted as 15-minute time-interval data from Big Sandy Creek. Air temperature was collected at Big Sandy Met and plotted on a daily time interval. Precipitation data are from the Westfall meteorological station operated by the US Army Corps of Engineers. Snow depth data are plotted using daily averages and spatial averages of all sensors across the Sugar Pine site.

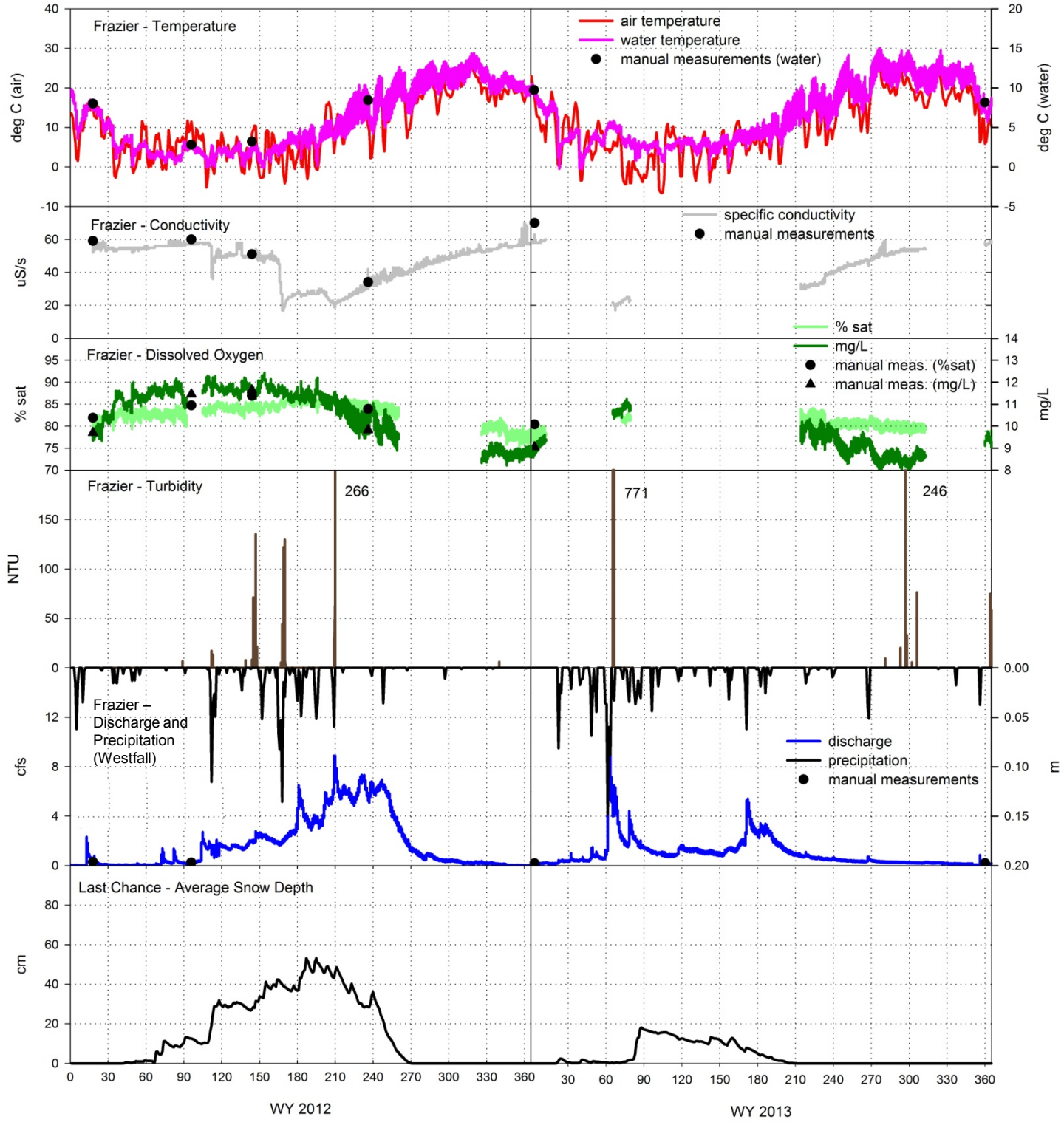

Figure 32. Frazier Creek water-quality data for WY 2012 and WY 2013. Water temperature, conductivity, dissolved oxygen, turbidity, and discharge are plotted as 15-minute time-interval data from Frazier Creek. Air temperature was collected at Bear Trap Met and plotted on a daily time interval. Precipitation data are from the Blue Canyon meteorological station operated by the US Bureau of Reclamation. Snow depth data are plotted using daily averages and spatial averages of all sensors across the Last Chance site.

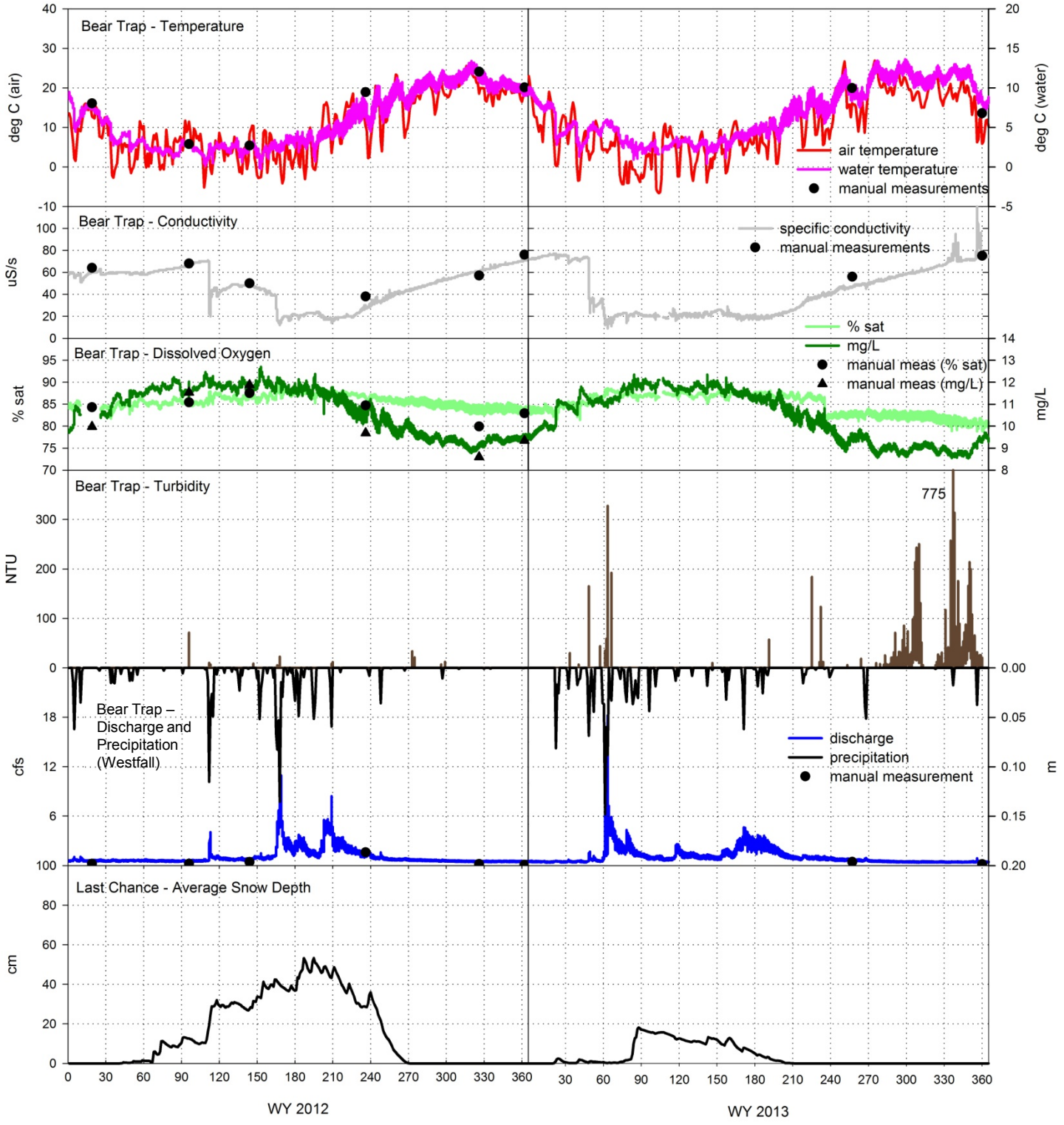

Figure 33. Bear Trap Creek water-quality data for WY 2012 and WY 2013. Water temperature, conductivity, dissolved oxygen, turbidity, and discharge are plotted as 15-minute time-interval data from Bear Trap Creek. Air temperature was collected at Bear Trap Met and plotted on a daily time interval. Precipitation data are from the Blue Canyon meteorological station operated by the US Bureau of Reclamation. Snow depth data are plotted using daily averages and spatial averages of all sensors across the Last Chance site.

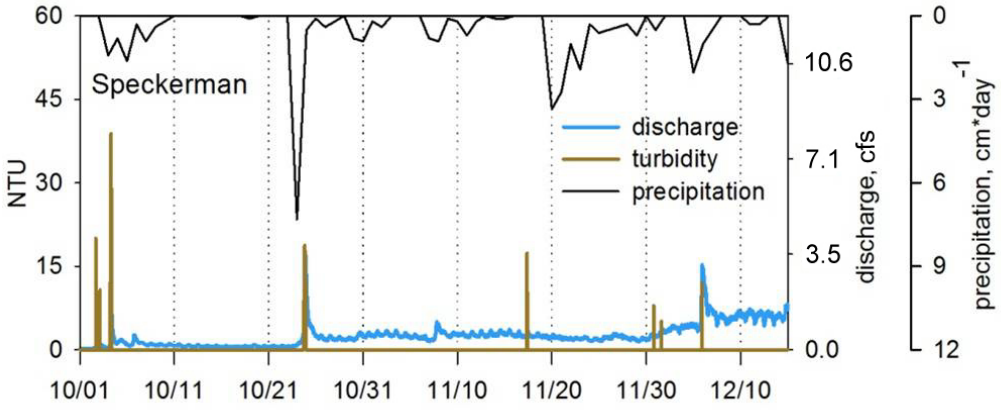

Figure 34. Turbidity, discharge, and precipitation data from Speckermen Creek for the fall rainy season, WY 2011.

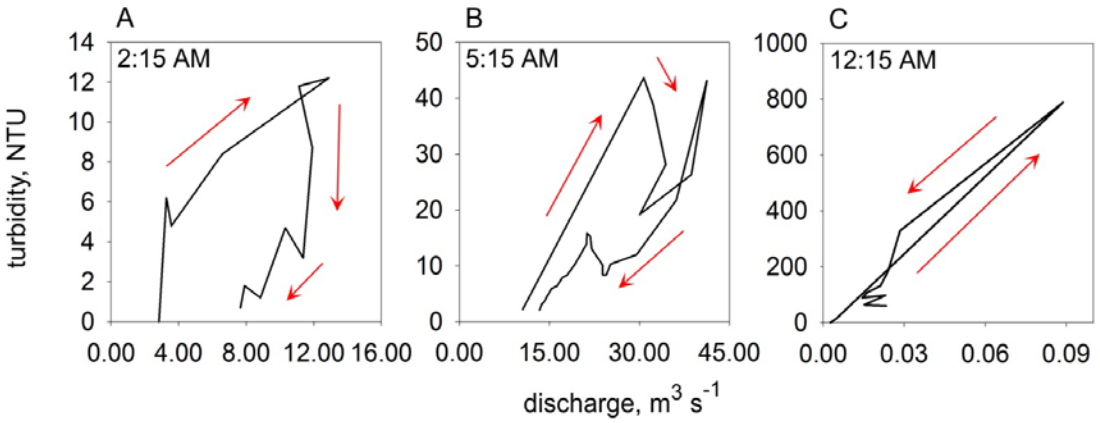

Figure 35. Hysteresis pattern progression seen within a multi-rise discharge event at Big Sandy Creek

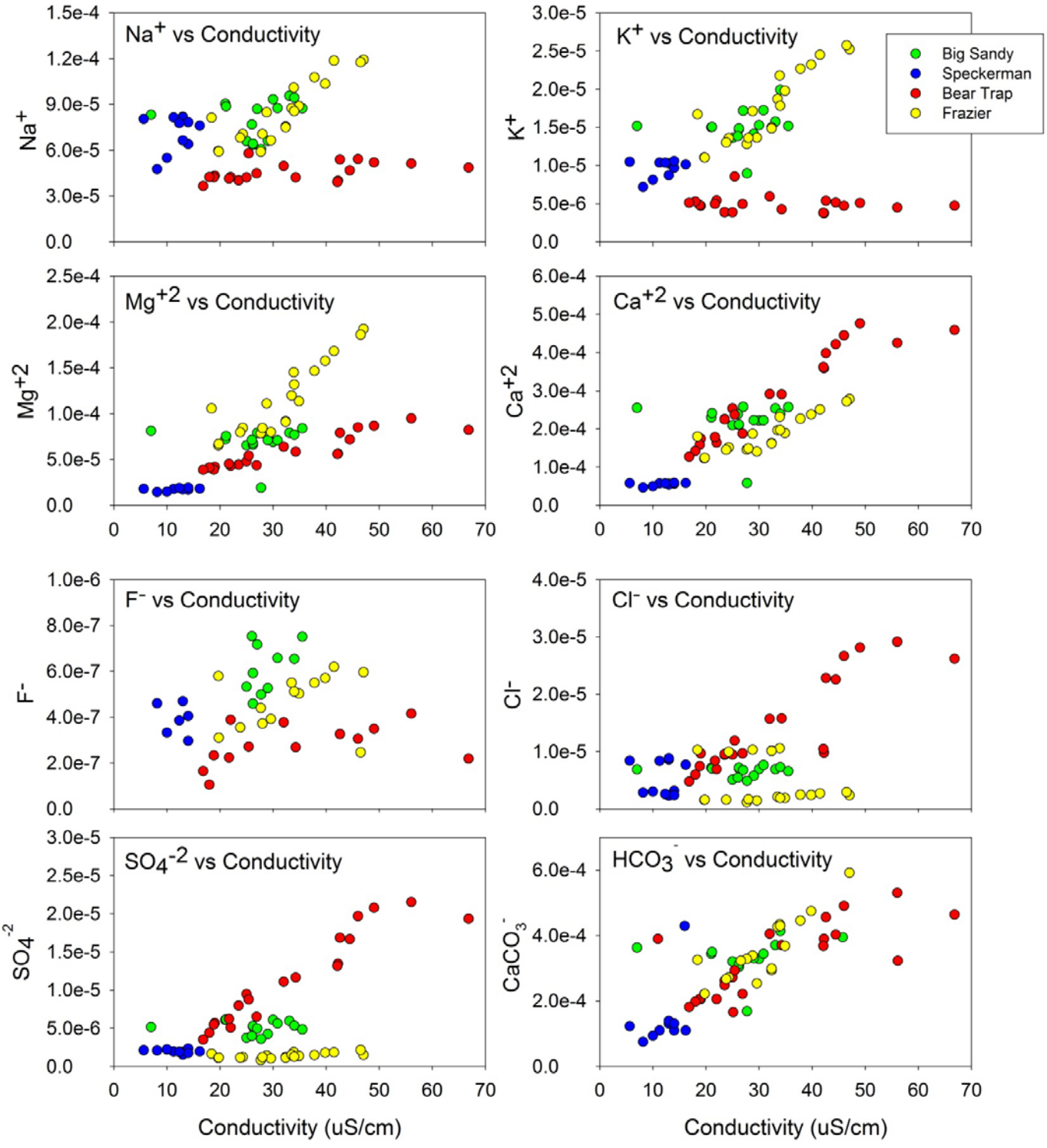

Figure 36. Major cation and anion data for stream water samples from WY's 2010-2013.

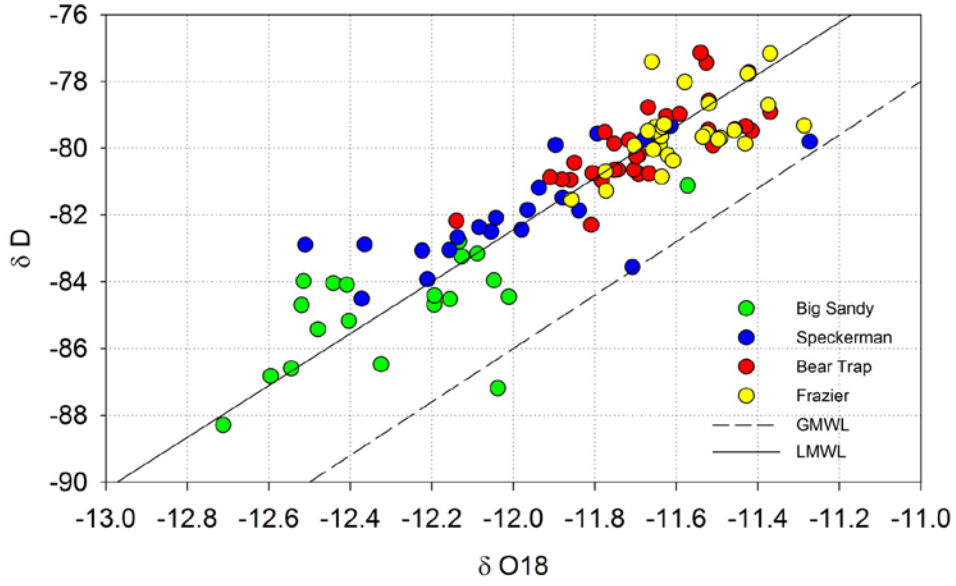

Figure 37. Stable isotopes from stream water samples in all four study catchments for WY's 2010 to 2013. The local meteoric water line (LMWL) was determined based on snow and stream samples from SNAMP watersheds and from Kings River Experimental Watershed.

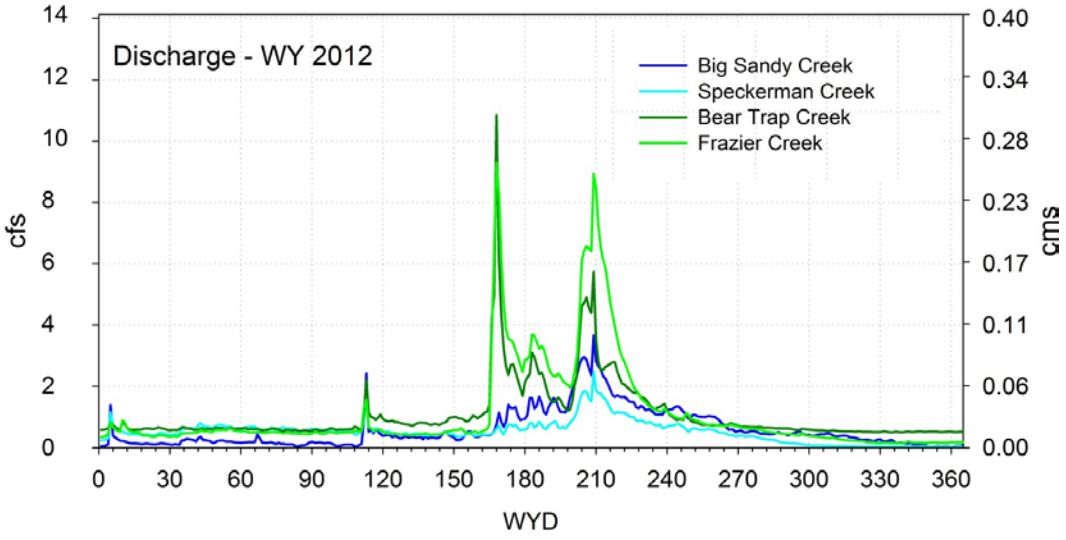

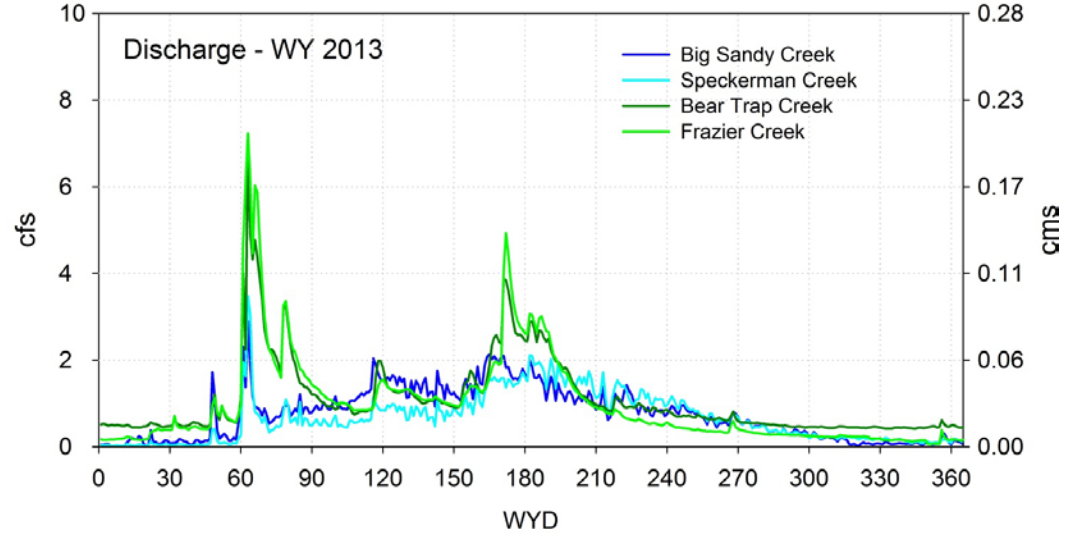

Figure 38. Water year 2012 and 2013 discharge data for the Sugar Pine and Last Chance sites.

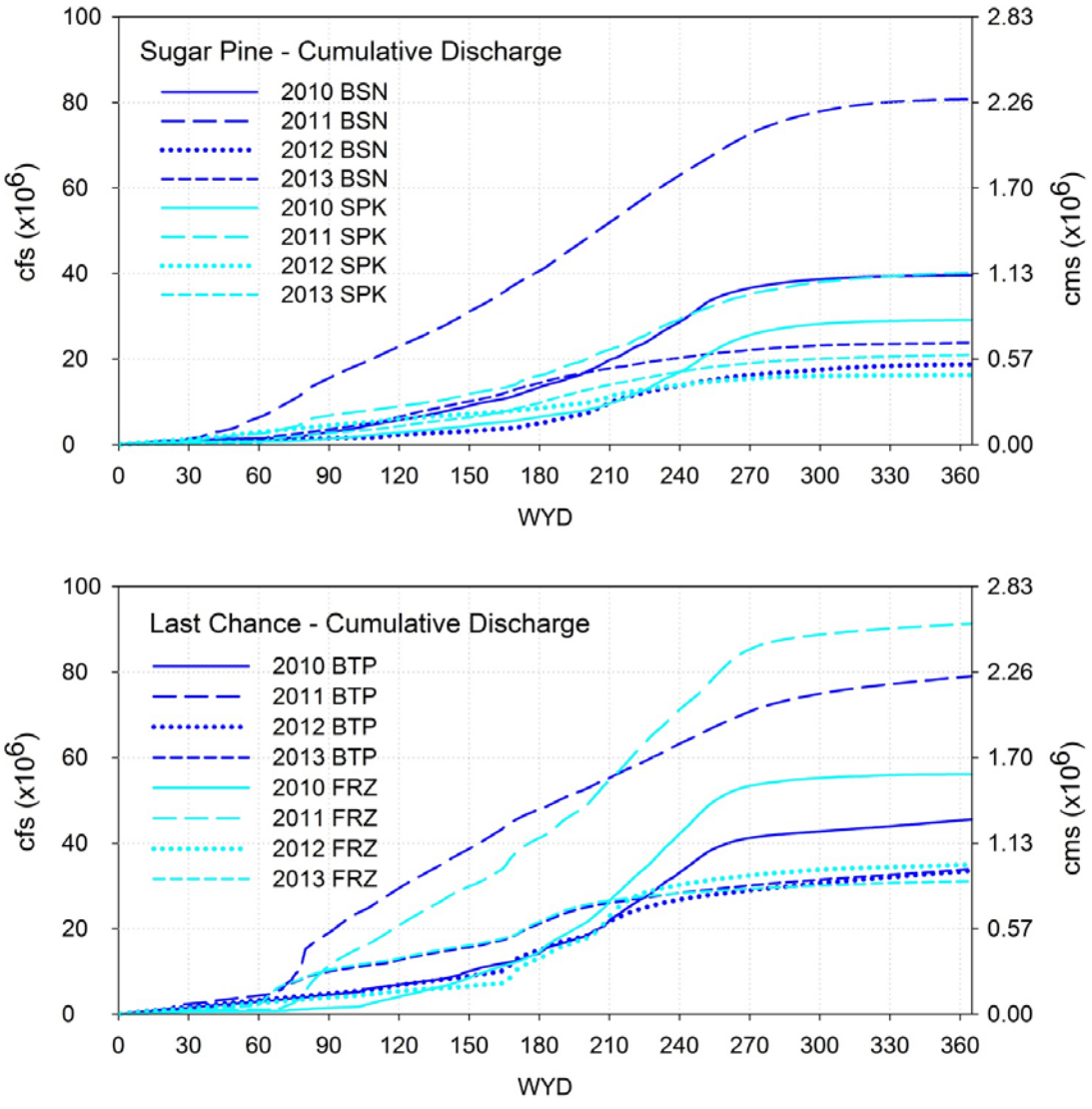

Figure 39. Cumulative discharge plots ta for Sugar Pine (Big Sandy – BSN, Speckerman – SPK) and Last Chance (Bear Trap – BTP, Frazier – FRZ) sites.

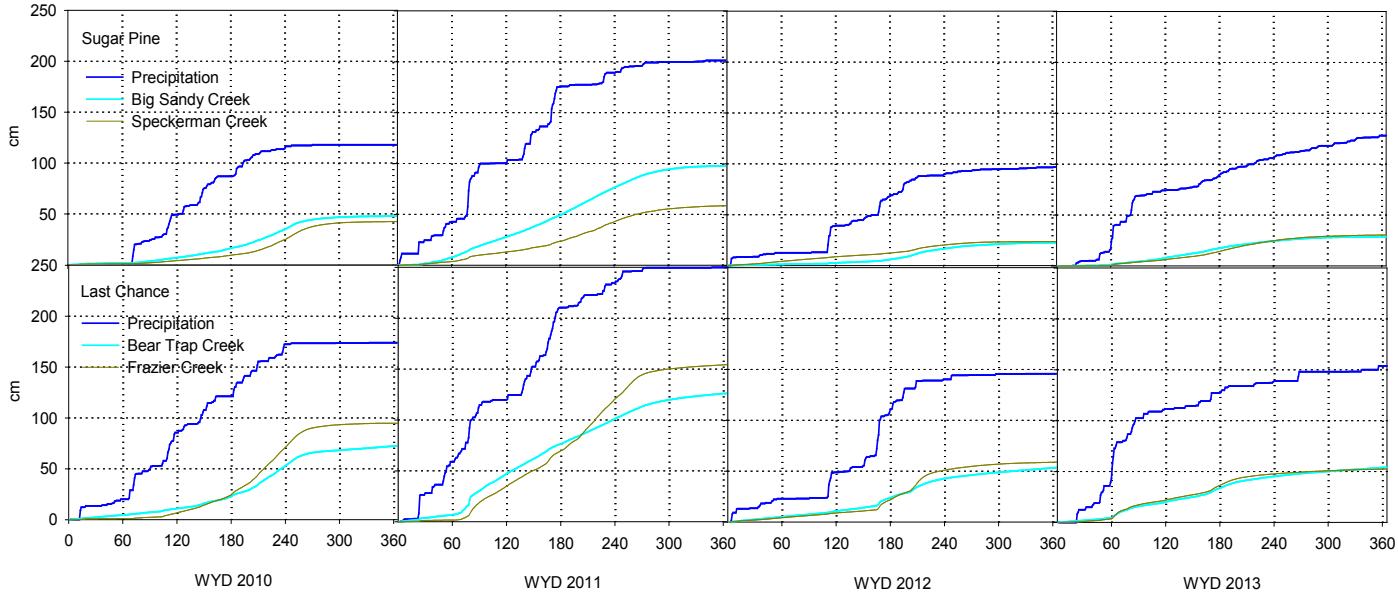

Figure 40. Cumulative precipitation and mean discharge for the Sugar Pine and Last Chance sites. Discharge data were collected at the study watersheds. Precipitation data are from the Westfall (Sugar Pine) and Blue Canyon (Last Chance) meteorological stations.

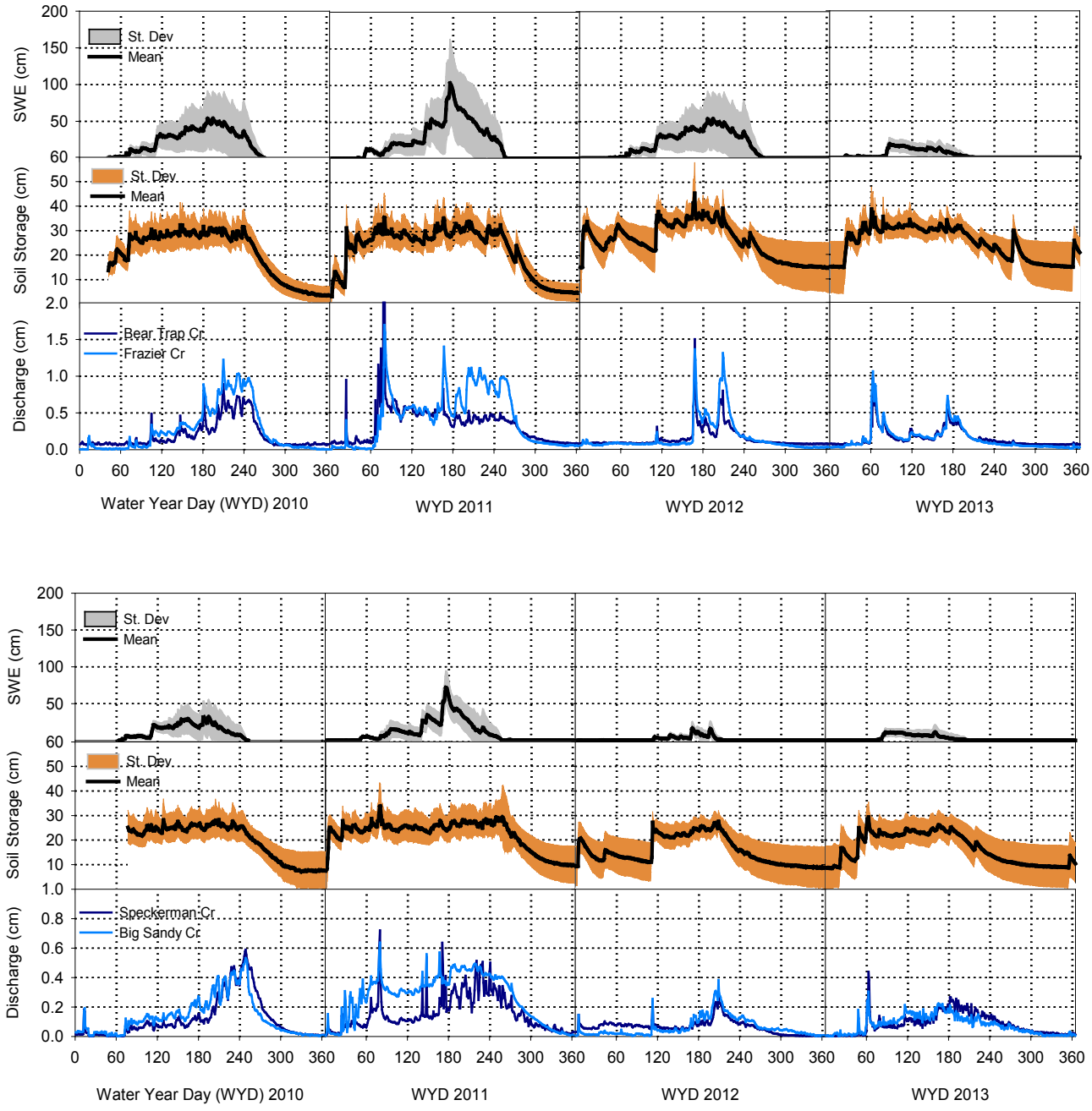

Figure 41: Water balance components of daily observed snow, soil moisture, and discharge for Last Chance (top) and Sugar Pine (bottom) for water years 2010-2013.

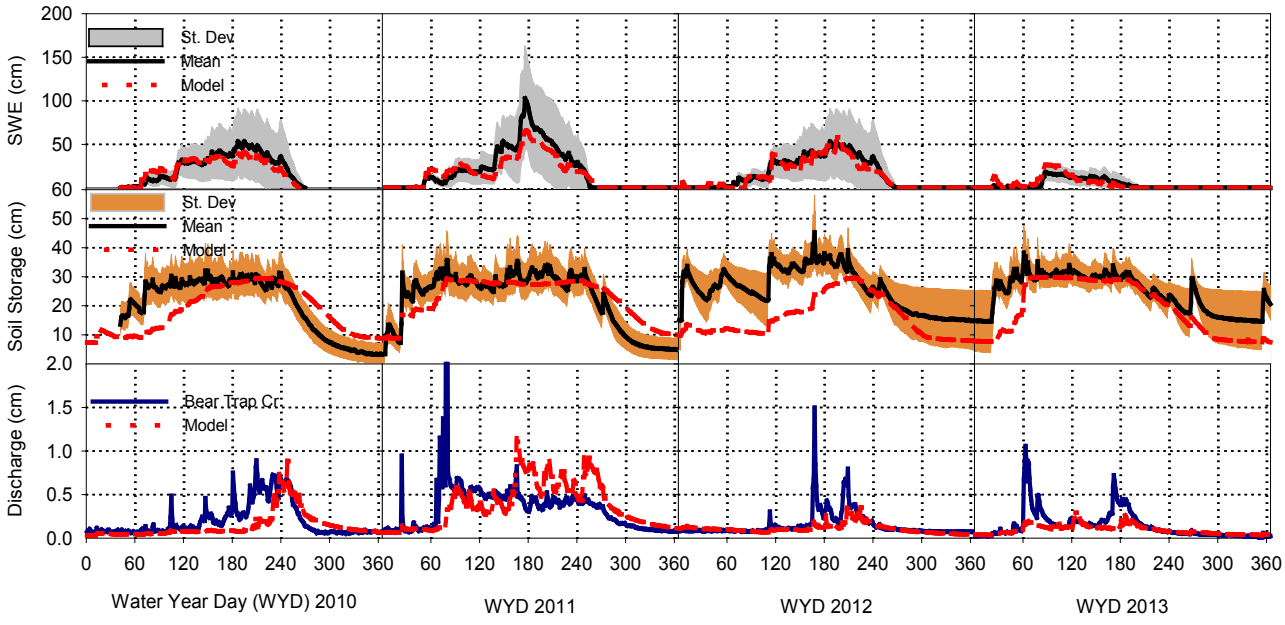

Figure 42: Regional Hydro-Ecological Simulation System (RHESSys) outputs compared to daily observed water balance components of snow, soil moisture, and discharge from Bear Trap Creek. Final parameterization is ongoing and is contingent upon the incorporation of the LiDAR-derived vegetation data that will be available shortly.

Appendix

A. Timeline of major field activities.

Year	Season	Activities
2007	Summer	2 Met station installed
	Fall	2 Met stations installed, Bear Trap Met moved**????**
2008	Winter	
	Spring	
	Summer	Streambank erosion pins installed at Sugarpine stream sites
	Fall	Snow depth sensors installed at all nodes
2009	Winter	Water quality sondes installed Solinst stream stage sensors installed Snow survey at Duncan Peak
	Spring	
	Summer	Soil moisture sensors installed at all nodes
	Fall	
2010	Winter	
	Spring	
	Summer	
	Fall	2 upstream scour sensors installed at Sugarpine stream sites DUST network partial installation 4 Culvert depth sensors installed
2011	Winter	Sugarpine TTS equipment installed
	Spring	YSI sonde calibrations (BTP creek, turbidity sondes)
	Summer	2 downstream scour sensors installed at Sugarpine stream sites 4 scour sensors installed at Last Chance stream sites YSI sonde calibrations Last Chance TTS equipment installed DUST network completion Stream reach cross-section surveys
	Fall	Speckerman Creek weir plate fabrication and fitting Turbidity sondes installed at Sugarpine sites
2012	Winter	Snow survey at Duncan Peak
	Spring	Turbidity sonde installed at Bear Trap Creek
	Summer	Instrument calibrations (Met Towers and YSI sondes) Stream reach cross-section surveys Longitudinal water chemistry surveys- all stream sites
	Fall	Tree fell on Fresno Dome north-facing node and was repaired
2013	Winter	
	Spring	
	Summer	The American Fire burns through the Last Chance study site, Duncan Peak south-facing site is removed by fire crews. YSI sondes recalibrated.
	Fall	Tree falls on Duncan Peak met station, which is destroyed.

B. Period of record by measurement type.

Site, measurement type	Period of record (water year)
METEOROLOGICAL STATIONS	
Big Sandy	
Meteorological Instrumentation	2008-2013
NF Snow Depth	2009-2013
NF Soil Moisture	2010-2013
SF Snow Depth	2009-2013
SF Soil Moisture	2010-2013
Bear Trap	
Meteorological Instrumentation	2008-2013
NF Snow Depth	2009-2013
NF Soil Moisture	2010-2013
SF Snow Depth	2009-2013
SF Soil Moisture	2010-2013
Duncan Peak	
Meteorological Instrumentation	2008-2013
NF Snow Depth	2009-2013
NF Soil Moisture	2010-2012
SF Snow Depth	2009-2013
SF Soil Moisture	2010-2013
DUST network	2011-2013
Fresno Dome	
Meteorological Instrumentation	2008-2013
NF Snow Depth	2009-2013
NF Soil Moisture	2010-2013
SF Snow Depth	2009-2013
SF Soil Moisture	2010-2013
STREAM SITES	
Big Sandy Creek	
NF Snow Depth	2009-2013
NF Soil Moisture	2010-2013
SF Snow Depth	2009-2013
SF Soil Moisture	2010-2013
Water Quality	2010-2013
Stage	2010-2013
Culvert Measurement	2011-2013

Site, Measurement Type	Period of Record (Water Year)
Big Sandy Creek (cont.)	
Scour Sensors	2011-2013
Bear Trap Creek	
NF Snow Depth	2009-2013
NF Soil Moisture	2010-2013
SF Snow Depth	2009-2013
SF Soil Moisture	2010-2013
Water Quality	2010-2013
Stage	2010-2013
Culvert Measurement	2011-2013
Scour Sensors	2011-2013
Frazier Creek	
NF Snow Depth	2008-2013
NF Soil Moisture	2009-2013
SF Snow Depth	2008-2013
SF Soil Moisture	2009-2013
Water Quality	2010-2013
Stage	2010-2013
Culvert Measurement	2011-2013
Scour Sensors	2011-2013
Speckerman Creek	
NF Snow Depth	2008-2013
NF Soil Moisture	2009-2013
SF Snow Depth	2008-2013
SF Soil Moisture	2009-2013
Water Quality	2010-2013
Stage	2010-2013
Culvert Measurement	2011-2013
Scour Sensors	2011-2013

C. Initial Report Text

Sierra Nevada Adaptive Management Project

Water-Team Field Activities, Methods and Results

Task Order #UC 10-6

Deliverable #4.3.2

Contract #4600008548

Martha Conklin, Ph.D., Co-Principal Investigator

Roger Bales, Ph.D., Co-Principal Investigator

Ram Ray, Ph.D., Postdoctoral Researcher

Sarah Martin, Ph.D. Student

Phil Saksa, Ph.D. Student

Patrick Womble, Field Hydrologist

Sierra Nevada Research Institute

University of California, Merced

2 July 2012

Table of Contents

Executive Summary

This report is a review of the purpose, design, and installation of the water component of the Sierra Nevada Adaptive Management Project (SNAMP), and contains a summary of the data developed from the field measurement program over the first four years of the planned seven-year study. SNAMP is an integrated effort designed to study forest management from an ecosystem perspective - more specifically, to assess the effects of Strategically Placed Landscaped Treatments (SPLATs) in the mixed-conifer zone of the Sierra Nevada. In addition to water, investigations of forest health, forest fire, wildlife, and spatial processes are being conducted simultaneously in the same region. The hydrology (water) component focuses on detecting and predicting changes in the movement and timing of water flowing through these mountain catchments as a result of vegetation management, and on detecting changes to water quality. We hypothesize that the tree thinning and prescribed burning implemented with SPLATs will alter the timing of streamflow, increase water yields, and increase sediment movement within the stream channel due to the increased water yield.

The two SNAMP study areas are Last Chance, in the Tahoe National Forest, and Sugar Pine, in the Sierra National Forest. Within each study area, two headwater catchments were chosen for intensive monitoring, providing a treated and untreated watershed in both areas. An upper and lower elevation meteorological station was installed in each study area to capture the range of conditions in each catchment. Stream instruments for monitoring water level and water quality were installed at the watershed outlets. Additional snow and soil moisture sensors were distributed on the landscape around the meteorological stations and watershed outlets to measure the variable conditions attributed to the heterogeneous nature of mountain terrain and vegetation.

Four years of meteorological data, three years of distributed snow depth data, and two years of distributed soil moisture, streamflow, and water quality data are reported here through water year 2011. These observations will be used in conjunction with the Regional Hydro-Ecological Simulation System (RHESSys), to assess the effect of forest treatments on water cycling. Preliminary model results are also displayed, though they are not yet complete. Operating continuously recording instruments that require access to a power source in remote mountain environments can be difficult, so a discussion of these challenges and lessons learned is also included. Forest treatments were started in the fall of 2011 and are expected to be finished in summer 2012.

The lower-elevation meteorological station at both the Last Chance (1590 m elevation) and Sugar Pine (1755 m) study sites had an annual average temperature of about 9.7-9.8^{o}C, and received

about an equal mix or rain and snow. The upper-elevation meteorological station in the north (2112 m) had an annual average temperature of about 7.1°C, versus 8.1 °C in the south (2176 m).

The data show a snowcover duration of 5-7 months for Last Chance, and about 2 weeks shorter at Sugar Pine. Snow accumulates from approximately mid-December through mid-March or early April, then melts through May (2009) or July (2011). Many sites had winter melt periods in all three years, but maintained some snowcover all winter.

Soil-moisture values remained high from about November through May, dropped following snowmelt in June-July, and were at season-low values during August-September. Soil-moisture levels in the Sugar Pine study area were generally higher above the stream banks than around the meteorological stations.

Discharges for the two sets of paired catchments were comparable, with differences in both peak and baseflow attributed to the degree of subsurface flow. The total stream discharge at the Sugar Pine catchments was about 50 cm in WY 2010 and 100 cm in WY 2011. Specific-yield values (discharge divided by precipitation) were about 0.4 for both years. Stream discharge at the Last Chance catchments was estimated to be about 100 cm in WY 2010 and 150 cm in WY 2011. Respective specific-yield values were about 0.5 for both years.

Introduction

The Sierra Nevada Adaptive Management Project (SNAMP) is a joint effort by the University of California, state and federal agencies, and the public to study management of forest lands in the Sierra Nevada. The SNAMP team is assessing how forest vegetation treatments to prevent wildfire affect fire risk, wildlife, forest health and water. The USDA Forest Service's 2004 Sierra Nevada Forest Plan Amendment calls for managing the forest using the best information available to protect forests and homes. Vegetation management treatments are planned or being conducted in several places in the Sierra Nevada where fire risk is high. Millions of acres of Sierra Nevada forest are endangered by wildfire.

The overall SNAMP team includes university scientists acting as an independent third party to assess the effects of vegetation management treatments in the Sierra Nevada. Results will be used to improve forest management, with important implications for water yield, runoff timing and water quality. The goals of the Water Team are:

1) To better understand and predict the timing and movement of water through the catchments

2) To assess and predict the effects of forest treatments on the route and timing of the water; and
3) To quantify erosion and sediment movement caused by the water routing.

Our working hypothesis is that treatments will alter the timing of flows and increase water quantity and sediment movement in the streams. Any changes in water quality (such as turbidity) will be due to in-streamflow changes from the increased discharges. Results thus also provide process understanding that is important for improving predictions of runoff for water supply and other downstream uses.

Field sites for this study consist of two locations, a northern and southern site. The southern site (Sugar Pine) is located on the Sierra National Forest near Fish Camp while the northern site (Last Chance) is located on the Tahoe National Forest near Foresthill (Figure 1). Two headwater catchments were chosen in each site for intensive measurements based on the comparable size, gradient, discharge, aspect, and vegetation cover as locations for aquatic and terrestrial monitoring instrumentation. These instrument clusters were located along a relatively low-gradient response reach where sediment scour and deposition are likely to occur. One instrument cluster in each site is located in a catchment subject to treatment to study the effects of those treatments while the other is located in an untreated catchment as an experimental control.

In addition to the two stream instrument clusters, two meteorological stations were located in each site. One station is located at an elevation similar to the upper portion of the basins and the other at an elevation similar to the stream instrument clusters. Instrument clusters and meteorological sites are further divided into two nodes; one located on a south-facing slope and another on a north-facing slope (Table 1).

The two southern watersheds chosen are Big Sandy Creek and Speckerman North Creek. From the junction between Jackson Rd and CA-41, Speckerman Creek is approximately 5.5 km east while Big Sandy Creek is nearly 9 km east. The two northern watersheds chosen are Frazier Creek and Bear Trap Creek, both of which are located along Forest Route 44. Frazier Creek is approximately 9.5 km north of Forest Route 96 (Mosquito Ridge Rd) and Bear Trap Creek is another 4 km north of Frazier Creek.

In the southern site, the upper meteorological station, Fresno Dome, is approximately 3.25 km northeast of the Fresno Dome campground along Sky Ranch Rd (Forest Route 6S10). The lower meteorological station, Big Sandy, is located just west of the Big Sandy campground. The upper meteorological station in the northern site, Duncan Peak, is approximately 1 km west of Robinson Flat campground along Forest Route 43. The lower meteorological station, Bear Trap, is situated between the stream sites approximately 2.5 km from Frazier Creek along Forest Route 44.

.

Table 1. Instrument nodes and watershed attributes

Forest (Site)	Instrument node	Area, km^2	Latitude, north	Longitude, west	Elevation, m
Sierra N.F. (Sugar Pine)	Speckerman Creek	1.62	37.4639	119.6051	1719
	Big Sandy Creek	2.47	37.4684	119.5819	1778
	Fresno Dome Met	--	37.4638	119.5362	2176
	Big Sandy Met	--	37.4684	119.5856	1755
Tahoe N.F. (Last Chance)	Bear Trap Creek	1.76	39.1067	120.5670	1560
	Frazier Creek	1.68	39.0851	120.5689	1605
	Duncan Peak Met	--	39.1546	120.5101	2112
	Bear Trap Met	--	39.0945	120.5769	1590

Methods

Field data collection started in late 2007 following the installation of the four meteorological stations. Snow-depth nodes were added in late 2008 to all sites and soil-moisture sensors were added to those nodes in the summer of 2009. Water quality and stage instrumentation was added to stream sites during the winter of 2009 (see Appendix A for timeline of major field activities). When not involved with installations, field personnel performed routine maintenance and repairs, stream sampling at regular intervals, data retrieval and processing, laboratory analysis, and public outreach as part of the SNAMP team.

Sampling

Water-quality samples were collected at stream sites year round at biweekly to bimonthly intervals. Samples were taken at or near the location of the water-quality instrumentation at each stream site in order to correlate sample results to stream conditions. Stream samples were analyzed for total suspended solids, major ions, and isotopes. Bottles and lids used during sampling were cleaned, triple rinsed with DI water prior to field work and then triple rinsed at the site with stream water. All samples were taken in the center of flow and bed sediment disturbance was avoided.

Snow samples were retrieved and analyzed for major ions and isotopes. Ion samples were taken at snow pit locations using a clean 10 cm diameter by 1-m long PVC pipe sampler inserted vertically near the edge of the pit. Snow from the samplers was placed in cleaned 4-L zip-top bags and once melted were combined and subsampled. Isotope samples were collected with a 500-mL snow cutter, placed in gallon zip-top bags, and once in the laboratory were melted put in isotope bottles.

Approximately 1 L of bulk soil was collected from each of the soil moisture sensor locations. Soil samples were air dried and sent to the University of California Analytical Laboratory (UC-ANL) in Davis, CA for texture analysis. At UC-ANL, the soil samples were ground in a Bico-Braun soil pulverizer until they were fine enough to pass through a 2 mm sieve. Soil particle size was then determined by measuring the settling rates of the sample in a sodium hexametaphosphate solution, using a hydrometer to record changes in suspension density (1% detection limit).

Total Suspended Solids

Total suspended solids (TSS) measurements were used to calculate the mass of all solids present in a volume of water. Total suspended solids samples were collected with a DH-48 depth integrated sampler, by dipping the bottle in the stream (referred to as grab samples), or with an automated water sampler. In all cases, labeled samples were stored in a refrigerator or out of the light to prevent algae

growth prior to analysis. Filters (0.45 micron) were dried in a 60-70 °C oven for 24 hours and weighed prior to filtering to establish the initial mass of the filter. The volume of sample was measured and then filtered using a vacuum chamber. Filters were dried in an oven for 24 hours, and then weighed to determine the total mass (filter + sediment). Data are currently being reported by the laboratory and analyzed, and results will be forthcoming.

Major Ions

Ion chemistry in stream water can help to identify sources and flow paths of water in that system. Grab samples of 500 mL of stream water and 500 mL of total snowpack water were collected for major cation and anion analysis. Regularly collected stream samples were taken adjacent to water quality instrumentation, and snow samples from snow pits adjacent to the meteorological stations. Samples were brought back to the laboratory and filtered using a vacuum-filtration system with a 0.45-µm filter. If samples could not be filtered immediately they were frozen to preserve the samples until they could be processed. Samples were analyzed by the Environmental Analytical Laboratory at University of California, Merced on a Dionex ICS-2000 integrated ion chromatography system. Cations measured included Na, NH_4, K, Mg, and Ca. Anions measured included F, Cl, SO_4, and NO_3. Data are currently being processed and results will be forthcoming

Isotopes

Like major cations and anions, isotopes can give information about water sources and flow paths. Isotope samples were collected with 30-mL glass vials with septum lids. Bottles were capped such that no air was present in the bottle. Regularly collected stream samples were taken adjacent to water quality instrumentation and snow samples from snow pits adjacent to the meteorological stations. Additional single samples were collected at various locations of interest within the watersheds (ie. springs, seeps, confluences) to provide additional information on water sources and pathways. Samples were stored refrigerated until they could be analyzed to prevent algae growth. Aliquots of 1 mL from each sample were analyzed for $\delta^{18}O$ and δD on an LGR DLT-100 liquid-water-isotope analyzer. Data are currently being processed and results will be forthcoming.

TTS program

Turbidity threshold sampling was used to observe how stream conditions change during turbid flows typical of precipitation or snowmelt events. Turbidity threshold sampling (TTS) stations consist of, at minimum, a water-quality sonde and an automated water sampler connected to and controlled by a datalogger. These stations also typically include instrumentation present at stream sites such as snow-

depth sensors, scour pans, and soil-moisture sensors. The program uploaded to the datalogger executes in-stream and on-bank instrument measurements at 15-minute intervals. The automatic water sampler is triggered weekly or when turbidity values exceed a site-specific turbidity value set by the field personnel.

Instrument Cluster Configurations

All instrument clusters consist of Campbell Scientific dataloggers that were used to control and record sensor output at two nodes (north facing and south facing). All nodes collect data at 15 minute intervals and are in operation year round. Clusters were visited by field personnel on a monthly basis to download data and perform any maintenance or repairs required.

Stream clusters were located upstream of access roads and were reached on foot. North facing nodes at Speckerman operate snow-depth and soil-moisture sensors (Table 2). Included on the north-facing node at Big Sandy Creek is a scour sensor. At Speckerman, Big Sandy, and Bear Trap Creeks the south-facing node houses a datalogger running a turbidity threshold sampling (TTS) program that records water-quality readings and controls an automated water sampler. At Frazier Creek, the TTS program is run on a datalogger independent of the stream nodes.

Table 2. In-stream and terrestrial instruments present at each stream instrument cluster

Site	In-stream Instruments	Terrestrial Instruments
Big Sandy Creek	YSI 6920V2-2 sonde Solinst Levelogger Gold YSI 600 OMS sonde (2) Rickly Scour Sensors (1 attached to NF node)	(3) Judd Ultrasonic Depth Sensors (2 on SF node, 1 on NF node) (16) Decagon 5TM soil moisture sensors (8 per node)
Speckerman Creek	YSI 6920V2-2 sonde Solinst Levelogger Gold YSI 600 OMS sonde (2) Rickly Scour Sensors	(3) Judd Ultrasonic Depth Sensors (2 on SF node, 1 on NF node) (16) Decagon 5TM soil moisture sensors (8 per node)
Bear Trap Creek	YSI 6920V2-2 sonde Solinst Levelogger Gold YSI 600 OMS sonde (2) Rickly Scour Sensors	(3) Judd Ultrasonic Depth Sensors (2 on SF node, 1 on NF node) (16) Decagon 5TM soil moisture sensors (8 per node)
Frazier Creek	YSI 6920V2-2 sonde Solinst Levelogger Gold (2) Rickly Scour Sensors	(3) Judd Ultrasonic Depth Sensors (1 on SF node, 1 on NF node) (16) Decagon 5TM soil moisture sensors (8 per node)

NF= North facing; SF= South facing

Meteorological sites consist of a central tower with meteorological instrumentation in addition to two nodes on adjacent NF and SF slopes. Parameters measured on the tower include snow depth, rainfall, air temperature, relative humidity, incoming solar radiation, net solar radiation, wind speed and direction, and barometric pressure (Table 3). Data are transmitted from the tower hourly via an on-board GOES satellite transmission platform and posted on the California Data Exchange Center website (http://cdec.water.ca.gov/). After quality assurance and quality control, data are archived in the SNAMP digital library (https://eng.ucmerced.edu/snsjho).

Table 3. Tower and node instruments at each meteorological station

Met Site	Tower Instrumentation	Node Instrumentation
Big Sandy	Judd Ultrasonic Depth Sensor Handar 444B Tipping Bucket LI-COR LI200X Pyranometer Solinst Barologger Gold Kipp & Zonen NR Lite2 Vaisala HMP155C Temp/RH RM Young 05103 Wind Monitor	NF: (4) Judd Ultrasonic Depth Sensors (10) Decagon 5TM soil moisture sensors SF: (4) Judd Ultrasonic Depth Sensors (12) Decagon 5TM soil moisture sensors
Fresno Dome	Judd Ultrasonic Depth Sensor Handar 444B Tipping Bucket LI-COR LI200X Pyranometer Solinst Barologger Gold Kipp & Zonene NR Lite2 Vaisala HMP155C Temp/RH Vaisala WMT700 Wind Monitor	NF: (3) Judd Ultrasonic Depth Sensors (10) Decagon 5TM soil moisture sensors SF: (3) Judd Ultrasonic Depth Sensors (10) Decagon 5TM soil moisture sensors
Bear Trap	Judd Ultrasonic Depth Sensor Handar 444B Tipping Bucket LI-COR LI200X Pyranometer Solinst Barologger Gold Kipp & Zonene NR Lite Vaisala HMP45C Temp/RH Vaisala WMT700 Wind Monitor	NF: (3) Judd Ultrasonic Depth Sensors (10) Decagon 5TM soil moisture sensors SF: (3) Judd Ultrasonic Depth Sensors (9) Decagon 5TM soil moisture sensors
Duncan Peak	Judd Ultrasonic Depth Sensor Handar 444B Tipping Bucket LI-COR LI200X Pyranometer Solinst Barologger Gold Kipp & Zonene NR Lite Vaisala HMP45C Temp/RH Vaisala WMT700 Wind Monitor	NF: (2) Judd Ultrasonic Depth Sensors (8) Decagon 5TM soil moisture sensors SF: (4) Judd Ultrasonic Depth Sensors (14) Decagon 5TM soil moisture sensors

Instrument and Equipment Descriptions

Due to the remote locations, all instrumentation is solar powered. Panel size ranged from 10 to 50 watts, with panels mounted facing south to maximize their exposure to the sun. At instrument clusters panels were attached to the top of rigid metal conduit or up in trees, whichever gave the best sun exposure. Solar panels on the met towers were mounted directly to the tower.

Solar panels are used to charge batteries through use of a charge controller. Sealed lead-acid batteries were used to supply power to dataloggers and all attached instrumentation. Battery size varied from 7.5 AH to 50 AH and was based on size and amount of sun exposure the solar panel had, how much equipment was present, as well as trial and error. At met towers 100+ AH marine batteries were used due to the demands of the instrumentation on the towers. Two different 12-volt charge controllers were used in this study. At instrument nodes, a 6-Amp controller (Morningstar Sunsaver 6) was used while at the met towers a larger 15-Amp controller (Morningstar ProSaver 15) was used.

NEMA 4x certified fiberglass and steel enclosures were used in this study to provide protect dataloggers, batteries, and charge controllers from the elements. Refrigerator putty was used to further weather proof the enclosures and desiccant packs were used to control moisture levels inside. At many sites the enclosures fared well. However, in several cases, the pressure exerted on the boxes by snow creep often resulted in the enclosures being torn from the mounting poles, typically accompanied by severed instrument and power cables.

A 9-m Rohn Products tower is the primary mounting platform for all of the meteorological stations in this study. These towers are freestanding and climbable for instrument access. Three of the towers are set into poured concrete footings and one is set on a base bolted directly into bedrock (Fresno Dome Met). Towers meet the following specifications:

1) Survive 125 mph winds
2) No horizontal or vertical movement (sliding once installed)
3) Withstand snow loads of typical high mountain locations
4) Support technical personnel on the tower while servicing all sensors
5) Provide adequate mounting surface and locations to meet sensor requirements (NFDRS)

Galvanized rigid metal conduit pipe was used as the primary means to mount instrument enclosures and snow-depth sensors at all instrument clusters. Conduit pipe had a 4-cm inside diameter and 3-m length. Pipes were bolted to U-channel posts that were driven into the ground. Extensions 1.5-m in length were installed at the higher elevation meteorological stations where potential snow depth exceeds 3-m.

Programmable dataloggers such as the Campbell Scientific CR1000 and CR200x enable many types of sensors to be deployed and controlled at a site and allow a high degree of customization by users. Most instruments were wired into Campbell Scientific CR1000 dataloggers. An AM16/32B multiplexer was typically connected to the CR1000 to expand the instrument capacity at instrument clusters to control soil-moisture sensors. The CR200X dataloggers are used at culvert measurement locations and Bear Trap Creek NF node where fewer instruments are connected and differential ports were unnecessary.

GOES satellite telemetry was used to provide real-time updates on weather conditions at Met stations and alert personnel to issues that need addressing. Each GOES platform consists of a transmitter in the enclosure, a GPS antenna, and a satellite antenna. A CR1000 datalogger is used to upload data at 15-minute intervals into the Campbell Scientific TX-312 transmitter buffer that is then relayed once an hour to a GOES satellite. To ensure accurate transmission times, the transmitter uses a GPS antenna to synchronize the datalogger clock.

A Solinst Barologger was used to record barometric pressure at meteorological stations. Instruments were housed in perforated PVC capsules to protect them and allow sufficient pressure equalization. Housings were mounted directly to the meteorological towers. Barometric data were used to remove the effects of barometric pressure on stream level data.

Two types of precipitation were measured during this study: rainfall and snow depth. Rainfall was measured at meteorological stations using a Handar 444b tipping-bucket rain gage. Each tipping-bucket assembly was mounted on the meteorological tower 4.5 to 5 m above the ground. Rain gages were unshielded and unheated. Snow depth was measured at all instrument nodes and meteorological stations using Judd ultrasonic depth sensors. Each Judd was mounted on the end of a 5-foot section of ½" rigid metal conduit and positioned so that the surface of the transducer was parallel to the ground.

Scour sensors were installed to monitor sediment movement through the stream system. Two Rickly Hydrological load cell sensors were buried 30 to 50-cm below the stream bed at each stream reach. The sensors operate by measuring the pressure of the water column and the pressure exerted on a water-filled pan buried in the sediment at the same depth. The difference between the two readings is the weight of the sediment present on top of the pan. Sensors are co-located at Bear Trap, Frazier, and Speckerman Creeks to provide redundant measurements. At Big Sandy Creek, one sensor was installed adjacent to the water quality instrumentation and the other was installed approximately 15 m downstream.

Decagon Devices ECH_20 TM soil temperature and moisture sensors were installed in soil pits at depths ranging from 10 to 90-cm. At met station nodes, EC-TMs were installed under each Judd depth sensor to examine the relationship between snow depth and soil moisture. However, the deployment was changed when installing sensors at stream nodes to see how soil moisture was related to orientation. At these sites a tree was chosen and pits were dug approximately 1 meter from its base in the four cardinal directions. Installation depths vary but were generally confined to 30 and 60 cm due to the shallow nature of the soils.

Incoming solar and net all-wave radiation measurements were used to quantify the energy balance at meteorological sites for use in evapotranspiration calculations. Incoming solar radiation was measured using a LI-COR LI200X pyranometer that detects the spectral range of 400-1100 nm using a silicone photovoltaic diode. Net solar radiation was measured using a Kipp & Zonen NR Lite or NR Lite2 net radiometer. Both NR Lites report the difference between all incoming solar and far infrared radiation and the reflected radiation from the surface of the soil under the assumption that all wavelengths are absorbed (manufacturer specifications are identical for both NR Lite and NR Lite2 sensors). The LI200X and NR Lite sensors are mounted near the top of the meteorological towers facing south to get the best view of the sky and avoid shading from the tower and nearby trees.

Temperature and relative humidity were measured using two different instruments from Vaisala. The older HMP45 was installed at the two northern meteorological stations. It has a measurement range of -40°C to +60°C for temperature and 0% to 100% for relative humidity. Newer HMP155 sensors were installed at the two meteorological stations in the southern sites as replacements for HMP45 sensors that were malfunctioning. The HMP155 can read temperatures down to -80°C and has an updated version of the HUMICAP humidity sensor. Each of the sensors were mounted inside a 9- or 14-layer radiation shield manufactured by RM Young.

Two different sensor platforms manufactured by YSI were used to measure *in situ* water quality. The YSI 6920 V2-2 is a robust and flexible platform that contains 2 optical ports, 1 conductivity/temperature port, 1 pH/ORP port (not used in this study), 1 nutrient ion-selective-electrode (ISE) port (not used in this study), and an integrated unvented pressure transducer. The 600 OMSV2-1 sonde is a smaller unit and contains 1 optical port and an integrated conductivity/temperature sensor.

The two optical sensors used in this study are the YSI 6150 ROX® dissolved oxygen and YSI 6136 turbidity sensors. The 6920 sondes houses both of these sensors while the 600OMS sondes only house the turbidity sensor. The ROX DO sensor uses the luminescence lifetime method for detecting oxygen

and does not require flow. The sensor is capable of measuring 0-100% dissolved oxygen with minimal drift. The turbidity sensor uses a near infrared LED to illuminate a sample and measures the light that is scattered with an adjacent photodiode. The range of the sensor is 0 to 1,000 NTU. Anti-fouling wipers are installed on both sensors to prevent buildup of sediment or algae on the optical ports.

The YSI 6560 conductivity/temperature sensor uses four nickel electrodes to measure conductivity and a thermistor to measure temperature. The temperature measurement range is -5 to 60°C and is used on-board by the sonde to calculate and output specific conductance. The range for conductivity measurements is 0 to 0.1 mS cm^{-1}.

Multiple in-stream sensors are employed at stream sites and in weir ponds to record changes in stream stage. Solinst Levelogger Gold pressure/temperature transducers are used near culverts and in weir ponds. The YSI sondes measure stage at the water quality instrument locations and Judd ultrasonic depth sensors measure stage inside the road culverts during high flow (winter/spring). Both the sonde and the Levelogger measure absolute pressure (barometric + water) and so data need to be processed after collection to reflect actual stage measurements. Rating curves developed from salt dilutions allow stage measurements to be converted into discharge values.

To better determine discharge during low flow times of the year, a v-notch weir was installed in the road culvert at the Speckerman outlet. The weir was constructed so that field personnel could easily remove it during high flow months to allow sediment and debris to move freely through the system. A Solinst Levelogger will be installed in the weir pond to log the stage of the pond during low flow. This will allow discharge to be calculated with standard engineering equations.

Two different wind monitors were used in this study: an RM Young 01503 and a Vaisala WINDCAP WMT700. On the 05103, wind speed is measured by a propeller and the direction is measured based on the orientation of the vane whereas on the WMT700, three ultrasonic transducers were used to measure both parameters. The 05103 sensors have a wind speed measurement range of 0-100 m s^{-1} and require a minimum of 1.1 m s^{-1} to accurately record wind direction. The WMT700 has a wind-speed measurement range of 0-75 m s^{-1} and require a minimum of 0.1 m s^{-1} to accurately measure wind direction. The 01503 is only used at Big Sandy meteorological station.

A wireless network prototype of snow depth nodes has been deployed around the Duncan Peak meteorological station. The goal of the network is to better capture terrain variability and reduce sensor downtime due to exposed wires that are susceptible to damage by rodents, bears and extreme weather conditions. This network consists of ten snow depth, temperature, and relative humidity measurements in a 1-km^2 area around Duncan Peak. Nodes are connected to a central computer via radio signals that

stores data and is capable of on-demand transmissions through a cell phone modem. Off-site access to the network helps project personnel keep track of field conditions and the status of instrumentation.

Data Management and Processing

Continuous data are downloaded from all dataloggers at one-month intervals. These raw files are compiled by water year to a “level 0” file for processing and analysis. The raw data are then reviewed for anything considered an erroneous measurement by a combination of visual review and filtering algorithms to upgrade the file to “level 1”. The level 1 file has time periods with missing data due to measurement error or battery failure. These missing data are filled in using linear relationships with the same type of measurements collected at a nearby site, putting the file at “level 2”. Most of the data in this report are at level 2 or higher. Higher-level processing, including using the continuous stream-stage measurements with individual discharge measurements, creating a stage-discharge relationship for continuous discharge estimates, are files at “level 3”or “level 4”.

Results

Meteorological Data

Hourly meteorological data were recorded at the four stations beginning in water-year 2008, capturing the range of environmental conditions present within the four study basins. Figures 2 and 3 show the daily observations of solar radiation, precipitation, temperature, relative humidity, and wind speed, as well as net radiation for observing energy exchanges between the ecosystem and atmosphere. Note that net radiation was not measured at Big Sandy until water year 2012, and is therefore not shown on these figures. The upper and lower elevations at Last Chance showed greater differences in the meteorological observations than the Sugar Pine stations.

Precipitation measured in Last Chance was 120 cm in 2008 versus 255 cm in 2011; while Sugar Pine had 83 and 214 cm in the same years. Spatial differences in precipitation showed the northern study region of Last Chance, located within the American River basin, with about 40-cm higher levels annually than the southern study region of Sugar Pine, located within the Merced River basin. Precipitation at the higher elevation stations of Duncan Peak and Fresno Dome (elevation >2100 m) is dominated by snowfall, while the lower elevation stations of Bear Trap and Big Sandy (1500-1800 m elevation) record similar levels of rain and snow.

Temperatures at Bear Trap averaged 9.8^{o}C (ranging -12.5 to 35.2) and Duncan Peak averaged 7.1^{o}C (-16.7 to 31.8) at Last Chance, while Big Sandy averaged 9.7^{o}C (-15.4 to 32.7) and Fresno Dome averaged 8.1^{o}C (-15.0 to 30.8) at Sugar Pine. This reflects a temperature difference of only 1.5 ^{o}C per 300 m elevation for Last Chance, and 1.2 ^{o}C for Sugar Pine. A broader analysis of southern Sierra Nevada stations shows values of 1.8-2.0 ^{o}C per 300 m elevation. The cause of these relatively small differences is being evaluated using regional data. However, it is apparent that Duncan Peak has a lower day-night temperature difference than does Bear Trap. Also, daily maximum temperatures between the two sites differ by about 1.8 ^{o}C, versus 1.0 ^{o}C for daily minimum temperatures.

Higher relative-humidity values were recorded at the lower-elevation sites, with mean daily wind speeds around 2 m s^{-1}, and the major wind direction being S-SE for all sites. Wind speed and direction were not able to be gap filled, due to the individual nature of wind conditions at each site.

Upper-elevation stations received slightly higher total daily solar radiation inputs during the summer than lower elevations due to the lower horizon, and the southern study site received more than the northern study site. Approximate maximum radiation values were 35 MJ m^{-2} day^{-2} at Fresno Dome, 30 MJ m^{-2} day^{-2} at Big Sandy, 30 MJ m^{-2} day^{-2} at Duncan Peak, and 25 MJ m^{-2} day^{-2} at Bear Trap.

Maximum summer net radiation followed a similar stratification with values of 25, 20, and 12 MJ m^{-2} day^{-2} at Fresno Dome, Duncan Peak, and Bear Trap respectively. Net solar radiation was small, and in many cases close to zero for water year days 60 to 150 for all sites. The Duncan Peak station (higher elevation) also showed greater variability in net radiation than did Bear Trap (lower elevation).

Snow Depth

Additional snow-depth measurements (2009-2011) were distributed around the meteorological stations and the stream instrument clusters to measure variability around the landscape (Figures 4-5). The data show a snowcover duration of 5-7 months for Last Chance, and about 2 weeks shorter at Sugar Pine. Snow accumulates from approximately mid-December through mid-March or early April, then melts through May (2009) or July (2011). Many sites had winter melt periods in all three years, but maintained some snowcover all winter.

Upper-elevation meteorological stations recorded the highest snow depths and latest snowmelt dates. Last Chance snow depth showed greater variability than did Sugar Pine, with Duncan Peak having the highest snow accumulations and Bear Trap showing intermittent snowcover throughout the three winter periods. Snow depth measured above the banks of the streams varied from the intermittent patterns seen at the lower meteorological stations to the higher accumulation and later melt out of the upper-elevation stations. Due to the greater precipitation levels in Last Chance, snow depth was notably higher at the upper elevation, but similar at lower versus higher elevations in Sugar Pine. With the exception of the time period around day 180 in WY 2011, mean snow depths over the three years in Last Chance were around 100-cm. In Sugar Pine, snow depth values were closer to 75-cm, also excluding the time around day 180 in WY 2011. Last Chance showed greater variability among measurement locations while Sugar Pine showed more daily variability over the winter seasons.

Wireless snow-depth sensors were installed around Duncan Peak to cover a greater variety of terrain and capture a greater fraction of snow depth variability. A grid survey of 119 points with 75-m spacing was completed around Duncan Peak on March 23-26, 2009 and showed the 7 wired nodes represented 20% of the variability measured with the survey. A second survey on April 15 and 26, 2012 showed the wired sensors represented 24% of the variability, with 9 of the new wireless sensors improving that number to 61% (Figure 6). In both cases, the snow-depth sensors did adequately represent the mean spatial value of snow depth.

Soil Texture and Moisture

Soil samples were collected at moisture-sensors locations and analyzed for soil texture (Figure 7). The results show that all the soil samples were in one of four USDA texture classifications: loam, sandy loam, loamy sand, or sand. Almost all of the soils had greater than 50% sand, while they all had less than 50% silt and 30% clay. Soils in the Sugar Pine study area were sandier than in the Last Chance area, with textures showing more similarity by sample site location than by depth.

Soil-moisture values remained high from about November through May, dropped following snowmelt in June-July, and were at season-low values during August-September (Figures 8-9). Soil-moisture levels in the Sugar Pine study area were generally higher above the stream banks than around the meteorological stations (Figure 8). Measurements at the Big Sandy Creek south-facing node more likely represent mean moisture content than variability due to data gaps that were filled in using the north-facing site. At Last Chance, soil-moisture levels showed more similarity between the sites, with the greatest variability at the Bear Trap meteorological station south-facing node due to intermittent snowcover (Figure 9). Monitoring soil moisture at Duncan Peak proved to be challenging, as the sensors exhibited erratic behavior that could not be reconciled with measurements recorded at the other sites, limiting observations at the upper elevations. On average, soils in Sugar Pine maintained 20-30% Volumetric Water Content (VWC) during the wet winter season while Last Chance soils sustained approximately 30% VWC. This may be due to the lower sand content in Last Chance soils.

Stream Water Quality and Quantity

The water-quality parameters of water temperature, conductivity, dissolved oxygen, turbidity, and stage were collected in all study catchments using multi-parameter continuously running sondes (Figures 10-13). Water-quality parameters and stream stage were collected on a 15-minute time interval at the upstream instrument locations approximately 0.3 km above the outlet culvert at the Sugar Pine sites and 30 m above the culverts at the Last Chance sites. Downstream stage measurements were collected using a pressure transducer near the outlet culverts and was also collected on a 15 minute time interval. The meteorological parameters of air temperature and precipitation, plotted on the following graphs, were collected at the lower met stations at corresponding hourly time intervals. The snow depths plotted below were collected on fifteen minute and hourly time intervals, from which daily means were calculated. The plotted values represent means of all snow depth measurements at a given site.

Gap filling was conducted on water temperature and discharge using the upstream or downstream measurements from the same catchment. Snow depth was gap filled from adjacent measurements prior to spatial averaging. The remaining parameters were not gap filled and contain data gaps due to battery failures and burial of the sonde during sediment movement.

Turbidity measurements had considerable noise with background values ranging from -5 to +5 NTU. To compensate for this noise, all values under 5 NTU were removed so that only significant spikes of 5 NTU or more would be considered. That is, spikes exceeding 5 NTU were considered to be water-quality events of potential interest.

Manual measurements of discharge, conductivity, and dissolved oxygen were made on a bi-weekly to bi-monthly basis. Discharge was measured using the salt-dilution slug method and rating curves were created for the continuous stage data. Conductivity and dissolved-oxygen measurements were made with a separately calibrated multi-parameter sonde identical to the continuous running sondes.

Temperature

Water temperature ranged for the period of record from 0 to 11.9 ^{o}C in Speckerman, 0 to 15.6 ^{o}C in Big Sandy, 0 to 12.9 ^{o}C in Frazier and 0 to 11.8 ^{o}C in Bear Trap. Yearly means were 5.0 ^{o}C for Speckerman, 5.1 ^{o}C for Big Sandy, 5.4 ^{o}C for Frazier, and 5.5 ^{o}C for Bear Trap. For all four catchments, water temperatures in WY 2010 were lowest in early winter and gradually rose through the season. In WY 2011, temperatures stayed steady for much of the winter. The higher summer temperatures at Big Sandy compared to Speckerman may be due to Big Sandy having less groundwater input and/or less shading of the stream by vegetation.

Conductivity

At both the Sugar Pine catchments, manual and continuous measurements of conductivity show low, relatively stable values with little seasonal variation. Mean values for WY 2010 and WY 2011 are 12.5 µS and 12.4 µS at Speckerman, and 25.9 µS and 29.0 µS at Big Sandy respectively. The low seasonal variation suggests that the water in these streams is relatively new water. A greater seasonal change would be seen between rain/snowmelt and baseflow if older, higher-conductivity groundwater that has had more time to interact with soil and bedrock was feeding the stream during baseflow. The roughly double conductivity values at Big Sandy suggests the presence of at least some water that is older/higher conductivity than that at Speckerman or differences between the catchments in soils and rock that the event water comes in contact with.

A step-wise pattern is seen in the first part of the Speckerman conductivity record. This is due to the sonde's default setting not recording a sufficient number of significant figures, rather than to the physical functioning of the stream. The problem was remedied part way through WY 2011. Continuous conductivity and dissolved oxygen values at Big Sandy are not shown due to frequent battery failures and sediment burial.

Mean conductivity values for the Last Chance catchments were 33.3 µS and 28.8 µS for Frazier for WY 2010 and WY 2011. For Bear Trap the mean value for WY 2010 was 27.8 µS. Bear Trap's WY 2011 mean were not calculated due to the amount of missing data. Frazier and Bear Trap show a much more pronounced seasonal trend in conductivity. For both streams, the highest conductivity values are seen during baseflow conditions and the lowest during peak spring snowmelt. This is to be expected because baseflow consists of a higher proportion of groundwater, which generally has higher conductivity. In the spring, this groundwater input is diluted by relatively low conductivity snowmelt. The dilution effect can also be seen on a storm-by-storm basis. A good example is the large discharge spike from early season snowmelt centered on WY 2011 day 80 for Frazier Creek. The addition of low-conductivity melt water caused a dilution of the stream and a corresponding dip in conductivity is seen.

Higher mean conductivities and more seasonal variation imply that the groundwater input at Last Chance may be older or that the soil/rock the water is in contact with is more easily reacted. The latter is plausible given that Sugar Pine has predominantly granitic bedrock that is slow to react, whereas the Last Chance catchments have a mixture of granitic and metamorphic rock types.

Dissolved Oxygen

Dissolved oxygen data in all four catchments show percent saturation values that are fairly stable ranging between 75% and 95% saturation, with means for WY 2010 and WY 2011 of 88% and 87% saturation for Speckerman, 91% and 87% saturation for Big Sandy, 86% and 84% saturation for Frazier, and 89% and 86% saturation for Bear Trap. The concentration values in all catchments show a slight seasonal trend as would be expected with higher values in winter/spring when water temperatures are lower. For 85% saturation at sea level, dissolved oxygen values range from 12.2 mg L^{-1} at 0^{o} C to 8.5 mg L^{-1} at 15^{o} C. Values of 7.0 mg L^{-1} or higher are recommended for streams. All four streams have values that fall between 8.0 and 13.0 mg L^{-1}, a healthy range for aquatic life.

Turbidity

In Speckerman, the highest turbidity values tended to occur during snowmelt periods and did not necessarily correspond to the highest flow peaks. In WY 2010, the largest spike was during early

snowmelt without any large discharge event associated with it. In WY 2011, the highest spikes were during the peak spring melt, but no spikes were associated with the largest discharge events in that year. An early spike in WY 2011 showed higher turbidity than the storm after it which was associated with a larger discharge event. Gaps in data make interpretation of Big Sandy turbidity difficult, but WY 2010 data shows spikes that correspond to winter and spring melt events as were seen in Speckerman.

Frazier has the most continuous turbidity record of the four catchments. In WY 2010, there is a significant peak that corresponds to the fall rain event, but the largest spikes for the water year were during small early winter snowmelt events and as in Speckerman did not seem to correspond to major discharge events. Two small spikes during spring snowmelt did correspond to some of the most significant discharge events of the year. Similar to Speckerman, one of the highest turbidity spikes in WY 2011 occurred during a rain fall that had a fairly small discharge peak associated with it. The following rainstorm had a much smaller turbidity spike, even thought it had a much larger discharge peak. This could imply a certain amount of sediment depletion occurring in early fall. The first event though smaller flushed out a large portion of the loose sediment leaving less material for the larger event following it to move. The Frazier data also showed a significant spike in turbidity in WY 2011 that in this case did correspond to the highest flow event of the year, an early season snowmelt.

Bear Trap had significant data gaps making interpretation difficult, but showed similar patterns to the other streams in that spikes were seen during snowmelt that did not necessarily correspond to large discharge event. There was also a similar pattern in the rain events in early WY 2011 where the earlier, smaller discharge event had the larger turbidity spike.

Another interesting pattern for all four streams was that significant spikes in turbidity occurred during baseflows when no discharge events were occurring. The exact reason for these spikes is unknown, but possible explanations may be wildlife using the stream or algae growth in the water column. Because the turbidity sensors are equipped with automatic wipers, biofilm buildup on the sensor is not a likely explanation for these spikes.

Discharge

In Speckerman and Big Sandy Creeks, WY 2010 had two fall rain events the first roughly equal to peak snowmelt discharge, the second significantly smaller. WY 2011 also had two fall rain events. In Speckerman, the second was the larger event and was roughly the same as spring snowmelt peaks. In Big Sandy, the second event was also larger, but was about 30% greater than spring snowmelt peaks. In Frazier and Bear Trap the early WY 2010 rain event had a discharge much smaller than that of peak

snowmelt. The second of the two early WY 2011 rain events at Frazier was larger than the first, but unlike at Sugar Pine, was less than the peak snowmelt discharges.

The highest WY 2010 discharge events were peak spring snowmelt at the Sugar Pine sites and mid-season melt events at Frazier and Bear Trap. In WY 2011, the highest discharges at all four sites were associated with large early winter melt out events.

The Bear Trap WY 2011 data are problematic in that the downstream instrument read higher values than are reasonable for this stream. It's suspected that accumulation of woody debris near the sensor caused water to back up and artificially elevate stage readings. Because the downstream discharge data were suspect, it was not used to gap fill the upstream discharge values during the time the sonde was pulled for repairs. Bear Trap WY 2011 downstream discharge data were included in Figure 13 to show timing of events only. Discounting the questionable Bear Trap data, spring snowmelt peaks in the remaining three catchments were of similar magnitude in WY 2010 and WY 2011. However, WY 2010 tended to have distinct spring melt peaks, and WY 2011 was long and drawn out extending later into the spring.

Basin Discharge Comparison

For both water years, Big Sandy had higher discharges than Speckerman during rain events; winter flows and the snowmelt period (Figures 14-15). During summer baseflows, the relationship switched and Speckerman had slightly higher discharges. This may be indicative of a greater amount of subsurface streamflow at Big Sandy and/or a greater amount of groundwater input from springs in the Speckerman catchment during the baseflow period. Based on the WY 2010 and early WY 2011 data, Frazier seems to generally have higher discharges than Bear Trap during winter flow and spring snowmelt (with the exception of a few short-duration early winter events where Bear Trap has slightly higher peak event flows). Like at Sugar Pine, that relationship switches during baseflow conditions and Bear Trap showed higher discharges. This may be due to the bedrock channel at Bear Trap preventing any channel bed infiltration or subsurface streamflow. Bear Trap may also have more flow from springs this time of year.

Cumulative discharge comparisons highlight the differences between the two water years and between streams. Total annual flows for WY 2010 and WY 2011 were calculated for each discharge instrument and averaged by stream (Figure 16). Total flow for Speckerman averaged 0.76 $x10^6$ m^3 ($27x10^6$ ft^3) for WY 2010 and 1.50 $x10^6$ m^3 ($53x10^6$ ft^3) for WY 2011. Annual totals at Big Sandy were 1.21 $x10^6$ m^3 ($43X10^6$ ft^3) and 2.60 $x10^6$ m^3 ($92x10^6$ ft^3) in WY 2010 and 2011 respectively. Due to a faulty

pressure transducer, the Big Sandy downstream data begins partway through WY 2011. To calculate the cumulative discharge for this instrument, the cumulative total for the downstream sensor at the time its record began was assumed to be equal to that of the cumulative total for the upstream sensor. Based on the discharge comparisons this may be a slight over estimation. Frazier had totals of 1.70 $x10^6$ m^3 ($60x10^6$ ft^3) and 2.58 $x10^6$ m^3 ($91x10^6$ ft^3) for WY 2010 and 2011. Bear Trap totaled 1.59 $x10^6$ m^3 ($56x10^6$ ft^3) for WY 2010. In both water years, Speckerman's total flows are about 60% of Big Sandy's and for both streams, the WY 2011 totals are roughly double that of WY 2010. For Last Chance, the differences are less drastic. Total flows for WY 2010 are tightly grouped and WY 2010 values are approximately 70% of WY 2011 values for Frazier. Bear Trap WY 2011 cumulative discharges were not included in the figure, but the downstream sensor measured a cumulative total of 4.56 $x10^6$ m^3 ($161x10^6$ ft^3), further indication that those data are suspect.

When discharge values are normalized over the watershed areas, the differences between streams become less apparent (Figure 17). The normalized total cumulative flow at Speckerman was 51.4 cm (upstream) and 42 cm (downstream) in WY 2010 and 92 cm (upstream) and 93 cm (downstream) in WY 2011. At Big Sandy they were 49 cm (upstream) in WY 2010 and 108 cm (upstream) and 104 cm (downstream) in WY 2011. Frazier's cumulative totals for WY 2010 were 96 cm (upstream) and 107 cm (downstream). For WY 2011 they were 162 cm (upstream) and 143 cm (downstream). Bear Trap WY 2010 cumulative flows were 92 cm (upstream) and 88 cm (downstream). When normalized the paired watersheds group closer together, but there is still a significant difference between the two water years. WY 2010 had normalized total discharge values that were between 46% and 67% of WY 2011 with the greater differences seen at the Sugar Pine sites.

Runoff coefficients, expressed as the fraction of precipitation leaving the basin as stream discharge, were associated more with precipitation levels than basin size (Figure 17). As a result, Last Chance showed higher runoff than Sugar Pine, and both increased from 2010 to 2011. Speckerman Creek and Big Sandy Creek had respective coefficients of 0.40 and 0.42 in 2010 and 0.46 and 0.53 in 2011, respectively. Bear Trap Creek and Frazier Creek had respective coefficients of 0.51 and 0.58 in 2010 and 0.55 and 0.61 in 2011.

Seasonal Stream Diel Cycles

Water-quality data were plotted for select ten-day periods to explore any diel cycles of the water-quality parameters. Frazier Creek and Speckerman Creek WY 2010 were used since their records had the fewest data gaps (Figures 18-19). Snowmelt, spring-recession, and baseflow periods were

selected for each stream. For each water-quality parameter in which a diel cycle was seen, the time of day of for the peak of each cycle was identified. Diel signals at Speckerman were seen in water temperature, dissolved oxygen, and discharge. For the Speckerman snowmelt period, a cold-air front drowned out the cycle around days 193-194, but it picked back up around day 195. Water temperature peaked at around 14:00, dissolved oxygen peaked at 12:30, and discharge peaked at 18:00. This reflects only a 4-hr lag between peak temperature, indicative of peak snowmelt, and peak discharge. The spring-recession period was identified as a time past peak snow accumulation along the recession limb of the yearly hydrograph. During this period, water temperature peaked at 15:00, dissolved oxygen peaked at 13:00, and discharge peaked at 14:30. During the baseflow period water temperature peaked at 15:30, dissolved oxygen peaked at 13:00, and discharge peaked at 11:45 (Table 4). A diel signal may also be present in conductivity, but was not visible due to data recording issue explained above.

As the melt season progressed peak temperature shifted to slightly later in the day, dissolved oxygen stayed relatively constant, and peak discharge shifted to earlier in the day. The results are as expected for discharge as early season discharge is dominated by snowmelt and typically peaks later in the day while late season discharge is dominated by evapotranspiration processes and tends to peak earlier in the day before ET reaches its peak. The somewhat unexpected results were in the temperature values. Typically during snowmelt, temperatures peaks are opposite those of discharge because during maximum snowmelt (max discharge) cold melt water is entering the stream dropping water temperature. The fact that these cycles are only slightly out of sync may be an indication that a piston-type flow model is occurring in this stream where snowmelt is immediately infiltrating into the soil, increasing the hydraulic head and pushing near stream soil water into the channel. Additional investigation will be necessary to confirm this conceptual model.

Table 4. Timing of diel cycles in Speckerman water quality data for three flow periods

	Snowmelt	Drawdown	Baseflow
Temperature, peak	14:00	15:00	15:30
Dissolved oxygen, peak	12:30	13:00	13:00
Discharge peak/minimum	18:00/04:00	14:30/04:00	11:45/00:00

At Frazier diel cycles were seen in water temperature, conductivity, and dissolved oxygen. No diel signal could be seen in the discharge for the time periods chosen. During the snowmelt period, temperature peaked at 13:45, conductivity peaked at 14:00, and dissolved oxygen peaked at 12:00. For the draw down period, temperature peaked at 14:14, conductivity peaked at 17:30, and dissolved

oxygen peaked at 12:00. The baseflow period showed temperature peaking at 16:00, the conductivity peaking at 15:30, and the dissolved oxygen peaking at 10:30 (Table 5).

The diel water temperature peaks shifted toward slightly later in the day. Conductivity varied widely, but did not show any discernible trend. Dissolved oxygen as in Speckerman did not show any significant shift in the daily peaks.

Table 5. Timing of diel cycles in Frazier water quality data for three flow periods

	Snowmelt	Drawdown	Baseflow
Temperature, peak	13:45	14:15	16:00
Conductivity, peak	14:00	17:30	15:30
Dissolved oxygen,peak	12:00	12:00	11:00

Regional Hydro-Ecological Simulation System (RHESSys)

RHESSys calibration and parameterization continues for the SNAMP basins, with additional input from the Kings River Experimental Watershed – Critical Zone Observatory (KREW-CZO). KREW-CZO has longer, richer data sets than do the SNAMP catchments, and catchments lie at similar elevations and are of comparable areas. Thus the KREW-CZO catchments are being used as part of a meta-analysis for KREW. Further, parameterization developed for CZO-KREW catchments will guide efforts on the SNAMP catchments and larger study areas.

Model results were obtained using observed temperatures and precipitation separated into rain and snow. The separation of rain and snow, as opposed to a single precipitation input, provides a more-accurate daily calculation of evapotranspiration, soil moisture and streamflow. Results for one Providence Creek catchment (P303, KREW-CZO) for water year 2006 (wet year) are shown (Figures 20-21), though modeling has been carried out for two catchments for 6 years. The model simulation was also adjusted using additional observed input parameters such as relative humidity, vapor-pressure deficit and wind speed for water years from 2003 to 2008. The presented results show a good agreement between the daily observed streamflow and simulated streamflow. Moving forward, additional observed parameters such as daily soil moisture, evapotranspiration, and snow depth/snow water equivalent will be compared with the model estimates to finalize the calibrated model.

The same model output is also shown for water year 2010 from Bear Trap Creek (Figures 22-23). It is evident comparing the streamflow output between this watershed and P303, that the model is not as mature for this basin. Calibration and parameterization of the four headwater catchments is still

ongoing, although model development of these basins has not yet reached the more advanced stage of P303. The KREW-CZO catchments have been useful for informing these model configurations, as they have provided a good starting point for parameter values, have a more extensive streamflow record for model testing, and have observed values not available at these sites: sapflow rates, fluxes of water vapor and carbon dioxide with the atmosphere, and chemical composition of wet and dry atmospheric deposition.

Project Challenges

Gaps are expected when collecting continuous datasets and were filled during post-processing. Gaps can be caused by many situations, some of which include instrument failure, power failure, damage, vandalism, and user error. Inclement weather and access difficulties occasionally prevented consistent site visits. This was especially prevalent during the fall and spring months when roads are only partially covered with snow. Under those conditions, access with either truck or snowmobile was difficult and often not possible. In these situations, sites were accessed on foot by personnel or field work was delayed until access by vehicle was possible. However, when large repairs were required the equipment needed couldn't always be carried and repairs had to be postponed.

Long stretches of cloud cover or accumulation of snow prevented solar panels from receiving enough incoming solar to keep batteries charged and resulted in station down time. It was expected that battery charge would drop during the winter months and so the initial approach was to replace batteries when they started getting low. Because the sites locations had poorer sun exposure than accounted for, batteries drained faster than could be replaced. Larger batteries helped solve power issues at some sites, however at sites with chronic power issues (typically north facing nodes) solar panels needed to be moved to locations with better sun exposure. This often required a professional tree climber to move the panels high enough in trees that ridgetops did not block low angle winter sun. The combination of increasing battery size and relocating solar panels largely resolved any power problems.

By far the most common damage to sites was from snow loads. The damage caused by snow creep on installations varied each season but common damage included: bent u-channels, mounting/instrument poles leaned downslope, enclosures torn from mounting poles, and cables ripped out of dataloggers. Damage was amplified during heavier snow years (e.g. WY 2011) and resulted in wide-spread power failures and instrument damage. Many of the snow depth sensors and instrument enclosures needed to be repaired or replaced during the life of this project. Duncan Peak was especially hard hit and required repairs to every instrument node following the 2010-2011 winter. Mitigating damage was difficult due to the constraints on field season length and budget. Sites were generally repaired with some minor modifications such as reinforcing connection, adding extensions, installing more robust hardware, and burying or using zip-ties to secure loose or exposed cables.

Two less-common forms of damage at sites were a result of vandalism and wildlife. Vandalism ranged from property destruction to theft and was usually confined to areas where summer recreation was popular (e.g. Big Sandy Campground). Solar panels became targets for both firearms and rocks but

those incidents usually did not result in much, if any, instrument downtime. Theft occurred once during the summer of 2011 at the Speckerman Creek culvert installation and required the replacement of all site components. Wildlife damage was focused around enclosures and cables. The most common damage was from rodents chewing through exposed cables cutting power to instrumentation. Bears focused their efforts on fiberglass enclosures and flexible conduit, chewing through or ripping out cables running along mounting poles. Trenching and running cables through conduit were the best ways to prevent wildlife damage but made troubleshooting cable connections was difficult and time consuming.

Operating a network of 8 instrument clusters that, in some cases, produce upwards of 30 individual 15-minute data streams each, results in a massive amount of data accrued annually. Processing the incoming data is time consuming and was difficult to keep up with while concurrently performing installations, routine maintenance and repairs. To address this issue, a protocol for managing incoming data streams was established. Through use of the protocol, a clear division of responsibilities, and additional project support, data streams are being processed in a timely manner and routinely examined throughout the year. Prioritizing the installations, measurements and data processing was also necessary given the lag and eventual reduction in funding relative to the project's original scope of work and accompanying budget.

Conclusions

The 2-4 years of water-quantity and energy-balance data assembled and presented here provides an adequate basis for developing a pre-treatment modeling capability for the SNAMP catchments. Use of the CZO-KREW data is important to help guide the modeling effort, and extend it to large areas. Forest treatments were started in the fall of 2011 and are expected to be finished in summer 2012. Thus water-year 2012 data represent a transition year. Water-year 2013 will be a post-treatment measurement year, and will be the main measurement basis for evaluating the effects of thinning. Extending measurements through water-year 2014 would enhance detecting the post-treatment effects; but that would necessitate data analysis and modeling through spring-summer 2015.

While it has been necessary to somewhat reduce the water-quality measurements and scope, measurements to date do establish baseline conditions from which to compare effects of treatments. The adequacy of this data set will depend in part on precipitation and hydrologic conditions in water-year 2013.